Application to Amend the Australia New Zealand Food Standards Code
Schedule 26 - *Food Produced Using Gene Technology*

OECD Unique Identifier: DP-91Ø521-2

DP910521 Maize

Submitting company:
Corteva Agriscience Australia Pty Ltd

Submitted by:
[redacted]

[redacted]
Regulatory Manager ANZ
Corteva Agriscience Australia Pty Ltd (ABN 24 003 771 659)
Level 9, 67 Albert Avenue
CHATSWOOD NSW 2067 Australia
Telephone: [redacted]
Email: [redacted]

July 2023

© 2023 Corteva Agriscience Australia Pty Ltd., All Rights Reserved.

®, TM, SM Trademarks and service marks of Corteva Agriscience and its affiliated companies or their respective owners.

This document is protected by copyright law. This document and material is for use only by the regulatory authority for the purpose that it is submitted by Corteva Agriscience Australia Pty Ltd, ("Corteva Agriscience"), its affiliates, or its licensees and only with the explicit consent of Corteva Agriscience. Except in accordance with law, any other use of this material, without prior written consent of Corteva Agriscience, is strictly prohibited. The intellectual property, information, and materials described in or accompanying this document are proprietary to Corteva Agriscience. By submitting this document, Corteva Agriscience does not grant any party or entity not authorized by Corteva Agriscience any right or license to the information or intellectual property described in this document.

SUMMARY

Corteva, Inc. is a publicly traded, global pure-play agriculture company that combines industry-leading innovation, high-touch customer engagement and operational execution to profitably deliver solutions for the world's most pressing agriculture challenges. Corteva generates advantaged market preference through its unique distribution strategy, together with its balanced and globally diverse mix of seed, crop protection, and digital products and services. With some of the most recognized brands in agriculture and a technology pipeline well positioned to drive growth, the company is committed to maximizing productivity for farmers, while working with stakeholders throughout the food system as it fulfills its promise to enrich the lives of those who produce and those who consume, ensuring progress for generations to come. More information can be found at www.corteva.com.Corteva Agriscience Australia Pty Ltd, member of Corteva Agriscience group of companies, is submitting this application to FSANZ to vary the Code to approve food uses of insect-resistant and herbicide-tolerant maize (*Zea mays* L.) event DP-91Ø521-2 (referred to as DP910521 maize), a new food produced using gene technology.

DP910521 maize was genetically modified to expresses the Cry1B.34 protein for protection against certain susceptible lepidopteran pests, the phosphinothricin acetyltransferase (PAT) protein for tolerance to glufosinate herbicide, and the phosphomannose isomerase (PMI) protein that was used as a selectable marker. The Cry1B.34 protein is presented to FSANZ for review for the first time. The PAT and PMI proteins present in DP910521 maize are found in several approved events that are currently in commercial use.

This application presents information supporting the safety and nutritional comparability of DP910521 maize. The molecular characterization analyses conducted on DP910521 maize demonstrate that the introduced genes are integrated at a single locus, stably inherited across multiple generations, and segregate according to Mendel's law of genetics. The allergenic and toxic potential of the Cry1B.34 protein was evaluated, and the Cry1B.34 protein was found unlikely to be allergenic or toxic to humans.

The allergenic and toxic potential of the PAT and PMI proteins was evaluated previously, and these proteins were found unlikely to be allergenic or toxic to humans. The updated bioinformatics analyses for the PAT and PMI proteins are referenced to Corteva's two recent applications currently under evaluation (A1270 and A1272). The results confirm the PAT and PMI proteins as unlikely to cause an adverse effect on humans.

Based on the weight of evidence, consumption of the Cry1B.34, PAT or PMI proteins in DP910521 maize is unlikely to cause an adverse effect on humans. A compositional equivalence assessment demonstrated that the nutrient composition of DP910521 maize grain is comparable to that of conventional maize, represented by non-genetically modified (non-GM) near-isoline maize and non-GM commercial maize.

Overall, data and information contained herein support the conclusion that DP910521 maize containing the Cry1B.34, PAT, and PMI proteins is as safe and nutritious as non-GM maize.

TABLE OF CONTENTS

SUMMARY **2**
Table of Contents **3**
List of Tables **5**
List of Figures **7**
Checklists **9**
Statutory Declaration **11**
GENERAL INFORMATION ON THE APPLICATION **12**
B. Applicant 12
C. Purpose of the application 12
D. Justification for the application 12
D(a) Need for the proposed change 12
D(b) Advantage of the genetically modified food 13
D.1 Regulatory impact 13
A.1 (b) GM Organism Identification 16
A.1 (c) Trade name 16
A.2 History of use of the host and donor organisms 17
A.2 (a) Donor organisms 17
A.2 (b) Host organism 18
A.3 Nature of the genetic modification 19
A.3 (a) Transformation Method 19
A.3(b) Description of the construct and the transformation vectors used 37
A.3(c) Molecular characterisation 37
A.3 (d) Breeding process 61
A.3 (e) Stability of the genetic changes 63
B. CHARACTERISATION AND SAFETY ASSESSMENT OF NEW SUBSTANCES **73**
B.1 Characterisation and safety assessment of new substances 73
B.2 New proteins 73
Cry1B.34 Protein 73
PAT protein 107
PMI Protein 117
B.3 Other (non-protein substances) 126
B.4 Novel herbicide metabolites in GM herbicide-tolerant plants 126
B.5 Compositional analyses of the food produced using gene technology 126
Trait Expression Assessment (PHI-2020-024 study) 126
Nutrient Composition Assessment (PHI-2020-025/021 study) 128
C. INFORMATION RELATED TO THE NUTRITIONAL IMPACT OF THE FOOD **150**
D. OTHER INFORMATION **151**
Overall Risk Assessment Conclusions for DAS1131 Maize 151
References **152**
Study Index **161**
Appendix A. Methods for Southern-by-Sequencing Analysis **163**
Appendix B. Methods for Southern Blot Analysis **182**
Appendix C. Methods for Multi-Generation Segregation Analysis **184**
Appendix D. Methods for Sanger Sequencing Analysis **186**
Appendix E. Methods for Characterization of Cry1B.34 Protein **188**
Appendix E.2 Characterization of Cry1B.34 (PCF-0059) Protein Derived from a Microbial Expression System 200
Appendix E.3. Methods for Characterization of Microbially Derived Cry1B.34 Protein (PCF-0059) 211

Appendix F. Methods for Characterization of PAT Protein..... 215
Appendix G. Methods for Characterization of PMI Protein..... 218
Appendix H. Methods for Trait Expression Analyses..... 221
Appendix I. Methods for Nutrient Composition Analysis..... 226

LIST OF TABLES

Table 1. List of Genetic Elements in Plasmids Used for Landing Pad Transformation and their Presence in DP910521 Maize 21
Table 2. List of Genetic Elements in Plasmid PHP79620 Recombination Fragment Region and Plasmids Used for SSI and their Presence in DP910521 Maize 21
Table 3. Description of the Genetic Elements in Plasmid PHP79620 33
Table 4. Description of the Genetic Elements in Recombination Fragment Region from Plasmid PHP79620 34
Table 5. Maize Endogenous Elements in Plasmids and DP910521 Insertion 40
Table 6. SbS Junction Reads 41
Table 7. Generations and Comparators Used for Analysis of DP910521 Maize 62
Table 8. Description of DNA Probes Used for Southern Hybridization 64
Table 9. Predicted and Observed Hybridization Bands on Southern Blots; Bcl I Digest 64
Table 10 . Summary of Genotypic and Phenotypic Segregation Analyses for Five Generations of DP910521 Maize 72
Table 11. Identified Tryptic Peptides of DP910521 Maize-Derived Cry1B.34 Protein Using LC MS Analysis 81
Table 12. Identified Chymotryptic Peptides of DP910521 Maize-Derived Cry1B.34 Protein Using LC MS Analysis 83
Table 13. Combined Sequence Coverage of Identified Tryptic and Chymotryptic Peptides of DP910521 Maize-Derived Cry1B.34 Protein Using LC-MS Analysis 85
Table 14. Identified Tryptic Peptides of Microbially Derived Cry1B.34 Protein Using LC-MS Analysis .. 87
Table 15. Identified Chymotryptic Peptides of Microbially Derived Cry1B.34 Protein Using LC-MS Analysis 88
Table 16. Combined Sequence Coverage of Identified Tryptic and Chymotryptic Peptides of Microbially Derived Cry1B.34 Protein Using LC-MS Analysis 90
Table 17. N-Terminal Amino Acid Sequence of the Cry1B.34 Protein 92
Table 18. Microbially Derived Cry1B.34 Protein Bioactivity Assay Using Spodoptera frugiperda 93
Table 19. Biological Activity of Heat-Treated Cry1B.34 Protein in Artificial Diet Fed to Spodoptera frugiperda 96
Table 20. Summary of Cry1B.34 Protein In Vitro Pepsin Resistance Analyses 97
Table 21. Summary of Cry1B.34 Protein In Vitro Pancreatin Resistance Analyses 100
Table 22. Identified Tryptic and Chymotryptic Peptides of DP910521 Maize-Derived PAT Protein Using LC-MS Analysis 114
Table 23. Combined Sequence Coverage of Identified Tryptic and Chymotryptic Peptides of DP910521 Maize-Derived PAT Protein Using LC-MS Analysis 114
Table 24. N-Terminal Amino Acid Sequence Analysis of DP910521 Maize-Derived PAT Protein 115
Table 25. Identified Tryptic Peptides of DP910521 Maize-Derived PMI Protein Using LC-MS Analysis 122
Table 26. Identified Chymotryptic Peptides of DP910521 Maize-Derived PMI Protein Using LC-MS Analysis 122
Table 27. Combined Sequence Coverage of Identified Tryptic and Chymotryptic Peptides of DP910521 Maize-Derived PMI Protein Using LC-MS Analysis 124
Table 28. Across-Site Summary of Cry1B.34 Protein Concentrations in DP910521 Maize 127

Table 29. Across-Site Summary of PAT Protein Concentrations in DP910521 Maize *127*
Table 30. Across-Site Summary of PMI Protein Concentrations in DP910521 Maize *128*
Table 31. Outcome of Nutrient Composition Assessment Across Sites *130*
Table 32. Proximate, Fiber, and Mineral Results for DP910521 Maize Forage *134*
Table 33. Proximate and Fiber Results for DP910521 Maize Grain *136*
Table 34. Fatty Acid Results for DP910521 Maize Grain *138*
Table 35. Amino Acid Results for DP910521 Maize Grain *140*
Table 36. Mineral Results for DP910521 Maize Grain *144*
Table 37. Vitamin Results for DP910521 Maize Grain *146*
Table 38. Secondary Metabolite and Anti-Nutrient Results for DP910521 Maize Grain *149*
Table D.1. PCR Amplification Conditions *186*
Table E.1. Control Samples for Simulated Gastric Fluid (SGF) Digestibility Analysis *194*
Table E.2. Control Samples for Simulated Intestinal Fluid (SIF) Digestibility Analysis *196*
Table E2.1. Tryptic Peptides of Microbially Derived Cry1B.34 Protein Identified Using LC-MS Analysis *205*
Table E2.2. Chymotryptic Peptides of Microbially Derived Cry1B.34 Protein Identified Using LC-MS Analysis *206*
Table E2.3. Combined Sequence Coverage of Identified Tryptic and Chymotryptic Peptides of Microbially Derived Cry1B.34 Protein Using LC-MS Analysis *208*
Table E2.4. Microbially Derived Cry1B.34 Protein Bioactivity Assay Using Spodoptera frugiperda *210*
Table H.1. Maize Growth Stage Descriptions *221*
Table I.1. Methods for Compositional Analysis *228*
Table I.2. Number of Sample Values Below the Lower Limit of Quantification (sprayed) *234*

LIST OF FIGURES

Figure 1. Map of Plasmid [redacted] 22
Figure 2. Map of Plasmid [redacted] 23
Figure 3. Map of Plasmid [redacted] 24
Figure 4. Map of Plasmid PHP21875 25
Figure 5. Map of the T-DNA Region from Plasmid [redacted] 26
Figure 6. Map of Plasmid PHP79620 27
Figure 7. Map of Plasmid PHP5096 28
Figure 8. Map of Plasmid PHP73572 29
Figure 9. Map of the Recombination Fragment Region from Plasmid PHP79620 30
Figure 10. Map of the DP910521 Maize Insertion 31
Figure 11. Schematic Diagram of the DP910521 Maize DNA Insertion 42
Figure 12. SbS Results for Control Maize 44
Figure 13. SbS Results for Positive Control Samples 47
Figure 14. SbS Results for DP910521 Maize (Plant ID 404181698) 50
Figure 15. SbS Results for Representative Null Segregant Plant (Plant ID 404181702) 53
Figure 16. Map of the Insert and Flanking Genomic Regions Sequenced for DP910521 Maize 56
Figure 17. Event Development Process of DP910521 Maize 61
Figure 18. Breeding Diagram for DP910521 Maize and Generations Used for Analysis 62
Figure 19. Map of Plasmid PHP79620 for Southern Analysis 65
Figure 20. Map of the Recombination Fragment Region from Plasmid PHP79620 66
Figure 21. Map of the DP910521 Insertion 67
Figure 22. Southern Blot Analysis of DP910521 Maize; Bcl I Digest with cry1B.34 Probe 68
Figure 23. Southern Blot Analysis of DP910521 Maize; Bcl I Digest with mo-pat Probe 69
Figure 24. Southern Blot Analysis of DP910521 Maize; Bcl I Digest with pmi Probe 70
Figure 25. Deduced Amino Acid Sequence of the Cry1B.34 Protein 73
Figure 26. SDS-PAGE Analysis of Cry1B.34 Protein 75
Figure 27. Western Blot Analysis of Cry1B.34 Protein 76
Figure 28. Glycosylation Analysis of DP910521 Maize-Derived Cry1B.34 Protein 78
Figure 29. Glycosylation Analysis of Microbially Derived Cry1B.34 Protein 79
Figure 30. Identified Tryptic and Chymotryptic Peptide Amino Acid Sequence of DP910521 Maize-Derived Cry1B.34 Protein Using LC-MS Analysis 86
Figure 31. Identified Tryptic and Chymotryptic Peptide Amino Acid Sequence of Microbially Derived Cry1B.34 Protein Using LC-MS Analysis 91
Figure 32. SDS-PAGE Analysis of Cry1B.34 Protein in Simulated Gastric Fluid Digestion Time Course 98
Figure 33. Western Blot Analysis of Cry1B.34 Protein in Simulated Gastric Fluid Digestion Time Course 99
Figure 34. SDS-PAGE Analysis of Cry1B.34 Protein in Simulated Intestinal Fluid Digestion Time Course 101
Figure 35. Western Blot Analysis of Cry1B.34 Protein in Simulated Intestinal Fluid Digestion Time Course 102
Figure 36. SDS-PAGE Analysis of Cry1B.34 Protein in a Sequential Digestion with Simulated Gastric Fluid and Simulated Intestinal Fluid 104

Figure 37. Alignment of the Deduced Amino Acid Sequence of PAT Protein Encoded by pat and mo-pat Genes 107
Figure 38. SDS-PAGE Analysis of DP910521 Maize-Derived PAT Protein 109
Figure 39. Western Blot Analysis of DP910521 Maize-Derived PAT Protein 110
Figure 40. Glycosylation Analysis of DP910521 Maize-Derived PAT Protein 112
Figure 41. Identified Tryptic and Chymotryptic Peptide Amino Acid Sequence of DP910521 Maize-Derived PAT Protein Using LC-MS Analysis 115
Figure 42. Deduced Amino Acid Sequence of PMI Protein 117
Figure 43. SDS-PAGE Analysis of DP910521 Maize-Derived PMI Protein 118
Figure 44. Western Blot Analysis of DP910521 Maize-Derived PMI Protein 119
Figure 45. Glycosylation Analysis of DP910521 Maize-Derived PMI Protein 120
Figure 46. Identified Tryptic and Chymotryptic Peptide Amino Acid Sequence of DP910521 Maize-Derived PMI Protein Using LC-MS Analysis 124
Figure A1. SbS Results for Plant ID 404181700 – DP910521 Maize (Transgenic) 168
Figure A2. SbS Results for Plant ID 404181703 – DP910521 Maize (Transgenic) 171
Figure A3. SbS Results for Plant ID 404181704 – DP910521 Maize (Transgenic) 174
Figure A4. SbS Results for Plant ID 404181705 – DP910521 Maize (Transgenic) 177
Figure A5. SbS Results for Plant ID 404181706 – DP910521 Maize (Transgenic) 180
Figure E2.1. SDS-PAGE Analysis of the Microbially Derived Cry1B.34 Protein 201
Figure E2.2. Western Blot Analysis of the Microbially Derived Cry1B.34 Protein 202
Figure E2.3. Glycosylation Analysis of Microbially Derived Cry1B.34 Protein 203
Figure E2.4. Amino Acid Sequence of Microbially Derived Cry1B.34 Protein Indicating Chymotryptic Peptides Identified Using LC-MS Analysis 209

CHECKLISTS

		General requirements (3.1.1)
Check	**Page No.**	**Mandatory requirements**
☑		A Form of application ☑ *Application in English* ☑ *Executive Summary (separated from main application electronically)* ☑ *Relevant sections of Part 3 clearly identified* ☑ *Pages sequentially numbered* ☑ *Electronic copy (searchable)* ☑ *All references provided*
☑	12	B Applicant details
☑	12	C Purpose of the application
☑	12	D Justification for the application ☑ *Regulatory impact information* ☑ *Impact on international trade*
☑		E Information to support the application ☑ *Data requirements*
☑		F Assessment procedure ☑ *General* *Major* *Minor* *High level health claim variation*
☑		G Confidential commercial information ☑ *CCI material separated from other application material* ☑ *Formal request including reasons* ☑ *Non-confidential summary provided*
☑		H Other confidential information ☑ *Confidential material separated from other application material* ☑ *Formal request including reasons*
☐		I Exclusive Capturable Commercial Benefit ☐ *Justification provided*

		J International and other national standards
☑		☑ *International standards* *Other national standards*
☑	11	K Statutory Declaration
☑	9	L Checklist/s provided with application ☑ *3.1.1 Checklist* ☑ *All page number references from application included* ☑ *Any other relevant checklists for Chapters 3.2–3.7*

		Foods produced using gene technology (3.5.1)
Check	**Page No.**	**Mandatory requirements**
☑	16	A.1 Nature and identity
☑	17	A.2 History of use of host and donor organisms
☑	19	A.3 Nature of genetic modification
☑	37	B.1 Characterisation and safety assessment
☑	73	B.2 New proteins
☑	126	B.3 Other (non-protein) new substances
☑	126	B.4 Novel herbicide metabolites in GM herbicide-tolerant plants
☑	126	B.5 Compositional analyses
☑	150	C Nutritional impact of GM food
☑	151	D Other information

STATUTORY DECLARATION

Statutory Declarations Act 1959 [1]

I, [redacted] Regulatory Manager of Corteva Agriscience, Level 9, 67 Albert Ave, Chatswood, NSW 2067 make the following declaration under the *Statutory Declarations Act 1959*:

1. the information provided in this application fully sets out the matters required
2. the information provided in this application is true to the best of my knowledge and belief
3. no information has been withheld that might prejudice this application, to the best of my knowledge and belief

I understand that a person who intentionally makes a false statement in a statutory declaration is guilty of an offence under section 11 of the *Statutory Declarations Act 1959*, and I believe that the statements in this declaration are true in every particular.

[redacted]

[*Signature of person making the declaration*]

Declared at Chatswood on 9th of February 2022

Before me, [redacted]

Legal Practitioner
Corteva Agriscience, Level 9, 67 Albert Ave, Chatswood, NSW 2067

[1] http://www.comlaw.gov.au/Series/C1959A00052.

GENERAL INFORMATION ON THE APPLICATION

The chapter numbering follows section numbers from the FSANZ Application Handbook (Chapters 3.1 and 3.5.1).

B. Applicant

This application is submitted by:

Corteva Agriscience Australia Pty Ltd
Member of Corteva Agriscience group of companies
Level 9, 67 Albert Ave
Chatswood
NSW 2067

The primary contact is:

[redacted]
Regulatory Manager
Corteva Agriscience
Ph: [redacted]
Email: [redacted]

The Managing Director of Corteva Agriscience Australia Pty Ltd is:

[redacted]
Ph: [redacted]
Email: [redacted]

C. Purpose of the application

Corteva Agriscience Australia Pty Ltd, member of Corteva Agriscience group of companies, and its affiliated companies (herein referred to collectively as Corteva), has developed DP910521 maize (OECD Unique Identifier DP-91Ø521-2), a new event that has been transformed to express the Cry1B.34 protein for protection against certain susceptible lepidopteran pests, the phosphinothricin acetyltransferase (PAT) protein for tolerance to glufosinate herbicide, and the phosphomannose isomerase (PMI) protein that was used as a selectable marker.

As a result of this application, Corteva seeks an amendment of Standard 1.5.2 *Food produced using gene technology* by inserting the following into table to Schedule 26 3(4) after the last entry: herbicide-tolerant and insect-protected corn line DP910521.

D. Justification for the application

D(a) Need for the proposed change

Corteva is a member of Excellence Through Stewardship™ (ETS). Corteva has developed the new maize event DP910521, which is being commercialized in accordance with the ETS Product Launch Stewardship Guidance and in compliance with Corteva polices regarding stewardship of

GM products. In line with these guidelines, Corteva's process for launches of new products includes a longstanding process to evaluate export market information, value chain consultations, and regulatory functionality. Corteva's application to amend Standard 1.5.2 with respect to DP910521 maize is in support of these policies.

D(b) Advantage of the genetically modified food

Maize has multiple downstream uses for feed, fuel, and food that are significant for the global supply of this crop commodity. The introduction of insect-resistant and herbicide-tolerant DP910521 maize is intended to help growers keep pace with increasing maize demand globally. The United States is one of the world's largest maize producers and a leading exporter of maize. In 2020, more than 14 billion bushels of maize were produced in the United States from approximately 90 million planted acres, valued at nearly $60 billion (NCGA, 2020; USDA-NASS, 2020).

Insect Resistance

Certain lepidopteran insects are serious pests of maize in the United States. Control of lepidopteran maize pests has historically been managed with crop rotation, broad-spectrum insecticides, and transgenic crops expressing crystalline (Cry) proteins. As adoption of Bt maize has increased, the selection pressure on target insects to develop resistance has become greater. Insect resistance to transgenic traits can reduce the efficacy of the traits over time, increasing costs of maize production and/or reducing yield.

Herbicide Tolerance

Genetically modified (GM) herbicide-tolerant maize lines are widely cultivated because they provide additional weed management options for growers. Herbicide-tolerant maize has a significant impact on growers' earnings as they can be used on an as-needed basis and can help growers to adopt reduced or no tillage practices (Fawcett and Towery, 2003; Fernandez-Cornejo et al., 2012).

The PAT protein is tolerant to the herbicidal active ingredient glufosinate-ammonium (CERA - ILSI Research Foundation, 2016). DP910521 maize provides farmers with an additional control option for weed management practices.

Selectable Marker

The PMI protein was incorporated into DP910521 maize to enable selection of plants containing the desired constructs during the event development process (Negrotto et al., 2000).

D.1 Regulatory impact

Corteva have developed the new maize line DP910521, which will be commercialized in accordance with the ETS Product Launch Stewardship Guidance and in compliance with Corteva polices regarding stewardship of GM products. In line with these guidelines, Corteva's approach to responsible launches of new products includes a longstanding process to evaluate export market information, value chain consultations, and regulatory functionality. Growers and end-users must

take all steps within their control to follow appropriate stewardship requirements and confirm their buyer's acceptance of the grain or other material being purchased.

Refer to the OECD Consensus Document on Compositional Considerations for New Varieties of Maize (Zea mays): Key Food and Feed Nutrients, Anti-nutrients and Secondary Plant Metabolites (OECD, 2002), for the following aspects of the food uses of maize:

- Production of maize for food and feed
- Processing of maize
- Wet Milling
- Dry Milling
- Masa Production
- Feed Processing

The majority of grain and forage derived from maize is used for animal feeds. Less than 10% of maize grain is processed for human food products. Maize grain is also processed into industrial products, such as ethyl alcohol by fermentation and highly refined starch by wet-milling to produce starch and sweetener products. In addition to milling, maize germ can be processed to obtain maize oil.

Domestic production of maize in Australia (ca. 440,000 t) and New Zealand is supplemented by import of a small amount of maize-based products, largely as high-fructose maize syrup, which is not currently manufactured in either Australia or New Zealand. Such products are processed into breakfast cereals, baking products, extruded confectionery and maize chips. Other maize products such as maize starch are also imported. This is used by the food industry for the manufacture of dessert mixes and canned foods (www.grdc.com.au).

D.1.1 Costs and benefits for industry, consumers and government

Corteva launches new products in accordance with the Corteva Product Launch Policy and Excellence Through Stewardship Product Launch Guidance. Our long-standing, multi-faceted approach includes evaluating export market information, performing value-chain consultations and consideration of regulatory functionality. Innovative technologies like DP910521 maize are designed to deliver exceptional value and needed performance to the farmers that produce grain from these products, along with helping farmers provide enough safe, nutritious food to meet global demand. In line with these guidelines, Corteva's approach to responsible launches of new products includes a long-standing process to evaluate export market information, value chain consultations, regulatory functionality, preparedness to meet product ramp up and demand plans, and other factors. Corteva continues to advocate for a global synchronous, science-based and predictable regulatory system. We also encourage farmers, industry, and consumer groups to continue to advocate for the acceptance of new, innovative technologies that help to improve farm productivity and profitability and contribute to the global economy and environmental sustainability.

Corteva does not develop nor import food or feed products into the Australian or New Zealand markets. The proposed amendment to the Standard, however, may result in increasing Australia and New Zealand's access to international grain food markets while supporting Corteva's sale of

seed in markets where DP910521 maize is to be cultivated. In this sense, and in an effort to maintain transparency with FSANZ, Corteva acknowledges that there may be a capturable commercial benefit to Corteva as defined in Section 8 of the FSANZ Act. Any relevant local costs are made up of Corteva personnel time both locally and globally as well as of the direct fees associated with the submission.

Most of the sweet corn consumed in Australia is grown domestically. Domestic production of corn in Australia and New Zealand is supplemented by importation of a small amount of corn-based products usually frozen or canned, largely as high-fructose corn syrup, which is not currently manufactured in either Australia or New Zealand (www.grdc.com.au). Although not requiring a FSANZ approval for livestock feed, from time to time, mainly during periods of drought where local supply of feed grain is limited, maize is imported from the United States for use as stock feed, predominantly in the pig and poultry markets. This variation to the Standard permits the import and use of food derived or developed from DP910521 maize. This offers benefits to the industry and consumers in Australia and New Zealand, which result from the advantages of DP910521 maize available to growers in cultivation countries (see Section D(b) Advantage of the genetically modified food of the dossier above).

While Corteva does not possess quantitative data, which would allow it to estimate the benefits in monetary terms, DP910521 maize is anticipated to contribute to the maintenance of stable global maize supply, choice and affordability for consumers. No specific costs associated with the approval of DP910521 maize for Australian and New Zealand consumers have been identified.

Similarly, an analysis in monetary terms for the grain and food industry is hard to determine, however, Australian and New Zealand importers are expected to benefit from trade access, which the approval of DP910521 maize will support (see Section D.1.2 Impact on international trade below). Compliance with import requirements is also anticipated to be simplified when sourcing from markets in which DP910521 maize is commercialized as a seed product. The only identified costs associated with the approval of DP910521 maize for Australian and New Zealand industry is meeting their GM labelling requirements for those foods derived from DP910521 maize which trigger them, similarly to other existing GM maize varieties.

No dollar value of the costs and benefits for the governments can be assigned with the available information. However, from the government perspective, approval of DP910521 maize will support global regulatory harmonization and limit potential instances of non-compliance related to the regulation of GM foods. No costs associated with the approval of DP910521 maize for the Australian and New Zealand governments have been identified.

D.1.2 Impact on international trade

The addition of DP910521 maize to Schedule 26 is anticipated to facilitate import access to maize from the applicable cultivation countries. Without such an approval, grain handlers may undertake a scientifically unnecessary and costly activities to segregate DP910521 maize and food products derived from it for Australian and New Zealand markets. Therefore, amending the Food Code to include DP910521 maize is anticipated to have a positive impact on Australian and New Zealand access to international commodity trade markets.

A. TECHNICAL INFORMATION ON THE FOOD PRODUCED USING GENE TECHNOLOGY

A.1 Nature and identity of the genetically of the genetically modified food

A.1 (a) Description of the GM organisms, nature and purpose of the genetic modification

DP910521 maize was genetically modified to express the Cry1B.34 protein for protection against certain susceptible lepidopteran pests, the phosphinothricin acetyltransferase (PAT) protein for tolerance to the glufosinate herbicide, and the phosphomannose isomerase (PMI) protein that was used as a selectable marker.

The Cry1B.34 protein is encoded by the *cry*1B.34 gene, a chimeric gene comprised of sequences from a *cry*1B-class gene, the *cry*1Ca1 gene, and the *cry*9Db1 gene, all derived from *Bacillus thuringiensis*. The expressed Cry1B.34 protein is effective against certain susceptible lepidopteran pests by causing disruption of the midgut epithelium. The Cry1B.34 protein binds to receptors in the brush border membrane of susceptible lepidopteran pests and causes cell death through the formation of non-specific, ion conducting pores in the apical membrane of the midgut epithelial cells.

The PAT protein, encoded by a maize-optimized version of the phosphinothricin acetyltransferase (*mo-pat*) gene from *Streptomyces viridochromogenes*, confers tolerance to the herbicidal active ingredient glufosinate-ammonium at current labeled rates by acetylating phosphinothricin to an inactive form. The PAT protein present in DP910521 maize is identical to the corresponding protein found in a number of approved events across several different crops that are currently commeralized and have a history of safe use (CERA - ILSI Research Foundation, 2011; CERA - ILSI Research Foundation, 2016; Hérouet et al., 2005).

The phosphomannose isomerase (PMI) protein, encoded by the *pmi* gene from *Escherichia coli*, serves as a selectable marker in plant tissue during transformation which allows for tissue growth using mannose as the carbon source. The PMI protein is found in several approved events that are currently in commercial use (ISAAA, 2020).

A.1 (b) GM Organism Identification

In accordance with OECD's "Guidance for the Designation of a Unique Identifier for Transgenic Plants", this event has an OECD identifier of DP-91Ø521-2, also referred to as DP910521 maize.

A.1 (c) Trade name

Maize event DP910521 is at pre-commercialization stage and has not yet been assigned a commercial product name.

A.2 History of use of the host and donor organisms

A.2 (a) Donor organisms

Bacillus thuringiensis (*Bt*): donor of the chimeric *cry*1B.34 gene comprised of sequences from a *cry*1B-class gene, the *cry*1Ca1 gene, and the *cry*9Db1 gene

- Class: Bacillus/Clostridium group (low G+C Gram-positive bacteria)
- Order: Bacillales
- Family: Bacillaceae
- Genus: *Bacillus*
- Species: *B. thuringiensis*

Bt is a diverse group of Gram-positive, spore-forming bacteria that has a history of safe use as a pesticide over several decades (US-EPA, 1998; US-EPA, 2001). It occurs ubiquitously in the soil and on plants including vegetables, cotton, tobacco, tree crops, and forest crops (Schnepf et al., 1998; Shelton, 2012). Several Cry proteins have been deployed as safe and effective pest control agents in microbial *Bt* formulations for almost 40 years. Several Cry proteins have also been effectively deployed as safe and effective pest control agents and have a history of safe use in genetically modified crops (ISAAA, 2019).

Streptomyces viridochromogenes: donor of the *mo-pat* gene

- Class: Actinobacteria (high G+C Gram-positive bacteria)
- Order: Actinomycetales
- Family: Streptomycetaceae
- Genus: *Streptomyces*
- Species: *S. viridochromogenes*
- Strain: Tü494

Streptomyces. viridochromogenes is a Gram-positive, saprophytic, aerobic bacterium commonly found in soil. *S. viridochromogenes* is not considered pathogenic to humans or animals and is not known to be an allergen or toxin. *S. viridochromogenes* produces the tripeptide L-phosphinothricyl-L-alanyl-alanine (L-PPT), which was developed as a non-selective herbicide (OECD, 1999).

Escherichia coli: donor of the *pmi* gene

- Class: Gammaproteobacteria
- Order: Enterobacteriales
- Family: Enterobacteriaceae
- Genus: *Escherichia*
- Species: *E. coli*
- Strain: K-12

Escherichia coli (*E. coli*) is a Gram-negative, facultatively anaerobic, rod-shaped bacterium. The strain *E. coli* K-12 is a strain which has been debilitated, does not normally colonize the human

intestine, and has a poor survival rate in the environment. *E. coli* K-12 has a history of safe use in human drug and specialty chemical production (US-EPA, 1997).

A.2 (b) Host organism

Information relating to maize, the host organism, was included in many previous safety assessments prepared by FSANZ. Repeating it is not considered necessary in this submission.

A.3 Nature of the genetic modification

A.3 (a) Transformation Method

DP910521 maize was developed by site-specific integration (SSI) using two sequential transformation steps to (1) insert an integration site sequence (referred to as a "landing pad" sequence) at a specific location of the maize genome using microprojectile bombardment, and (2) insert the intended expression cassettes from the plasmid PHP79620 recombination fragment region into the landing pad in the maize genome using microprojectile bombardment. After each transformation step, a line containing only the intended insertion with no unintended plasmid-derived sequences was selected for the next step in the process. The use of SSI for targeted transgene insertion has advantages compared to random transformation by allowing the ability to pre-select the insertion location to avoid endogenous gene disruption and pre-test the genomic location for agronomic neutrality (Gao *et al.*, 2020). Thus, the SSI approach can simplify risk assessment of the event intended for commercialization as it concerns potential for insertional effects.

First Transformation Step: Insertion of the Landing Pad Sequence from the Plasmid [redacted] T-DNA Region into the Maize Genome

The first transformation step utilized microprojectile co-bombardment with [redacted] plasmids ([redacted], and PHP21875) to insert the SSI landing pad sequence into a pre-selected integration site in the maize genome using [redacted] (Table 1; Figure 1 - Figure 4).

Following microprojectile co-bombardment, the *zm*-84CR1 guide RNA and [redacted] gene from plasmid [redacted] (Figure 2), the *zm-wus2* gene from plasmid [redacted] (Figure 3), and the *zm-odp2* gene from plasmid PHP21875 (Figure 4) were transiently expressed without integration into the maize genome. The *zm*-84CR1 guide RNA directed the [redacted] protein, an RNA-guided DNA endonuclease, to produce a double-stranded DNA break between the continuous and endogenous [redacted] and [redacted] sequences in the maize genome. These endogenous sequences are identical to the [redacted] and [redacted] sequences flanking the landing pad sequence in the [redacted] T-DNA (Figure 5). The landing pad was inserted into the maize genome by a cellular mechanism known as homology-directed repair (HDR). During HDR, crossovers (homologous recombination) occurred between the [redacted] and [redacted] sequences in the [redacted] T-DNA (Figure 5) and the identical endogenous [redacted] and [redacted] sequences in the maize genome, thus introducing the landing pad sequence into the maize genome at the targeted location. The introduced landing pad sequence consists of the *lox*P site, *ubi*ZM1 promoter region including 5' UTR and intron, FRT1 recombination target site, *nptII* gene, *pin*II terminator, and FRT87 recombination target site (Figure 5). The transient expression of the WUS protein from plasmid [redacted] and the ODP2 protein from plasmid PHP21875 allowed for the improved regeneration of maize plants from the transformation process.

Table 1 lists the relevant genetic elements used in this transformation step and indicates whether they are present in the final DP910521 maize event.

Maize plants were regenerated after transformation. A maize line that contained the expected landing pad sequence but did not contain unintended plasmid DNA sequences was selected and advanced to the next step in the transformation process.

Second Transformation Step: Site-Specific Integration of Trait Gene Cassettes from the Plasmid PHP79620 Recombination Fragment Region into the DP910521 Maize Genome

The second transformation step used to create DP910521 maize utilized microprojectile co-bombardment with [redacted] plasmids (PHP79620, PHP5096, PHP21875, PHP73572) to insert the trait genes from PHP79620 into the landing pad (Table 2; Figure 6, Figure 7, Figure 4, and Figure 8). The FLP recombinase encoded by the *mo-Flp* gene in PHP5096 (Figure 7) exchanged the *nptII* gene and *pin*II terminator in the landing pad for the intended trait gene cassettes between the FRT1 and FRT87 recombination sites from PHP79620 (referred to as PHP79620 recombination fragment region, Figure 9) to result in the intended insertion. Following transformation, the *mo-Flp* gene from plasmid PHP5096 (Figure 7), the *zm-odp2* gene from plasmid PHP21875 (Figure 4), and the *zm-wus2* gene from plasmid PHP73572 (Figure 8) are transiently expressed without integration into the maize genome. The flippase recombinase exchanges the *nptII* gene and *pin*II terminator, located between the FRT1 and FRT87 sites in the landing pad, for the *cry*1B.34*, mo-pat,* and *pmi* gene cassettes between the FRT1 and FRT87 sites in PHP79620, therefore allowing for the utilization of the *ubi*ZM1 promoter region in the landing pad to facilitate the expression of the *pmi* gene used for selection. The transient expression of WUS2 and ODP2 allows for improved regeneration of maize plants from the transformation process.

Table 2 lists the relevant genetic elements within the plasmid PHP79620 recombination fragment region, as well as other elements from PHP5096, PHP21875, and PHP73572 relevant to the transformation step, and indicates whether they are present in the final DP910521 maize event (Figure 10).

Maize plants were regenerated after transformation and molecular characterization was conducted. A maize line that contained the intended DNA insertion but did not contain unintended plasmid DNA sequences was selected and advanced to the next step in the event development process.

In summary, DP910521 maize is a genetically modified event wherein [redacted] has been used to insert the landing pad sequence. The SSI landing pad sequence was incorporated into the pre-selected insertion location in the maize genome by HDR; then the intended expression cassettes were further inserted into the SSI landing pad through recombination. It is worthwhile to note that gene edited organisms, for example, by a CRISPR system, are not always counted as genetically modified organisms (GMOs).

Table 1. List of Genetic Elements in Plasmids Used for Landing Pad Transformation and their Presence in DP910521 Maize

Plasmid	Genetic element	Description	Present in DP910521
[redacted] (landing pad)	[redacted]	Genomic recognition site for HDR	Yes*
	*lox*P	Cre recombination site	Yes
	*ubi*ZM1	Promoter region	Yes
	FRT1	Flippase recombination target site	Yes
	nptII	Neomycin phosphotransferase II gene	No
	*pin*II terminator	Terminator	No
	FRT87	Flippase recombination target site	Yes
	[redacted]	Genomic recognition site for HDR	Yes*
[redacted]	[redacted] exons 1 and 2	[redacted] nuclease gene	No
	zm-84CR1	Guide RNA	No
[redacted]	*zm-wus2*	Developmental gene for regeneration	No
PHP21875	*zm-odp2*	Developmental gene for regeneration	No

* As [redacted] and [redacted] are endogenous sequences in the maize genome, they are part of the maize genome and not the DP910521 insertion. Their role in [redacted] was targeting of the landing pad between the endogenous [redacted] and [redacted] sequences in the maize genome.

Table 2. List of Genetic Elements in Plasmid PHP79620 Recombination Fragment Region and Plasmids Used for SSI and their Presence in DP910521 Maize

Plasmid	Genetic element	Description	Present in DP910521
PHP79620 (trait genes)	FRT1	Flippase recombination target site	Yes
	pmi	Phosphomannose isomerase gene	Yes
	mo-pat	Phosphinothricin acetyltransferase gene	Yes
	*cry*1B.34	Insect protection protein gene	Yes
	FRT87	Flippase recombination target site	Yes
PHP5096	*mo-Flp*	Flippase recombinase gene	No
PHP21875	*zm-odp2*	Developmental gene for regeneration	No
PHP73572	*zm-wus2*	Developmental gene for regeneration	No

Figure 1. Map of Plasmid

Schematic diagram of plasmid indicating the . The size of plasmid is bp. The portion flanked by sequences, referred to as a "landing pad", was inserted into the maize genome during homology-directed repair (HDR) following a endonuclease-mediated double-stranded break. In the second transformation step, the region between the recombination sites was replaced by site-specific integration (SSI) with the intended *pmi, mo-pat,* and *cry*1B.34 gene cassettes from the plasmid PHP79620 recombination fragment region (Figure 9) that is flanked by the same FRT1 and FRT87 recombination sites.

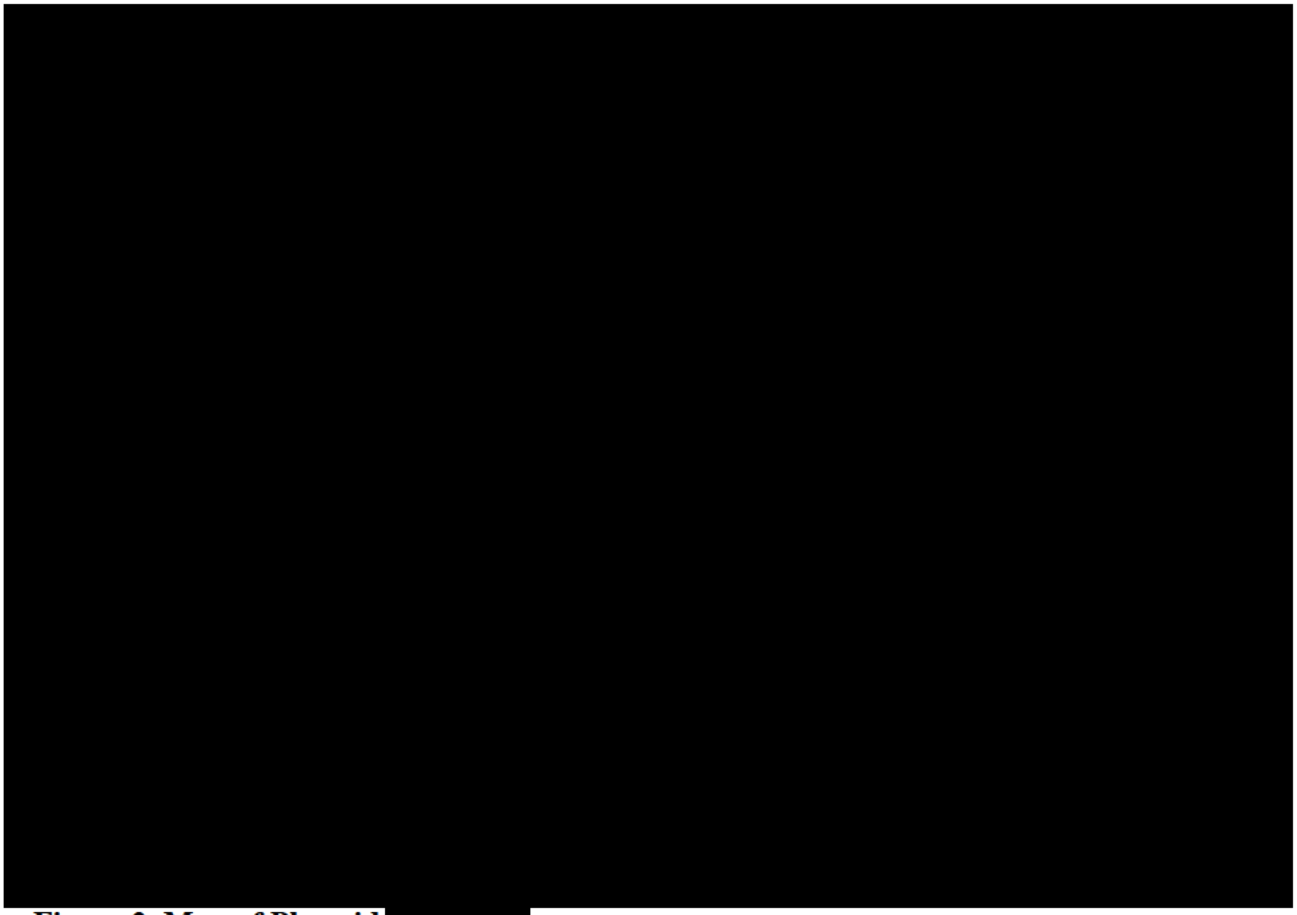

Figure 2. Map of Plasmid

Schematic diagram of plasmid indicating the gene cassette and cassette. The size of plasmid is bp.

Figure 3. Map of Plasmid

Schematic diagram of plasmid indicating the . The size of plasmid is bp. Plasmid

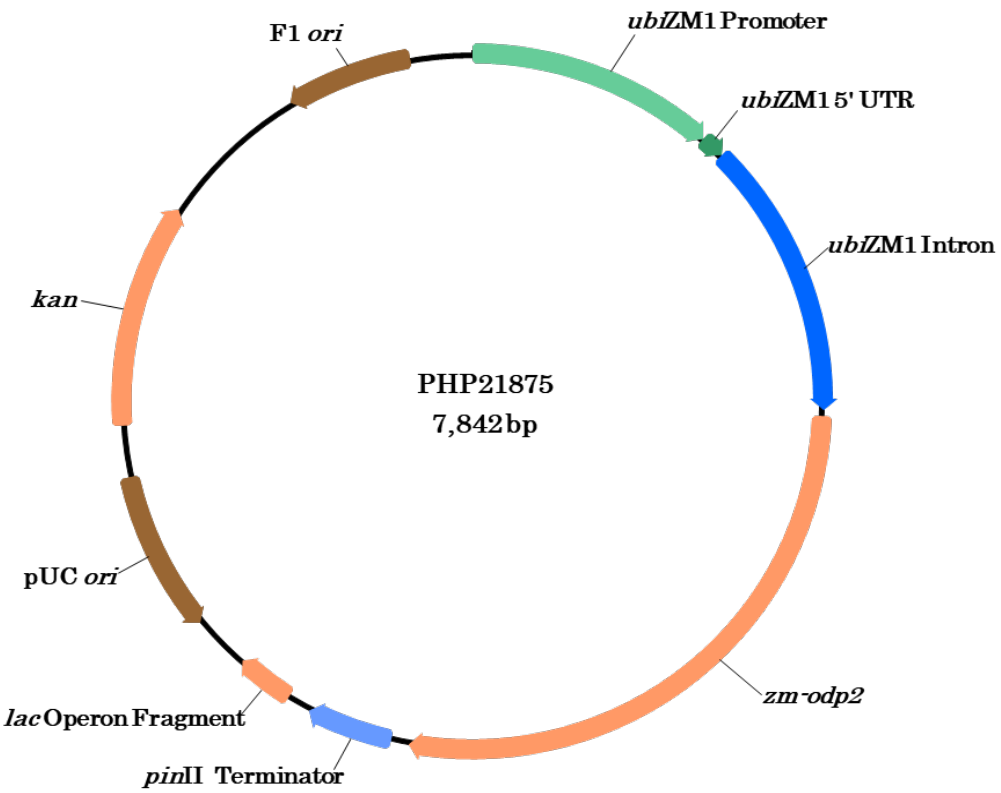

Figure 4. Map of Plasmid PHP21875

Schematic diagram of plasmid PHP21875 indicating the *zm-odp2* gene cassette. The size of plasmid PHP21875 is 7,842 bp. Plasmid PHP21875 was used in both transformation steps to enhance transformation and plant regeneration but was not incorporated into the genome of the maize.

Figure 5. Map of the T-DNA Region from Plasmid [redacted]

Schematic diagram of the T-DNA region from plasmid [redacted] indicating the *nptII* gene cassette, along with the [redacted], *lox*P, FRT1, FRT87, and [redacted] elements. The size of the T-DNA is 5,116 bp. The portion flanked by the [redacted] sequences, referred to as a "landing pad", was inserted into the maize genome during homology-directed repair (HDR) following a [redacted] endonuclease-mediated double-stranded break. In the second transformation step, the region between the FRT1 and FRT87 recombination sites was replaced by site-specific integration (SSI) with the intended *pmi*, *mo-pat*, and *cry*1B.34 gene cassettes from the plasmid PHP79620 recombination fragment region (Figure 9) that is flanked by the same FRT1 and FRT87 recombination sites.

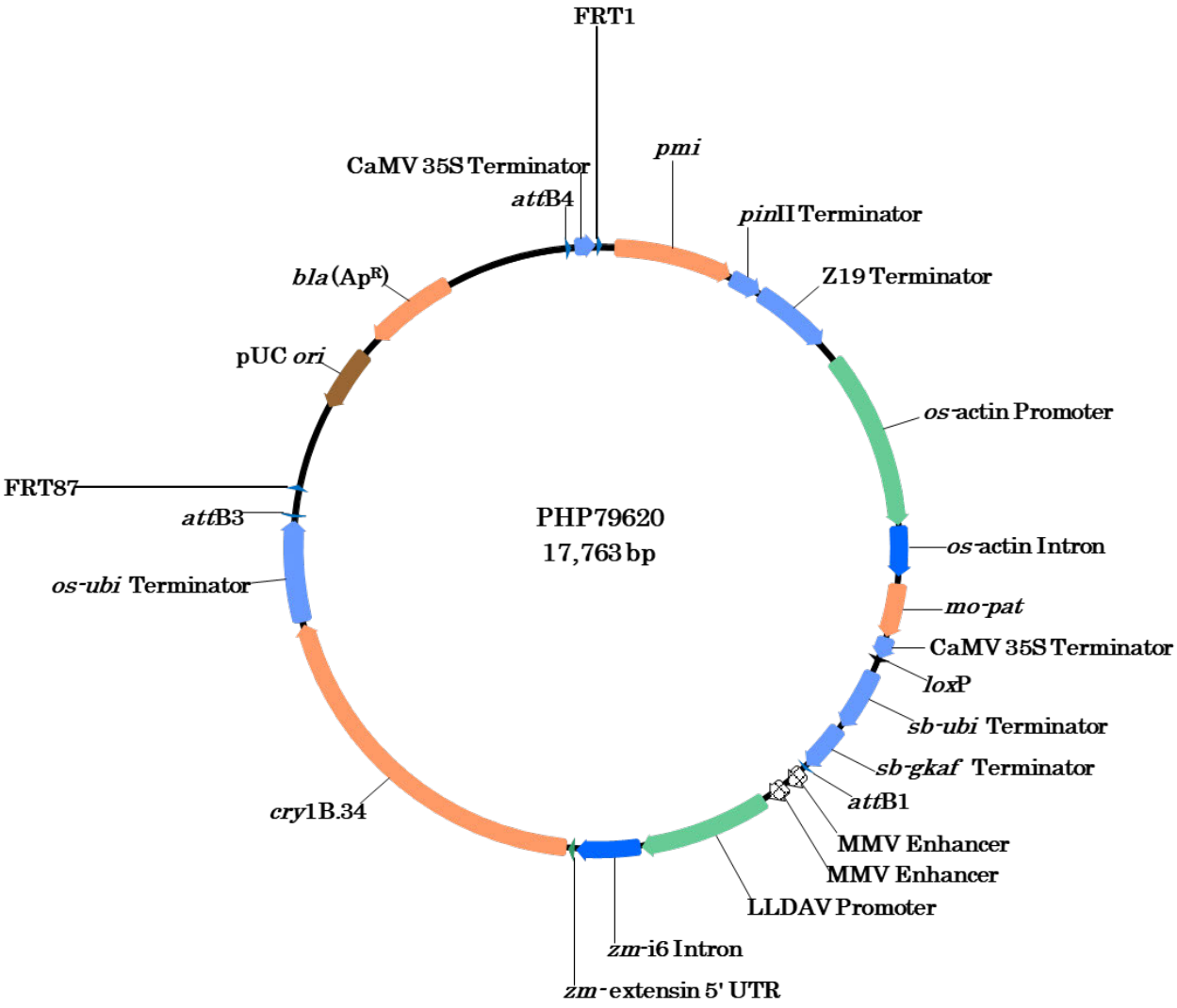

Figure 6. Map of Plasmid PHP79620

Schematic diagram of plasmid PHP79620 indicating the *pmi*, *mo-pat*, and *cry*1B.34 gene cassettes. The size of plasmid PHP79620 is 17,763 bp. The recombination fragment region flanked by the FRT1 and FRT87 recombination sites was inserted into the maize genome during microprojectile bombardment-mediated transformation.

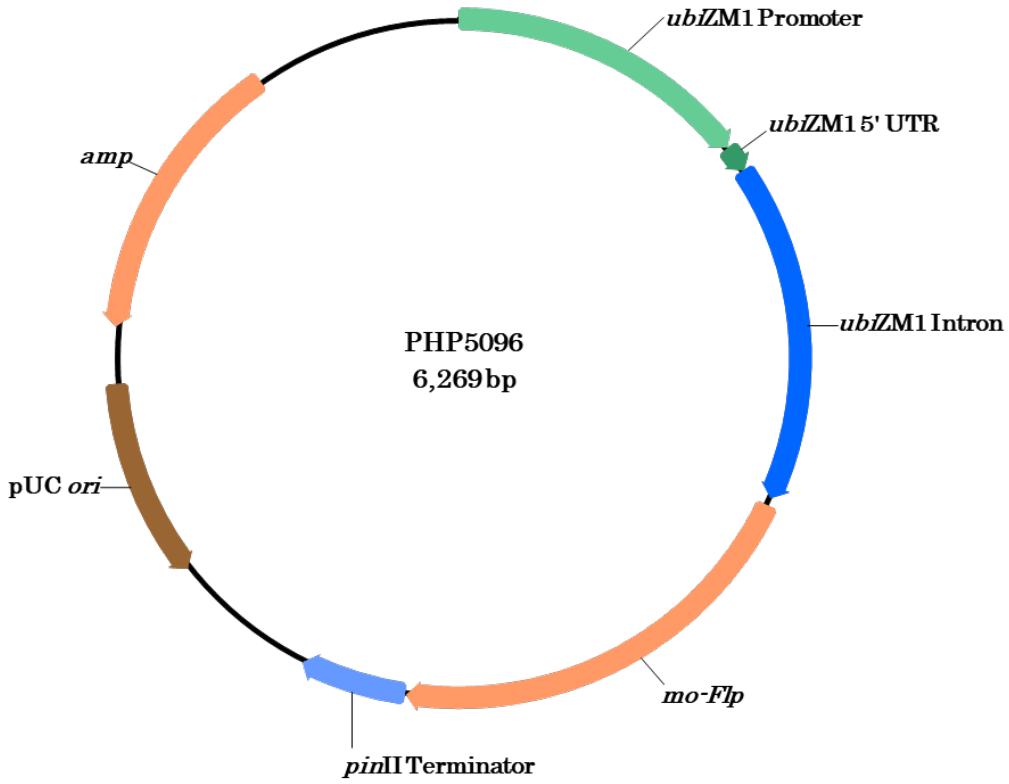

Figure 7. Map of Plasmid PHP5096

Schematic diagram of plasmid PHP5096 indicating the *mo-Flp* gene cassette. The size of plasmid PHP5096 is 6,269 bp. Plasmid PHP5096 was used during the second transformation step to express the FLP recombinase but was not incorporated into the maize genome. The FLP recombinase exchanged the *nptII* gene and *pin*II terminator in the landing pad for the intended trait gene cassettes between the FRT1 and FRT87 recombination sites from PHP79620 to result in DP910521 maize.

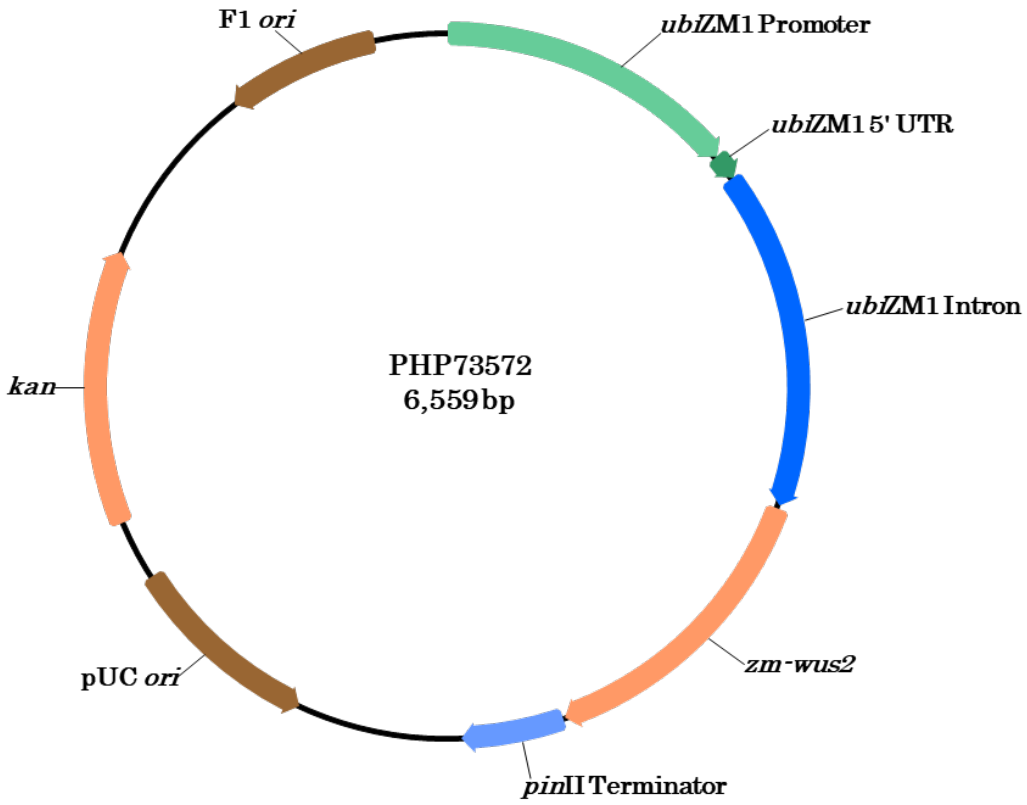

Figure 8. Map of Plasmid PHP73572

Schematic diagram of plasmid PHP73572 indicating the *zm-wus2* gene cassette. The size of plasmid PHP73572 is 6,559 bp. Plasmid PHP73572 was used during the second transformation step to enhance transformation and plant regeneration but was not incorporated into the genome of the maize.

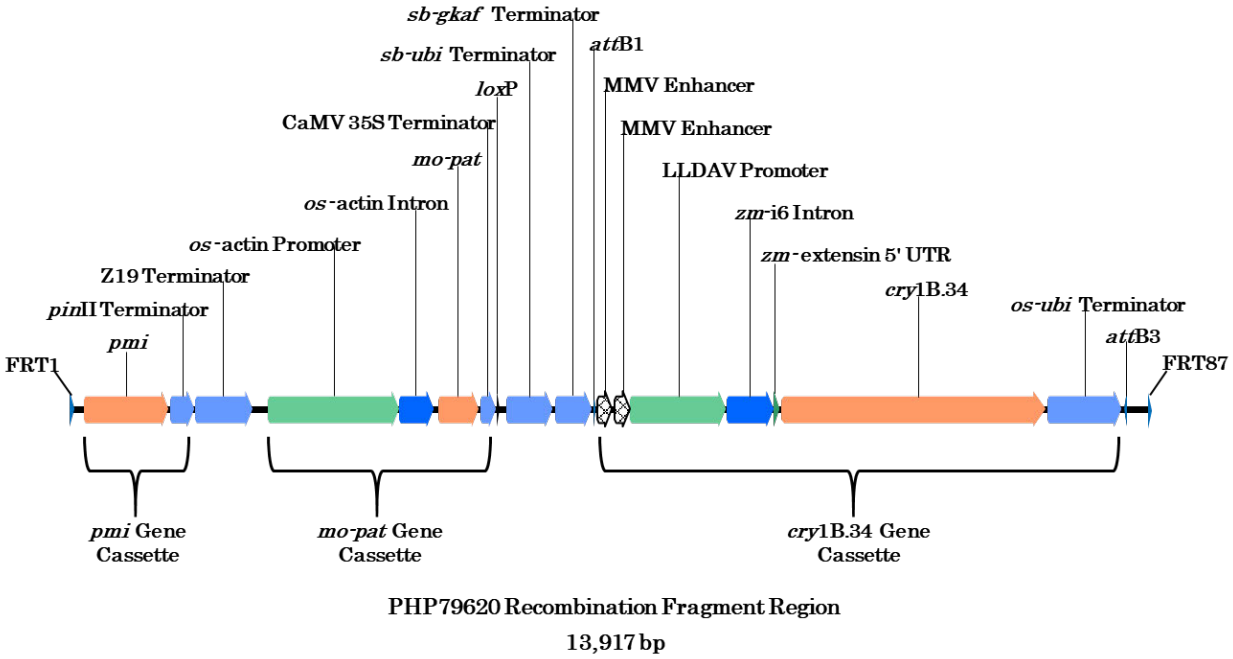

Figure 9. Map of the Recombination Fragment Region from Plasmid PHP79620

Schematic diagram of the PHP79620 recombination fragment region from plasmid PHP79620 indicating the *pmi*, *mo-pat*, and *cry*1B.34 gene cassettes. The size of the recombination fragment is 13,917 bp.

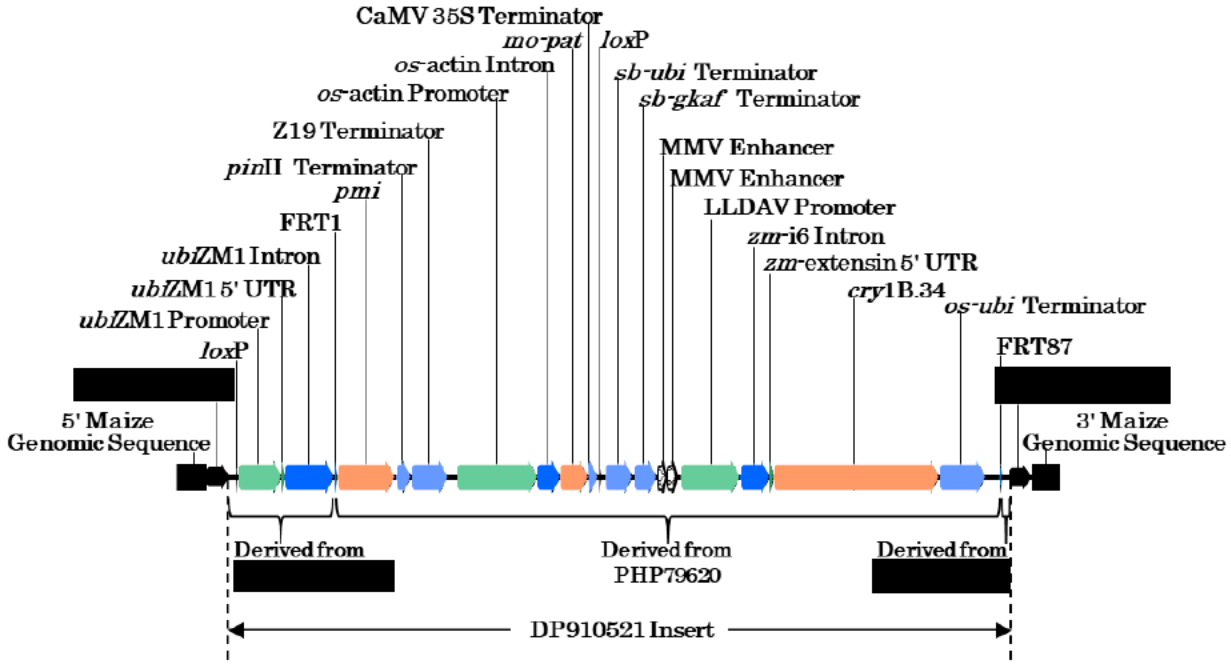

Figure 10. Map of the DP910521 Maize Insertion

Schematic diagram of the insertion in the DP910521 maize genome following SSI at the FRT1 and FRT87 recombination sites. The size of the inserted DNA in DP910521 maize is 16,269 bp, and it includes sequences from the PHP79620 recombination fragment region (Figure 9) and the [redacted] T-DNA (Figure 5). The flanking maize genomic regions are represented by horizontal black bars, and the vertical dash lines represent the junctions between the insertion and flanking maize genome. Although [redacted] are present in [redacted], they are derived from the maize genome and appear in their natural context in the chromosome, so are considered to be part of the flanking maize genome and are not included in the insertion.

Description of the Recombination Fragment Region of Plasmid PHP79620

The recombination fragment region of plasmid PHP79620 contains three gene cassettes (Figure 9) that are intended for incorporation into the DP910521 maize genome. Description of the gene cassettes included in the PHP79620 recombination fragment region is provided below. The PHP79620 recombination fragment region also contains the FRT1 and FRT87 recombination sites (Proteau *et al.*, 1986; Tao *et al.*, 2007 respectively) as well as the *lox*P (Dale and Ow, 1990), *att*B1 (Hartley *et al.*, 2000; Katzen, 2007), and *att*B3 sites (Cheo *et al.*, 2004). Summaries of the genetic elements within plasmid PHP79620 and the PHP79620 recombination fragment region are provided in Table 3 and Table 4, respectively.

The *pmi* gene cassette contains the phosphomannose isomerase (*pmi*) gene from *Escherichia coli* (Negrotto et al., 2000). The expressed PMI protein in plant tissue serves as a selectable marker during transformation which allows for tissue growth using mannose as the carbon source. The PMI protein is 391 amino acids in length and has a molecular weight of approximately 43 kDa. As present in the PHP79620 recombination fragment region, the *pmi* gene lacks a promoter, but its location next to the flippase recombination target site, FRT1, allows post-recombination expression by the promoter region from the maize ubiquitin gene 1 (*ubi*ZM1), including the 5' untranslated region (5' UTR) and intron, contained in the landing pad. The terminator for the *pmi* gene is the terminator region from the potato (*Solanum tuberosum*) proteinase inhibitor II (*pin*II) gene (An et al., 1989; Keil et al., 1986). One additional terminator is present between the first and second cassettes: the terminator region from the maize 19-kDa zein (Z19) gene (GenBank accession KX247647; Dong *et al.*, 2016). This additional terminator element is intended to prevent any potential transcriptional interference with the downstream cassettes. Transcriptional interference is defined as the transcriptional suppression of one gene on another when both are in close proximity (Shearwin et al., 2005). The placement of one or multiple transcriptional terminators between gene cassettes has been shown to reduce the occurrence of transcriptional interference (Greger et al., 1998).

The *mo-pat* gene cassette contains a maize-optimized version of the phosphinothricin acetyltransferase (*mo-pat*) gene from *Streptomyces viridochromogenes* (Wohlleben *et al.*, 1988) encoding the PAT protein. The expressed PAT protein confers tolerance to phosphinothricin. The PAT protein is 183 amino acids in length and has a molecular weight of approximately 21 kDa. Expression of the *mo-pat* gene is controlled by the promoter and intron region of the rice (*Oryza sativa*) actin (*os*-actin) gene (GenBank accession CP018159; GenBank accession EU155408.1), in conjunction with the 35S terminator region from the cauliflower mosaic virus genome (CaMV 35S terminator; Franck *et al.*, 1980; Guilley *et al.*, 1982). Two additional terminators are present between the second and third cassettes to prevent transcriptional interference: the terminator regions from the sorghum (*Sorghum bicolor*) ubiquitin (*sb-ubi*) gene (Phytozome gene ID Sobic.004G049900.1; (US Patent 9725731 Abbitt, 2017)) and γ-kafirin (*sb-gkaf*) gene (de Freitas et al., 1994), respectively.

The *cry*1B.34 gene cassette contains the *cry*1B.34 gene, a chimeric gene comprised of sequences from a *cry*1B-class gene, the *cry*1Ca1 gene, and the *cry*9Db1 gene, all derived from *Bacillus thuringiensis* (WO Patent 2016061197 Izumi Wilcoxon and Yamamoto, 2016)]; GenBank accession CAA30396.1; (US Patent 7541517 Flannagan and Abad, 2009), respectively). The expressed Cry1B.34 protein confers control of certain susceptible lepidopteran pests. The Cry1B.34 protein is 1,149 amino acids in length and has a molecular weight of approximately 129 kDa. Expression of the *cry*1B.34 gene is controlled by two copies of the enhancer region from

the mirabilis mosaic virus (MMV) genome (Dey and Maiti, 1999), the promoter region from the lamium leaf distortion-associated virus (LLDAV) genome (Zhang et al., 2008), the intron region from the maize translation initiation factor 6 (*zm*-i6) gene (Phytozome gene ID GRMZM2G318475; US Patent 10344290 Diehen *et al.*, 2019), and the 5′ untranslated region (UTR) from the maize extensin (*zm*-extensin) gene (GenBank accession NM001111947.2; UniProt accession P14918). The terminator for the *cry*1B.34 gene is the terminator region from the rice (*Oryza sativa*) ubiquitin (*os-ubi*) gene (Phytozome gene ID LOC_Os06g46770.1; Wang *et al.*, 2000).

Table 3. Description of the Genetic Elements in Plasmid PHP79620

Region	Location on Plasmid (bp to bp)	Genetic Element	Size (bp)	Description
Recombination Fragment	**1 – 13,917**		**13,917**	**See Table 4 for information on the elements in this region**
Plasmid Construct	**13,918 – 17,763**	**Includes Elements Below**	**3,846**	**DNA from various sources for plasmid construction and plasmid replication**
	14,704 – 15,292 (complementary)	pUC *ori*	589	Origin of replication from *Escherichia coli* pUC19 plasmid (GenBank accession KP700956.1; Yanisch-Perron *et al.*, 1985)
	15,463 – 16,323 (complementary)	*bla* (Ap^R)	861	β-lactamase (ampicillin resistance) gene from *Escherichia coli* (Sutcliffe, 1978; Yanisch-Perron *et al.*, 1985)
	17,455 – 17,475	*att*B4	21	Bacteriophage lambda integrase recombination site (Cheo *et al.*, 2004)
	17,555 – 17,748	CaMV 35S Terminator	194	35S terminator region from the cauliflower mosaic virus genome (Franck *et al.*, 1980; Guilley *et al.*, 1982)

Table 4. Description of the Genetic Elements in Recombination Fragment Region from Plasmid PHP79620

Gene Cassette	Location on Recombination Fragment (bp to bp)	Genetic Element	Size (bp)	Description
	1 – 48	FRT1	48	Flippase recombination target site from *Saccharomyces cerevisiae* (Proteau *et al.*, 1986)
	49 – 66	Intervening Sequence	18	DNA sequence used for cloning
pmi gene cassette	67 – 1,282	*pmi*	1,216	Phosphomannose isomerase gene from *Escherichia coli* including 5′ and 3′ untranslated regions (UTR) (Negrotto *et al.*, 2000) as described below: 5′ UTR at bp 67-70 (4 bp long) Coding sequence at bp 71-1,246 (1,176 bp long) 3′ UTR at bp 1,247-1,282 (36 bp long)
	1,283 – 1,292	Intervening Sequence	10	DNA sequence used for cloning
	1,293 – 1,603	*pin*II Terminator	311	Terminator region from the *Solanum tuberosum* (potato) proteinase inhibitor II gene (An *et al.*, 1989; Keil *et al.*, 1986)
	1,604 – 1,613	Intervening Sequence	10	DNA sequence used for cloning
	1,614 – 2,355	Z19 Terminator	742	Terminator region from the *Zea mays* 19-kDa zein gene (GenBank accession KX247647; Dong *et al.*, 2016)
	2,356 – 2,558	Intervening Sequence	203	DNA sequence used for cloning
mo-pat gene cassette	2,559 – 4,240	*os*-actin Promoter	1,682	Promoter region from the *Oryza sativa* (rice) actin gene (GenBank accession CP018159; GenBank accession EU155408.1)
	4,241 – 4,709	*os*-actin Intron	469	Intron region from the *Oryza sativa* (rice) actin gene (GenBank accession CP018159; GenBank accession EU155408.1)
	4,710 – 4,724	Intervening Sequence	15	DNA sequence used for cloning
	4,725 – 5,276	*mo-pat*	552	Maize-optimized phosphinothricin acetyltransferase gene from *Streptomyces viridochromogenes* (Wohlleben *et al.*, 1988)
	5,277 – 5,294	Intervening Sequence	18	DNA sequence used for cloning
	5,295 – 5,488	CaMV 35S Terminator	194	35S terminator region from the cauliflower mosaic virus genome (Franck *et al.*, 1980; Guilley *et al.*, 1982)

Table 4. Description of Genetic Elements in the Recombination Fragment Region from Plasmid PHP79620 (continued)

Gene Cassette	Location on Recombination Fragment (bp to bp)	Genetic Element	Size (bp)	Description
	5,489 – 5,509	Intervening Sequence	21	DNA sequence used for cloning
	5,510 – 5,543	*lox*P	34	Bacteriophage P1 recombination site recognized by Cre recombinase (Dale and Ow, 1990)
	5,544 – 5,639	Intervening Sequence	96	DNA sequence used for cloning
	5,640 – 6,223	*sb-ubi* Terminator	584	Terminator region from the Sorghum bicolor (sorghum) ubiquitin gene (Phytozome gene ID Sobic.004G049900.1; US Patent 9725731 Abbitt, 2017)
	6,224 – 6,264	Intervening Sequence	41	DNA sequence used for cloning
	6,265 – 6,728	*sb-gkaf* Terminator	464	Terminator region from the *Sorghum bicolor* (sorghum) γ-kafirin gene (de Freitas *et al.*, 1994)
	6,729 – 6,761	Intervening Sequence	33	DNA sequence used for cloning
	6,762 – 6,785	*att*B1	24	Bacteriophage lambda integrase recombination site from the Invitrogen Gateway® cloning system (Hartley *et al.*, 2000; Katzen, 2007)
	6,786 – 6,823	Intervening Sequence	38	DNA sequence used for cloning
*cry*1B.34 gene cassette	6,824 – 7,010	MMV Enhancer	187	Enhancer region from the mirabilis mosaic virus genome (Dey and Maiti, 1999)
	7,011 – 7,020	Intervening Sequence	10	DNA sequence used for cloning
	7,021 – 7,207	MMV Enhancer	187	Enhancer region from the mirabilis mosaic virus genome (Dey and Maiti, 1999)
	7,208 – 7,230	Intervening Sequence	23	DNA sequence used for cloning
	7,231 – 8,456	LLDAV Promoter	1,226	Promoter region from the lamium leaf distortion-associated virus genome (Zhang *et al.*, 2008)
	8,457 – 8,474	Intervening Sequence	18	DNA sequence used for cloning

Table 4. Description of Genetic Elements in the Recombination Fragment Region from Plasmid PHP79620 (continued)

Gene Cassette	Location on Recombination Fragment (bp to bp)	Genetic Element	Size (bp)	Description
*cry*1B.34 gene cassette (cont.)	8,475 – 9,078	*zm*-i6 Intron	604	Intron region from the *Zea mays* translation initiation factor 6 gene (Phytozome gene ID GRMZM2G318475; US Patent 10344290 Diehen *et al.*, 2019)
	9,079 – 9,084	Intervening Sequence	6	DNA sequence used for cloning
	9,085 – 9,151	*zm*-extensin 5' UTR	67	5' untranslated region from a *Zea mays* extensin gene (GenBank accession NM001111947.2; UniProt accession P14918)
	9,152 – 9,163	Intervening Sequence	12	DNA sequence used for cloning
	9,164 – 12,613	*cry*1B.34	3,450	Chimeric gene comprised of sequences from a *cry*1B-class gene, the *cry*1Ca1[1] gene, and the *cry*9Db1 gene, all derived from *Bacillus thuringiensis* (WO Patent 2016061197 Izumi Wilcoxon and Yamamoto, 2016); (GenBank accession CAA30396.1; US Patent 7541517 Flannagan and Abad, 2009), respectively) as described below: *cry*1B-class at bp 9,164 - 10,633(1,470 bp long) *cry*1Ca1 at bp 10,634 - 11,155 (522 bp long) *cry*9Db1 at bp 11,156 - 12,613 (1,458 bp long)
	12,614 – 12,619	Intervening Sequence	6	DNA sequence used for cloning
	12,620 – 13,569	*os-ubi* Terminator	950	Terminator region from the *Oryza sativa* (rice) ubiquitin gene (Phytozome gene ID LOC Os06g46770.1; Wang *et al.*, 2000)
	13,570 – 13,613	Intervening Sequence	44	DNA sequence used for cloning
	13,614 – 13,634 (complimentary)	*att*B3	21	Bacteriophage lambda integrase recombination site (Cheo *et al.*, 2004)
	13,635 – 13,869	Intervening Sequence	235	DNA sequence used for cloning
	13,870 – 13,917	FRT87	48	Modified flippase recombination target site derived from *Saccharomyces cerevisiae* (Tao *et al.*, 2007)

[1] Nomenclature defined according to Bacterial Pesticidal Protein Resource Center (www.bpprc.org; Crickmore *et al.*, 2021)

A.3(b) Description of the construct and the transformation vectors used

Please refer to Section *A.3 (a) Transformation Method* for the vectors used in transformation and to Table 3 for the description of the genetic elements in Plasmid PHP79620, Table 4 for the description of the genetic elements in recombination fragment region from Plasmid PHP79620, and to Figures 1-4; 6-8 for the maps of plasmids [redacted], PHP21875, PHP79620, PHP5096 and PHP73572, respectively.

A.3(c) Molecular characterisation

Characterization of the inserted DNA in DP910521 maize was conducted using a Next Generation Sequencing (NGS) method known as Southern-by-Sequencing (SbS™ technology, hereafter referred to as SbS) to determine the insertion copy number and organization within the plant genome and to confirm the absence of plasmid backbone and other unintended plasmid sequences. Southern blot analysis was performed to confirm stable genetic inheritance of the inserted *cry*1B.34, *mo-pat*, and *pmi* gene cassettes across multiple generations during the breeding process (see also *A.3 (e) Stability of the genetic changes*). Segregation analysis was conducted for five generations of DP910521 maize to confirm stable Mendelian inheritance (presented in *A.3 (e) Stability of the genetic changes*). Sanger sequencing was conducted to determine the DNA sequence of the DP910521 insert and flanking genomic regions. Based on the determined genomic border sequences, nucleotide (BLASTN) searches were performed to identify the genomic location of the insert and to determine if any endogenous genes were disrupted by the insert. Additionally, a bioinformatic safety assessment of translated stop-codon-bracketed frames within an insertion or crossing the boundary between an insertion and its genomic borders was conducted to evaluate for similarity to known and putative allergens and toxins. An event-specific quantitative real-time PCR method was developed and validated for detection of event DP-91Ø521-2 in maize.

Southern-by-Sequencing (SbS) Analysis to Determine Insertion Copy Number and Organization and Confirm the Absence of Plasmid Backbone and Other Unintended Plasmid Sequences (PHI-2021-045 study)

SbS analysis utilizes probe-based sequence capture, Next Generation Sequencing (NGS) techniques, and bioinformatics procedures to capture, sequence, and identify inserted DNA within the maize genome. By compiling a large number of unique sequencing reads and mapping them against the transformation plasmid and control maize genome, unique junctions due to inserted DNA are identified in the bioinformatics analysis and used to determine the insertion copy number and organization within the plant genome, and confirm the absence of plasmid backbone and other unintended plasmid sequences.

The SbS technique utilizes capture probes homologous to the transformation plasmid to isolate genomic DNA that hybridizes to the probe sequences (Zastrow-Hayes et al., 2015). Captured DNA is then sequenced using a Next Generation Sequencing (NGS) procedure and the results are analyzed using bioinformatics tools. During the analysis, junction reads are identified as those sequence reads where part of the read shows exact homology to the plasmid DNA sequence while the rest of the read does not match the contiguous plasmid. Junctions may occur between inserted DNA and genomic DNA, or between insertions of two plasmid-derived DNA sequences that are

not contiguous in the transformation plasmid. Multiple sequence reads are generated for each junction and are compiled into a consensus sequence for the junction. By compiling a large number of unique sequencing reads and comparing them to the transformation plasmid and control maize genome, unique junctions due to inserted DNA are identified. A unique junction is defined as one in which the adjacent sequences are the same across multiple reads, although the overall length of the multiple reads for that junction will vary due to the sequencing process. The number of unique junctions is related to the number of plasmid insertions present in the maize genome (for example, a single T-DNA insertion is expected to have two unique junctions). Detection of additional unique junctions beyond the two expected for a single insertion would indicate the presence of rearrangements or additional insertions derived from plasmid DNA. The absence of any junctions indicates there are no detectable insertions within the maize genome.

The segregating T1 generation of DP910521 maize was analyzed by SbS, using capture probes targeting all sequences of the trait plasmid PHP79620, the landing pad plasmid [redacted], and the helper plasmids [redacted], PHP21875, PHP73572, and PHP5096, to determine the insertion copy number and organization and to confirm the absence of plasmid backbone and other unintended plasmid sequences. SbS was also performed on one PH184C control maize plant, and on positive control samples for each plasmid, to confirm that the assay could reliably detect plasmid DNA spiked into control maize genomic DNA at a level equivalent to one copy of plasmid per genome copy. Based on the results obtained for DP910521 maize, a schematic diagram of the DP910521 insertion was developed and is provided in Figure 11.

Several genetic elements in the plasmids used in the positive control samples are derived from maize, and thus the homologous elements in the PH184C maize genome will be captured by the full-coverage probes used in the SbS analysis. These endogenous elements ([redacted]; *ubi*ZM1 promoter, 5′ UTR, and intron; [redacted]; Z19 terminator; *zm*-i6 intron; *zm*-extensin 5' UTR; [redacted]; Table 5 and Figure 12 - Figure 15) will have sequencing reads in the SbS results due to the homologous elements in the PH184C maize genome. However, if no junctions are detected, these sequencing reads only indicate the presence of the endogenous elements in their normal context of the maize genome and are not from inserted DNA.

SbS analysis results for the control maize are shown in Figure 12 and the positive control samples are presented in Figure 13. Results from the segregating T1 generation of DP910521 maize are presented in Figure 14 - Figure 15 and Appendix A - Figures A1 to A5.

SbS Analysis of the PH184C Control Maize

Sequencing reads of the PH184C control maize were aligned to the intended insertion and plasmid maps (Figure 12); however, coverage was obtained only for the endogenous genetic elements derived from the maize genome. These sequence reads were due to capture and sequencing of these genetic elements in their normal context within the PH184C control maize genome (Table 5). Variation in coverage of the maize endogenous elements is due to sequence variations between the PH184C control maize and the maize varieties from which the genetic elements in the plasmids were derived. No junctions were detected between plasmid sequences and the maize genome (Table 6), indicating that there are no plasmid DNA insertions in the control maize, and the sequence reads were solely due to the endogenous genetic elements present in the PH184C control maize genome.

SbS Analysis of the Positive Control Samples Containing Spiked-in Plasmid DNA

SbS analysis of the positive control samples resulted in sequence coverage across the entire length of each plasmid (Figure 13), indicating that the SbS assay utilizing the full-coverage probe library is sensitive enough to detect PHP79620, [redacted], PHP21875, PHP73572, or PHP5096 sequences at a concentration equivalent to one copy of plasmid per copy of the maize genome. No junctions were detected between plasmid and genomic sequences (Table 6), indicating that the sequence reads were due to either the spiked-in plasmid or the endogenous maize genetic elements that were detected in the PH184C control maize.

SbS Analysis of the T1 Generation of DP910521 Maize

SbS analysis of ten plants of the segregating T1 generation of DP910521 maize showed six positive plants that contained the inserted DNA (Table 6; Figure 14; and Appendix A - Figures A1 to A5). Each of these plants contained two unique genome-insertion junctions, one at each end of the insertion, that were identical across the six plants. The insertion, derived from PHP79620 and [redacted] starts with the 5′ junction at bp 1 and ends with the 3′ junction at bp 16,269 (Figure 11). The number of sequencing reads at the 5′ and 3′ junctions is provided in Table 6. There were no other junctions between the PHP79620, [redacted], PHP21875, PHP73572, or PHP5096 plasmid sequences and the maize genome detected in the plants, indicating that there are no additional plasmid-derived insertions present in DP910521 maize.

Alignments of the reads from the six positive plants to the seven plasmid maps (Figure 14 and Appendix A - Figures A1 to A5) show coverage of the genetic elements found in the intended insertion, along with coverage of the endogenous elements in the plasmids that were not incorporated into the insertion [redacted]). Reads also aligned to the *pin*II terminator elements located outside of the intended insertion regions in [redacted], PHP21875, PHP73572, and PHP5096 although these elements were not incorporated into the insertion. The NGS reads that aligned to these copies of the *pin*II terminator are from fragments containing the *pin*II terminator in the *pmi* cassette of the intended insertion; however, the reads from this single copy align to all copies of the *pin*II terminator in the plasmid maps. There were no unexpected junctions between non-contiguous regions of the intended insertion identified, indicating that there are no rearrangements, deletions, or duplications in the inserted DNA. Furthermore, there were no junctions between the unintended sequence of any of the plasmids involved in the production of DP910521 maize and maize genome sequences, demonstrating that no plasmid backbone or other unintended plasmid sequences were incorporated into DP910521 maize.

Each of the four DP910521 maize plants from the T1 generation that was determined to be negative for the DP910521 insertion yielded sequencing reads for the endogenous genetic elements derived from the maize genome (a representative plant is presented in Figure 15). There were no junctions between plasmid sequences and the maize genome detected in these plants, indicating that these plants did not contain any insertions derived from PHP79620, [redacted] PHP21875, PHP73572, or PHP5096.

SbS analysis of the T1 generation of DP910521 maize demonstrated that DP910521 maize contains a single copy of the inserted DNA derived from PHP79620 and [redacted], with the

expected organization, and that no additional insertions, plasmid backbone, or other unintended plasmid sequences are present in its genome.

Additional details regarding analytical methods for SbS analysis are provided in Appendix A.

Table 5. Maize Endogenous Elements in Plasmids and DP910521 Insertion

Number[a]	Name of Endogenous Element[b]	Present in Plasmid(s) or Insertion
1	[redacted]	[redacted]
2	*ubi*ZM1 promoter, 5′ UTR, and intron	[redacted], PHP21875, PHP73572, PHP5096, DP910521 insertion
3	[redacted]	[redacted]
4	Z19 terminator	PHP79620, DP910521 insertion
5	*zm*-i6 intron	PHP79620, DP910521 insertion
6	*zm*-extensin 5' UTR	PHP79620, DP910521 insertion
7	[redacted]	[redacted]
8	[redacted]	[redacted]
9	[redacted]	[redacted]
10	[redacted]	[redacted]
11	*zm-wus2*	[redacted], PHP73572
12	[redacted]	[redacted]
13	*zm-odp2*	PHP21875

[a] The numbers indicating endogenous genetic elements are shown as circled numbers found below the linear maps in Figure 12 and Figure 13 and Appendix A - Figures A1-A5.

[b] As shown in the plasmid and recombination fragment maps in Figure 1 to Figure 4 and Figure 6 to Figure 9 and the intended insertion map in Figure 10.

[c] [redacted] (Figure 10).

Table 6. SbS Junction Reads

Sample Description	Total Reads at 5′ Genomic Junction[a]	Unique Reads at 5′ Genomic Junction[b]	Total Reads at 3′ Genomic Junction[c]	Unique Reads at 3′ Genomic Junction[d]	DP910521 Insertion
T1 Generation Plant ID 404181697	0	0	0	0	-
T1 Generation Plant ID 404181698	1494	284	1326	373	+
T1 Generation Plant ID 404181699	0	0	0	0	-
T1 Generation Plant ID 404181700	920	213	697	216	+
T1 Generation Plant ID 404181701	0	0	0	0	-
T1 Generation Plant ID 404181702	0	0	0	0	-
T1 Generation Plant ID 404181703	1678	300	1148	343	+
T1 Generation Plant ID 404181704	1382	298	1262	341	+
T1 Generation Plant ID 404181705	1667	303	1269	332	+
T1 Generation Plant ID 404181706	1429	295	1310	321	+
PH184C Control Maize	0	0	0	0	-
PHP79620 Positive Control	0	0	0	0	-
[redacted] Positive Control	0	0	0	0	-
[redacted] Positive Control	0	0	0	0	-
PHP21875 Positive Control	0	0	0	0	-
PHP73572 Positive Control	0	0	0	0	-
[redacted] Positive Control	0	0	0	0	-
PHP5096 Positive Control	0	0	0	0	-

[a] Total number of sequence reads across the 5′ junction of the DP910521 insert.

[b] Unique sequence reads establishing the location of the 5′ genomic junction of the DP910521 insert (Figure 10). Multiple identical NGS-supporting reads are condensed into each unique read.

[c] Total number of sequence reads across the 3′ junction of the DP910521 insert.

[d] Unique sequence reads establishing the location of the 3′ genomic junction of the DP910521 insert (Figure 10). Multiple identical NGS-supporting reads are condensed into each unique read.

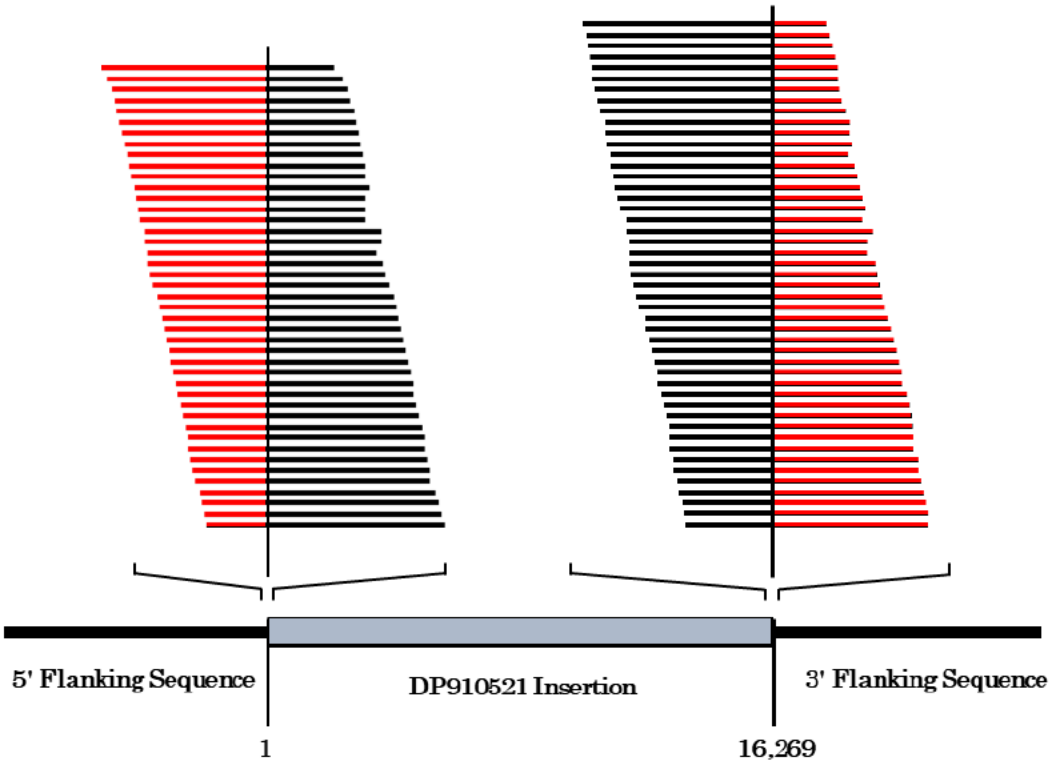

Figure 11. Schematic Diagram of the DP910521 Maize DNA Insertion

Schematic diagram of the DNA insertion in DP910521 maize based on the SbS analysis described. The flanking maize genomic regions, including [redacted], are indicated in the map by black bars. A single copy of the insertion, derived from PHP79620 and [redacted] and shown by the gray box, is integrated into the DP910521 maize genome. Vertical lines show the locations of the two unique genome-insertion junctions. The numbers below the map indicate the bp location of the junction nucleotide in reference to the sequence of the intended insertion (Figure 10). Representative individual sequencing reads across the junctions are shown as horizontally stacked lines above each junction (not to scale); red indicates genomic flanking sequence and black indicates inserted DNA sequence within each read.

A. Alignment to Intended Insertion

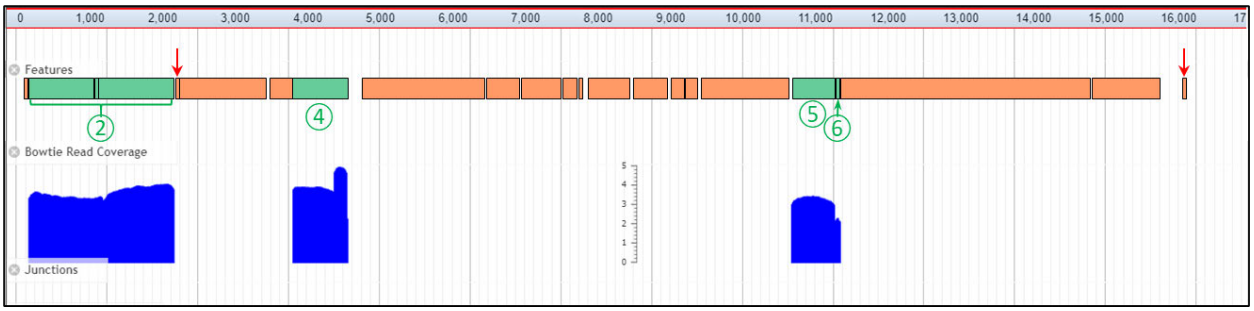

B. Alignment to PHP79620

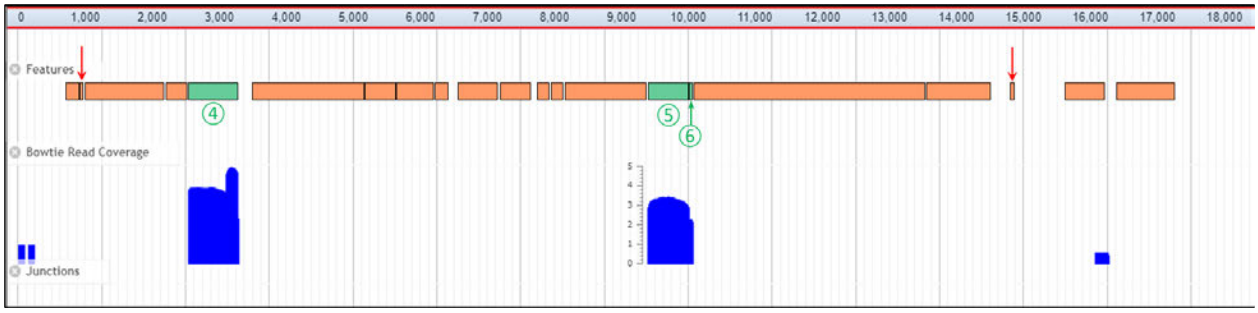

C. Alignment to [redacted]

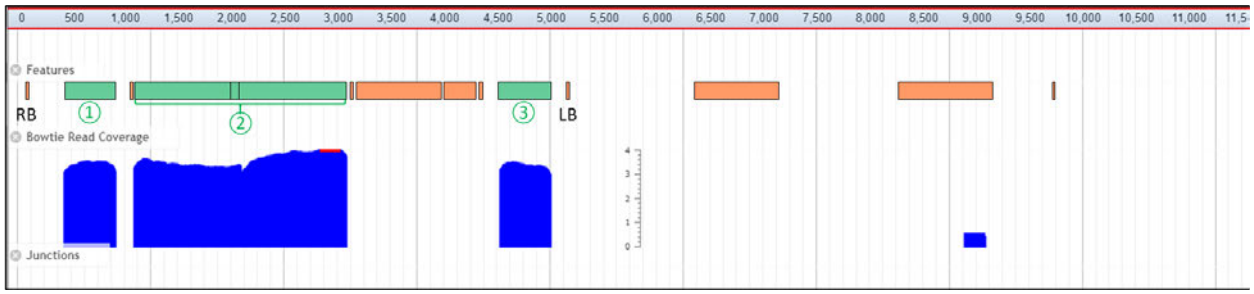

D. Alignment to [redacted]

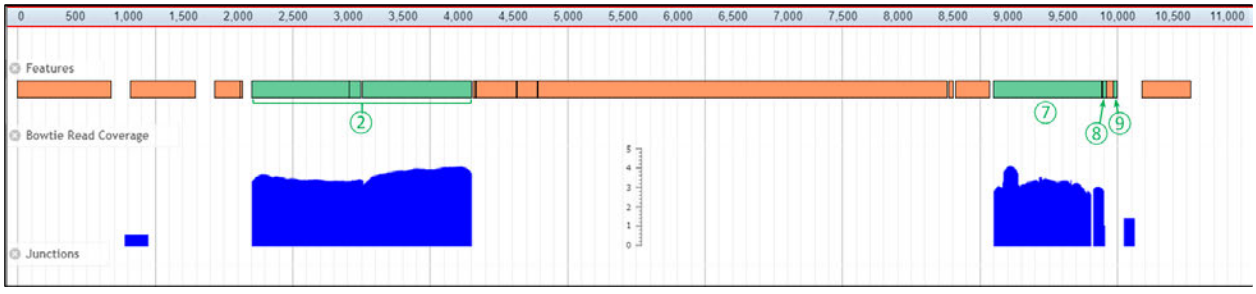

E. Alignment to [redacted]

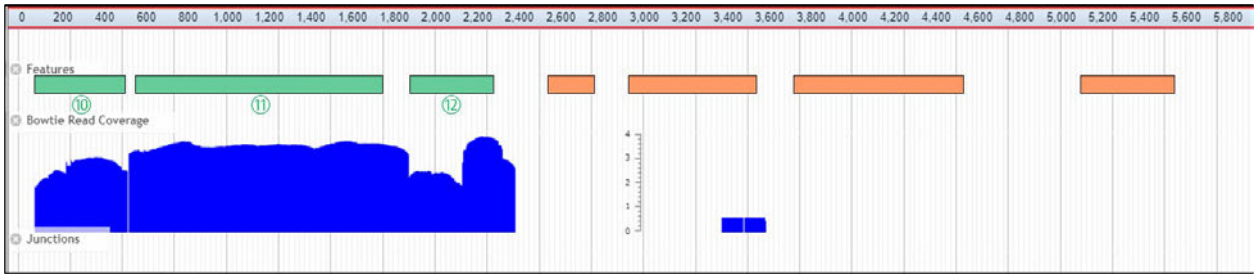

F. Alignment to PHP21875

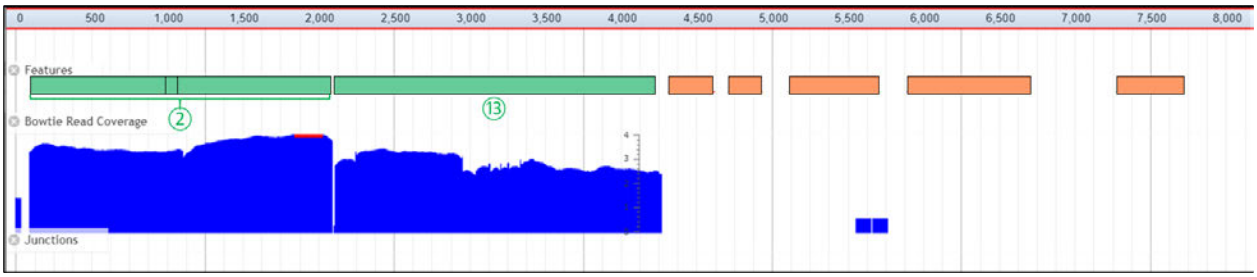

G. Alignment to PHP73572

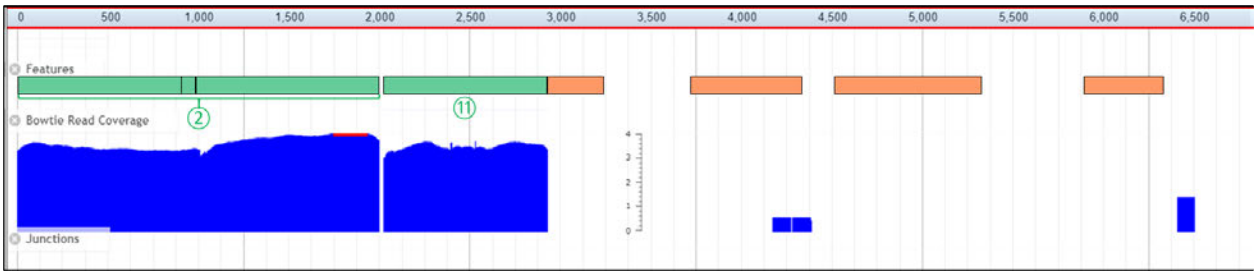

H. Alignment to PHP5096

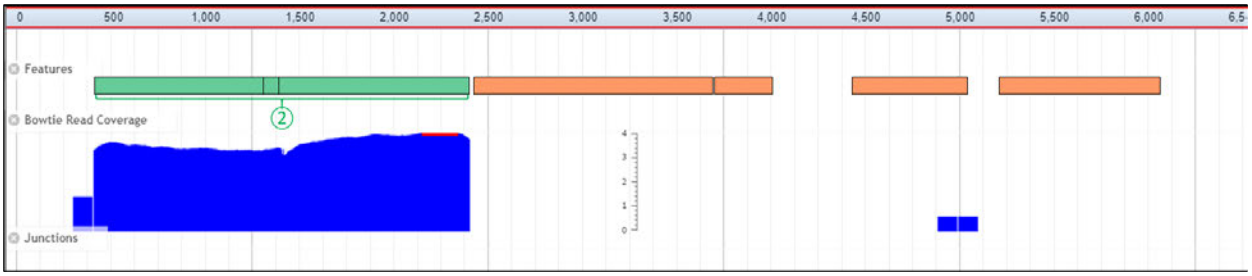

Figure 12. SbS Results for Control Maize

The blue coverage graph shows the number of individual NGS reads aligned at each point on the intended insertion or plasmid using a logarithmic scale at the middle of the graph. Green bars above the coverage graph indicate endogenous genetic elements in each plasmid derived from the maize genome (identified by numbers; Table 5), while tan bars indicate genetic elements derived from other sources. The absence of any junctions between plasmid and genomic sequences indicates that there are no insertions, plasmid

backbone, or other unintended plasmid sequences present in the PH184C control maize. FRT sites are indicated by red arrows. **A)** SbS results for PH184C control maize aligned against the intended insertion (16,269 bp; Figure 10). Coverage was obtained only for regions derived from maize endogenous elements. Variation in coverage of the endogenous elements is due to sequence variations between the control maize and the source of the corresponding genetic elements. As no junctions were detected between plasmid sequences and the maize genome, there are no DNA insertions identified in the PH184C control maize, and the sequence reads are solely due to the endogenous elements present in the PH184C genome. **B)** SbS results aligned against the plasmid PHP79620 sequence (17,763 bp; Figure 6). Coverage was obtained only for the endogenous elements. **C)** SbS results aligned against the plasmid [redacted] sequence [redacted] bp; Figure 1). Coverage was obtained only for the endogenous elements. **D)** SbS results aligned against the plasmid [redacted] sequence ([redacted] bp; Figure 2). Coverage was obtained only for the endogenous elements. **E)** SbS results aligned against the plasmid [redacted] sequence ([redacted] bp; Figure 3). Coverage was obtained only for the endogenous elements. **F)** SbS results aligned against the plasmid PHP21875 sequence (7,842 bp; Figure 4). Coverage was obtained only for the endogenous elements. **G)** SbS results aligned against the plasmid PHP73572 sequence (6,559 bp; Figure 8). Coverage was obtained only for the endogenous elements. **H)** SbS results aligned against the plasmid PHP5096 sequence (6,269 bp; Figure 7). Coverage was obtained only for the endogenous elements.

A. Alignment to PHP79620

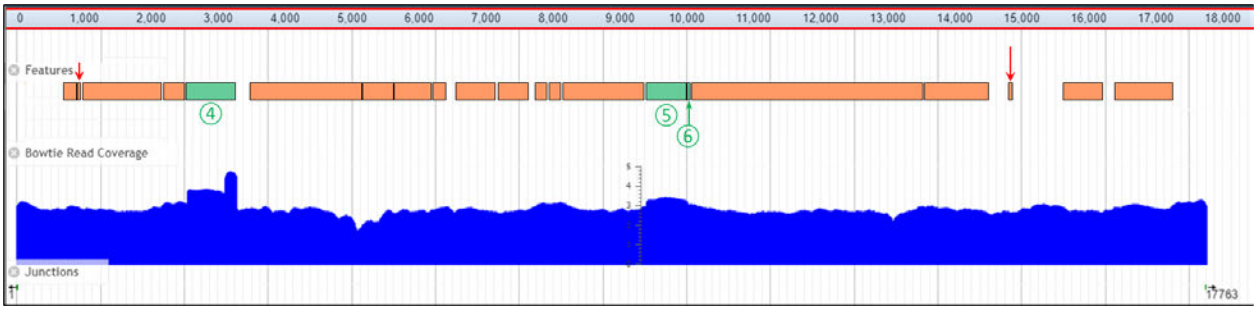

B. Alignment to [redacted]

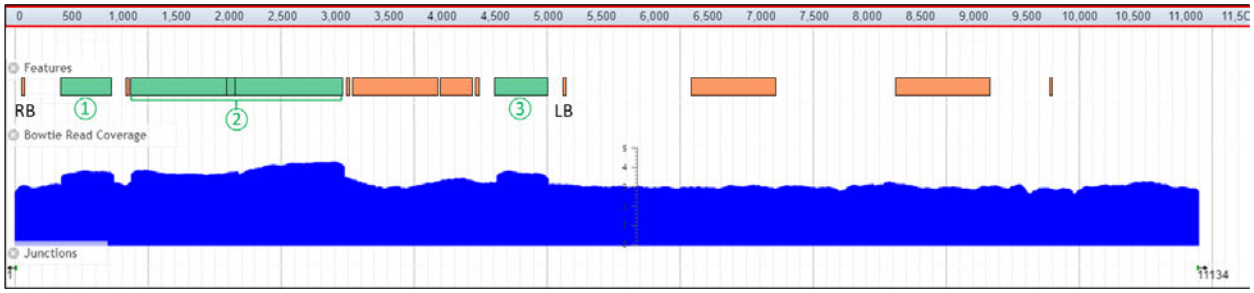

C. Alignment to [redacted]

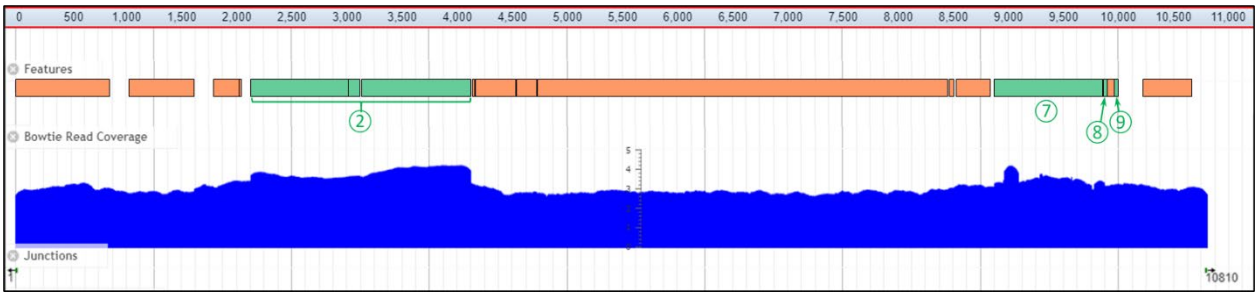

D. Alignment to [redacted]

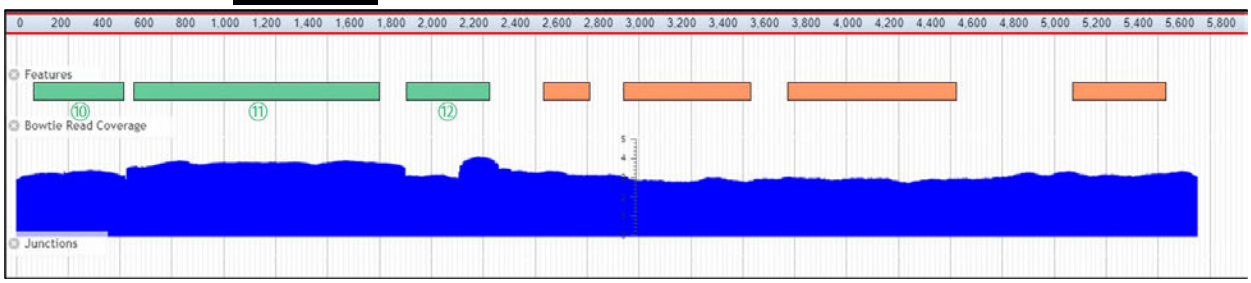

E. Alignment to PHP21875

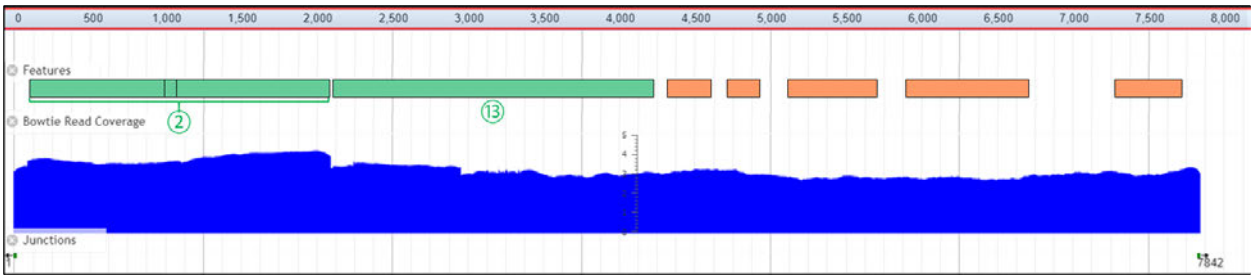

F. Alignment to PHP73572

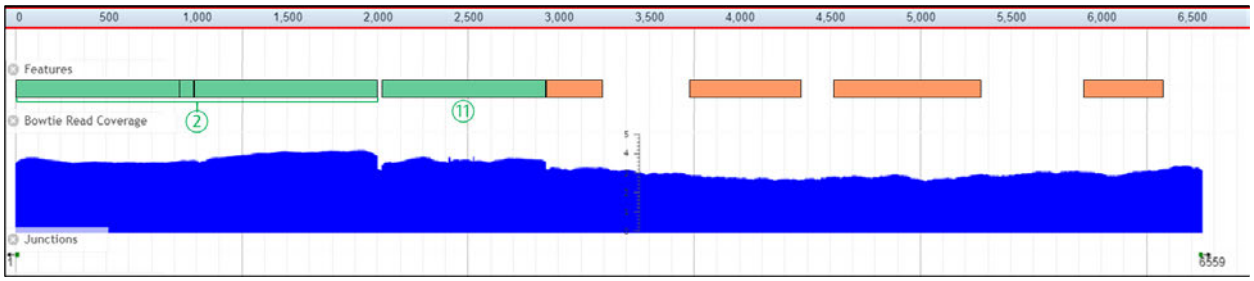

G. Alignment to PHP5096

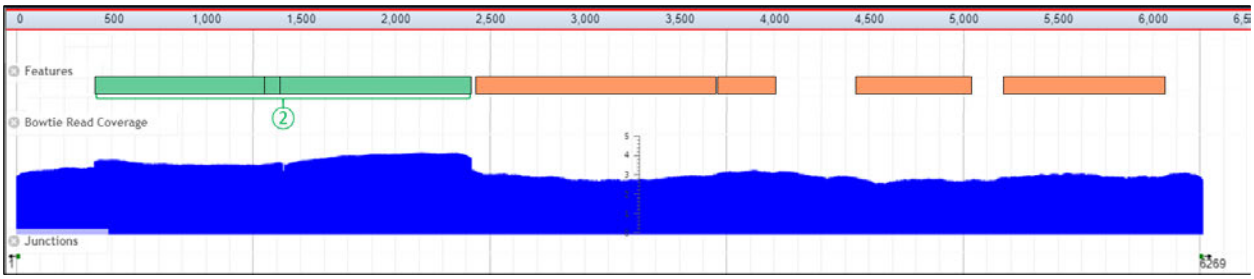

Figure 13. SbS Results for Positive Control Samples

The positive control samples consisted of separate control maize DNA samples individually spiked with each plasmid at a level corresponding to one copy of plasmid per copy of the maize genome. The blue coverage graph shows the number of individual NGS reads aligned at each point on the intended insertion or plasmid using a logarithmic scale at the middle of the graph. Green bars above the coverage graph indicate endogenous genetic elements in the plasmid derived from the maize genome (identified by numbers; Table 5), while tan bars indicate genetic elements derived from other sources. FRT sites are indicated by red arrows. Junctions shown at the bottom of the graphs are artifacts of mapping a circular plasmid to a linear map and show the start and end points of the plasmid sequence but do not indicate insertions in genomic DNA. **A)** SbS results of the PHP79620 positive control sample aligned against PHP79620 (17,763 bp; Figure 6). Coverage was obtained across the full length of the plasmid, indicating successful capture of PHP79620 sequences by the SbS probe library. **B)** SbS results of the [redacted] positive control sample aligned against [redacted] ([redacted] bp; Figure 1). Coverage was obtained across the full length of the plasmid, indicating successful capture of [redacted] sequences by the SbS probe library. **C)** SbS results of the [redacted] positive control sample aligned against [redacted] ([redacted] bp; Figure 2). Coverage was obtained across the full length of the plasmid, indicating successful capture of [redacted] sequences by the SbS probe library. **D)** SbS results of the [redacted] positive control sample

aligned against [redacted] [redacted] bp; Figure 3). Coverage was obtained across the full length of the plasmid, indicating successful capture of [redacted] sequences by the SbS probe library. **E)** SbS results of the PHP21875 positive control sample aligned against PHP21875 (7,842 bp; Figure 4). Coverage was obtained across the full length of the plasmid, indicating successful capture of PHP21875 sequences by the SbS probe library. **F)** SbS results of the PHP73572 positive control sample aligned against PHP73572 (6,559 bp; Figure 8). Coverage was obtained across the full length of the plasmid, indicating successful capture of PHP73572 sequences by the SbS probe library. **G)** SbS results of the PHP5096 positive control sample aligned against PHP5096 (6,269 bp; Figure 7). Coverage was obtained across the full length of the plasmid, indicating successful capture of PHP5096 sequences by the SbS probe library.

A. Alignment to Intended Insertion

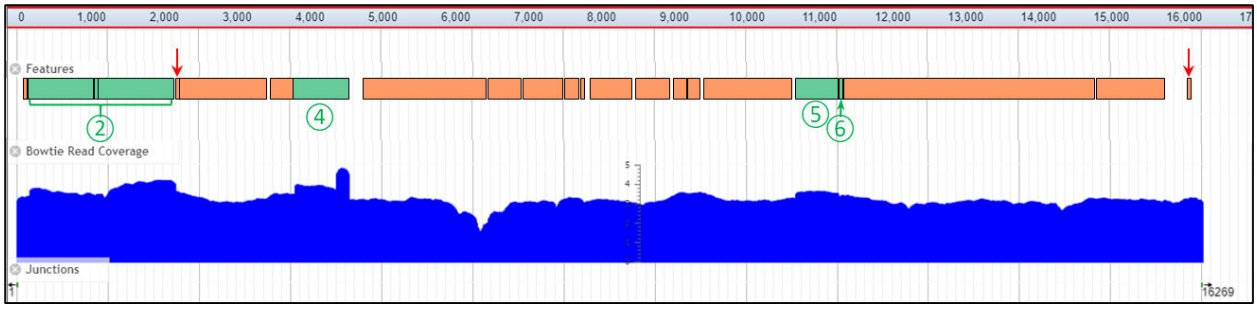

B. Alignment to PHP79620

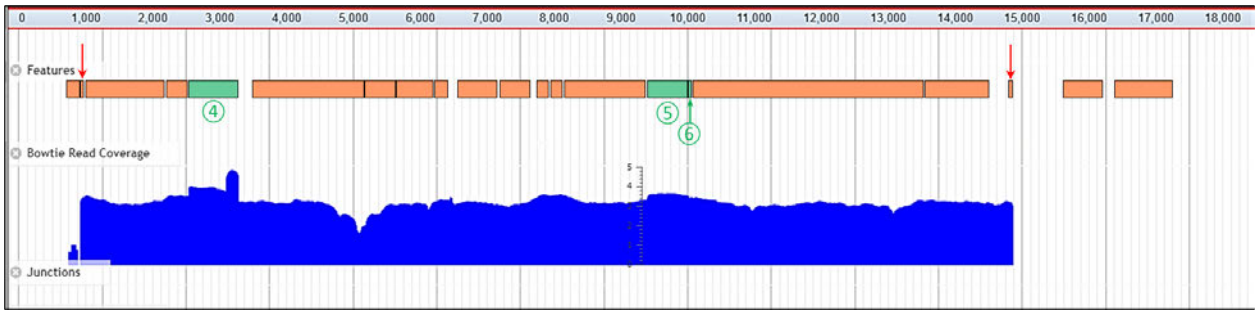

C. Alignment to [redacted]

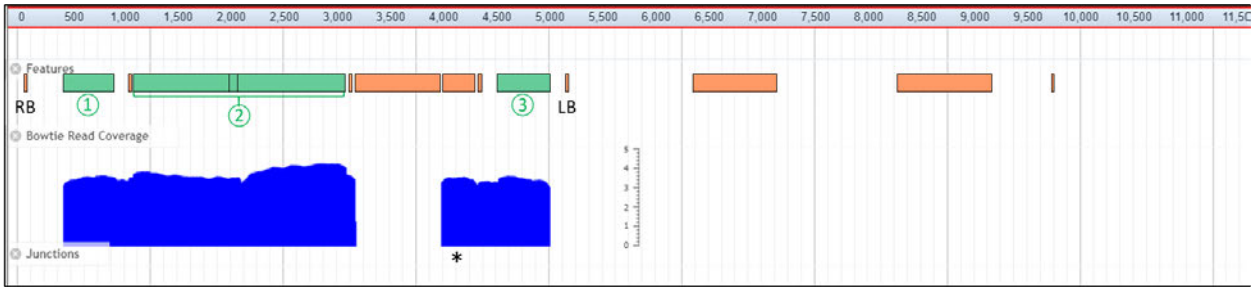

D. Alignment to [redacted]

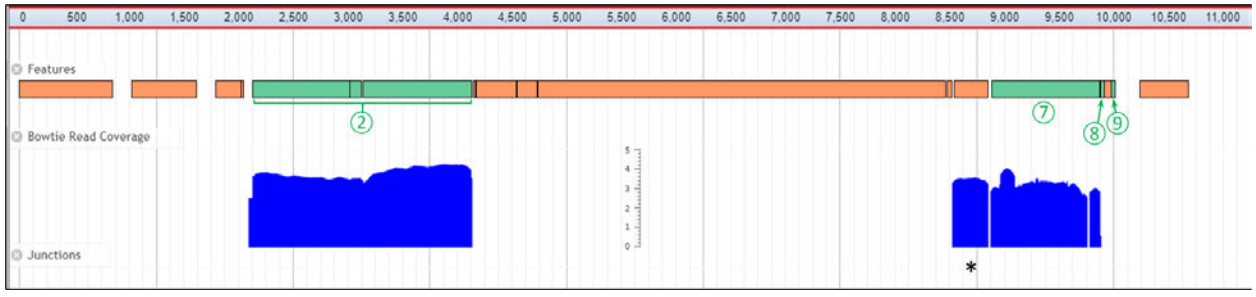

E. Alignment to [redacted]

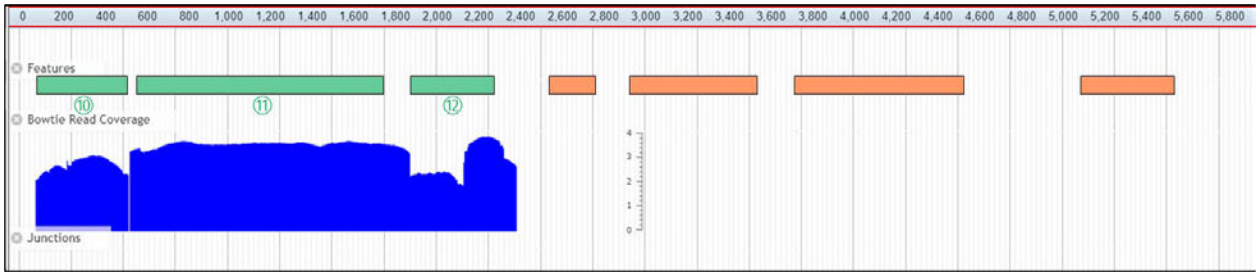

F. Alignment to PHP21875

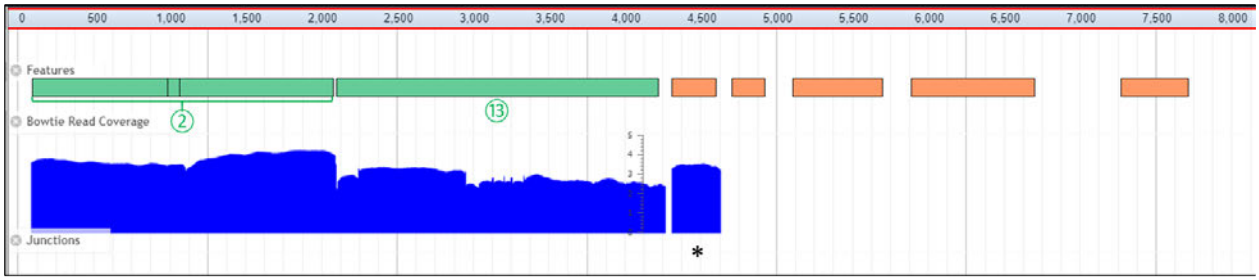

G. Alignment to PHP73572

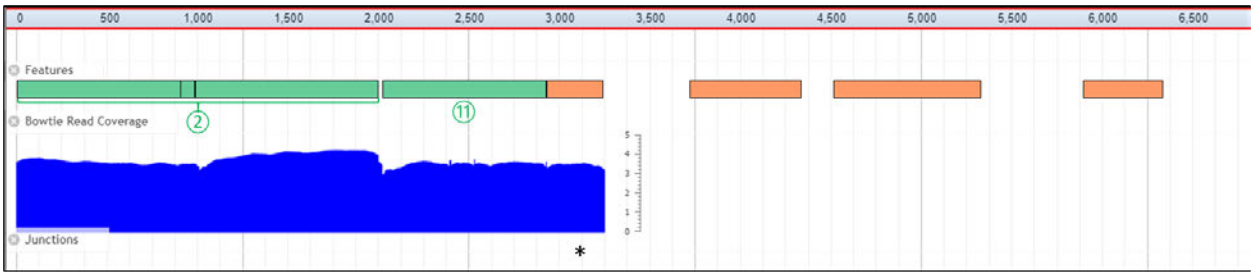

H. Alignment to PHP5096

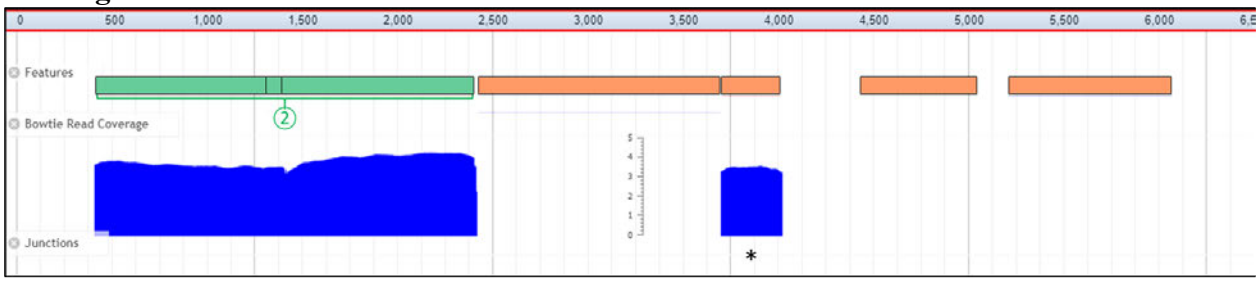

Figure 14. SbS Results for DP910521 Maize (Plant ID 404181698)

The blue coverage graph shows the number of individual NGS reads aligned at each point on the intended insertion or plasmid using a logarithmic scale at the middle of the graph. Green bars above the coverage graph indicate endogenous genetic elements in each plasmid derived from the maize genome (identified by numbers; Table 5), while tan bars indicate genetic elements derived from other sources. FRT sites are

indicated by red arrows. **A)** SbS results aligned against the intended insertion (16,269 bp; Figure 10), indicating that this plant contains the intended insertion. Arrows below the graph indicate the two plasmid-to-genome sequence junctions identified by SbS; the numbers below the arrows refer to the bp location of the junction relative to the intended insertion (Figure 10). The presence of only two junctions demonstrates the presence of a single insertion in the DP910521 maize genome. **B)** SbS results aligned against the plasmid PHP79620 sequence (17,763 bp; Figure 6). Coverage was obtained for the elements between FRT1 and FRT87 transferred into DP910521 maize (region between the red arrows at top of graph). **C)** SbS results aligned against the plasmid [redacted] sequence [redacted] bp; Figure 1). Coverage was obtained for [redacted], and the elements found in the intended insertion (between [redacted] to FRT1 and between FRT87 to [redacted]), along with the *pin*II terminator element (*) in [redacted] due to alignment of reads derived from the *pin*II terminator in the *pmi* cassette of the intended insertion to the copy of this element in [redacted]. **D)** SbS results aligned against the plasmid [redacted] sequence [redacted] bp; Figure 2). Coverage was obtained only for the endogenous elements along with the *pin*II terminator element (*). **E)** SbS results aligned against the plasmid [redacted] sequence [redacted] bp; Figure 3). Coverage was obtained only for the endogenous elements. **F)** SbS results aligned against the plasmid PHP21875 sequence (7,842 bp; Figure 4). Coverage was obtained for the endogenous elements along with the *pin*II terminator element (*). **G)** SbS results aligned against the plasmid PHP73572 sequence (6,559 bp; Figure 8). Coverage was obtained for the endogenous elements along with the *pin*II terminator element (*). **H)** SbS results aligned against the plasmid PHP5096 sequence (6,269 bp; Figure 7). Coverage was obtained for the endogenous elements along with the *pin*II terminator element (*). The absence of any junctions other than to the intended insertion indicates that there are no additional insertions, plasmid backbone, or other unintended plasmid sequences present in DP910521 maize.

A. Alignment to Intended Insertion

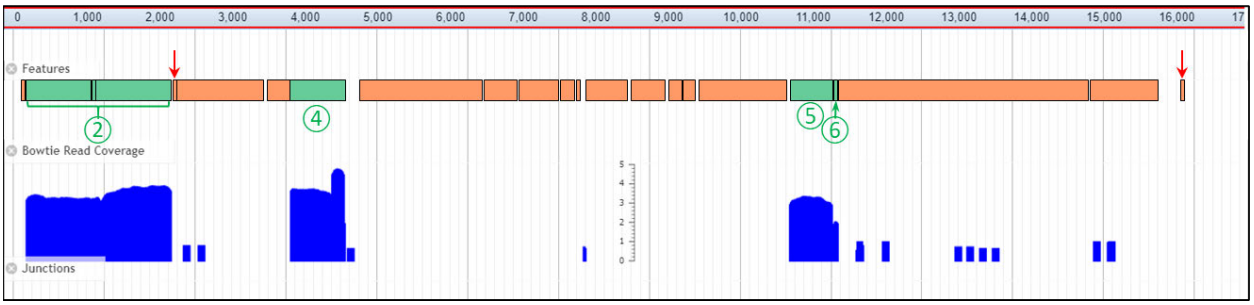

B. Alignment to PHP79620

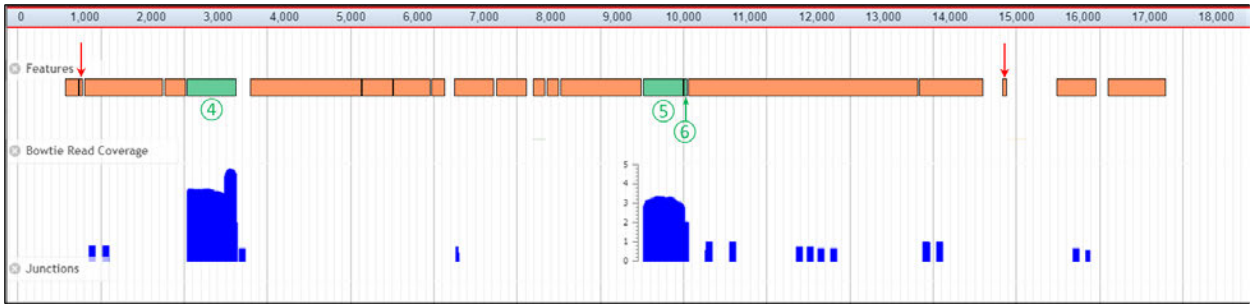

C. Alignment to [redacted]

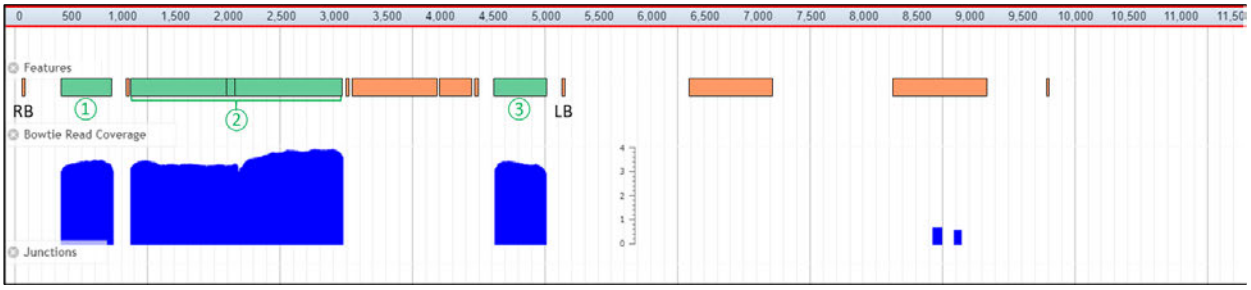

D. Alignment to [redacted]

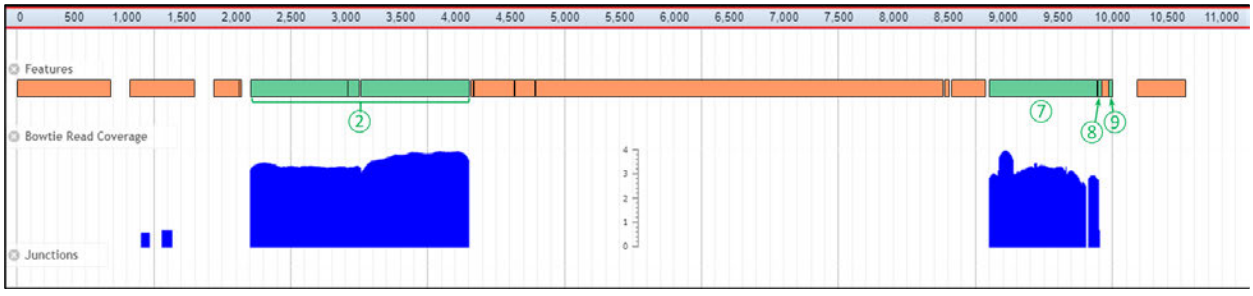

E. Alignment to [redacted]

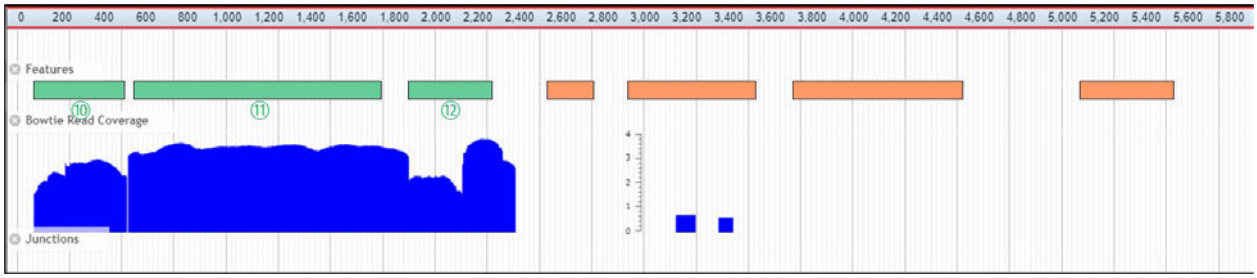

F. Alignment to PHP21875

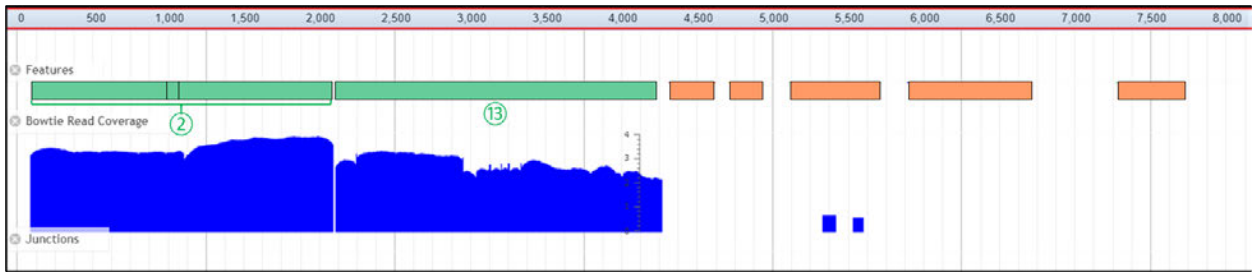

G. Alignment to PHP73572

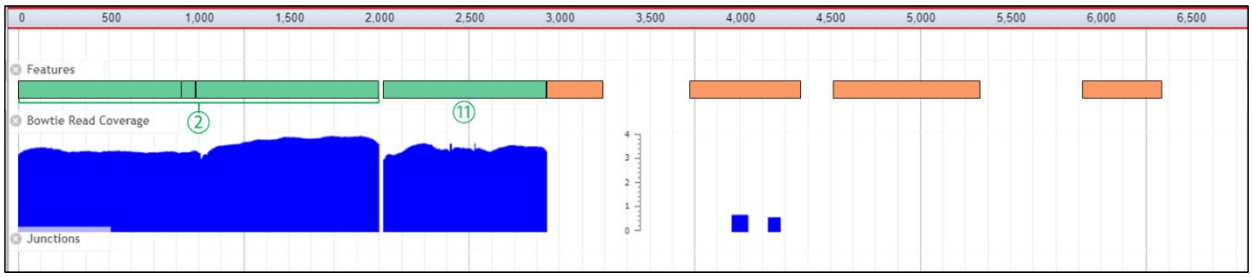

H. Alignment to PHP5096

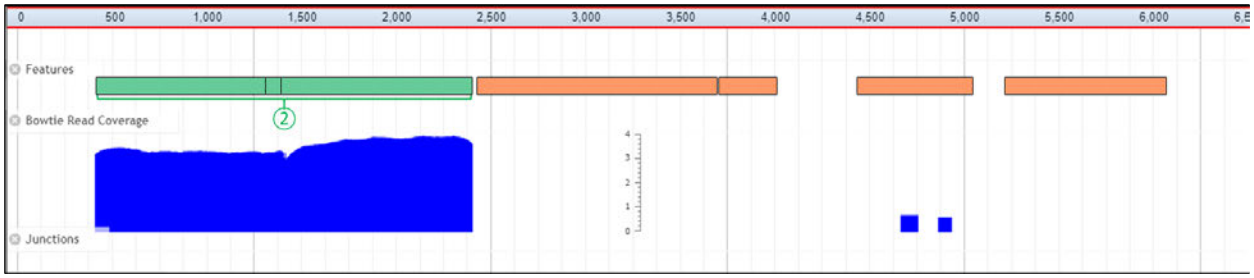

Figure 15. SbS Results for Representative Null Segregant Plant (Plant ID 404181702)

The blue coverage graph shows the number of individual NGS reads aligned at each point on the intended insertion or plasmid using a logarithmic scale at the middle of the graph. Green bars above the coverage graph indicate endogenous genetic elements in each plasmid derived from the maize genome (identified by numbers; Table 5), while tan bars indicate genetic elements derived from other sources. FRT sites are indicated by red arrows. The absence of any junctions between plasmid and genomic sequences indicates

that there are no insertions, plasmid backbone, or other unintended plasmid sequences present in this plant. **A)** SbS results aligned against the intended insertion (16,269 bp; Figure 9). Coverage was obtained only for regions derived from maize endogenous elements. As no junctions were detected between plasmid sequences and the maize genome, there are no DNA insertions identified in this plant, and the sequence reads are solely due to the endogenous elements present in the PH184C genome. **B)** SbS results aligned against the plasmid PHP79620 sequence (17,763 bp; Figure 6). Coverage was obtained only for the endogenous elements. **C)** SbS results aligned against the plasmid [redacted] sequence ([redacted] bp; Figure 1). Coverage was obtained only for the endogenous elements. **D)** SbS results aligned against the plasmid [redacted] sequence ([redacted] bp; Figure 2). Coverage was obtained only for the endogenous elements. **E)** SbS results aligned against the plasmid [redacted] sequence ([redacted] bp; Figure 3). Coverage was obtained only for the endogenous elements. **F)** SbS results aligned against the plasmid PHP21875 sequence (7,842 bp; Figure 4). Coverage was obtained only for the endogenous elements. **G)** SbS results aligned against the plasmid PHP73572 sequence (6,559 bp; Figure 8). Coverage was obtained only for the endogenous elements. **H)** SbS results aligned against the plasmid PHP5096 sequence (6,269 bp; Figure 7). Coverage was obtained only for the endogenous elements.

Sequence of Insert and Genomic Border Regions (PHI-2021-064 study)

Sequence characterization analysis was performed to determine the DNA sequence of the DP910521 insert and flanking genomic regions. It should be noted that while DNA sequencing provides certain molecular information, the exact nucleotide sequence should not be viewed as static. Spontaneous mutations are a very common phenomenon in plants, presenting a biological mechanism of adaptation to constantly changing environment (Weber et al., 2012). Spontaneous mutations can occur in any part of the plant genome and in both non-GM and GM plants (Waigmann et al., 2013). In GM plants, there is no scientific basis to expect that the frequency of spontaneous mutations in transgenic insert or flanking genomic regions would be greater than in the rest of the plant genome, or that they would have a differential impact on safety (La Paz et al., 2010; Waigmann et al., 2013).

The sequence of the DP910521 insert and flanking genomic regions was determined to confirm the integrity of the inserted DNA derived from [redacted] and PHP79620. PCR primers were designed to amplify six overlapping PCR products spanning the insert and the 5' and 3' flanking genomic regions (Figure 16). The overlapping consensus sequences from all PCR fragments were then used to assemble the final bi-directional consensus sequence for the entirety of the DP910521 insert and flanking genomic regions. The total length of sequence determined in DP910521 maize is 18,420 bp, comprised of 1,097 bp of the 5′ flanking genomic sequence, 1,054 bp of the 3′ flanking genomic sequence and 16,269 bp of inserted DNA.

The sequence of the DP910521 insert was compared with the intended landing pad sequence from plasmid [redacted] and the sequence from the PHP79620 recombination fragment region. The DP910521 insert was confirmed to have the expected sequences derived from both [redacted] and PHP79620.

Additional details regarding analytical methods for Sanger sequencing analysis are provided in Appendix D.

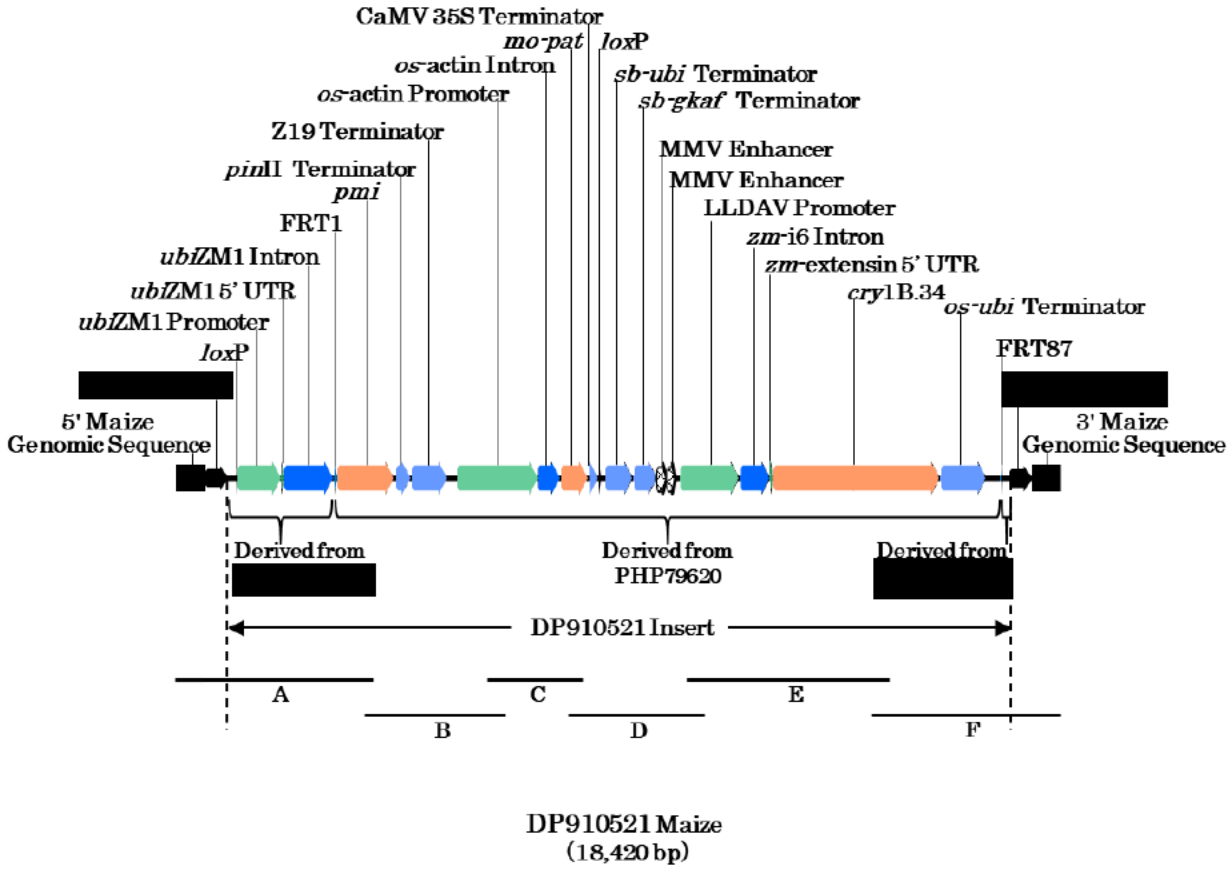

Figure 16. Map of the Insert and Flanking Genomic Regions Sequenced for DP910521 Maize

Six overlapping PCR fragments (**A**, **B**, **C**, **D**, **E**, and **F**) for the DP910521 insert and its flanking genomic regions were amplified from the genomic DNA of DP910521 maize. Each black horizontal bar represents the relative position of the PCR fragment, and the vertical dash lines represent the genomic border/insert junctions. The total length of the genomic sequence determined from the DP910521 maize is 18,420 bp, composed of 1,097 bp of the 5' flanking maize genomic sequence, 1,054 bp of the 3' flanking maize genomic sequence, and 16,269 bp of the inserted DNA (referred to as DP910521 insert) derived from both plasmids [redacted] and PHP79620.

Flanking Border Analysis (PHI-2021-194/230 study)

A bioinformatic assessment of the genomic border flanking the DP910521 maize insertion was conducted to determine the chromosomal location of the insertion and confirm there was no disruption of endogenous genes or regulatory elements. It should be noted that while bioinformatic assessment of the border flanking an insertion in a GM plant provides some molecular information, genes and regulatory elements may be disrupted or deleted in a plant without any safety risks. For example, genes are disrupted or deleted in conventionally bred plants, and it is the high plasticity of plant genomes that enables selective breeding for desired traits. Conventional breeding is generally regarded as safe, and the likelihood and risks of a gene disruption or deletion occurring in a GM plant is the same as in a conventionally bred plant (Herman *et al.*, 2011). Flanking border analysis confirmed the chromosomal location of the insertion and confirmed no known genes or regulatory elements were disrupted or deleted.

Detailed methods and results are provided in the PHI-2021-194/230 study.

Open Reading Frame Analysis of the Insert/Border Junctions (PHI-2021-195/225 study)

Assessing potentially-expressed peptides (i.e., translated stop codon-bracketed frames) within an insertion or crossing the boundary between an insertion and its genomic borders for similarity to known and putative allergens and toxins is a critical part of the weight-of-evidence approach used to evaluate the safety of genetically-modified plant products (Codex Alimentarius Commission, 2003). Here, a bioinformatics assessment of translated stop codon-bracketed frames was conducted following established international criteria (Codex Alimentarius Commission, 2003; EFSA, 2010; EFSA Panel on Genetically Modified Organisms (GMO), 2011; FAO/WHO, 2001). All translated stop codon-bracketed frames of length ≥ eight amino acids in the maize (*Zea mays* L.) event DP-91Ø521-2 (referred to as DP910521 maize) sequence that are within the insertion or that cross the boundary between the insertion and its genomic borders were identified and evaluated.

Nine hundred twenty-five (925) stop codon-bracketed frames ≥ eight amino acids were identified for the DP910521 maize sequence.

The allergen database used for the searches was the Comprehensive Protein Allergen Resource (COMPARE) 2021 database (January 2021), compiled through a collaborative effort of the Health and Environmental Sciences Institute (HESI) Protein Allergens, Toxins and Bioinformatics (PATB) Committee. This database is peer-reviewed and contains 2348 sequences.

Searches of the translated stop codon-bracketed frames of DP910521 maize against the COMPARE allergen database revealed seven (DP910521_224, DP910521_361, DP910521_364, DP910521_370, DP910521_728, DP910521_729, and DP910521_889) displaying > 35% identity with eleven known allergens over "sliding windows" of 80 amino acids. The DP910521_224 translated stop codon-bracketed frame showed 35.6% to 37.0% identity (*E*-values from 0.03 to 7.4) to a bovine collagen α2 chain type 1 precursor (1364 aa; GenBank Accession NP_776945.1), 36.3% to 37.8% identity (*E*-values from 6.8 to 10) to a parasitic fish worm Ani s 11-like protein 2 precursor (287 aa; GenBank Accession BAJ78222.1), and 36.1% identity (*E*-values from 15 to 94) to rainbow trout collagen alpha 2 chain (1356 aa; GenBank Accession BAB55663.1). The DP910521_361 translated stop codon-bracketed frame showed 36.3% identity (*E*-value = 0.00029) to allergen Der f 15, a chitinase from house dust mite (555 aa; GenBank Accession AAD52672.1),

36.3% identity (*E*-value = 0.012) to a group 15 allergen protein from house dust mite (558 aa; GenBank Accession AAY84564.2), 35.4% to 36.6% identity (*E*-values from 0.037 to 0.75) to allergen Alt a 4, a protein disulfide-isomerase (PDI) from *Alternaria alternata*, a fungus (436 aa; GenBank Accession Q00002.2), and 36.9% identity (*E*-value = 0.14) to villin 2 from tobacco (520 aa; GenBank Accession CAE17317.1). The DP910521_364 translated stop codon-bracketed frame showed 36.3% to 37.6% identity (*E*-values from 0.29 to 0.64) to a bovine collagen α2 chain type 1 precursor (1364 aa; GenBank Accession NP_776945.1) and 36.4% to 37.3% identity (*E*-values from 1.6 to 17) to a 7S globulin/vicilin-like protein from English walnut (593 aa; GenBank Accession AAF18269.1). The DP910521_370 translated stop codon-bracketed frame showed 36.3% identity (*E*-values from 0.13 to 0.21) to villin 2 from tobacco (520 aa; GenBank Accession CAE17317.1), 36.2% to 40.7% identity (*E*-values from 0.0002 to 0.0011) to a group 15 allergen protein from house dust mite (558 aa; GenBank Accession AAY84564.2), and 35.4% to 37.6% identity (*E*-values from 0.0022 to 0.0073) to allergen Der f 15, a chitinase from house dust mite (555 aa; GenBank Accession AAD52672.1). The DP910521_728 translated stop codon-bracketed frame showed 36.3% identity (*E*-value = 0.00013) to a putative ragweed homolog of Art v 1 (164 aa; GenBank Accession CBJ24286.1) and 36.3% identity (*E*-value = 0.00013) to an allergen also described as a putative ragweed homolog of Art v 1 (164 aa; GenBank Accession CBK52317.1). The DP910521_729 translated stop codon-bracketed frame showed 35.4% identity (*E*-values from 0.037 to 0.065) to blue lupin conglutin beta 5 (637 aa; GenBank Accession F5B8W3.1) and 35.1% to 37.0% identity (*E*-values from 25 to 93) to rainbow trout collagen alpha 2 chain (1356 aa; GenBank Accession BAB55663.1). The DP910521_889 translated stop codon-bracketed frame showed 35.8% to 36.3% identity (*E*-values from 3.2 to 6.9) to rainbow trout collagen alpha 2 chain (1356 aa; GenBank Accession BAB55663.1).

While transcription of the region where the DP910521_224 frame is located would be expected given an upstream promoter element that drives the *mo-pat* gene, the only methionine residue (start codon) in DP910521_224 lies 19 amino acids from the C-terminal of the theoretical peptide, making only translation of a very short peptide viable. In any event, one would expect preferential translation of the intended PAT protein in this region. Furthermore, the methionine residue lies well downstream of the region of the frame involved in the alignments to allergens, so even if an unlikely translation product were produced, it would not be implicated in any possible cross-reactivity. In general, the alignments between translated frame DP910521_224 and the allergens are made possible only by gaps and the large number of proline, arginine, and glycine identities. Additionally, the alignments exhibit both low-level percent identity (> 35% to < 38%) and moderate to very high *E*-values (0.03 to 94).

While transcription of the region where the DP910521_361 frame is located would be expected given an upstream promoter element that drives the *cry1B.34* gene, it contains no start codons to drive translation. In any event, one would expect preferential translation of the intended Cry1B.34 protein in this region. In general, the alignments between translated frame DP910521_361 and the allergens are made possible only by the large number of proline, threonine, and serine identities. Additionally, the alignments exhibit both low-level percent identity (> 35% to < 37%) and moderate *E*-values (0.00029 to 0.75).

While transcription of the region where the DP910521_364 frame is located would be expected given an upstream promoter element that drives the *cry1B.34* gene, it contains no start codons to drive translation. In any event, one would expect preferential translation of the intended Cry1B.34 protein in this region. In general, the alignments between translated frame DP910521_364 and the

allergens are made possible only by gaps and the large number of proline, arginine, glutamine, glutamic acid, and glycine identities. Additionally, the alignments exhibit both low-level percent identity (> 35% to < 38%) and moderate to high *E*-values (0.29 to 17).

While transcription of the region where the DP910521_370 frame is located would be expected given an upstream promoter element that drives the *cry1B.34* gene, it contains no start codons to drive translation. In any event, one would expect preferential translation of the intended Cry1B.34 protein in this region. In general, the alignments between translated frame DP910521_370 and the allergens are made possible only by gaps and the large number of serine and arginine identities. Additionally, the alignments exhibit both low-level percent identity (> 35% to < 41%) and moderate *E*-values (0.0002 to 0.21).

For DP910521_728, DP910521_729, and DP910521_889, there are no upstream promoter elements, making transcription extremely unlikely. DP910521_728 and DP910521_729 lack methionine residues, making translation extremely unlikely even in the event of transcription. DP910521_889 does possess several methionine residues, but the fact that it almost certainly cannot be transcribed renders the presence of those moot. In any event, the alignments between translated frame DP910521_889 and the rainbow trout allergen are made possible only by gaps and the large number of proline and glycine identities. Additionally, the alignments exhibit both low-level percent identity (> 35% to < 37%) and high *E*-values (3.2 to 6.9).

Collectively, the results of this bioinformatics analysis suggest that the alignments produced between these seven translated stop codon-bracketed frames and the allergens, when using an extremely conservative approach, are likely false positive hits without biological relevance and impart negligible risk of producing allergenic proteins. These data indicate that no allergenicity concerns arose from the alignments produced in the bioinformatics assessment of the translated stop codon-bracketed frames in DP910521 maize.

Three translated stop codon-bracketed frames (DP910521_99, DP910521_209, and DP910521_728) produced 8-contiguous amino acid matches to allergens in the COMPARE allergen database. Upon analysis of the matches produced in this bioinformatics assessment of the translated stop codon-bracketed frames in DP910521 maize, no allergenicity concerns arose.

No alignments with an *E*-value $\leq 10^{-4}$ were returned between a translated stop codon-bracketed frame and any protein sequence in an internal toxin database. Seventeen translated stop codon-bracketed frames produced alignments to proteins in the National Center for Biological Information (NCBI) non-redundant (nr) protein database with *E*-values $\leq 10^{-4}$. None of the sequence alignments are related to any known toxic proteins that are harmful to humans; while they do show expected alignments with non-toxic proteins, many are already present in the food and/or feed chain. Therefore, no toxicity concerns for humans arose from the bioinformatics assessment of the translated stop codon-bracketed frames in DP910521 maize.

Bioinformatics evaluation of the DP910521 insert did not generate biologically relevant amino acid sequence similarities to known allergens, toxins, or other proteins that would be harmful to humans.

Detailed methods and results are provided in the PHI-2021-195/225 study.

Event-Specific Detection Methodology (PHI-2021-104 study)

An event-specific quantitative real-time PCR method was developed and validated for detection of event DP-91Ø521-2 (referred to as DP910521) in maize. The event-specific assay for DP910521 maize is designed to amplify the target sequence at the 5' junction between the DP910521 maize insert and the maize genomic DNA. The binding site of the forward primer is within the maize genomic DNA, the binding site of the reverse primer is within the DP910521 maize insert, and the binding site of the probe spans the junction of the maize genomic DNA and the DP910521 maize insert. The event-specific PCR assay for DP910521 maize amplifies a 108-bp product.

Conclusions on the Characterization of the Inserted DNA in DP910521 Maize

SbS, Southern blot, and multi-generation segregation, Sanger sequencing of the insert and genomic border regions, and bioinformatic analyses of the flanking border and putative translated stop-codon-bracketed frames, were conducted to characterize the inserted DNA in DP910521 maize.

SbS analysis confirmed that DP910521 maize contains a single copy of the inserted DNA with the expected organization, and that no additional insertions, plasmid backbone, or other unintended plasmid sequences are present in DP910521 maize. As the data presented in *A.3 (e) Stability of the genetic changes*, Southern blot analysis of five generations of DP910521 maize confirmed that the inserted DNA in DP910521 maize is consistent and stable across multiple generations during the breeding process. Segregation analysis (presented in *A.3 (e) Stability of the genetic changes*) confirmed that the inserted DNA segregated as a single locus according to Mendelian rules of inheritance across five generations of DP910521 maize, and the stability of the insertion and of the herbicide tolerance phenotype was demonstrated in these populations.

Sanger sequencing analysis determined the sequence of the insert and flanking genomic regions in DP910521 maize. The total length of sequence determined in DP910521 maize is 18420 bp, composed of 1097 bp of the 5′ flanking genomic region, 1054 bp of the 3′ flanking genomic region, and 16269 bp of inserted DNA. Upon comparing the sequence of the DP910521 insert with the intended landing pad sequence from plasmid [redacted] and the sequence from the PHP79620 recombination fragment region, the DP910521 insert was confirmed to have the expected sequence derived from both [redacted] and PHP79620.

Together, these analyses confirmed that a single copy of the inserted DNA, with no plasmid backbone sequences or other unintended plasmid sequences, is present in the DP910521 maize genome. The introduced genes are stably inherited across multiple generations and segregated according to Mendel's law of inheritance during the breeding process. Nucleotide (BLASTN) searches of the genomic border flanking the DP910521 maize insertion confirmed the chromosomal location of the insertion and confirmed there was no disruption of endogenous genes. Bioinformatic safety evaluation of the translated stop-codon-bracketed frames at the DP910521 insertion site support the conclusion that there are no allergenicity or toxicity concerns for humans. Additionally, an event-specific quantitative real-time PCR detection method was developed and validated for detection of DP910521 maize.

A.3 (d) Breeding process

Plants that were regenerated from transformation and tissue culture (designated T0 plants) were selected for further characterization. A schematic overview of the transformation and event development process for DP910521 maize is provided in Figure 17.

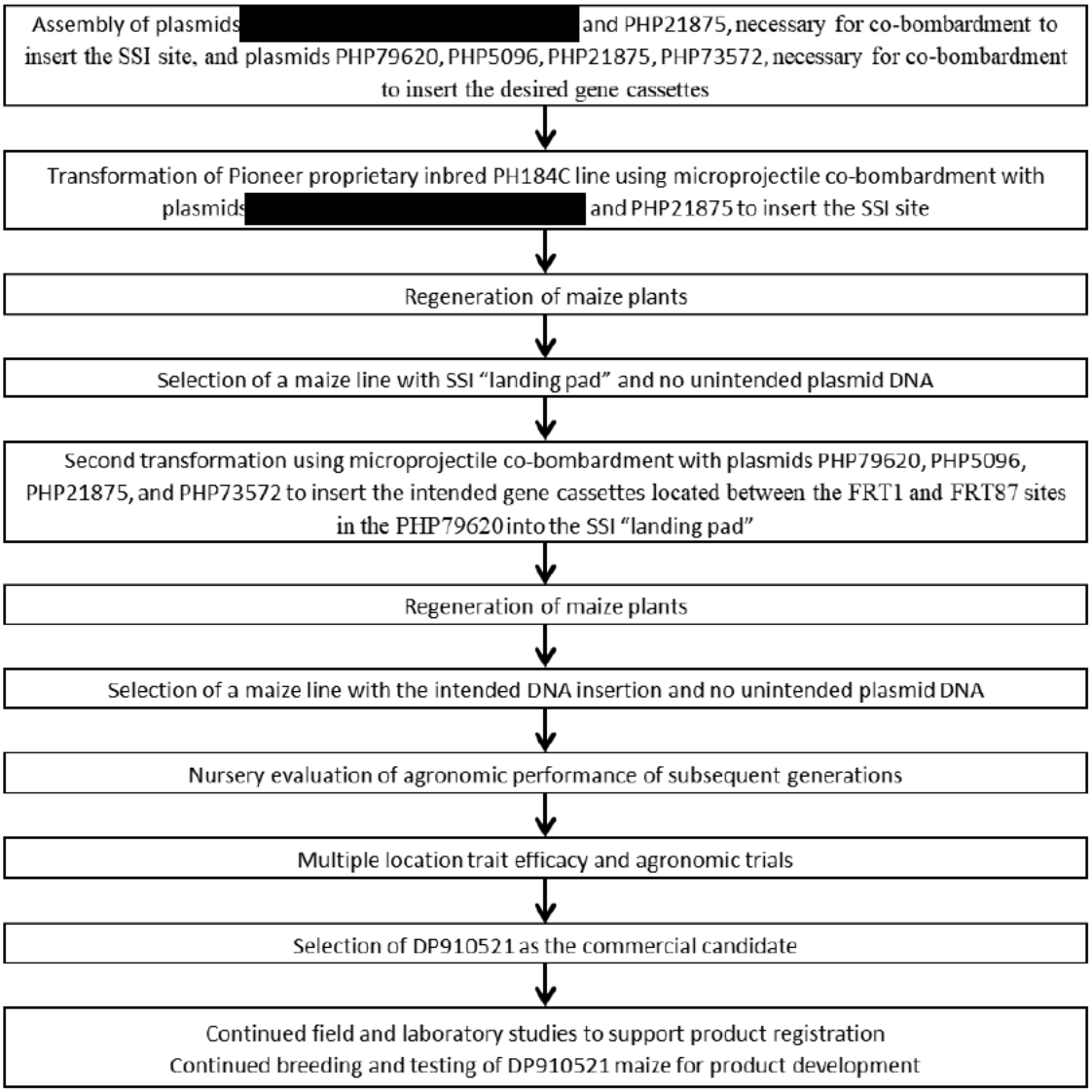

Figure 17. Event Development Process of DP910521 Maize

The subsequent breeding of DP910521 maize proceeded as indicated in Figure 18 to produce specific generations for the characterization and assessments conducted, as well as for the development of commercial maize lines. Table 7 provides the generations used for each characterization study.

Figure 18. Breeding Diagram for DP910521 Maize and Generations Used for Analysis

The breeding steps to produce the generations used for characterization, assessment, and the development of commercial lines are shown schematically. Proprietary inbred PH184C was used for transformation to produce DP910521 maize.

Table 7. Generations and Comparators Used for Analysis of DP910521 Maize

Analysis	Seed Generation(s) Used	Comparators
Insertion copy number, insertion organization, and the absence of plasmid backbone and other unintended plasmid sequences by SbS	T1	PH184C
Insertion organization and stability by Southern blot analysis	T1, BC1, BC1S1, BC1S2, and BC1S3	PH184C
Sanger sequencing	BC1S2	PH184C
Mendelian inheritance by multi-generation segregation analysis	F1 (PH2SRH/PH184C), F2, BC1, BC1S1, BC1S3	
Composition and expression analysis	F1 (PH47K2/PH184C)	PH47K2xPH184C

Selection of Comparators

For the characterization of DP910521 maize, proprietary maize inbred (PH184C) and F1 hybrid (PH47K2/PH184C) were used as experimental controls (Table 7). The control lines selected are non-genetically modified (non-GM) and represent the same genetic background of the maize lines used to produce the DP910521 maize generations used in analysis (Figure 18).

In addition, conventionally bred (conventional) non-GM maize hybrid lines (i.e., reference lines), were used to obtain tolerance intervals for compositional analyses. These maize hybrids were chosen to represent a wide range of conventional non-GM varieties. These tolerance intervals help represent the biological variation of the maize crop for compositional analytes and further helped to determine the comparability of DP910521 maize to conventional non-GM maize.

A.3 (e) Stability of the genetic changes

Southern Analysis to Determine Stable Genetic Inheritance across Generations (PHI-2021-052 study)

Southern blot analysis was performed on five generations of DP910521 maize to evaluate the stability of the inserted *cry*1B.34, *mo-pat*, and *pmi* gene cassettes across multiple generations.

Restriction enzyme *Bcl* I (indicated in Figure 19 and Figure 20) was selected to verify the stability of the DP910521 maize insertion across the five generations (T1, BC1, BC1F1, BC1F2, and BC1F3) of DP910521 maize plants. *Bcl* I was selected because there is a single *Bcl* I restriction site within the DP910521 maize insertion, which provides a means to uniquely identify the event, as additional sites would be in the adjacent flanking genomic DNA (Figure 21).

Genomic DNA samples isolated from leaf tissues of the five generations of DP910521 maize and the PH184C control maize were digested with *Bcl* I and hybridized with the the *cry*1B.34, *mo-pat*, and *pmi* gene probes for Southern analysis. Hybridization patterns of these probes exhibited event-specific bands unique to the DP910521 maize insertion, and thus provided a means of verification that the genomic border regions of the DP910521 maize insertion were not changed across the five generations during breeding. Plasmid PHP79620 was added to control maize DNA, digested with *Bcl* I, and included on the blot to verify successful probe hybridization. The probes used for Southern hybridization are described in Table 8 and shown in Figure 19.

Hybridization of the *cry*1B.34 probes to *Bcl* I-digested genomic DNA resulted in a single band of approximately 6,500 bp in all five generations of DP910521 maize samples analyzed (Table 9, Figure 22). This result confirmed that the 3' border fragment, containing the *cry*1B.34 gene in the DP910521 maize insertion, is intact and stable across the five generations of DP910521 maize. The lanes containing PHP79620 plasmid DNA showed the expected band of 17,763 bp, confirming successful hybridization of the *cry*1B.34 probe.

Hybridization of the *mo-pat* and *pmi* probes to *Bcl* I-digested genomic DNA resulted in a consistent band of approximately 10,000 bp in all five generations of DP910521 maize (Table 9, Figure 23 and Figure 24, respectively). These results confirmed that the 5' border fragment, containing the *mo-pat* and *pmi* genes in the DP910521 maize insertion, is intact and stable across the five

generations of DP910521 maize. The lanes containing PHP79620 plasmid DNA showed the expected band of 17,763 bp, confirming successful hybridization of the *mo-pat* and *pmi* probes.

The presence of equivalent bands from hybridization with each of the *cry*1B.34, *mo-pat*, and *pmi* gene probes within the plants from all five generations analyzed confirms that the inserted DNA in DP910521 maize is consistent and stable across multiple generations during the breeding process.

Additional details regarding analytical methods for Southern analysis are provided in Appendix B.

Table 8. Description of DNA Probes Used for Southern Hybridization

Genetic Element/ Probe Name	Probe Length (bp)	Position on DP910521 Insertion Map (bp to bp)[a]
pmi[b]	569	2,257 to 2,825
	660	2,795 to 3,454
mo-pat	582	6,904 to 7,485
*cry*1B.34[c]	699	11,341 to 12,009
	652	11,982 to 12,633
	756	12,598 to 13,353
	745	13,328 to 14,072
	774	14,041 to 14,814

[a] The probe position is based on the DP910521 insertion map (Figure 21).
[b] These probes comprise two fragments that are combined in a single hybridization solution.
[c] These probes comprise five fragments that are combined in a single hybridization solution.

Table 9. Predicted and Observed Hybridization Bands on Southern Blots; *Bcl* I Digest

Probe Name	Predicted and Observed Fragment Size from Plasmid PHP79620 (bp)[a]	Predicted Fragment Size from DP910521 Insertion Map (bp)[b]	Observed Fragment Size in DP910521 Maize[c] (bp)	Figure
*cry*1B.34	17,763	>6,378	~6,500	Figure 22
mo-pat	17,763	>9,891	~10,000	Figure 23
pmi	17,763	>9,891	~10,000	Figure 24

[a] Predicted and observed fragment sizes are based on the PHP79620 plasmid map (Figure 19).
[b] Predicted sizes are based on the DP910521 insertion map (Figure 21).
[c] Observed fragment sizes are approximated from the DIG-labeled DNA Molecular Weight Marker III and VII fragments on the Southern blots. Due to inability to determine the exact sizes on the blot, all approximated values are rounded to the nearest 100 bp.

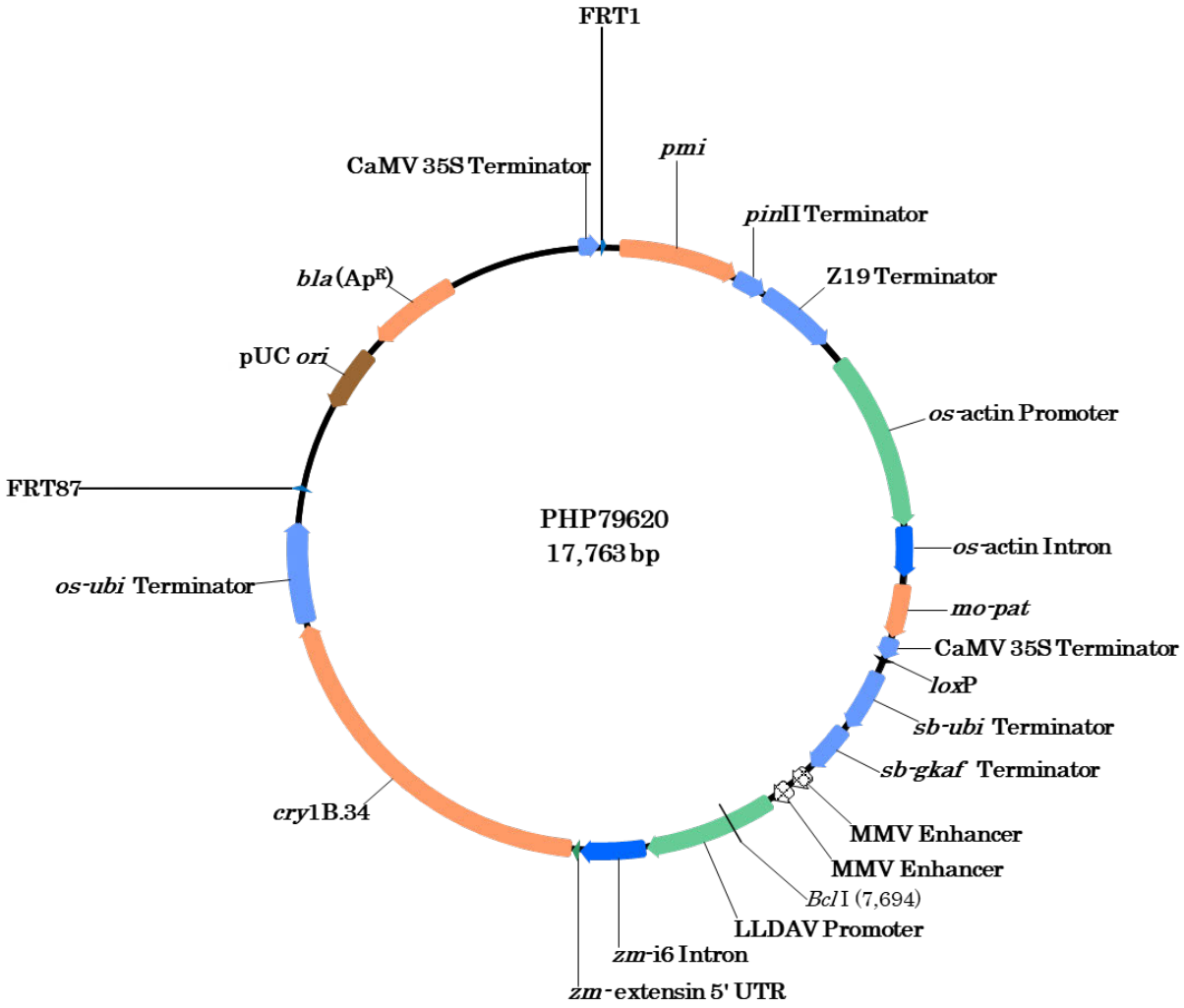

Figure 19. Map of Plasmid PHP79620 for Southern Analysis

Schematic diagram of plasmid PHP79620 indicating the *Bcl* I restriction enzyme site with base pair position and the *pmi*, *mo-pat*, and *cry*1B.34 gene cassettes between the FRT1 and FRT87 sites (the PHP79620 recombination fragment; Figure 20) intended for insertion into the landing pad. The size of plasmid PHP79620 is 17,763 bp. The genetic elements between the FRT1 and FRT87 sites were incorporated in the final DP910521 insertion (Figure 21).

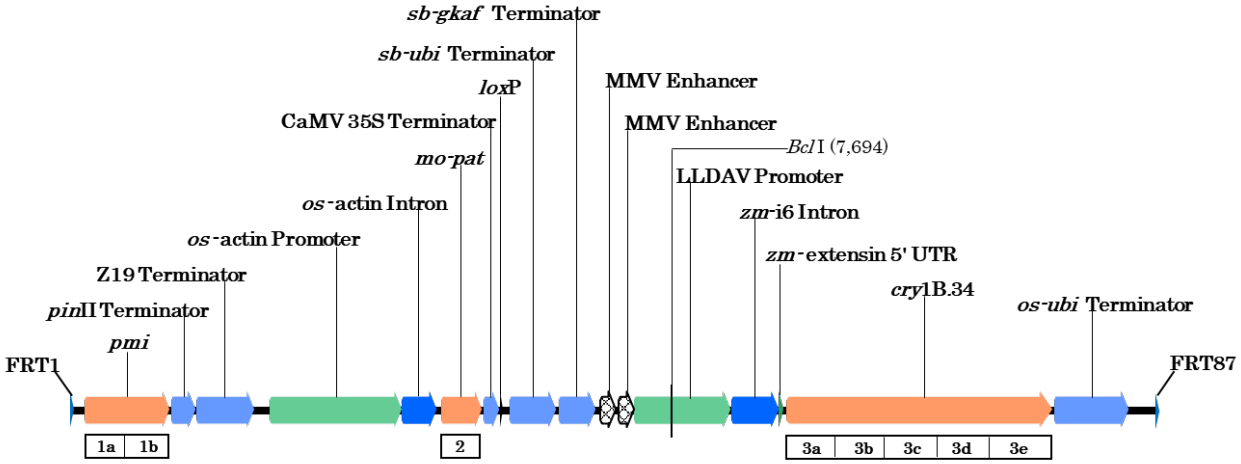

Number	Probe Name
1a & 1b	*pmi*
2	*mo-pat*
3a, 3b, 3c, 3d & 3e	*cry*1B.34

Figure 20. Map of the Recombination Fragment Region from Plasmid PHP79620

Schematic diagram of the PHP79620 recombination fragment region indicating the *Bcl* I restriction enzyme site with base pair position and the *pmi*, *mo-pat*, and *cry*1B.34 gene gene cassettes between the FRT1 and FRT87 sites intended for insertion into the landing pad. The PHP79620 recombination fragment region size is 13,917 bp. The genetic elements between the FRT1 and FRT87 sites were incorporated in the final DNA insertion (Figure 21). The locations of the Southern blot probes are shown by the boxes below the map.

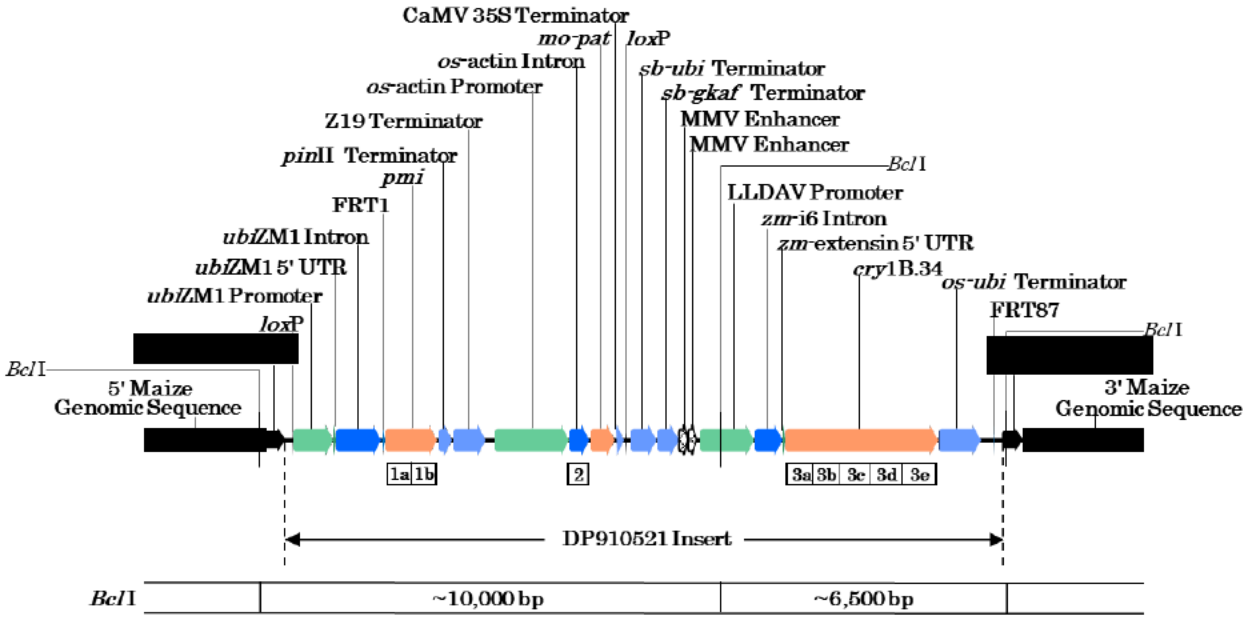

Number	Probe Name
1a & 1b	*pmi*
2	*mo-pat*
3a, 3b, 3c, 3d & 3e	*cry*1B.34

Figure 21. Map of the DP910521 Insertion

Schematic diagram of the DP910521 maize insertion following SSI integration of the gene cassettes from the PHP79620 recombination fragment region (Figure 20) indicating the *Bcl* I restriction enzyme sites. The DP910521 insert comprises sequences from two sources: the sequences of the landing pad outside the FRT1 and FRT87 sites and the sequences from the PHP79620 recombination fragment region within the FRT1 and FRT87 sites (with *pmi*, *mo-pat*, and *cry*1B.34 gene cassettes). The flanking maize genomic regions are represented by the horizontal black rectangular bars. The locations of the Southern blot probes are shown by the boxes below the map. The *Bcl* I restriction sites are indicated with the sizes of observed fragments on Southern blots shown below the map in base pairs (bp). The locations of restriction enzyme sites in the flanking maize genomic DNA are not to scale.

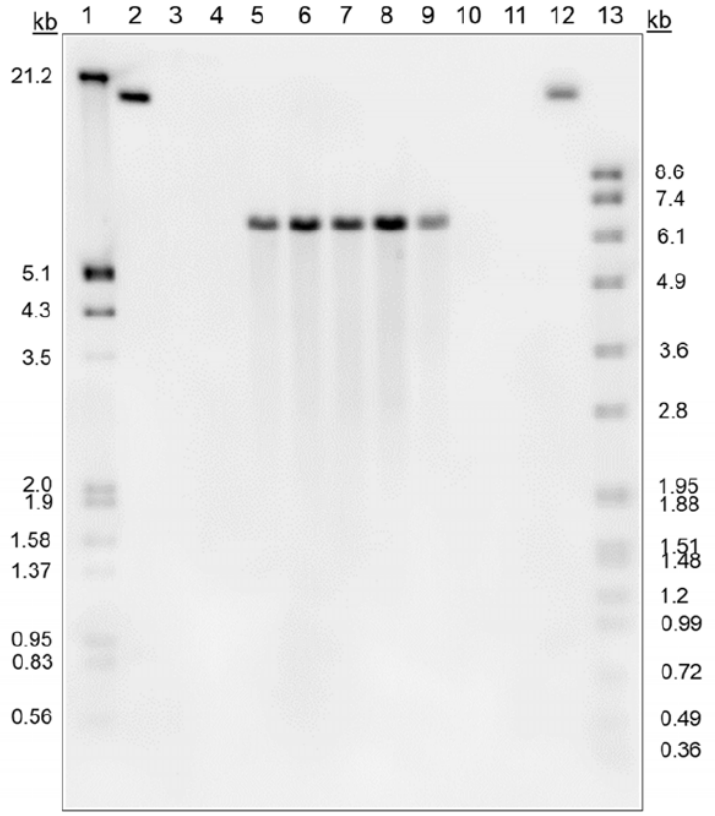

Lane	Sample
1	DIG-labeled DNA marker III
2	1 copy of PHP79620 + PH184C control maize
3	PH184C Control maize
4	Blank
5	DP910521 maize BC1 generation
6	DP910521 maize BC1F2 generation
7	DP910521 maize BC1F1 generation

Lane	Sample
8	DP910521 maize BC1F3 generation
9	DP910521 maize T1 generation
10	Blank
11	PH184C Control maize
12	1 copy of PHP79620 + PH184C control maize
13	DIG-labeled DNA marker VII

Figure 22. Southern Blot Analysis of DP910521 Maize; Bcl I Digest with cry1B.34 Probe

Genomic DNA isolated from leaf tissues of DP910521 maize from T1, BC1, BC1F1, BC1F2, and BC1F3 generations and PH184C control maize plants was digested with *Bcl* I and hybridized to the *cry*1B.34 probe. Approximately 10 µg of genomic DNA was digested and loaded per lane. Positive control lanes include PHP79620 plasmid DNA at approximately one gene copy number and 10 µg of control maize DNA. Sizes of the DIG-labeled DNA Molecular Weight Marker III and VII are indicated adjacent to the blot image in kilobases (kb).

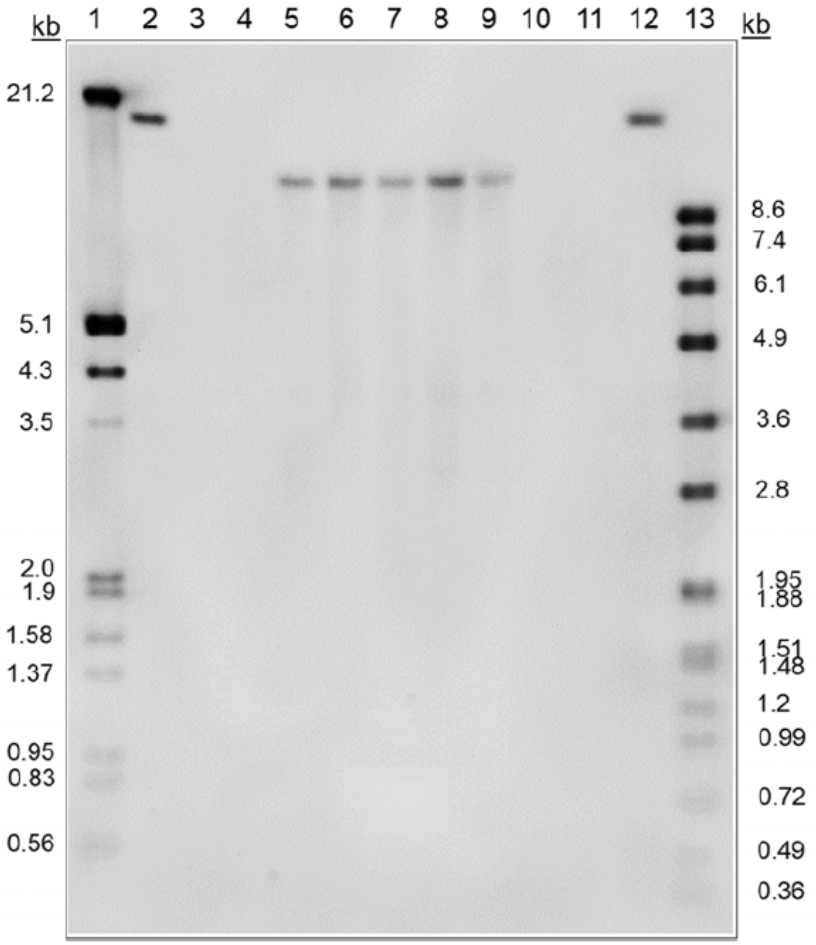

Lane	Sample
1	DIG-labeled DNA marker III
2	1 copy of PHP79620 + PH184C control maize
3	PH184C Control maize
4	Blank
5	DP910521 maize BC1 generation
6	DP910521 maize BC1F2 generation
7	DP910521 maize BC1F1 generation

Lane	Sample
8	DP910521 maize BC1F3 generation
9	DP910521 maize T1 generation
10	Blank
11	PH184C Control maize
12	1 copy of PHP79620 + PH184C control maize
13	DIG-labeled DNA marker VII

Figure 23. Southern Blot Analysis of DP910521 Maize; *Bcl* I Digest with *mo-pat* Probe

Genomic DNA isolated from leaf tissues of DP910521 maize from T1, BC1, BC1F1, BC1F2, and BC1F3 generations and PH184C control maize plants was digested with *Bcl* I and hybridized to the *mo-pat* probe. Approximately 10 µg of genomic DNA was digested and loaded per lane. Positive control lanes include PHP79620 plasmid DNA at approximately one gene copy number and 10 µg of control maize DNA. Sizes of the DIG-labeled DNA Molecular Weight Marker III and VII are indicated adjacent to the blot image in kilobases (kb).

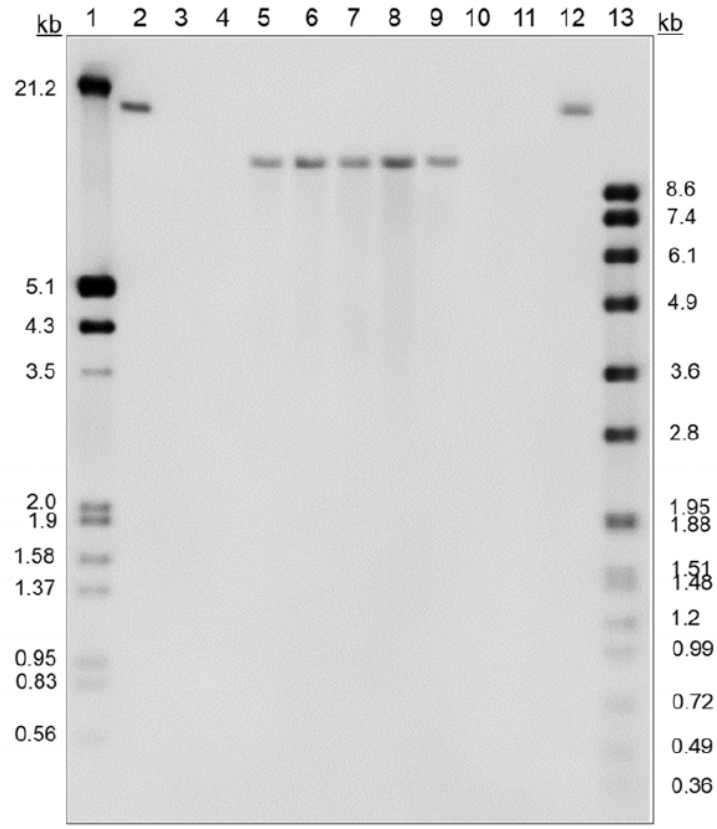

Lane	Sample
1	DIG-labeled DNA marker III
2	1 copy of PHP79620 + PH184C control maize
3	PH184C Control maize
4	Blank
5	DP910521 maize BC1 generation
6	DP910521 maize BC1F2 generation
7	DP910521 maize BC1F1 generation

Lane	Sample
8	DP910521 maize BC1F3 generation
9	DP910521 maize T1 generation
10	Blank
11	PH184C Control maize
12	1 copy of PHP79620 + PH184C control maize
13	DIG-labeled DNA marker VII

Figure 24. Southern Blot Analysis of DP910521 Maize; *Bcl* I Digest with *pmi* Probe

Genomic DNA isolated from leaf tissues of DP910521 maize from T1, BC1, BC1F1, BC1F2, and BC1F3 generations and PH184C control maize plants was digested with *Bcl* I and hybridized to the *pmi* probe. Approximately 10 µg of genomic DNA was digested and loaded per lane. Positive control lanes include PHP79620 plasmid DNA at approximately one gene copy number and 10 µg of control maize DNA. Sizes of the DIG-labeled DNA Molecular Weight Marker III and VII are indicated adjacent to the blot image in kilobases (kb).

Multi-Generation Segregation Analysis (PHI-2020-067 study)

Segregation analysis was performed on five generations of DP910521 maize (F1, F2, BC1, BC1S1, and BC1S3) to confirm the Mendelian inheritance pattern of the inserted DNA during the breeding process. The selected maize generations represent a range of different genotypes, created through crossing, backcrossing, and selfing, in a typical maize breeding program. The observed inheritance pattern predicts the segregation of these genes and/or traits as a single unit and as a single genetic locus throughout the commercial breeding process. For F1, BC1, and BC1S3 generations, a total of 100 maize plants from each generation were analyzed using genotypic and phenotypic analyses; for the F2 and BC1S1 generations, 252 and 168 seeds, respectively, were analyzed using genotypic and phenotypic analyses.

The genotypic analyses utilized a quantitative polymerase chain reaction (qPCR) assay to confirm the copy number of event DP-91Ø521-2 (F1, BC1, BC1S1 and BC1S3 generations) or endpoint PCR to confirm the presence or absence of event DP-91Ø521-2 (F2 generation). The phenotypic analysis utilized a visual herbicide injury evaluation to confirm the presence or absence of tolerance to glufosinate for each individual plant. The individual results for each plant were compared to the qPCR results to verify co-segregation of genotype with phenotype. A chi-square test was performed at the 0.05 significance level to compare the observed segregation ratios of the F1, F2, BC1 and BC1S1 generations of DP910521 maize to the expected segregation ratios (1:1 for the F1 and BC1 generations, 3:1 for the F2 and BC1S1 generations). A chi-square test was not performed for the BC1S3 generation of DP910521 maize as all plants were identified as positive as expected for a homozygous generation.

A summary of segregation results for DP910521 maize (F1, F2, BC1, BC1S1, and BC1S3 generations) is provided in Table 10. No statistically significant deviation from the expected segregation ratio was found in the F1, F2, BC1, and BC1S1 generations of DP910521 maize, and the BC1S3 generation was confirmed to be non-segregating. Genotypic results based on qPCR and endpoint PCR results demonstrated that the observed segregation ratios matched the expected segregation ratios for all five generations. Results of phenotypic analysis for tolerance to glufosinate herbicide aligned with the genotypic results.

The results of the multi-generation segregation analysis demonstrated that the inserted DNA in DP910521 maize segregated as a single locus in accordance with Mendelian rules of inheritance for a single genetic locus, indicating stable integration of the insert into the maize genome and a stable genetic inheritance pattern across generations during the breeding process.

Additional details regarding analytical methods for the multi-generation segregation analysis are provided in Appendix C.

Table 10 . Summary of Genotypic and Phenotypic Segregation Analyses for Five Generations of DP910521 Maize

Entry	Generation	Expected Segregation Ratio (Positive:Negative)	Observed Segregation[ab]			Statistical Analysis	
			Positive	Negative	Total	Chi-Square[a]	P-Value
1	F1	1:1	46	53	99	0.49	0.4817
3	BC1	1:1	47	53	100	0.36	0.5485
5	BC1S3	Homozygous	100	0	100	--	--
8	BC1S1	3:1	130	35	165	1.26	0.2612
10	F2	3:1	175	68	243	1.15	0.2828

Note: One Entry 1 plant was excluded from statistical analysis as the phenotype and genotype did not align. Three Entry 8 plants and nine Entry 10 plants were excluded from statistical analysis due to undetermined or not conclusive results obtained during the PCR analyses.

[a] Degrees of freedom = 1. A chi-square value greater than 3.84 (P-value less than 0.05) would indicate a significant difference.

[b] The observed segregation ratio was determined based on genotypic results.

B. CHARACTERISATION AND SAFETY ASSESSMENT OF NEW SUBSTANCES

B.1 Characterisation and safety assessment of new substances

There are no new substances associated with DP910521 maize other than the Cry1B.34 protein (see Section B.2 New proteins below).

B.2 New proteins

Cry1B.34 Protein

Amino Acid Sequence of the Cry1B.34 Protein

The deduced amino acid sequence from the translation of the *cry*1B.34 gene encodes a full-length protein that is 1,149 amino acids in length and has a molecular weight of approximately 129 kDa (Figure 25).

```
   1   MAPSNRKNEN EIINAVSNHS AQMDLSLDAR IEDSLCVAEV NNIDPFVSAS
  51   TVQTGISIAG RILGVLGVPF AGQLASFYSF LVGELWPSGR DPWEIFLEHV
 101   EQLIRQQVTE NTRNTAIARL EGLGRGYRSY QQALETWLDN RNDARSRSII
 151   LERYVALELD ITTAIPLFSI RNQEVPLLMV YAQAANLHLL LLRDASLFGS
 201   EWGMSSADVN QYYQEQIRYT EEYSNHCVQW YNTGLNNLRG TNAESWLRYN
 251   QFRRDLTLGV LDLVALFPSY DTRTYPINTS AQLTREIYTD PIGRTNAPSG
 301   FASTNWFNNN APSFSAIEAA IFRPPHLLDF PEQLTIYSAS SRWSSTQHMN
 351   YWVGHRLNFR PIGGTLNTST QGLTNNTSIN PVTLQFTSRD VYRTESNAGT
 401   NILFTTPVNG VPWARFNFIN PQNIYERGAT TYSQPYQGVG IQLFDSETEL
 451   PPETTERPNY ESYSHRLSHI GLIIGNTLRA PVYSWTHRSA TLTNTIDPER
 501   INQIPLVKGF RVWGGTSVIT GPGFTGGDIL RRNTFGDFVS LQVNINSPIT
 551   QRYRLRFRYA SSRDARVIVL TGAASTGVGG QVSVNMPLQK TMEIGENLTS
 601   RTFRYTDFSN PFSFRANPDI IGISEQPLFG AGSISSGELY IDKIEIILAD
 651   ATFEAESDLE RAQKAGAGLF TRTRDGLQVN VTDYQVDRAA NLVSCLSDEQ
 701   YSHDKKMLME AVRAAKRLSR ERNLLQDPDF NEINSTEENG WKASNGIIIS
 751   EGGPFFKGRV LQLASARENY PTYIYQKVDA SVLKPYTRYR LDGFVKSSED
 801   LEIDLVHQHK VHLVKNVPDN LVSDTYPDGS CRGVNRCDEQ HQVDVQIDTE
 851   HHPMDCCEAA QTHEFSSYIN TGDLNSSVDQ GIWVVLKVRT ADGYATLGNL
 901   ELVEVGPLSG ESLEREQRDN AKWNAELGRE RAETDRVYLA AKQAINHLFV
 951   DYQDQQLNPE IGLAEINEAS NLVESITGVY SDTVLQIPGI SYEIYTELSD
1001   RLQQASYLYT SRNAVQNGDF DSGLDSWNAT TDASVQQDGN MHFLVLSHWD
1051   AQVTQQLRVN PNCKYVLRVT ARKVGGGDGY VTIRDGAHHR ETLTFNACDY
1101   DVNGTYVNDN TYITKEVVFY PHTEHTWVEV SESEGAFYID SIELIETQE*
```

Figure 25. Deduced Amino Acid Sequence of the Cry1B.34 Protein

The deduced amino acid sequence from the translation of the *cry*1B.34 gene from plasmid PHP79620. The asterisk (*) indicates the translational stop codon. The full-length protein is 1,149 amino acids in length and has a molecular weight of approximately 129 kDa.

Function and Activity of the Cry1B.34 Protein

The Cry1B.34 protein is encoded by the *cry*1B.34 gene, a chimeric gene comprised of sequences from a *cry*1B-class gene, the *cry*1Ca1 gene, and the *cry*9Db1 gene, all derived from *Bacillus thuringiensis*. The expressed Cry1B.34 protein is effective against certain susceptible lepidopteran pests by causing disruption of the midgut epithelium. The Cry1B.34 protein binds to receptors in the brush border membrane of susceptible lepidopteran pests and causes cell death through the formation of non-specific, ion conducting pores in the apical membrane of the midgut epithelial cells.

Characterization of Cry1B.34 Protein Derived from DP910521 Maize and Microbial System (PHI-2021-115, PHI-2020-093 and PHI-2021-027 studies)

The Cry1B.34 protein expressed in DP910521 maize was purified from the leaf tissue using immunoaffinity chromatography.

In order to have sufficient amounts of purified Cry1B.34 protein for the multiple studies required to assess its safety, the Cry1B.34 protein was expressed in an *Escherichia coli* protein expression system. The microbially derived protein was purified using pellet washing and ion exchange chromatography.

The biochemical characteristics of the microbially derived Cry1B.34 protein and the DP910521 maize-derived Cry1B.34 protein were characterized using sodium dodecyl sulfate polyacrylamide gel electrophoresis (SDS-PAGE), western blot, glycosylation, mass spectrometry, and N-terminal amino acid sequence analyses. For the microbially derived Cry1B.34 protein, the bioactivity was verified by insect bioassays. The results showed that the DP910521 maize-derived and microbially derived Cry1B.34 proteins are of the expected molecular weight, immunoreactivity, lack of glysoylation, and amino acid sequence. The microbially derived Cry1B.34 protein was demonstrated to be an appropriate test substance for use in safety studies.

SDS-PAGE Analysis

Samples of the DP910521 maize-derived Cry1B.34 protein and the microbially derived Cry1B.34 protein were analyzed by SDS-PAGE. As expected, the Cry1B.34 proteins derived from both DP910521 maize and the microbial system migrated as a predominant band consistent with the expected molecular weight of approximately 129 kDa, as shown in Figure 26.

Additional details regarding SDS-PAGE analytical methods are provided in Appendix E.

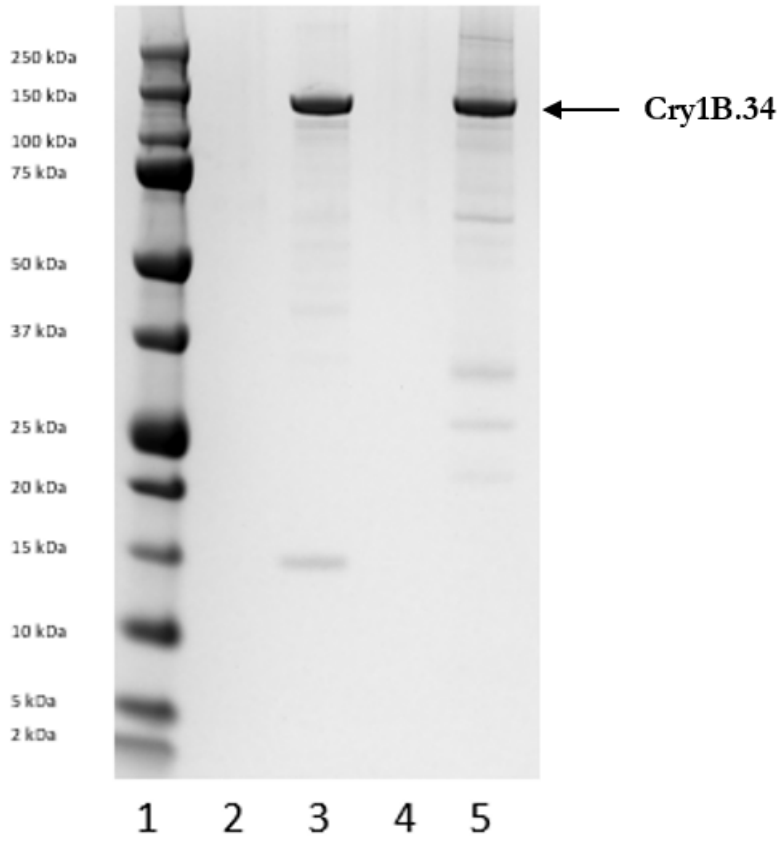

Lane	Sample Identification
1	Pre-stained Protein Molecular Weight Marker[a]
2	1X LDS/DTT Sample Buffer Blank
3	Microbially Derived Cry1B.34 Protein (Lot # PRCH-004)[b]
4	1X LDS/DTT Sample Buffer Blank
5	DP910521 Maize-Derived Cry1B.34 Protein

Note: kilodalton (kDa) and lithium dodecyl sulfate containing dithiothreitol (LDS/DTT).

[a] Molecular weight markers were included to provide a visual verification that migration was within the expected range of the predicted molecular weight.

[b] PRCH-004 was prepared from solubilization of lyophilized protein (Lot# PCF-0042). Target loading amount of 1 µg.

Figure 26. SDS-PAGE Analysis of Cry1B.34 Protein

Western Blot Analysis

Samples of the DP910521 maize-derived Cry1B.34 protein and the microbially derived Cry1B.34 protein were analyzed by Western blot. As expected, the Cry1B.34 proteins derived from both DP910521 maize and the microbial system were immunoreactive to a Cry1B.34 monoclonal antibody and visible as a predominant band consistent with the expected molecular weight of approximately 129 kDa, as shown in Figure 27.

Additional details regarding Western blot analytical methods are provided in Appendix E.

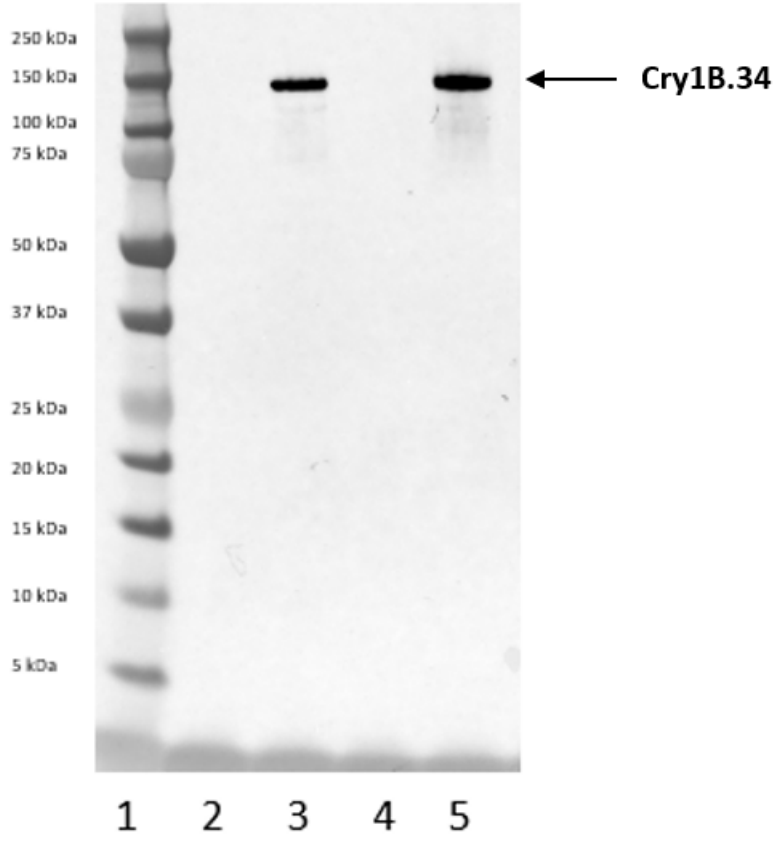

Lane	Sample Identification
1	Pre-stained Protein Molecular Weight Marker[a]
2	1X LDS/DTT Sample Buffer Blank
3	Microbially Derived Cry1B.34 Protein (Lot # PRCH-004)[b]
4	1X LDS/DTT Sample Buffer Blank
5	DP910521 Maize-Derived Cry1B.34 Protein

Note: kilodalton (kDa) and lithium dodecyl sulfate containing dithiothreitol (LDS/DTT).

[a] Molecular weight markers were included to provide a visual verification that migration was within the expected range of the predicted molecular weight.

[b] PRCH-004 was prepared from solubilization of lyophilized protein (Lot# PCF-0042). Target loading amount of 5 ng.

Figure 27. Western Blot Analysis of Cry1B.34 Protein

Protein Glycosylation Analysis

Samples of the DP910521 maize- derived Cry1B.34 protein and the microbially derived Cry1B.34 protein were analyzed by SDS-PAGE for glycosylation analysis. Each gel also included a positive control (horseradish peroxidase) and negative control (soybean trypsin inhibitor). The gels were stained using a Pierce Glycoprotein Staining Kit to visualize any glycoproteins. The gels were imaged and then stained with Coomassie based GelCode™ Blue Stain reagent to visualize all protein bands.

Glycosylation was determined to be negative for both the DP910521 maize-derived and microbially derived Cry1B.34 proteins (Figure 28 and Figure 29, respecctively). A very faint band was captured by the imaging system for the maize-derived Cry1B.34 protein sample. This was attributed to non-specific staining which is not due to glycosylation (Roth *et al.*, 2012). The horseradish peroxidase positive control was stained as a magenta-colored band. The soybean trypsin inhibitor negative control was not stained by the glycoprotein stain.

Additional details regarding glycosylation analytical methods are provided in Appendix E.

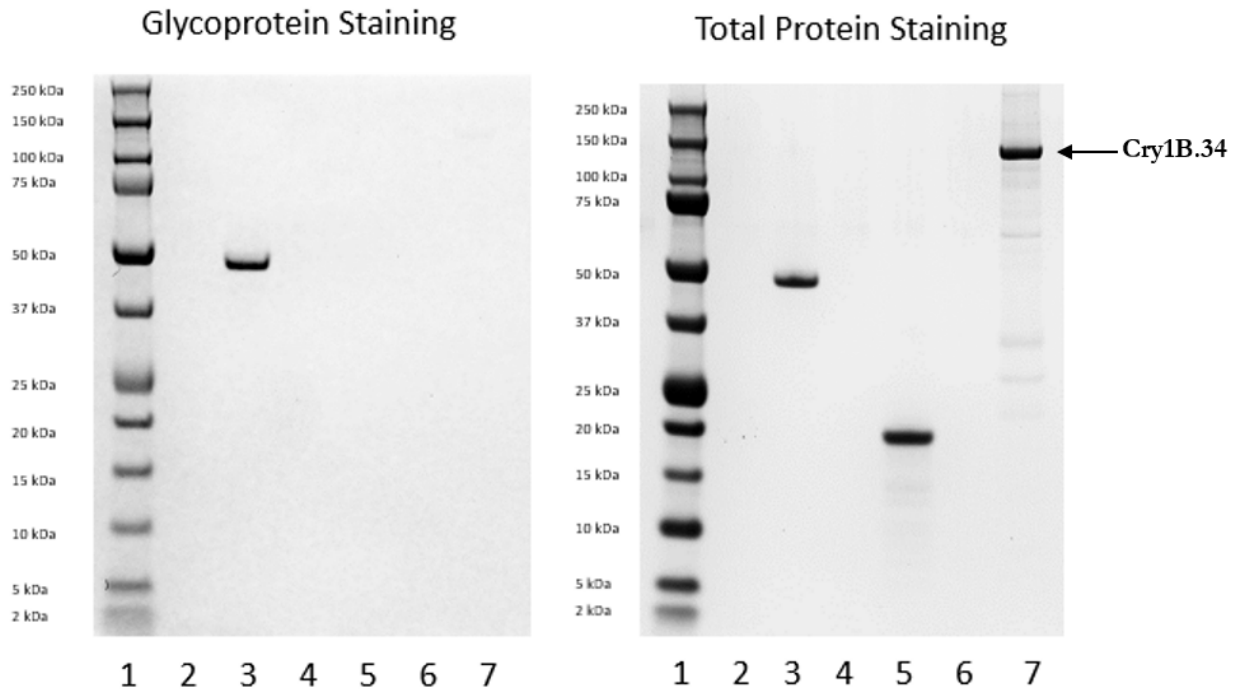

Lane	Sample Identification
1	Pre-stained Protein Molecular Weight Marker[a]
2	1X LDS/DTT Sample Buffer Blank
3	Horseradish Peroxidase (1.0 µg)
4	1X LDS/DTT Sample Buffer Blank
5	Soybean Trypsin Inhibitor (1.0 µg)
6	1X LDS/DTT Sample Buffer Blank
7	DP910521 Maize-Derived Cry1B.34 Protein

Note: The glycoprotein gel was stained with glycoprotein staining reagent. The total protein stain gel was stained with glycoprotein staining reagent followed by staining with Coomassie blue reagent for total proteins. Kilodalton (kDa) and lithium dodecyl sulfate containing dithiothreitol (LDS/DTT).

[a] Molecular weight markers were included to provide a visual verification that migration was within the expected range of the predicted molecular weight

Figure 28. Glycosylation Analysis of DP910521 Maize-Derived Cry1B.34 Protein

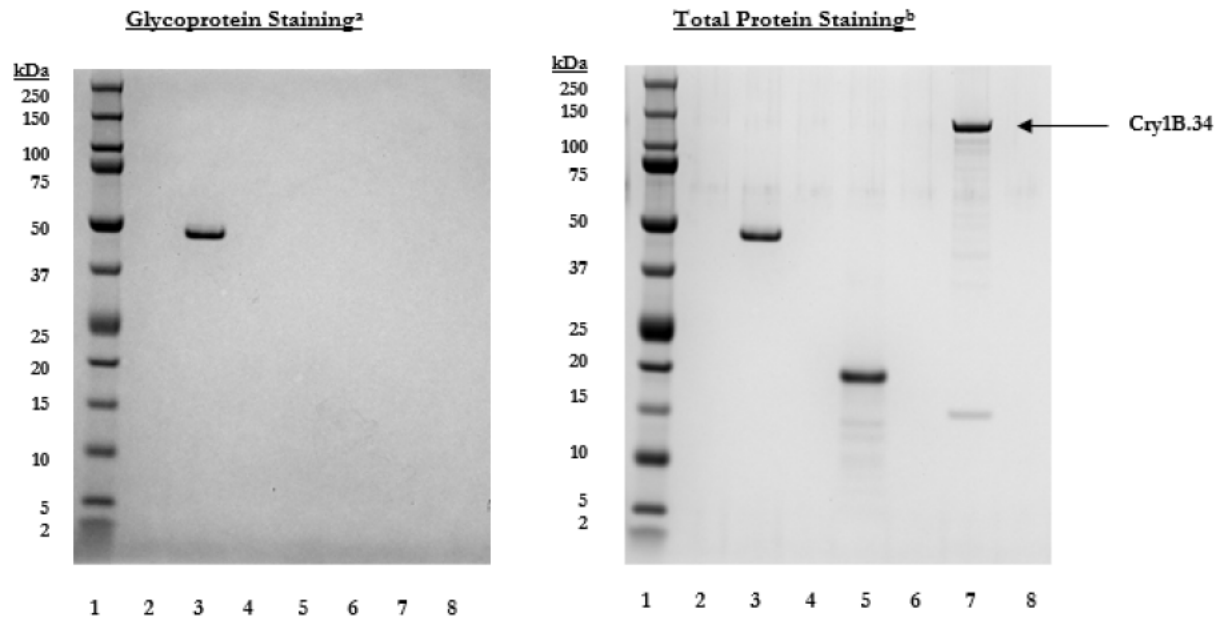

Lane	Sample Identification
1	Pre-stained Protein Molecular Weight Marker[c]
2	1X LDS Sample Buffer Blank
3	Horseradish Peroxidase (1 µg)
4	1X LDS Sample Buffer Blank
5	Soybean Trypsin Inhibitor (1 µg)
6	1X LDS Sample Buffer Blank
7	Microbially Derived Cry1B.34 Protein (1 µg)
8	1X LDS Sample Buffer Blank

Note: kilodalton (kDa) and microgram (µg).

[a] Gel was stained with glycoprotein staining reagent.

[b] Gel was stained with glycoprotein staining reagent followed by staining with Coomassie Blue G-250 for total proteins.

[c] Molecular weight markers were included to provide a visual estimate that migration was within the expected range of the predicted molecular weight.

Figure 29. Glycosylation Analysis of Microbially Derived Cry1B.34 Protein

Mass Spectrometry Peptide Mapping Analysis

Samples of the DP910521 maize- derived Cry1B.34 protein and the microbially derived Cry1B.34 protein were analyzed by SDS-PAGE. Protein bands were stained with Coomassie stain reagent, and bands containing the Cry1B.34 protein were excised for each sample.

The excised Cry1B.34 protein bands were digested with trypsin or chymotrypsin. Digested samples were analyzed with ultra-performance liquid chromatography-mass spectrometry (LC-MS). The resulting MS data were used to search and match the peptides from the expected Cry1B.34 protein sequence, and the combined sequence coverage was calculated.

The identified tryptic and chymotrypic peptides for the DP910521 maize-derived Cry1B.34 protein are shown in Table 11 and Table 12, respectively. The combined sequence coverage for the DP910521 maize-derived Cry1B.34 protein was 93.8% (1077/1148) of the expected Cry1B.34 amino acid sequence (Table 13 and Figure 30). The identified tryptic and chymotryptic peptides for microbially derived Cry1B.34 protein are shown in Table 14 and Table 15, respectively. The combined sequence coverage for the microbially derived Cry1B.34 protein was 90.8% (1042/1147) of the expected amino acid sequence (Table 16 and Figure 31).

Additional details regarding peptide mapping analytical methods are provided in Appendix E.

Table 11. Identified Tryptic Peptides of DP910521 Maize-Derived Cry1B.34 Protein Using LC MS Analysis

Matched Residue Position	Experimental Mass[a]	Theoretical Mass[b]	Identified Peptide Sequence
6–29	2668.2971	2668.2874	KNENEIINAVSNHSAQMDLSLDAR
7–29	2540.2027	2540.1925	NENEIINAVSNHSAQMDLSLDAR
30–60	3261.6516	3261.6187	IEDSLCVAEVNNIDPFVSASTVQTGISIAGR
90–104	1922.9985	1922.9890	DPWEIFLEHVEQLIR
105–112	974.4794	974.4781	QQVTENTR
119–124	643.3661	643.3653	LEGLGR
128–140	1622.7751	1622.7689	SYQQALETWLDNR
128–144	2078.9816	2078.9769	SYQQALETWLDNRNDAR
147–170	2745.5970	2745.5680	SIILERYVALELDITTAIPLFSIR
153–170	2034.1152	2034.1401	YVALELDITTAIPLFSIR
153–192	4534.5906	4534.5389	YVALELDITTAIPLFSIRNQEVPLLMVYAQAANLHLLLLR
171–192	2518.4306	2518.4093	NQEVPLLMVYAQAANLHLLLLR
171–217	5380.7268	5380.6648	NQEVPLLMVYAQAANLHLLLLRDASLFGSEWGMSSADVNQYYQEQIR
193–217	2880.2931	2880.2661	DASLFGSEWGMSSADVNQYYQEQIR
218–238	2660.1770	2660.1714	YTEEYSNHCVQWYNTGLNNLR
248–252	726.3450	726.3449	YNQFR
253–272	2263.2377	2263.2212	RDLTLGVLDLVALFPSYDTR
254–272	2107.1331	2107.1201	DLTLGVLDLVALFPSYDTR
273–284	1363.7133	1363.7096	TYPINTSAQLTR
285–293	1062.5381	1062.5346	EIYTDPIGR
294–341	5253.6188	5253.5584	TNAPSGFASTNWFNNNAPSFSAIEAAIFRPPHLLDFPEQLTIYSASSR
342–355	1787.7996	1787.7951	WSSTQHMNYWVGHR
356–388	3561.8847	3561.8540	LNFRPIGGTLNTSTQGLTNNTSINPVTLQFTSR
389–414	2877.4632	2877.4410	DVYRTESNAGTNILFTTPVNGVPWAR
393–414	2344.1824	2344.1812	TESNAGTNILFTTPVNGVPWAR
415–426	1553.7690	1553.7626	FNFINPQNIYER
427–465	4447.0456	4447.0517	GATTYSQPYQGVGIQLFDSETELPPETTERPNYESYSHR
466–478	1405.8446	1405.8405	LSHIGLIIGNTLR
479–487	1115.5540	1115.5512	APVYSWTHR
488–499	1316.6625	1316.6572	SATLTNTIDPER
488–507	2222.2418	2222.2270	SATLTNTIDPERINQIPLVK
500–507	923.5839	923.5804	INQIPLVK
511–530	1989.0431	1989.0320	VWGGTSVITGPGFTGGDILR
511–531	2145.1465	2145.1331	VWGGTSVITGPGFTGGDILRR
531–551	2405.2476	2405.2452	RNTFGDFVSLQVNINSPITQR
532–551	2249.1599	2249.1441	NTFGDFVSLQVNINSPITQR
566–589	2325.2884	2325.2726	VIVLTGAASTGVGGQVSVNMPLQK
590–600	1249.6020	1249.5972	TMEIGENLTSR
604–614	1379.6211	1379.6146	YTDFSNPFSFR
615–642	2890.4875	2890.4600	ANPDIIGISEQPLFGAGSISSGELYIDK
615–660	4906.5197	4906.4651	ANPDIIGISEQPLFGAGSISSGELYIDKIEIILADATFEAESDLER
643–660	2034.0272	2034.0157	IEIILADATFEAESDLER
664–671	791.4307	791.4290	AGAGLFTR
672–687	1877.9328	1877.9232	TRDGLQVNVTDYQVDR
674–687	1620.7718	1620.7744	DGLQVNVTDYQVDR
688–704	1935.8729	1935.8632	AANLVSCLSDEQYSHDK
688–705	2063.9675	2063.9582	AANLVSCLSDEQYSHDKK

Table 11. Identified Tryptic Peptides of DP910521 Maize-Derived Cry1B.34 Protein Using LC-MS Analysis (continued)

Matched Residue Position	Experimental Mass[a]	Theoretical Mass[b]	Identified Peptide Sequence
705–712	976.5204	976.5198	KMLMEAVR
706–712	848.4274	848.4248	MLMEAVR
720–741	2647.2228	2647.2150	ERNLLQDPDFNEINSTEENGWK
742–756	1535.7942	1535.7984	ASNGIIISEGGPFFK
759–766	856.5150	856.5130	VLQLASAR
767–776	1317.6304	1317.6241	ENYPTYIYQK
777–787	1247.6918	1247.6874	VDASVLKPYTR
788–795	996.5419	996.5393	YRLDGFVK
790–795	677.3763	677.3748	LDGFVK
796–809	1648.8135	1648.8056	SSEDLEIDLVHQHK
815–831	1907.8454	1907.8320	NVPDNLVSDTYPDGSCR
889–914	2689.3686	2689.3446	TADGYATLGNLELVEVGPLSGESLER
922–928	844.4210	844.4191	WNAELGR
931–941	1235.6510	1235.6510	AETDRVYLAAK
936–941	663.3961	663.3955	VYLAAK
1001–1011	1328.6772	1328.6724	LQQASYLYTSR
1012–1057	5115.3843	5115.3442	NAVQNGDFDSGLDSWNATTDASVQQDGNMHFLVLSHWDAQVTQQLR
1072–1083	1220.6549	1220.6514	KVGGGDGYVTIR
1073–1083	1092.5591	1092.5564	VGGGDGYVTIR
1073–1089	1765.8661	1765.8609	VGGGDGYVTIRDGAHHR
1090–1114	2930.3061	2930.2916	ETLTFNACDYDVNGTYVNDNTYITK
1115–1148	4011.9006	4011.8578	EVVFYPHTEHTWVEVSESEGAFYIDSIELIETQE

[a] The experimental mass is the uncharged mass calculated from the mass to charge ratio of the observed ion.
[b] The theoretical mass is the *in silico* generated mass that matches closest to the experimental mass.

Table 12. Identified Chymotryptic Peptides of DP910521 Maize-Derived Cry1B.34 Protein Using LC MS Analysis

Matched Residue Position	Experimental Mass[a]	Theoretical Mass[b]	Identified Peptide Sequence
1–24	2651.2859	2651.2721	APSNRKNENEIINAVSNHSAQMDL
25–34	1117.5681	1117.5615	SLDARIEDSL
25–45	2376.1753	2376.1267	SLDARIEDSLCVAEVNNIDPF
27–45	2176.0567	2176.0106	DARIEDSLCVAEVNNIDPF
46–62	1671.9652	1671.9519	VSASTVQTGISIAGRIL
80–92	1510.7796	1510.7569	LVGELWPSGRDPW
81–92	1397.6900	1397.6728	VGELWPSGRDPW
81–95	1786.902	1786.8679	VGELWPSGRDPWEIF
93–102	1255.6562	1255.6448	EIFLEHVEQL
96–102	866.4510	866.4498	LEHVEQL
103–119	1983.1126	1983.0973	IRQQVTENTRNTAIARL
120–126	750.3679	750.3660	EGLGRGY
127–136	1280.6254	1280.6149	RSYQQALETW
137–150	1641.9073	1641.8910	LDNRNDARSRSIIL
137–153	2090.1108	2090.0980	LDNRNDARSRSIILERY
138–153	1977.0304	1977.0140	DNRNDARSRSIILERY
154–166	1367.8068	1367.7912	VALELDITTAIPL
157–167	1231.6826	1231.6700	ELDITTAIPLF
167–176	1201.6547	1201.6455	FSIRNQEVPL
168–180	1560.8578	1560.8334	SIRNQEVPLLMVY
181–189	949.5387	949.5345	AQAANLHLL
191–197	820.4463	820.4443	LRDASLF
198–211	1529.6283	1529.6093	GSEWGMSSADVNQY
202–211	1070.4378	1070.4339	GMSSADVNQY
212–222	1520.6923	1520.6783	YQEQIRYTEEY
213–222	1357.6253	1357.615	QEQIRYTEEY
219–229	1451.5887	1451.5776	TEEYSNHCVQW
219–230	1614.6592	1614.6409	TEEYSNHCVQWY
223–229	929.3836	929.3814	SNHCVQW
223–230	1092.4507	1092.4447	SNHCVQWY
231–245	1645.8000	1645.7808	NTGLNNLRGTNAESW
235–245	1260.5920	1260.5847	NNLRGTNAESW
235–246	1373.6809	1373.6687	NNLRGTNAESWL
238–245	919.4159	919.4148	RGTNAESW
238–246	1032.5045	1032.4988	RGTNAESWL
238–248	1351.6753	1351.6633	RGTNAESWLRY
246–251	839.4302	839.4290	LRYNQF
252–260	1041.6350	1041.6295	RRDLTLGVL
263–282	2256.1930	2256.1426	VALFPSYDTRTYPINTSAQL
270–282	1478.7510	1478.7365	DTRTYPINTSAQL
288–300	1331.6578	1331.6470	TDPIGRTNAPSGF
306–321	1711.8518	1711.8206	FNNNAPSFSAIEAAIF
307–321	1564.7770	1564.7521	NNNAPSFSAIEAAIF
322–333	1460.7852	1460.7776	RPPHLLDFPEQL
343–350	966.3891	966.3865	SSTQHMNY
343–351	1152.4713	1152.4658	SSTQHMNYW
352–358	841.4564	841.4559	VGHRLNF
357–365	973.5396	973.5345	NFRPIGGTL
357–372	1674.8903	1674.8689	NFRPIGGTLNTSTQGL
359–372	1413.7706	1413.7576	RPIGGTLNTSTQGL
359–383	2568.3879	2568.3508	RPIGGTLNTSTQGLTNNTSINPVTL
366–383	1873.9648	1873.9381	NTSTQGLTNNTSINPVTL
366–385	2149.1120	2149.0651	NTSTQGLTNNTSINPVTLQF
373–383	1172.6118	1172.6037	TNNTSINPVTL
373–385	1447.7496	1447.7307	TNNTSINPVTLQF
384–391	1014.4805	1014.4771	QFTSRDVY
386–391	739.3506	739.3501	TSRDVY

Table 12. Identified Chymotryptic Peptides of DP910521 Maize-Derived Cry1B.34 Protein Using LC-MS Analysis (continued)

Matched Residue Position	Experimental Mass[a]	Theoretical Mass[b]	Identified Peptide Sequence
392–403	1321.6743	1321.6626	RTESNAGTNILF
416–424	1121 5588	1121.5505	NFINPQNIY
416–431	1899.9396	1899.9115	NFINPQNIYERGATTY
418–424	860.4429	860.4392	INPQNIY
418–431	1638.822	1638.8002	INPQNIYERGATTY
425–431	796.3718	796.3715	ERGATTY
443–462	2403.1051	2403.039	FDSETELPPETTERPNYESY
444–462	2255.9960	2255.9706	DSETELPPETTERPNYESY
463–471	1018.5702	1018.5672	SHRLSHIGL
463–477	1629.9508	1629.9315	SHRLSHIGLIIGNTL
478–484	877.4472	877.4446	RAPVYSW
485–491	784.4193	784.4191	THRSATL
492–505	1622.8850	1622.8628	TNTIDPERINQIPL
492–509	2054.1427	2054.1160	TNTIDPERINQIPLVKGF
513–529	1547.8074	1547.7832	GGTSVITGPGFTGGDIL
530–540	1310.6799	1310.6731	RRNTFGDFVSL
535–552	2050.0887	2050.0484	GDFVSLQVNINSPITQRY
541–552	1431.7197	1431.7470	QVNINSPITQRY
557–569	1504.8549	1504.8474	RYASSRDARVIVL
570–587	1644.8374	1644.8141	TGAASTGVGGQVSVNMPL
570–597	2788.4247	2788.3735	TGAASTGVGGQVSVNMPLQKTMEIGENL
588–597	1161 5768	1161.5699	QKTMEIGENL.T
603–611	1145 5225	1145.5142	RYTDFSNPF
612–627	1755.9439	1755.9155	SFRANPDIIGISEQPL
612–628	1903.0133	1902.9839	SFRANPDIIGISEQPLF
614–627	1521.8275	1521.8151	RANPDIIGISEQPL
614–628	1668.9107	1668.8835	RANPDIIGISEQPLF
614–638	2527.3392	2527.2918	RANPDIIGISEQPLFGAGSISSGEL
639–652	1623.9001	1623.8759	YIDKIEIILADATF
640–652	1460.8221	1460.8126	IDKIEIILADATF
653–668	1643.8278	1643.8114	EAESDLERAQKAGAGL
653–669	1790.8955	1790.8799	EAESDLERAQKAGAGLF
669–683	1783.9025	1783.8853	FTRTRDGLQVNVTDY
670–683	1636.8273	1636.8169	TRTRDGLQVNVTDY
684–695	1344.6940	1344.6820	QVDRAANLVSCL
684–700	1966.9051	1966.9054	QVDRAANLVSCLSDEQY
701–707	857.4427	857.4429	SHDKKML
708–717	1143.6533	1143.6546	MEAVRAAKRL
741–754	1388.7418	1388.7300	KASNGIIISEGGPF
741–755	1535.8214	1535.7984	KASNGIIISEGGPFF
755–760	718.3750	718.4490	FKGRVL
761–772	1411.6840	1411.6732	QLASARENYPTY
761–774	1687.8404	1687.8205	QLASARENYPTYIY
763–772	1170 5355	1170.5305	ASARENYPTY
763–774	1446.6910	1446.6779	ASARENYPTYIY
773–782	1134.6322	1134.6285	IYQKVDASVL
773–785	1522.8492	1522.8395	IYQKVDASVLKPY
775–782	858.4816	858.4811	QKVDASVL
775–785	1246.6949	1246.6921	QKVDASVLKPY
794–812	2225.1942	2225.1804	VKSSEDLEIDLVHQHKVHL
813–820	897.4949	897.4920	VKNVPDNL
865–882	1954.9298	1954.8909	SSYINTGDLNSSVDQGIW
868–882	1617.7874	1617.7635	INTGDLNSSVDQGIW
883–893	1219.6949	1219.6925	VVLKVRTADGY
883–896	1504.8698	1504.8613	VVLKVRTADGYATL
886–896	1193.6436	1193.6404	KVRTADGYATL
897–907	1138.6331	1138.6234	GNLELVEVGPL

Table 12. Identified Chymotryptic Peptides of DP910521 Maize-Derived Cry1B.34 Protein Using LC-MS Analysis (continued)

Matched Residue Position	Experimental Mass[a]	Theoretical Mass[b]	Identified Peptide Sequence
908–922	1803.8562	1803.8499	SGESLEREQRDNAKW
913–922	1330.6381	1330.6378	EREQRDNAKW
923–937	1777.8817	1777.8707	NAELGRERAETDRVY
923–938	1890.9772	1890.9547	NAELGRERAETDRVYL
927–937	1350.6690	1350.6640	GRERAETDRVY
927–938	1463.7604	1463.7481	GRERAETDRVYL
938–947	1077.6331	1077.6294	LAAKQAINHL
938–948	1224.6976	1224.6979	LAAKQAINHLF
939–947	964.5471	964.5454	AAKQAINHL
939–948	1111.6164	1111.6138	AKQAINHLF
939–951	1488.7819	1488.7725	AAKQAINHLFVDY
957–979	2431.2821	2431.2118	NPEIGLAEINEASNLVESITGVY
963–979	1807.9198	1807.8839	AEINEASNLVESITGVY
980–991	1291.6803	1291.6660	SDTVLQIPGISY
980–994	1696.8866	1696.8560	SDTVLQIPGISYEIY
985–994	1181.6075	1181.5968	QIPGISYEIY
992–1001	1237.6287	1237.6190	EIYTELSDRL
995–1001	832.4308	832.4290	TELSDRL
995–1006	1409.6924	1409.6786	TELSDRLQQASY
998–1006	1066.5377	1066.5043	SDRLQQASY
1009–1026	1967.8858	1967.8610	TSRNAVQNGDFDSGLDSW
1027–1042	1734.7447	1734.7268	NATTDASVQQDGNMHF
1027–1043	1847.8354	1847.8108	NATTDASVQQDGNMHFL
1027–1045	2060.0022	2059.9633	NATTDASVQQDGNMHFLVL
1043–1048	753.4186	753.4174	LVLSHW
1046–1056	1311.6317	1311.6208	SHWDAQVTQQL
1049–1056	901.4546	901.4505	DAQVTQQ
1065–1079	1546.8640	1546.8580	VLRVTARKVGGGDGY
1067–1079	1334.7085	1334.7055	RVTARKVGGGDGY
1067–1092	2820.5033	2820.4856	RVTARKVGGGDGYVTIRDGAHHRETL
1080–1092	1503.7939	1503.7906	VTIRDGAHHRETL
1080–1094	1751.9133	1751.9067	VTIRDGAHHRETLTF
1106–1118	1540.7956	1540.7773	VNDNTYITKEVVF
1112–1118	834.4876	834.4851	ITKEVVF
1112–1126	1885.9481	1885.9363	ITKEVVFYPHTEHTW
1112–1136	2920.4344	2920.3920	ITKEVVFYPHTEHTWVEVSESEGAF
1119–1126	1069.4656	1069.4617	YPHTEHTW
1119–1136	2103.9370	2103.9174	YPHTEHTWVEVSESEGAF
1119–1137	2267.0073	2266.9807	YPHTEHTWVEVSESEGAFY
1137–1148	1451.7218	1451.7031	YIDSIELIETQE
1138–1148	1288.6528	1288.6398	IDSIELIETQE

[a] The experimental mass is the uncharged mass calculated from the mass to charge ratio of the observed ion.
[b] The theoretical mass is the *in silico* generated mass that matches closest to the experimental mass.

Table 13. Combined Sequence Coverage of Identified Tryptic and Chymotryptic Peptides of DP910521 Maize-Derived Cry1B.34 Protein Using LC-MS Analysis

Protease	% Coverage	Combined % Sequence Coverage
Trypsin	79	93.8
Chymotrypsin	84	

```
   1  MAPSNRKNEN EIINAVSNHS AQMDLSLDAR IEDSLCVAEV NNIDPFVSAS
  51  TVQTGISIAG RILGVLGVPF AGQLASFYSF LVGELWPSGR DPWEIFLEHV
 101  EQLIRQQVTE NTRNTAIARL EGLGRGYRSY QQALETWLDN RNDARSRSII
 151  LERYVALELD ITTAIPLFSI RNQEVPLLMV YAQAANLHLL LLRDASLFGS
 201  EWGMSSADVN QYYQEQIRYT EEYSNHCVQW YNTGLNNLRG TNAESWLRYN
 251  QFRRDLTLGV LDLVALFPSY DTRTYPINTS AQLTREIYTD PIGRTNAPSG
 301  FASTNWFNNN APSFSAIEAA IFRPPHLLDF PEQLTIYSAS SRWSSTQHMN
 351  YWVGHRLNFR PIGGTLNTST QGLTNNTSIN PVTLQFTSRD VYRTESNAGT
 401  NILFTTPVNG VPWARFNFIN PQNIYERGAT TYSQPYQGVG IQLFDSETEL
 451  PPETTERPNY ESYSHRLSHI GLIIGNTLRA PVYSWTHRSA TLTNTIDPER
 501  INQIPLVKGF RVWGGTSVIT GPGFTGGDIL RRNTFGDFVS LQVNINSPIT
 551  QRYRLRFRYA SSRDARVIVL TGAASTGVGG QVSVNMPLQK TMEIGENLTS
 601  RTFRYTDFSN PFSFRANPDI IGISEQPLFG AGSISSGELY IDKIEIILAD
 651  ATFEAESDLE RAQKAGAGLF TRTRDGLQVN VTDYQVDRAA NLVSCLSDEQ
 701  YSHDKKMLME AVRAAKRLSR ERNLLQDPDF NEINSTEENG WKASNGIIIS
 751  EGGPFFKGRV LQLASARENY PTYIYQKVDA SVLKPYTRYR LDGFVKSSED
 801  LEIDLVHQHK VHLVKNVPDN LVSDTYPDGS CRGVNRCDEQ HQVDVQIDTE
 851  HHPMDCCEAA QTHEFSSYIN TGDLNSSVDQ GIWVVLKVRT ADGYATLGNL
 901  ELVEVGPLSG ESLEREQRDN AKWNAELGRE RAETDRVYLA AKQAINHLFV
 951  DYQDQQLNPE IGLAEINEAS NLVESITGVY SDTVLQIPGI SYEIYTELSD
1001  RLQQASYLYT SRNAVQNGDF DSGLDSWNAT TDASVQQDGN MHFLVLSHWD
1051  AQVTQQLRVN PNCKYVLRVT ARKVGGGDGY VTIRDGAHHR ETLTFNACDY
1101  DVNGTYVNDN TYITKEVVFY PHTEHTWVEV SESEGAFYID SIELIETQE
```

Red/shaded type	Bold red type indicates maize-derived Cry1B.34 peptides identified using LC-MS analysis. The gray-shaded N-terminal methionine is included in the Cry1B.34 sequence deduced by the translation of the *cry*1B.34 gene but is not expected to be present in the Cry1B.34 protein for DP910521 maize and is not included in the 1148-amino acid sequence used in LC-MS analysis.
Amino acid residue abbreviations	alanine (A), aspartic acid (D), glutamic acid (E), phenylalanine (F), glycine (G), histidine (H), isoleucine (I), lysine (K), leucine (L), methionine (M), asparagine (N), proline (P), glutamine (Q), arginine (R), serine (S), threonine (T), tryptophan (W), tyrosine (Y), and valine (V).

Figure 30. Identified Tryptic and Chymotryptic Peptide Amino Acid Sequence of DP910521 Maize-Derived Cry1B.34 Protein Using LC-MS Analysis

Table 14. Identified Tryptic Peptides of Microbially Derived Cry1B.34 Protein Using LC-MS Analysis

Matched Residue Position	Experimental Mass[a]	Theoretical Mass[b]	Identified Peptide Sequence
5–28	2668.2911	2668.2874	KNENEIINAVSNHSAQMDLSLDAR
6–28	2540.1955	2540.1925	NENEIINAVSNHSAQMDLSLDAR
29–59	3261.6255	3261.6187	IEDSLCVAEVNNIDPFVSASTVQTGISIAGR
104–111	974.4781	974.4781	QQVTENTR
112–117	644.3633	644.3606	NTAIAR
118–123	643.3685	643.3653	LEGLGR
127–139	1622.7725	1622.7689	SYQQALETWLDNR
146–151	729.4406	729.4385	SIILER
192–216	2880.2695	2880.2661	DASLFGSEWGMSSADVNQYYQEQIR
217–237	2660.1780	2660.1714	YTEEYSNHCVQWYNTGLNNLR
238–246	1032.5013	1032.4988	GTNAESWLR
247–251	726.3483	726.3449	YNQFR
272–283	1363.7107	1363.7096	TYPINTSAQLTR
284–292	1062.5364	1062.5346	EIYTDPIGR
341–354	1787.8043	1787.7951	WSSTQHMNYWVGHR
414–425	1553.7589	1553.7626	FNFINPQNIYER
426–464	4447.0558	4447.0517	GATTYSQPYQGVGIQLFDSETELPPETTERPNYESYSHR
465–477	1405.8469	1405.8405	LSHIGLIIGNTLR
478–486	1115.5562	1115.5512	APVYSWTHR
487–498	1316.6560	1316.6572	SATLTNTIDPER
499–506	923.5832	923.5804	INQIPLVK
510–529	1989.0360	1989.0320	VWGGTSVITGPGFTGGDILR
531–550	2249.1521	2249.1441	NTFGDFVSLQVNINSPITQR
565–588	2325.2734	2325.2726	VIVLTGAASTGVGGQVSVNMPLQK
589–599	1249.5973	1249.5972	TMEIGENLTSR
603–613	1379.6139	1379.6146	YTDFSNPFSFR
614–641	2890.4647	2890.4600	ANPDIIGISEQPLFGAGSISSGELYIDK
642–659	2034.0204	2034.0157	IEIILADATFEAESDLER
663–670	791.4314	791.4290	AGAGLFTR
671–686	1877.9262	1877.9232	TRDGLQVNVTDYQVDR
673–686	1620.7727	1620.7744	DGLQVNVTDYQVDR
687–703	1935.8642	1935.8632	AANLVSCLSDEQYSHDK
687–704	2063.9617	2063.9582	AANLVSCLSDEQYSHDKK
705–711	848.4260	848.4248	MLMEAVR
721–740	2362.0604	2362.0713	NLLQDPDFNEINSTEENGWK
741–755	1535.7972	1535.7984	ASNGIIISEGGPFFK
758–765	856.5155	856.513	VLQLASAR
766–775	1317.6250	1317.6241	ENYPTYIYQK
776–786	1247.6930	1247.6874	VDASVLKPYTR
787–794	996.5450	996.5393	YRLDGFVK
789–794	677.3776	677.3748	LDGFVK
795–808	1648.8080	1648.8056	SSEDLEIDLVHQHK
814–830	1907.8315	1907.8320	NVPDNLVSDTYPDGSCR
835–885	5941.6096	5941.5989	CDEQHQVDVQIDTEHHPMDCCEAAQTHEFSSYINTGDLNSSVDQGIWVVLK
888–913	2689.3489	2689.3446	TADGYATLGNLELVEVGPLSGESLER
921–927	844.4216	844.4191	WNAELGR
928–934	875.4121	875.4097	ERAETDR
935–940	663.3985	663.3955	VYLAAK
1000–1010	1328.6716	1328.6724	LQQASYLYTSR
1057–1062	730.3450	730.3432	VNPNCK
1071–1082	1220.6567	1220.6514	KVGGGDGYVTIR
1072–1082	1092.5565	1092.5564	VGGGDGYVTIR
1083–1088	691.3183	691.3150	DGAHHR
1089–1113	2930.2850	2930.2916	ETLTFNACDYDVNGTYVNDNTYITK
1114–1147	4011.8659	4011.8578	EVVFYPHTEHTWVEVSESEGAFYIDSIELIETQE

[a] The experimental mass is the uncharged mass calculated from the mass to charge ratio of the observed ion.
[b] The theoretical mass is the *in silico* generated mass that matches closest to the experimental mass.

Table 15. Identified Chymotryptic Peptides of Microbially Derived Cry1B.34 Protein Using LC-MS Analysis

Matched Residue Position	Experimental Mass[a]	Theoretical Mass[b]	Identified Peptide Sequence
1–23	2580.2360	2580.2350	PSNRKNENEIINAVSNHSAQMDL
24–33	1117.5605	1117.5615	SLDARIEDSL
24–44	2376.1295	2376.1267	SLDARIEDSLCVAEVNNIDPF
26–33	917.4474	917.4454	DARIEDSL
26–44	2176.0168	2176.0106	DARIEDSLCVAEVNNIDPF
34–44	1276.5769	1276.5758	CVAEVNNIDPF
79–91	1510.7607	1510.7569	LVGELWPSGRDPW
80–91	1397.6739	1397.6728	VGELWPSGRDPW
80–94	1786.8702	1786.8679	VGELWPSGRDPWEIF
92–101	1255.6454	1255.6448	EIFLEHVEQL
95–101	866.4509	866.4498	LEHVEQL
102–118	1983.1006	1983.0973	IRQQVTENTRNTAIARL
119–125	750.3677	750.3660	EGLGRGY
126–135	1280.6148	1280.6149	RSYQQALETW
129–135	874.4207	874.4185	QQALETW
129–136	987.5037	987.5025	QQALETWL
136–149	1641.8984	1641.8910	LDNRNDARSRSIIL
136–152	2090.1039	2090.0980	LDNRNDARSRSIILERY
137–152	1977.0173	1977.0140	DNRNDARSRSIILERY
153–165	1367.7922	1367.7912	VALELDITTAIPL
156–165	1084.6032	1084.6016	ELDITTAIPL
166–175	1201.6466	1201.6455	FSIRNQEVPL
167–175	1054.5784	1054.5771	SIRNQEVPL
167–179	1576.8293	1576.8283	SIRNQEVPLLMVY (Oxidation -M)[c]
180–187	836.4511	836.4504	AQAANLHL
180–188	949.5352	949.5345	AQAANLHLL
190–196	820.4470	820.4443	LRDASLF
197–210	1529.6089	1529.6093	GSEWGMSSADVNQY
201–210	1070.4322	1070.4339	GMSSADVNQY
211–217	998.4830	998.4821	YQEQIRY
211–221	1520.6788	1520.6783	YQEQIRYTEEY
212–217	835.4205	835.4188	QEQIRY
212–221	1357.6149	1357.6150	QEQIRYTEEY
222–228	929.3818	929.3814	SNHCVQW
230–244	1645.7794	1645.7808	NTGLNNLRGTNAESW
234–245	1373.6692	1373.6687	NNLRGTNAESWL
237–244	919.4147	919.4148	RGTNAESW
237–245	1032.4986	1032.4988	RGTNAESWL
245–250	839.4310	839.4290	LRYNQF
269–281	1478.7351	1478.7365	DTRTYPINTSAQL
287–299	1331.6455	1331.6470	TDPIGRTNAPSGF
305–312	909.4002	909.3981	FNNNAPSF
305–320	1711.8202	1711.8206	FNNNAPSFSAIEAAIF
306–320	1564.7545	1564.7521	NNNAPSFSAIEAAIF
321–332	1460.7801	1460.7776	RPPHLLDFPEQL
336–341	692.3263	692.3242	SASSRW
342–349	966.3867	966.3865	SSTQHMNY
342–350	1152.4650	1152.4658	SSTQHMNYW
351–357	841.4550	841.4559	VGHRLNF
356–364	973.5359	973.5345	NFRPIGGTL
356–371	1674.8707	1674.8689	NFRPIGGTLNTSTQGL
358–364	712.4250	712.4232	RPIGGTL
358–371	1413.7574	1413.7576	RPIGGTLNTSTQGL
365–382	1873.9357	1873.9381	NTSTQGLTNNTSINPVTL
372–382	1172.6028	1172.6037	TNNTSINPVTL
372–384	1447.7324	1447.7307	TNNTSINPVTLQF
383–390	1014.4779	1014.4771	QFTSRDVY

Table 15. Identified Chymotryptic Peptides of Microbially Derived Cry1B.34 Protein Using LC-MS Analysis (continued)

Matched Residue Position	Experimental Mass[a]	Theoretical Mass[b]	Identified Peptide Sequence
385–390	739.3523	739.3501	TSRDVY
391–401	1174.5959	1174.5942	RTESNAGTNIL
391–402	1321.6620	1321.6626	RTESNAGTNILF
415–423	1121.5511	1121.5505	NFINPQNIY
417–423	860.4408	860.4392	INPQNIY
424–430	796.3728	796.3715	ERGATTY
435–442	860.4776	860.4756	QGVGIQLF
443–461	2255.9694	2255.9706	DSETELPPETTERPNYESY
462–470	1018.5725	1018.5672	SHRLSHIGL
466–476	1136.6548	1136.6554	SHIGLIIGNTL
477–483	877.4460	877.4446	RAPVYSW
484–490	784.4214	784.4191	THRSATL
491–504	1622.8639	1622.8628	TNTIDPERINQIPL
512–522	991.4986	991.4975	GGTSVITGPGF
512–528	1547.7876	1547.7832	GGTSVITGPGFTGGDIL
540–551	1431.7459	1431.7470	QVNINSPITQRY
558–568	1185.6821	1185.6830	ASSRDARVIVL
569–586	1644.8155	1644.8141	TGAASTGVGGQVSVNMPL
587–596	1161.5688	1161.5699	QKTMEIGENL
602–610	1145.5143	1145.5142	RYTDFSNPF
611–626	1755.9189	1755.9155	SFRANPDIIGISEQPL
613–626	1521.8167	1521.8151	RANPDIIGISEQPL
613–627	1668.8875	1668.8835	RANPDIIGISEQPLF
613–637	2527.2968	2527.2918	RANPDIIGISEQPLFGAGSISSGEL
627–638	1186.5501	1186.5506	FGAGSISSGELY
638–651	1623.8784	1623.8759	YIDKIEIILADATF
639–646	955.5970	955.5954	IDKIEIIL
639–651	1460.813	1460.8126	IDKIEIILADATF
652–668	1790.8825	1790.8799	EAESDLERAQKAGAGLF
669–682	1636.8164	1636.8169	TRTRDGLQVNVTDY
683–690	885.4683	885.4668	QVDRAANL
683–694	1344.6826	1344.6820	QVDRAANLVSCL
691–699	1099.4481	1099.4492	VSCLSDEQY
740–753	1388.7280	1388.7300	KASNGIIISEGGPF
754–759	718.4511	718.4490	FKGRVL
760–771	1411.6730	1411.6732	QLASARENYPTY
760–773	1687.8234	1687.8205	QLASARENYPTYIY
762–771	1170.5293	1170.5305	ASARENYPTY
762–773	1446.6787	1446.6779	ASARENYPTYIY
772–781	1134.6273	1134.6285	IYQKVDASVL
772–784	1522.8417	1522.8395	IYQKVDASVLKPY
774–781	858.4818	858.4811	QKVDASVL
774–784	1246.6967	1246.6921	QKVDASVLKPY
812–819	897.4933	897.4920	VKNVPDNL
864–881	1954.8904	1954.8909	SSYINTGDLNSSVDQGIW
867–881	1617.7657	1617.7635	INTGDLNSSVDQGIW
882–892	1219.6953	1219.6925	VVLKVRTADGY
885–895	1193.6435	1193.6404	KVRTADGYATL
896–906	1138.6243	1138.6234	GNLELVEVGPL
907–921	1803.8487	1803.8499	SGESLEREQRDNAKW
912–921	1330.6421	1330.6378	EREQRDNAKW
922–936	1777.8729	1777.8707	NAELGRERAETDRVY
926–936	1350.6671	1350.6640	GRERAETDRVY
937–946	1077.6289	1077.6294	LAAKQAINHL
937–947	1224.7031	1224.6979	LAAKQAINHLF
938–947	1111.6139	1111.6138	AAKQAINHLF
962–978	1807.8866	1807.8839	AEINEASNLVESITGVY

Table 15. Identified Chymotryptic Peptides of Microbially Derived Cry1B.34 Protein Using LC-MS Analysis (continued)

Matched Residue Position	Experimental Mass[a]	Theoretical Mass[b]	Identified Peptide Sequence
971–978	866.4410	866.4386	VESITGVY
979–990	1291.6678	1291.6660	SDTVLQIPGISY
979–993	1696.8585	1696.8560	SDTVLQIPGISYEIY
984–993	1181.5963	1181.5968	QIPGISYEIY
991–996	766.3768	766.3749	EIYTEL
991–1000	1237.6179	1237.6190	EIYTELSDRL
994–1000	832.4308	832.4290	TELSDRL
994–1005	1409.6770	1409.6786	TELSDRLQQASY
997–1005	1066.5032	1066.5043	SDRLQQASY
1008–1025	1967.8584	1967.8610	TSRNAVQNGDFDSGLDSW
1026–1041	1734.7264	1734.7268	NATTDASVQQDGNMHF
1026–1042	1847.8101	1847.8108	NATTDASVQQDGNMHFL
1026–1044	2059.9662	2059.9633	NATTDASVQQDGNMHFLVL
1042–1047	753.4179	753.4174	LVLSHW
1043–1047	640.3363	640.3333	VLSHW
1045–1055	1311.6192	1311.6208	SHWDAQVTQQL
1048–1055	901.4523	901.4505	DAQVTQQL
1056–1063	1049.5077	1049.5076	RVNPNCKY
1079–1091	1503.7959	1503.7906	VTIRDGAHHRETL
1092–1104	1538.5938	1538.5984	TFNACDYDVNGTY
1094–1104	1290.4731	1290.4823	NACDYDVNGTY
1111–1117	834.4873	834.4851	ITKEVVF
1111–1125	1885.9421	1885.9363	ITKEVVFYPHTEHTW
1118–1125	1069.4665	1069.4617	YPHTEHTW
1118–1135	2103.9199	2103.9174	YPHTEHTWVEVSESEGAF
1118–1136	2266.9823	2266.9807	YPHTEHTWVEVSESEGAFY
1126–1135	1052.4668	1052.4662	VEVSESEGAF
1126–1136	1215.5290	1215.5295	VEVSESEGAFY
1136–1147	1451.7053	1451.7031	YIDSIELIETQE
1137–1147	1288.6399	1288.6398	IDSIELIETQE

[a] The experimental mass is the uncharged mass calculated from the mass to charge ratio of the observed ion.
[b] The theoretical mass is the *in silico* generated mass that matches closest to the experimental mass.
[c] This peptide was modified by methionine oxidation (Oxidation-M).

Table 16. Combined Sequence Coverage of Identified Tryptic and Chymotryptic Peptides of Microbially Derived Cry1B.34 Protein Using LC-MS Analysis

Protease	% Coverage	Combined % Coverage
Trypsin	65	90.8
Chymotrypsin	77	

```
1    PSNRKNENEI INAVSNHSAQ MDLSLDARIE DSLCVAEVNN IDPFVSASTV
51   QTGISIAGRI LGVLGVPFAG QLASFYSFLV GELWPSGRDP WEIFLEHVEQ
101  LIRQQVTENT RNTAIARLEG LGRGYRSYQQ ALETWLDNRN DARSRSIILE
151  RYVALELDIT TAIPLFSIRN QEVPLLMVYA QAANLHLLLL RDASLFGSEW
201  GMSSADVNQY YQEQIRYTEE YSNHCVQWYN TGLNNLRGTN AESWLRYNQF
251  RRDLTLGVLD LVALFPSYDT RTYPINTSAQ LTREIYTDPI GRTNAPSGFA
301  STNWFNNNAP SFSAIEAAIF RPPHLLDFPE QLTIYSASSR WSSTQHMNYW
351  VGHRLNFRPI GGTLNTSTQG LTNNTSINPV TLQFTSRDVY RTESNAGTNI
401  LFTTPVNGVP WARFNFINPQ NIYERGATTY SQPYQGVGIQ LFDSETELPP
451  ETTERPNYES YSHRLSHIGL IIGNTLRAPV YSWTHRSATL TNTIDPERIN
501  QIPLVKGFRV WGGTSVITGP GFTGGDILRR NTFGDFVSLQ VNINSPITQR
551  YRLRFRYASS RDARVIVLTG AASTGVGGQV SVNMPLQKTM EIGENLTSRT
601  FRYTDFSNPF SFRANPDIIG ISEQPLFGAG SISSGELYID KIEIILADAT
651  FEAESDLERA QKAGAGLFTR TRDGLQVNVT DYQVDRAANL VSCLSDEQYS
701  HDKKMLMEAV RAAKRLSRER NLLQDPDFNE INSTEENGWK ASNGIIISEG
751  GPFFKGRVLQ LASARENYPT YIYQKVDASV LKPYTRYRLD GFVKSSEDLE
801  IDLVHQHKVH LVKNVPDNLV SDTYPDGSCR GVNRCDEQHQ VDVQIDTEHH
851  PMDCCEAAQT HEFSSYINTG DLNSSVDQGI WVVLKVRTAD GYATLGNLEL
901  VEVGPLSGES LEREQRDNAK WNAELGRERA ETDRVYLAAK QAINHLFVDY
951  QDQQLNPEIG LAEINEASNL VESITGVYSD TVLQIPGISY EIYTELSDRL
1001 QQASYLYTSR NAVQNGDFDS GLDSWNATTD ASVQQDGNMH FLVLSHWDAQ
1051 VTQQLRVNPN CKYVLRVTAR KVGGGDGYVT IRDGAHHRET LTFNACDYDV
1101 NGTYVNDNTY ITKEVVFYPH TEHTWVEVSE SEGAFYIDSI ELIETQE
```

Red type	Red type indicates microbially-derived Cry1B.34 peptides identified using LC-MS analysis.
Amino acid residue abbreviations	alanine (A), cysteine (C), aspartic acid (D), glutamic acid (E), phenylalanine (F), glycine (G), histidine (H), isoleucine (I), lysine (K), leucine (L), methionine (M), asparagine (N), proline (P), glutamine (Q), arginine (R), serine (S), threonine (T), tryptophan (W), tyrosine (Y), and valine (V).

Figure 31. Identified Tryptic and Chymotryptic Peptide Amino Acid Sequence of Microbially Derived Cry1B.34 Protein Using LC-MS Analysis

N-Terminal Amino Acid Sequence Analysis

The Edman sequencing analysis of the DP910521 maize-derived Cry1B.34 sample identified an N-terminal sequence (APS). In addition, the N-terminal peptide (APSNRKNENEIINAVSNHSAQMDL) was identified from the chymotryptic digestion of the DP910521 maize-derived protein using LC-MS analysis (Table 12 and Table 17), indicating the N-terminal methionine was absent as expected (Dummitt et al., 2003; Sherman et al., 1985). The analysis of the microbially derived Cry1B.34 protein using Edman sequencing identified an N-terminal sequence (PSNRKNENEI). Additionally, the N-terminal peptide (PSNRKNENEIINAVSNHSAQMDL) was identified from the chymotryptic digestion of the microbially derived protein using LC-MS analysis (Table 15 and Table 17), indicating the N-terminal methionine and next alanine are absent.

Additional details regarding N-terminal amino acid sequence analytical methods are provided in Appendix E.

Table 17. N-Terminal Amino Acid Sequence of the Cry1B.34 Protein

Description		Amino Acid Sequence
DP910521 Maize-Derived Cry1B.34 Protein	Deduced Sequence[a]	M – A – P – S – N – R – K – N – E – N – E – I – I – N – A – V – S – N – H – S – A – Q – M – D – L
	Identified Sequence	A – P – S – N – R – K – N – E – N – E – I – I – N – A – V – S – N – H – S – A – Q – M – D – L
Microbially Derived Cry1B.34 Protein	Identified Sequence	P – S – N – R – K – N – E – N – E – I – I – N – A – V – S – N – H – S – A – Q – M – D – L

[a] The deduced Cry1B.34 protein sequence is a result of the translation of the gene.

Bioactivity assay

The bioactivity of the microbially derived Cry1B.34 protein was evaluated by conducting a 7-day bioassay using *Spodoptera frugiperda* (fall armyworm; Lepidoptera: Noctuidae), a species sensitive to the Cry1B.34 protein.

Bioactivity analysis demonstrated that the microbially derived Cry1B.34 protein had insecticidal activity toward a target insect, *S. frugiperda* (Table 18). The biological activity of the test diets containing 1.563 - 12.5 ng Cry1B.34 protein was demonstrated by the increased mortality and decreased weight of *S. frugiperda* fed the test diets. The biological activity of the test diets containing 25 and 50 ng Cry1B.34 protein was demonstrated by 100% mortality of *S. frugiperda* fed the test diet.

Additional details are provided in Appendix E.

Table 18. Microbially Derived Cry1B.34 Protein Bioactivity Assay Using *Spodoptera frugiperda*

Treatment	Treatment Description	Protein Concentration (ng Cry1B.34/mg)	Total Number of Observations	Mortality (%)	Number of Surviving Organisms	Weight of Surviving Organisms (mg)	
						Mean ± Standard Deviation	Range
1	Buffer Control Diet	0	20	10	18	36.6 ± 7.5	22.5 - 49.0
2	Test Diet	1.563	20	15	17	0.6 ± 0.4	0.2 - 1.7
3	Test Diet	3.125	20	25	15	0.3 ± 0.3	0.1 - 1.3
4	Test Diet	6.25	20	50	10	0.1 ± 0.1	0 - 0.2
5	Test Diet	12.5	20	85	3	0.1 ± 0.1	0.1 - 0.2
6	Test Diet	25	19[a]	100	0	NA	NA
7	Test Diet	50	19[a]	100	0	NA	NA

Note: The concentration of the Cry1B.34 protein in Treatments 2-7 was based on the wet weight of the artificial diet. The summary of *Spodoptera frugiperda* mortality data consisted of the calculation of dead larvae divided by the total number of observed larvae at the end of the study and multiplied by 100. Not applicable (NA); there were no surviving organisms in this diet group.

[a] Organisms counted as missing during the bioassay were not included in the total number of observations for a given treatment.

Allergenicity and Toxicity Analyses of the Cry1B.34 Protein

A weight-of-evidence approach was applied to determine the allergenic and toxic potentials of the Cry1B.34 protein expressed in DP910521 maize, including an assessment of the following: a bioinformatic comparison of the amino acid sequence of the Cry1B.34 protein to known or putative protein allergen and toxin sequences, evaluation of the stability of the Cry1B.34 protein using *in vitro* gastric and intestinal digestion models, determination of the Cry1B.34 protein glycosylation status, evaluation of the heat lability of the Cry1B.34 protein using a sensitive insect bioassay, and an evaluation of acute toxicity in mice following oral exposure to the Cry1B.34 protein.

Bioinformatic Analysis of Homology to Known or Putative Allergens (PHI-2021-195/225 and PHI-2021-106/201 studies)

Assessing newly expressed proteins for potential cross-reactivity with known or putative allergens is an important part of the weight-of-evidence approach used to evaluate the safety of these proteins in genetically-modified plant products (Codex Alimentarius Commission, 2003). A bioinformatic assessment of the Cry1B.34 protein sequence for potential cross-reactivity with known or putative allergens was conducted according to relevant guidelines (Codex Alimentarius Commission, 2003; FAO/WHO, 2001).

Two separate searches for the Cry1B.34 protein sequence were performed using the Comprehensive Protein Allergen Resource (COMPARE) 2021 database (January 2021) available at http://comparedatabase.org. This peer-reviewed database is a collaborative effort of the Health and Environmental Sciences Institute (HESI) Protein Allergens, Toxins, and Bioinformatics (PATB) Committee and is comprised of 2,348 sequences. The first search used the Cry1B.34 protein sequence as the query in a FASTA v35.4.4 (Pearson and Lipman, 1988) search against the allergen sequences. The search was conducted using default parameters, except the *E*-score threshold was set to 10^{-4}. An *E*-score threshold of 10^{-4} has been shown to be an appropriate value for allergenicity searches (Mirsky *et al.*, 2013). The generated alignments were examined to identify any that are 80 residues or longer and possess a sequence identity of greater than 35%. The second search used the FUZZPRO program (Emboss Package v6.4.0) to identify any contiguous 8-residue identical matches between the Cry1B.34 protein sequence and the allergen sequences.

Results of the search of the Cry1B.34 protein sequence against the COMPARE database of known and putative allergens found no alignments that were 80 residues or longer with a sequence identity of greater than 35%. No contiguous 8-residue matches between the Cry1B.34 protein sequence and the allergen sequences were identified in the second search. Collectively, these data indicate that no allergenicity concern arose from the bioinformatics assessment of the Cry1B.34 protein.

Collectively, these data indicate that no allergenicity concern arose from the bioinformatics assessment of the Cry1B.34 protein.

Bioinformatic Analysis of Homology to Known or Putative Toxins (PHI-2021-204/211 study)

Assessing newly expressed proteins for potential toxicity is a critical part of the weight-of-evidence approach used to evaluate the safety of these proteins in genetically modified plant products (Codex Alimentarius Commission, 2003). The potential toxicity of the Cry1B.34 protein was assessed by comparison of its sequence to the sequences in an internal toxin database. The internal toxin database is a subset of sequences found in UniProtKB/Swiss-Prot (https://www.uniprot.org/). To produce the internal toxin database, the proteins in UniProtKB/Swiss-Prot are filtered for molecular function by keywords that could imply toxicity or adverse health effects on humans (e.g., toxin, hemagglutinin, vasoactive, etc.). The internal toxin database is updated annually. The search between the Cry1B.34 protein sequence and protein sequences in the internal toxin database was conducted with BLASTP using default parameters, except that low complexity filtering was turned off, the E-value threshold was set to 10^{-4}, and unlimited alignments were returned.

No alignments with an E-value $\leq 10^{-4}$ were returned between the Cry1B.34 protein sequence and any protein sequence in the internal toxin database. Therefore, no human toxicity concern arose from the bioinformatics assessment of the Cry1B.34 protein.

Thermolability Analysis (PHI-2021-067 study)

Thermal stability of the Cry1B.34 protein was characterized by determining the biological activity of the heat-treated Cry1B.34 protein when incorporated in an artificial diet and fed to *Spodoptera frugiperda*, an insect sensitive to the test substance. The Cry1B.34 protein was incubated at various temperatures for approximately 30-35 minutes before incorporation into the artificial diet. Larvae were exposed via oral ingestion to the diets in a 7-day bioassay. A positive control diet containing the unheated Cry1B.34 protein and a bioassay control diet containing buffer were included in the bioassay to verify assay performance. After seven days, statistical analyses were conducted to evaluate *S. frugiperda* mortality of the heat-treated test groups relative to the unheated test group.

The results demonstrated that Cry1B.34 protein heated for approximately 30 minutes at temperatures of 75 °C or higher were inactive against *S. frugiperda* when incorporated in an artificial insect diet (Table 19).

Additional details regarding thermolability analytical methods are provided in Appendix E.

Table 19. Biological Activity of Heat-Treated Cry1B.34 Protein in Artificial Diet Fed to *Spodoptera frugiperda*

Treatment	Treatment Description	Test Dosing Solution Incubation Condition	Total Number of Observations	Mortality (%)	Fisher's Test P-Value	Number of Surviving Organisms	Weight of Surviving Organisms (mg)	
							Mean ± Standard Deviation	Range
1	Buffer Control Diet	NA	20	0	--	20	36.7 ± 13.9	2.3 - 50.1
2	Unheated Control Diet	Unheated	20	100	--	0	NA	NA
3	Test Diet	25 °C	20	100	1.0000	0	NA	NA
4	Test Diet	50 °C	20	95.0	0.5000	1	0.100[a]	NA
5	Test Diet	75 °C	20	0	<0.0001[b]	20	13.8 ± 7.88	0.2 - 34.7
6	Test Diet	95 °C	20	0	<0.0001[b]	20	41.1 ± 8.55	24.0 - 59.4

Note: The unheated control diet and the test diets contained a targeted concentration of 25 ng Cry1B.34 protein per mg diet wet weight. Not applicable (NA).

[a] The reported mean is the weight value of the one surviving larva after the 7-day feeding period.

[b] A statistically significant difference (P-value < 0.05) was observed in comparison to Treatment 2.

Digestibility Analysis with Simulated Gastric Fluid (PHI-2021-055 study)

Simulated gastric fluid (SGF) containing pepsin at pH ~1.2 was used to assess the susceptibility of the Cry1B.34 protein to proteolytic digestion by pepsin *in vitro*. The Cry1B.34 protein was incubated in SGF for 0, 0.5, 1, 2, 5, 10, 20, and 60 minutes. A positive control (bovine serum albumin) and a negative control (β-lactoglobulin) were included in the assay and were incubated in SGF for 0, 1, and 60 minutes. After incubation in SGF, the samples were analyzed by SDS-PAGE. Coomassie-based stain or western blot was used to detect protein bands.

A summary of the SGF results is provided in Table 20. The Cry1B.34 protein migrating at 129 kDa was digested (within 0.5 minutes) in SGF as demonstrated by both SDS-PAGE and western blot analysis (Table 19 and Table 20). A band migrating at ~20 kDa was digested within 5 minutes in SGF. On the SDS-PAGE gel, low molecular weight bands (~2-5 kDa) remained detectable in the Cry1B.34 protein samples for up to 60 minutes in SGF. As expected, the BSA control was digested within 1 minute and low molecular weight bands remained detectable at 60 minutes. The β-lactoglobulin control remained detectable after 60 minutes in SGF.

Additional details regarding SGF analytical methods are provided in Appendix E.

Table 20. Summary of Cry1B.34 Protein *In Vitro* Pepsin Resistance Analyses

Protein	Approximate Molecular Weight (kDa)	Digestion Time Determined by SDS-PAGE (minutes)	Digestion Time Determined by Western Blot (minutes)
Cry1B.34	129	< 0.5	< 0.5
Bovine Serum Albumin	66	< 1	NA
β-lactoglobulin	18	> 60	NA

Note: kilodalton (kDa), sodium dodecyl sulfate polyacrylamide gel electrophoresis (SDS-PAGE), and not applicable (NA).

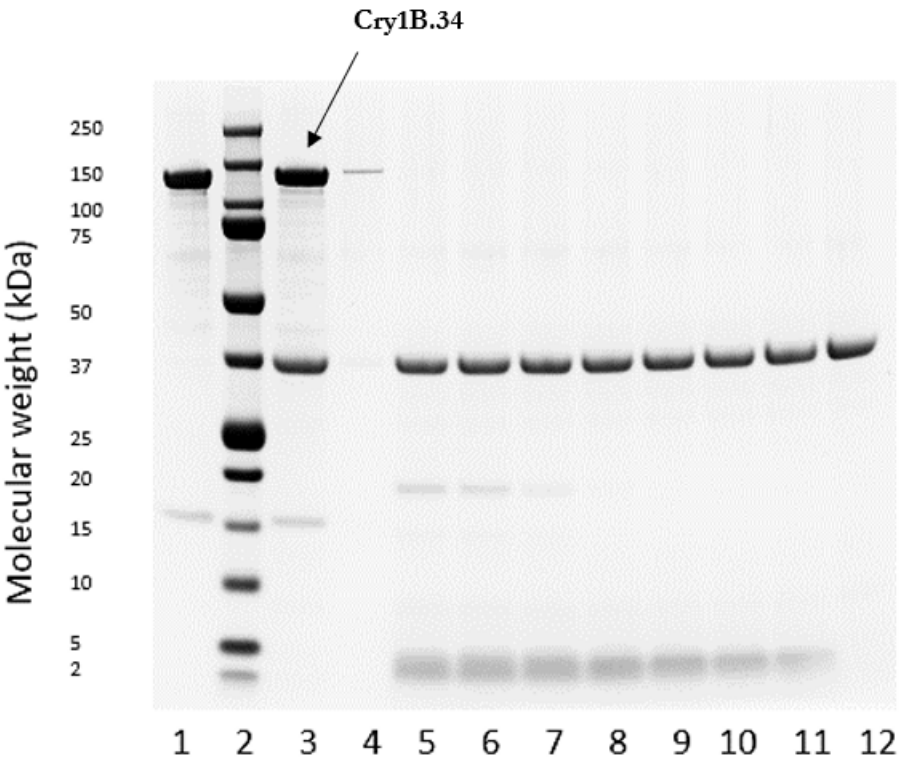

Lane	Sample Descriptions
1	Cry1B.34 protein in 10 mM CAPS buffer (no SGF), Time 0
2	Pre-stained protein molecular weight marker[a]
3	Cry1B.34 protein in SGF, Time 0
4	Cry1B.34 protein in SGF, Time 0; 1:20 dilution
5	Cry1B.34 protein in SGF, 0.5 minutes
6	Cry1B.34 protein in SGF, 1 minute
7	Cry1B.34 protein in SGF, 2 minutes
8	Cry1B.34 protein in SGF, 5 minutes
9	Cry1B.34 protein in SGF, 10 minutes
10	Cry1B.34 protein in SGF, 20 minutes
11	Cry1B.34 protein in SGF, 60 minutes
12	SGF Control, 60 minutes

Note: kilodalton (kDa), simulated gastric fluid (SGF), sodium dodecyl sulfate polyacrylamide gel electrophoresis (SDS-PAGE).

[a] Molecular weight markers were included to provide a visual estimate that migration was within the expected range of the predicted molecular weight.

Figure 32. SDS-PAGE Analysis of Cry1B.34 Protein in Simulated Gastric Fluid Digestion Time Course

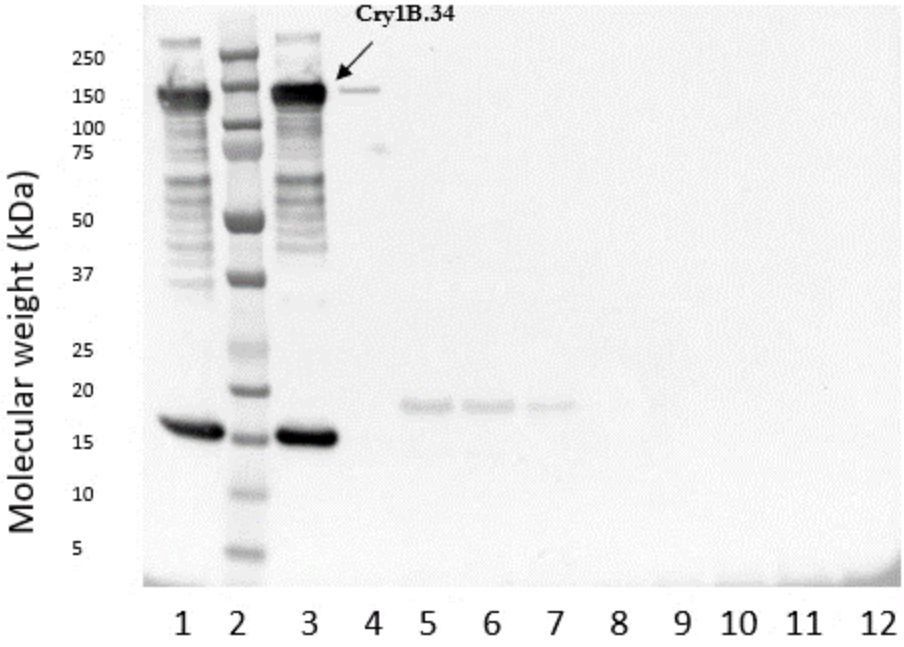

Lane	Sample Descriptions
1	Cry1B.34 protein in 10 mM CAPS buffer (no SGF), Time 0
2	Pre-stained protein molecular weight marker[a]
3	Cry1B.34 protein in SGF, Time 0
4	Cry1B.34 protein in SGF, Time 0; 1:200 dilution
5	Cry1B.34 protein in SGF, 0.5 minutes
6	Cry1B.34 protein in SGF, 1 minute
7	Cry1B.34 protein in SGF, 2 minutes
8	Cry1B.34 protein in SGF, 5 minutes
9	Cry1B.34 protein in SGF, 10 minutes
10	Cry1B.34 protein in SGF, 20 minutes
11	Cry1B.34 protein in SGF, 60 minutes
12	SGF Control, 60 minutes

Note: kilodalton (kDa) and simulated gastric fluid (SGF).

[a] Molecular weight markers were included to provide a visual estimate that migration was within the expected range of the predicted molecular weight.

Figure 33. Western Blot Analysis of Cry1B.34 Protein in Simulated Gastric Fluid Digestion Time Course

Digestibility Analysis with Simulated Intestinal Fluid (PHI-2021-078 study)

Simulated intestinal fluid (SIF) containing pancreatin at ~pH 7.5 was used to assess the susceptibility of the Cry1B.34 protein to proteolytic digestion by pancreatin *in vitro*. The Cry1B.34 protein was incubated in SIF for 0, 0.5, 1, 2, 5, 10, 20, 30, and 60 minutes. A positive control (β-lactoglobulin) and a negative control (bovine serum albumin) were included in the assay and were incubated in SIF for 0, 1, and 60 minutes. After incubation in SIF, the samples were analyzed by SDS-PAGE. Coomassie-based stain or western blot was used to detect protein bands.

A summary of the SIF assay results is provided in Table 21. The Cry1B.34 protein migrating at ~129 kDa was digested into smaller fragments migrating at less than 75 kDa within 0.5 minutes in SIF as was evident on the stained SDS-PAGE gel and within 1 minute as was evident on the western blot (Figure 34 and Figure 35, respectively). These smaller fragments remained detectable for up to 60 minutes. As expected, the β-lactoglobulin control was digested within 60 minutes in SIF. The BSA control remained detectable after 60 minutes in SIF.

Additional details regarding SIF analytical methods are provided in Appendix E.

Table 21. Summary of Cry1B.34 Protein *In Vitro* Pancreatin Resistance Analyses

Protein	Approximate Molecular Weight (kDa)	Digestion Time Determined by SDS-PAGE (minutes)	Digestion Time Determined by Western Blot (minutes)
Cry1B.34	129	< 0.5[a]	< 1
β-lactoglobulin	18	< 60	NA
Bovine Serum Albumin	66	> 60	NA

Note: kilodalton (kDa), sodium dodecyl sulfate polyacrylamide gel electrophoresis (SDS-PAGE), and not applicable (NA).

[a] The full-length Cry1B.34 protein migrating at ~129 kDa was digested into smaller fragments migrating at less than 75 kDa; these smaller fragments remained detectable for up to 60 minutes in simulated intestinal fluid (SIF).

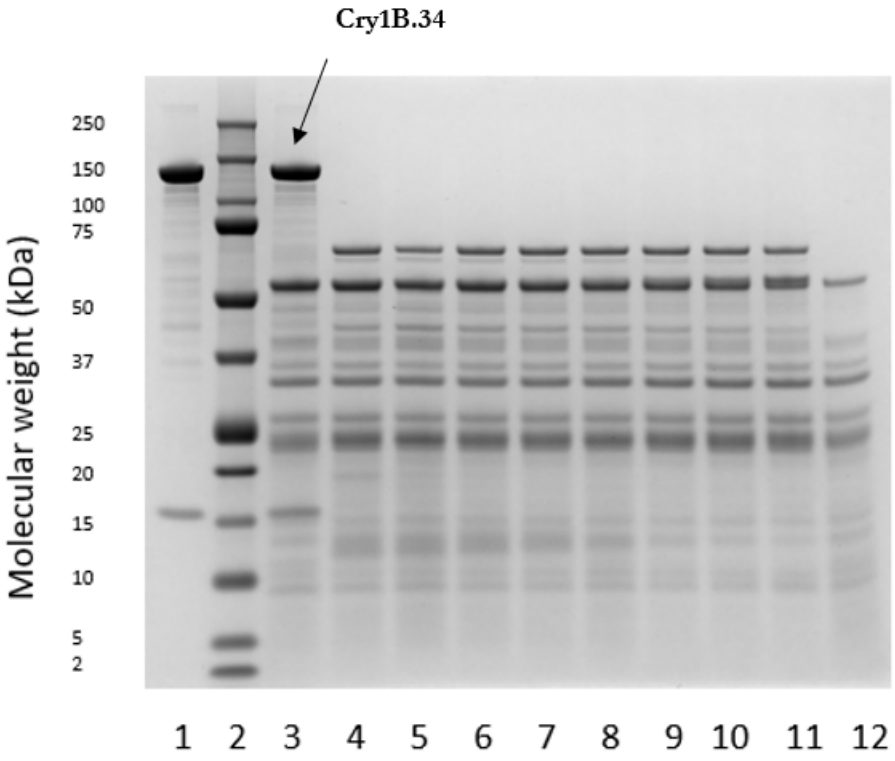

Lane	Sample Descriptions
Lane	**Sample Descriptions**
1	Cry1B.34 protein in 10 mM CAPS buffer (no SIF), Time 0
2	Pre-stained protein molecular weight markera
3	Cry1B.34 protein in SIF, Time 0
4	Cry1B.34 protein in SIF, 0.5 minutes
5	Cry1B.34 protein in SIF, 1 minute
6	Cry1B.34 protein in SIF, 2 minutes
7	Cry1B.34 protein in SIF, 5 minutes
8	Cry1B.34 protein in SIF, 10 minutes
9	Cry1B.34 protein in SIF, 20 minutes
10	Cry1B.34 protein in SIF, 30 minutes
11	Cry1B.34 protein in SIF, 60 minutes

Note: kilodalton (kDa), simulated intestinal fluid (SIF), and sodium dodecyl sulfate polyacrylamide gel electrophoresis (SDS-PAGE).

[a] Molecular weight markers were included to provide a visual estimate that migration was within the expected range of the predicted molecular weight

Figure 34. SDS-PAGE Analysis of Cry1B.34 Protein in Simulated Intestinal Fluid Digestion Time Course

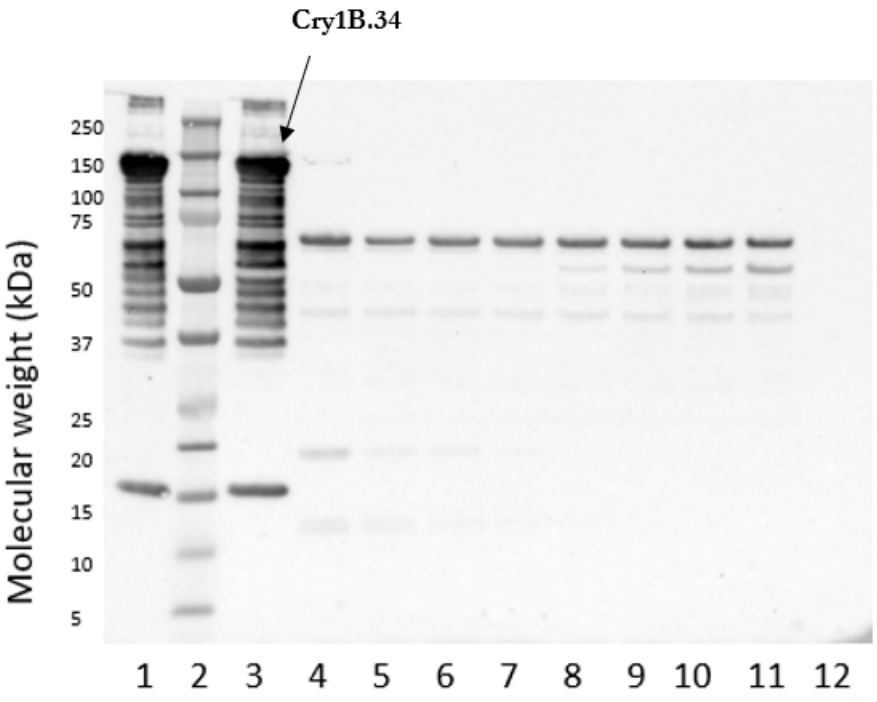

Lane	Sample Descriptions
1	Cry1B.34 protein in 10 mM CAPS buffer (no SIF), Time 0
2	Pre-stained protein molecular weight marker[a]
3	Cry1B.34 protein in SIF, Time 0
4	Cry1B.34 protein in SIF, 0.5 minutes
5	Cry1B.34 protein in SIF, 1 minute
6	Cry1B.34 protein in SIF, 2 minutes
7	Cry1B.34 protein in SIF, 5 minutes
8	Cry1B.34 protein in SIF, 10 minutes
9	Cry1B.34 protein in SIF, 20 minutes
10	Cry1B.34 protein in SIF, 30 minutes
11	Cry1B.34 protein in SIF, 60 minutes
12	SIF Control, 60 minutes

Note: kilodalton (kDa) and simulated intestinal fluid (SIF).

[a] Molecular weight markers were included to provide a visual estimate that migration was within the expected range of the predicted molecular weight.

Figure 35. Western Blot Analysis of Cry1B.34 Protein in Simulated Intestinal Fluid Digestion Time Course

Sequential Digestibility Analysis with Simulated Gastric Fluid (SGF) and Simulated Intestinal Fluid (SIF) (PHI-2021-056 study)

Sequential digestion in simulated intestinal fluid (SIF) following a digestion in SGF was used to assess the susceptibility of the low molecular weight SGF fragments (~2-5 kDa, Figure 32) of the Cry1B.34 protein. The Cry1B.34 protein was incubated for 10 minutes in SGF and then incubated for 0, 0.5, 1, 2, 5, 10, 20, and 30 minutes in SIF.

Sequential pepsin and pancreatin digestion results indicated the low molecular weight bands (~2-5 kDa) observed in SGF digestion (Figure 32) were digested within 0.5 minutes during sequential SIF digestion (Figure 36).

Additional details regarding analytical methods are provided in Appendix E.

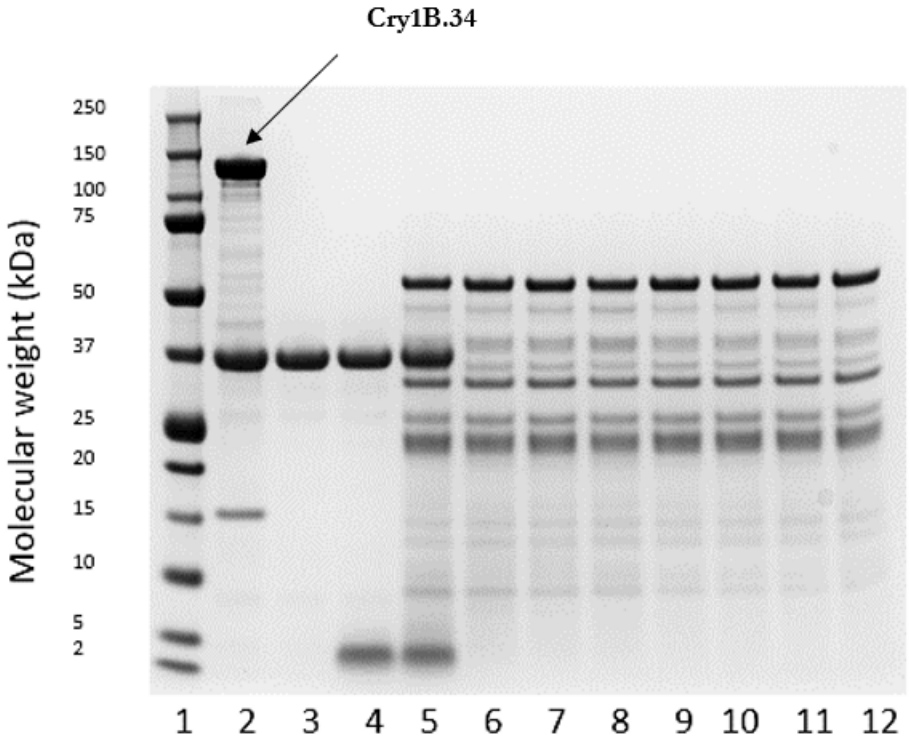

Lane	Sample Descriptions
1	Pre-stained protein molecular weight marker[a]
2	Cry1B.34 Protein in SGF, Time 0
3	SGF Control, 10 minutes
4	Cry1B.34 Protein in SGF, 10 minutes
5	Cry1B.34 Protein in SGF 10 minutes, SIF Time 0
6	Cry1B.34 Protein in SGF 10 minutes, SIF 0.5 minutes
7	Cry1B.34 Protein in SGF 10 minutes, SIF 1 minute
8	Cry1B.34 Protein in SGF 10 minutes, SIF 2 minutes
9	Cry1B.34 Protein in SGF 10 minutes, SIF 5 minutes
10	Cry1B.34 Protein in SGF 10 minutes, SIF 10 minutes
11	Cry1B.34 Protein in SGF 10 minutes, SIF 20 minutes
12	Cry1B.34 Protein in SGF 10 minutes, SIF 30 minutes

Note: kilodalton (kDa), simulated gastric fluid (SGF), simulated intestinal fluid (SIF), and sodium dodecyl sulfate polyacrylamide gel electrophoresis (SDS-PAGE).

[a] Molecular weight markers were included to provide a visual estimate that migration was within the expected range of the predicted molecular weight.

Figure 36. SDS-PAGE Analysis of Cry1B.34 Protein in a Sequential Digestion with Simulated Gastric Fluid and Simulated Intestinal Fluid

Glycoprotein Analysis (PHI-2021-115 study)

As stated previously in the characterization section, the results from glycoprotein staining analysis confirmed the absence of glycosylation for the Cry1B.34 protein isolated and purified from DP910521 maize tissue.

Evaluation of the Acute Toxicity of Cry1B.34 Protein (PHI-2020-188 study)

A study was conducted to evaluate the potential acute toxicity of the test substance, Cry1B.34 protein, in [redacted] mice following oral exposure at the limit dose (5000 mg/kg body weight, adjusted for Cry1B.34 content). Cry1B.34 protein and Bovine Serum Albumin (BSA) protein were each reconstituted in deionized water. Vehicle control, BSA comparative control and Cry1B.34 test substance formulations were administered orally by gavage in three split doses, separated by approximately four hours; the BSA comparative control was administered at an equivalent target dose to that of the test substance. The mice were fasted prior to and throughout the dosing procedure.

Body weights were evaluated on test days 1 (prior to fasting and shortly prior to administration of the first dose), 2, 3, 5, 8, and 15. Clinical signs were evaluated ten times on test day 1 (distributed before and after each dose) and daily thereafter. On test day 15, all surviving mice were euthanized and given a gross pathological examination.

All animals survived to scheduled euthanasia. There were no test substance-related clinical observations and all animals gained weight during the 2-week observation period prior to euthanasia. No gross lesions were observed in this study.

Under the conditions of this study, intragastric exposure of Cry1B.34 protein to male and female mice at 5000 mg/kg body weight did not result in mortality or other evidence of acute oral toxicity, based on evaluation of body weight, clinical signs, and gross pathology. Therefore, the acute oral toxicity tolerant dose and the LD50 of Cry1B.34 protein was determined to be greater than 5000 mg/kg body weight.

Conclusions on the Safety of Cry1B.34 Protein in DP910521 Maize

In conclusion, protein characterization results via SDS-PAGE, western blot, glycosylation, mass spectrometry, and N-terminal amino acid sequence analysis have demonstrated that the Cry1B.34 protein derived from DP910521 maize is of the expected molecular weight, immunoreactivity, lack of glysoylation, and amino acid sequence. Characterization of the microbially derived Cry1B.34 protein demonstrated that it is an appropriate test substance for use in safety studies.

The allergenic and toxic potential of the Cry1B.34 protein was assessed using a bioinformatic comparison of the amino acid sequence of the Cry1B.34 protein to known or putative protein allergen and toxin sequences, evaluation of the stability of the Cry1B.34 protein using *in vitro* gastric and intestinal digestion models, determination of the Cry1B.34 protein glycosylation status, evaluation of the heat lability of the Cry1B.34 protein using a sensitive insect bioassay, and an evaluation of acute toxicity in mice following oral exposure to the Cry1B.34 protein.

The bioinformatic comparisons of the Cry1B.34 protein sequence to known and putative allergen and toxin sequences showed that the Cry1B.34 protein is unlikely to be allergenic or toxic for

humans. The Cry1B.34 protein migrating at ~129 kDa was digested within 0.5 minutes in SGF. The band migrating at ~20 kDa was digested within 5 minutes in SGF and some low molecular weight bands (~2-5 kDa) remained detectable in the Cry1B.34 protein samples for up to 60 minutes in SGF. The protein was digested in SIF, and some bands remained visible after 60 minutes. The low molecular weight bands remaining from SGF digestion were digested (< 0.5 minutes) in sequential SIF. The Cry1B.34 protein was not glycosylated. The Cry1B.34 protein heated for approximately 30 minutes at 75 °C or higher was inactive against *Spodoptera frugiperda* when incorporated in an artificial diet. The acute oral toxicity assessment determined the LD50 of the Cry1B.34 protein to be greater than 5000 mg/kg. These data support the conclusion that the Cry1B.34 protein in DP910521 maize is as safe as conventional maize for the food and feed supply.

Based on this weight of evidence, consumption of the Cry1B.34 protein is unlikely to cause an adverse effect on humans.

PAT protein

Amino Acid Sequence of the PAT Protein

The gene encoding the PAT protein in DP910521 maize, referred to as the *mo-pat* gene, was derived from *Streptomyces viridochromogenes* with codon-optimization for expression in maize. The deduced amino acid sequence from the translation of the *mo-pat* gene is identical to the deduced amino acid sequence from the translation of the *pat* gene. The PAT protein encoded by the *pat* and *mo-pat* genes is 183 amino acids in length and has a molecular weight of approximately 21 kDa (Figure 37).

```
PAT(pat)          1   MSPERRPVEI RPATAADMAA VCDIVNHYIE TSTVNFRTEP QTPQEWIDDL
PAT(mo-pat)   1       MSPERRPVEI RPATAADMAA VCDIVNHYIE TSTVNFRTEP QTPQEWIDDL

PAT(pat)      51      ERLQDRYPWL VAEVEGVVAG IAYAGPWKAR NAYDWTVEST VYVSHRHQRL
PAT(mo-pat)   51      ERLQDRYPWL VAEVEGVVAG IAYAGPWKAR NAYDWTVEST VYVSHRHQRL

PAT(pat)      101     GLGSTLYTHL LKSMEAQGFK SVVAVIGLPN DPSVRLHEAL GYTARGTLRA
PAT(mo-pat)   101     GLGSTLYTHL LKSMEAQGFK SVVAVIGLPN DPSVRLHEAL GYTARGTLRA

PAT(pat)      151     AGYKHGGWHD VGFWQRDFEL PAPPRPVRPV TQI*
PAT(mo-pat)   151     AGYKHGGWHD VGFWQRDFEL PAPPRPVRPV TQI*
```

Figure 37. Alignment of the Deduced Amino Acid Sequence of PAT Protein Encoded by *pat* and *mo-pat* Genes

Deduced amino acid sequence alignment, where PAT (*pat*) represents the deduced amino acid sequence from the translation of the *pat* gene that is found in a number of authorized events across several different crops that are currently commeralized and have a history of safe use (Christensen *et al.*, 2019; Hérouet *et al.*, 2005; USDA-APHIS, 2001; USDA-APHIS, 2005; USDA-APHIS, 2013; USDA-APHIS, 2020). The PAT (*mo-pat*) sequence represents the deduced amino acid sequence from translation of the *mo-pat* gene. The asterisk (*) indicates the translational stop codon.

As shown in Figure 37, the deduced amino acid sequence from translation of the *mo-pat* gene is identical to that of the already-deregulated PAT protein from translation of the *pat* gene, for which safety has been confirmed (Hérouet et al., 2005) in a number of approved events across several different crops that are currently in commercial use.

Function and Activity of the PAT Protein

The mode of action of the PAT protein has been previously characterized and described (CERA - ILSI Research Foundation, 2011; Hérouet et al., 2005). The PAT protein confers tolerance to the herbicidal active ingredient glufosinate-ammonium, the active ingredient in phosphinothricin herbicides. Glufosinate chemically resembles the amino acid glutamate and acts to inhibit an enzyme called glutamine synthetase, which is involved in the synthesis of glutamine. Glutamine

synthetase is also involved in ammonia detoxification. Due to its similarity to glutamate, glufosinate blocks the activity of glutamine synthetase, resulting in reduced glutamine levels and a corresponding increase in concentrations of ammonia in plant tissues, leading to cell membrane disruption and cessation of photosynthesis resulting in plant death. The PAT protein confers tolerance to glufosinate-ammonium herbicides by acetylating phosphinothricin, an isomer of glufosinate-ammonium, thus detoxifying the herbicide (CERA - ILSI Research Foundation, 2011; Hérouet et al., 2005).

Characterization of the PAT Protein Derived from DP910521 Maize (PHI-2021-134 study)

The DP910521 maize-expressed PAT protein was characterized using SDS-PAGE, western blot, protein glycosylation analysis, mass spectrometry peptide mapping, and N-terminal amino acid sequence analyses. The results demonstrated that the PAT protein derived from DP910521 maize is of the expected molecular weight, immunoreactivity, amino acid sequence, and had the expected lack of glycosolation.

SDS-PAGE Analysis

Samples of the PAT protein purified from DP910521 leaf tissue were analyzed by SDS-PAGE. As expected, the DP910521 maize derived PAT protein migrated as a predominant band consistent with the expected molecular weight of approximately 21 kDa and a PAT protein reference substance (Figure 38).

Additional details regarding SDS-PAGE analytical methods are provided in Appendix F.

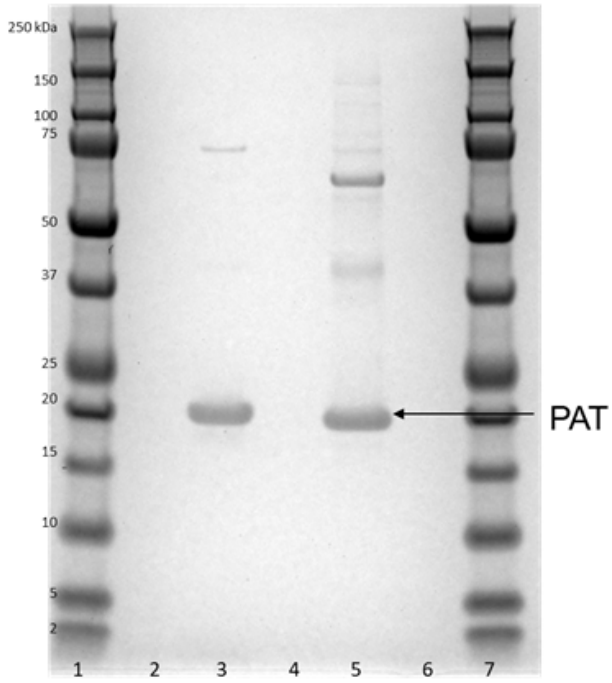

Lane	Sample Identification
1	Pre-stained Protein Molecular Weight Marker[a]
2	1X LDS/DTT Sample Buffer Blank
3	Microbially Derived PAT Protein (Lot PCF-0038)[b]
4	1X LDS/DTT Sample Buffer Blank
5	DP910521 Maize-Derived PAT Protein[c]
6	1X LDS/DTT Sample Buffer Blank
7	Pre-stained Protein Molecular Weight Marker[a]

Note: kilodalton (kDa).

[a] Molecular weight markers were included to provide a visual estimate that migration was within the expected range of the predicted molecular weight.

[b] Diluted to 1 µg per lane.

[c] After 1:4 dilution.

Figure 38. SDS-PAGE Analysis of DP910521 Maize-Derived PAT Protein

Western Blot Analysis

Samples of the PAT protein purified from DP910521 maize leaf tissue were analyzed by Western blot. As expected, the DP910521 maize-derived PAT was immunoreactive to a PAT monoclonal antibody and visible as a predominant band consistent with the expected molecular weight of approximately 21 kDa and a PAT protein reference substance (Figure 39).

Additional details regarding Western blot analytical methods are provided in Appendix F.

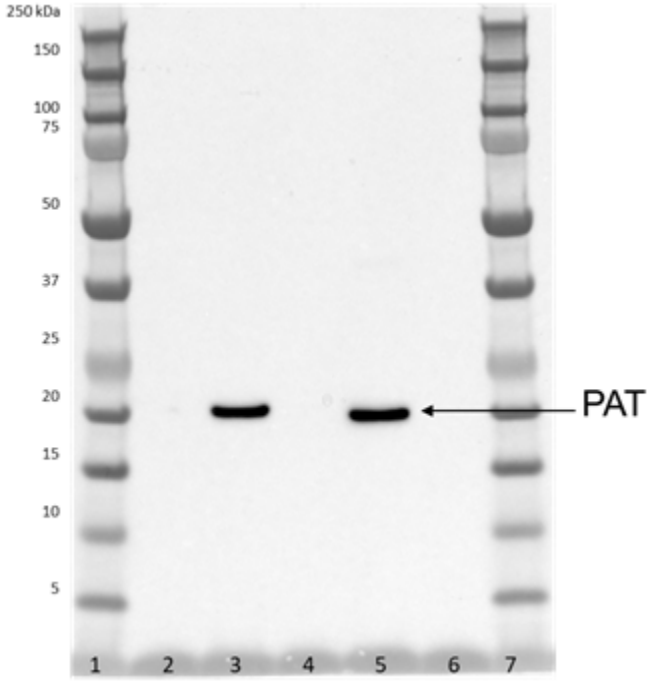

Lane	Sample Identification
1	Pre-stained Protein Molecular Weight Marker[a]
2	1X LDS/DTT Sample Buffer Blank
3	Microbially Derived PAT Protein (Lot PCF-0038)[b]
4	1X LDS/DTT Sample Buffer Blank
5	DP910521 Maize-Derived PAT Protein[c]
6	1X LDS/DTT Sample Buffer Blank
7	Pre-stained Protein Molecular Weight Marker[a]

Note: kilodalton (kDa).

[a] Molecular weight markers were included to provide a visual estimate that migration was within the expected range of the predicted molecular weight.

[b] Diluted to 10 ng per lane.

[c] After 1:80 dilution.

Figure 39. Western Blot Analysis of DP910521 Maize-Derived PAT Protein

Protein Glycosylation Analysis

The PAT protein purified from DP910521 maize leaf tissue was analyzed by SDS-PAGE. The gel also included a positive control (horseradish peroxidase) and a negative control (soybean trypsin inhibitor). The gel was stained using a Pierce Glycoprotein Staining Kit to visualize any glycoproteins. The gel was imaged and then stained with Coomassie based GelCode Blue Stain Reagent to visualize all protein bands.

Glycosylation was not detected for the DP910521 maize-derived PAT protein (Figure 40). The horseradish peroxidase positive control was stained and clearly visible as a magenta-colored band. The soybean trypsin inhibitor negative control was not stained by the glycoprotein stain.

Additional details regarding glycosylation analytical methods are provided in Appendix F.

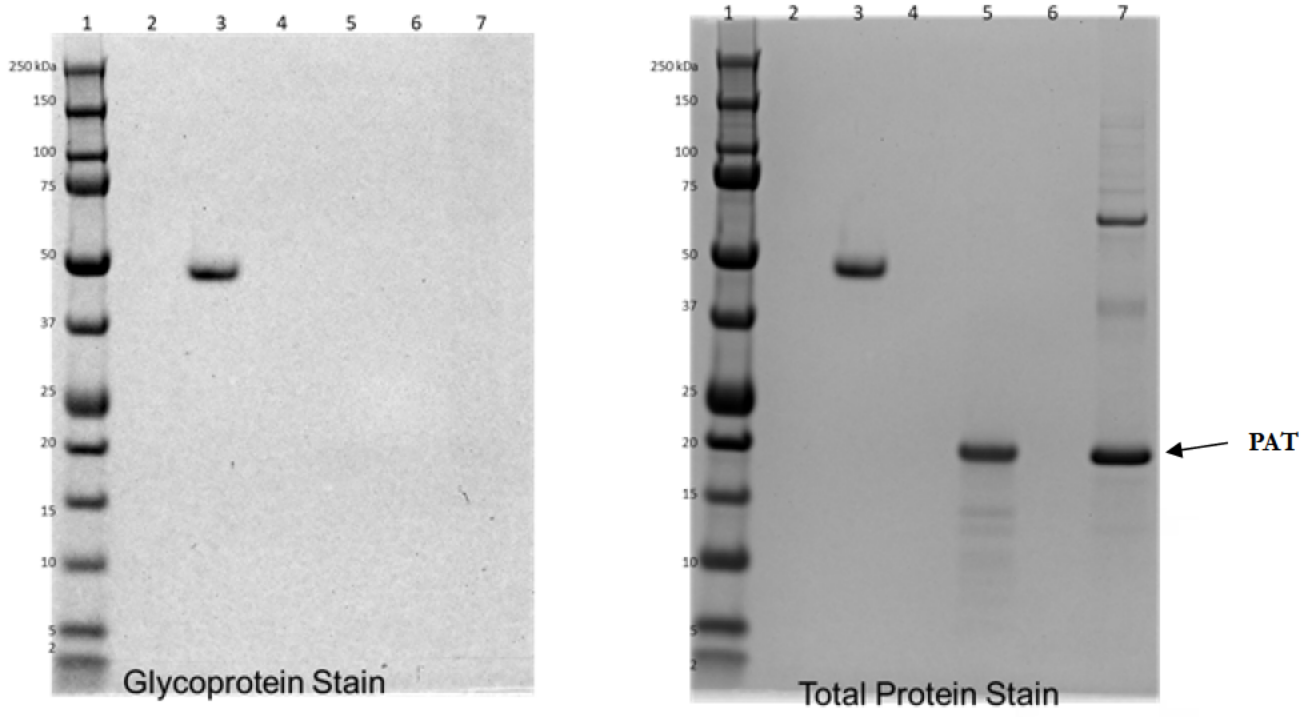

Lane	Sample Identification
1	Pre-stained Protein Molecular Weight Marker[a]
2	1X LDS/DTT Sample Buffer Blank
3	Horseradish Peroxidase (1.0 µg)
4	1X LDS/DTT Sample Buffer Blank
5	Soybean Trypsin Inhibitor (1.0 µg)
6	1X LDS/DTT Sample Buffer Blank
7	DP910521 Maize-Derived PAT Protein[b]

Note: The glycoprotein gel was stained with glycoprotein staining reagent. The total protein stain gel was stained with glycoprotein staining reagent followed by staining with Coomassie GelCode Blue Stain Reagent for total proteins. Kilodalton (kDa) and microgram (µg).

[a] Molecular weight markers were included to provide a visual estimate that migration was within the expected range of the predicted molecular weight.

[b] Sample diluted 1:4.

Figure 40. Glycosylation Analysis of DP910521 Maize-Derived PAT Protein

Mass Spectrometry Peptide Mapping Analysis

Samples of the PAT protein purified from DP910521 maize leaf tissue were analyzed by SDS-PAGE. Protein bands were stained with Coomassie stain reagent, and the band containing the PAT protein was excised for each sample. The excised PAT protein bands were digested with trypsin or chymotrypsin. Digested samples were analyzed using LC-MS, and an MS/MS ion search was used to match the detected peaks to peptides from the expected PAT protein sequence.

The identified tryptic and chymotrypic peptides for DP910521 maize-derived PAT protein are shown in Table 22. The combined sequence coverage was 95.1% (173/182) of the expected PAT amino acid sequence (Table 23). The deduced amino acid sequence includes an additional amino acid, an N-terminal methionine, that is not included in the expected 182-amino acid sequence for DP910521 maize used in LC-MS analysis (Figure 41).

Additional details regarding peptide mapping analytical methods are provided in Appendix F.

Table 22. Identified Tryptic and Chymotryptic Peptides of DP910521 Maize-Derived PAT Protein Using LC-MS Analysis

Matched Residue Position	Experimental Mass[a]	Theoretical Mass[b]	Identified Peptide Sequence
Tryptic Peptides			
5–36	3615 8385	3615 7926	RPVEIRPATAADMAAVCDIVNHYIETSTVNFR
37–51	1855 8831	1855 8588	TEPQTPQEWIDDLER
37–55	2368 1652	2368 1295	TEPQTPQEWIDDLERLQDR
80–95	1925 8973	1925 8908	NAYDWTVESTVYYVSHR
99–111	1414 8375	1414 8184	LGLGSTLYTHLLK
112–119	896 4186	896 4062	SMEAQGFK
120–134	1521 8736	1521 8515	SVVAVIGLPNDPSVR
135–144	1129 6007	1129 588	LHEALGYTAR
154–165	1480 6954	1480 6749	HGGWHDVGFWQR
166–182	1931 0918	1931 0629	DFELPAPPRPVRPVTQI
Chymotryptic Peptides			
1–27	3037 5342	3037 4862	SPERRPVEIRPATAADMAAVCDIVNHY
1–35	3928 9906	3928 92	SPERRPVEIRPATAADMAAVCDIVNHYIETSTVNF
28–35	909 4575	909 4444	IETSTVNF
36–45	1270 6096	1270 5942	RTEPQTPQEW
36–52	2125 0796	2125 044	RTEPQTPQEWIDDLERL
46–52	872 4719	872 4603	IDDLERL
46–58	1717 8657	1717 8424	IDDLERLQDRYPW
53–58	863 4051	863 3926	QDRYPW
59–72	1388 7776	1388 7551	LVAEVEGVVAGIAY
77–82	721 3971	721 3871	KARNAY
77–84	1022 5055	1022 4933	KARNAYDW
77–91	1801 8886	1801 8635	KARNAYDWTVESTVY
92–99	1031 5881	1031 5737	VSHRHQRL
92–101	1201 6968	1201 6792	VSHRHQRLGL
106–110	645 3587	645 3486	YTHLL
107–118	1360 7009	1360 6809	THLLKSMEAQGF
110–118	1009 5035	1009 4902	LKSMEAQGF
111–118	896 4195	896 4062	KSMEAQGF
119–135	1763 0584	1763 0305	KSVVAVIGLPNDPSVRL
119–139	2213 2833	2213 2532	KSVVAVIGLPNDPSVRLHEAL
119–141	2433 3777	2433 338	KSVVAVIGLPNDPSVRLHEALGY
142–147	617 3587	617 3497	TARGTL
153–163	1324 6299	1324 6102	KHGGWHDVGFW
158–163	759 3442	759 334	HDVGFW
164–182	2215 2522	2215 2226	QRDFELPAPPRPVRPVTQI
168–182	1668 9898	1668 9675	ELPAPPRPVRPVTQI

[a] The experimental mass is the uncharged mass calculated from the mass to charge ratio of the observed ion.

[b] The theoretical mass is the in silico generated mass that matches closest to the experimental mass.

Table 23. Combined Sequence Coverage of Identified Tryptic and Chymotryptic Peptides of DP910521 Maize-Derived PAT Protein Using LC-MS Analysis

Protease	% Coverage	Combined % Coverage
Trypsin	78	95.1
Chymotrypsin	92	

```
  1    MSPERRPVEI RPATAADMAA VCDIVNHYIE TSTVNFRTEP QTPQEWIDDL
 51    ERLQDRYPWL VAEVEGVVAG IAYAGPWKAR NAYDWTVEST VYVSHRHQRL
101    GLGSTLYTHL LKSMEAQGFK SVVAVIGLPN DPSVRLHEAL GYTARGTLRA
151    AGYKHGGWHD VGFWQRDFEL PAPPRPVRPV TQI
```

Red/shaded type	Bold red type indicates maize-derived PAT peptides identified using LC-MS analysis. The gray-shaded N-terminal methionine is included in the deduced amino acid sequence for PAT protein but is not expected to be present in the PAT protein for DP910521 maize and is not included in the 182-amino acid sequence used for LC-MS analysis.
Amino acid residue abbreviations	alanine (A), aspartic acid (D), glutamic acid (E), phenylalanine (F), glycine (G), histidine (H), isoleucine (I), lysine (K), leucine (L), methionine (M), asparagine (N), proline (P), glutamine (Q), arginine (R), serine (S), threonine (T), tryptophan (W), tyrosine (Y), and valine (V).

Figure 41. Identified Tryptic and Chymotryptic Peptide Amino Acid Sequence of DP910521 Maize-Derived PAT Protein Using LC-MS Analysis

N-Terminal Amino Acid Sequence Analysis

Samples of the PAT protein purified from DP910521 maize leaf tissue were analyzed by SDS-PAGE, followed by electrophoretic protein transfer to a polyvinylidene difluoride (PVDF) membrane. The membrane was stained using GelCode™ Blue Stain Reagent to visualize the proteins, and the band containing the PAT protein was excised. The excised band was analyzed using Edman degradation (Edman sequencing) to determine the N-terminal amino acid sequence.

The analysis identified a sequence (SPERRPVEIR) matching amino acid residues 1-10 of the expected the DP910521 maize-derived PAT protein sequence (Table 24), indicating the N-terminal methionine was absent as expected (Dummitt et al., 2003; Sherman et al., 1985).

Additional details regarding N-terminal amino acid sequence analytical methods are provided in Appendix F.

Table 24. N-Terminal Amino Acid Sequence Analysis of DP910521 Maize-Derived PAT Protein

Deduced PAT Sequence	M – S – P – E – R – R – P – V – E – I – R
Expected PAT Sequence	S – P – E – R – R – P – V – E – I – R
Identified PAT Sequence	S – P – E – R – R – P – V – E – I – R

Note: The deduced PAT sequence is a result of the translation of the gene and includes an N-terminal methionine. The expected PAT sequence does not include the N-terminal methionine as it is anticipated to be absent for the PAT protein in DP910521 maize.

Allergenicity and Toxicity Analyses of the PAT Protein

The PAT protein present in DP910521 maize is found in several approved events that are currently in commercial use. In accordance with the FSANZ Application Handbook, only the updated bioinformatics analysis is required for safety assessment in such a case. However, Corteva has very recently submitted bioinformatics data for the PAT protein to FSANZ within the A1270 and A1272 applications. Referrencing these two ongoing applications is considered sufficient for the assessment of DAS1131 maize. The data in question indicate that no new allergenicity or toxicity concern for humans arose from the updated bioinformatics assessment of the PAT protein.

Conclusions on the Safety of the PAT Protein in DP910521 Maize

The amino acid sequence of the PAT protein present in DP910521 maize was demonstrated to be identical to the corresponding protein found in a number of authorized GM events across several different crops that are currently commeralized and have a history of safe use.

Protein characterization results via SDS-PAGE, western blot, glycosylation, mass spectrometry peptide mapping, and N-terminal amino acid sequence analysis, have demonstrated that the PAT protein derived from DP910521 maize is of the expected molecular weight, immunoreactivity, lack of glycosylation, and amino acid sequence.

Currect bioinformatics analysis for the PAT protein, recently provided by Corteva within the A1270 and A1272 applications, indicate that no new allergenicity or toxicity concern for humans arose from the updated bioinformatics assessment of the PAT protein.

Based on this information there are no grounds to review the conclusions previously reached by FSANZ for the PAT protein that its consumption is unlikely to cause an adverse effect on humans.

PMI Protein

Amino Acid Sequence of the PMI Protein

The gene encoding the PMI protein in DP910521 maize, referred to as the *pmi* gene, was isolated from *Escherichia coli*. PMI served as a selectable marker during transformation which allowed for tissue growth using mannose as the carbon source. The deduced amino acid sequence from translation of the *pmi* gene is 391 amino acids in length and has a molecular weight of approximately 43 kDa (Figure 42).

```
  1   MQKLINSVQN YAWGSKTALT ELYGMENPSS QPMAELWMGA HPKSSSRVQN
 51   AAGDIVSLRD VIESDKSTLL GEAVAKRFGE LPFLFKVLCA AQPLSIQVHP
101   NKHNSEIGFA KENAAGIPMD AAERNYKDPN HKPELVFALT PFLAMNAFRE
151   FSEIVSLLQP VAGAHPAIAH FLQQPDAERL SELFASLLNM QGEEKSRALA
201   ILKSALDSQQ GEPWQTIRLI SEFYPEDSGL FSPLLLNVVK LNPGEAMFLF
251   AETPHAYLQG VALEVMANSD NVLRAGLTPK YIDIPELVAN VKFEAKPANQ
301   LLTQPVKQGA ELDFPIPVDD FAFSLHDLSD KETTISQQSA AILFCVEGDA
351   TLWKGSQQLQ LKPGESAFIA ANESPVTVKG HGRLARVYNK L*
```

Figure 42. Deduced Amino Acid Sequence of PMI Protein

The deduced amino acid sequence from the translation of the *pmi* gene from plasmid PHP79620. The asterisk (*) indicates the translational stop codon. The full-length protein is 391 amino acids in length and has a molecular weight of approximately 43 kDa.

Function and Activity of the PMI Protein

The mode of action of PMI has been previously characterized and described (Negrotto et al., 2000; Privalle, 2002; Reed et al., 2001; Weisser et al., 1996). PMI is widely present in nature and is expressed in fungi, insects, plants, and mammals (Slein, 1950; US-EPA, 2004). The United States EPA has granted an exemption from the requirement of a tolerance for the PMI protein as an inert ingredient in plants (US-EPA, 2004). The PMI protein catalyzes the reversible interconversion between mannose-6-phosphate and fructose-6-phosphate. Mannose is phosphorylated by hexokinase to mannose-6-phosphate and in the presence of PMI enters the glycolytic pathway after isomerization to fructose 6-phosphate. In the absence of PMI, mannose-6-phosphate accumulates in the plant cells and inhibits glycolysis; additionally, high levels of mannose can lead to other impacts on photosynthesis and ATP production (Negrotto et al., 2000; Privalle, 2002). However, in the presence of PMI, plant cells may survive on media containing mannose as a carbon source, thus allowing PMI to be utilized as a selectable marker (Negrotto et al., 2000; Reed et al., 2001).

Characterization of the PMI Protein Derived from DP910521 Maize (PHI-2021-153 study)

The DP910521 maize-expressed PMI protein was characterized using SDS-PAGE, western blot, glycosylation, mass spectrometry peptide mapping, and N-terminal amino acid sequence. The

results demonstrated that the PMI protein derived from DP910521 maize is of the expected molecular weight, immunoreactivity, lack of glycosylation, and amino acid sequence.

SDS-PAGE Analysis

Samples of PMI protein purified from DP910521 leaf tissue were analyzed by SDS-PAGE. As expected, the DP910521 maize derived PMI protein migrated as a predominant band consistent with the expected molecular weight of approximately 43 kDa and a PMI protein reference substance (Figure 43).

Additional details regarding SDS-PAGE analytical methods are provided in Appendix G.

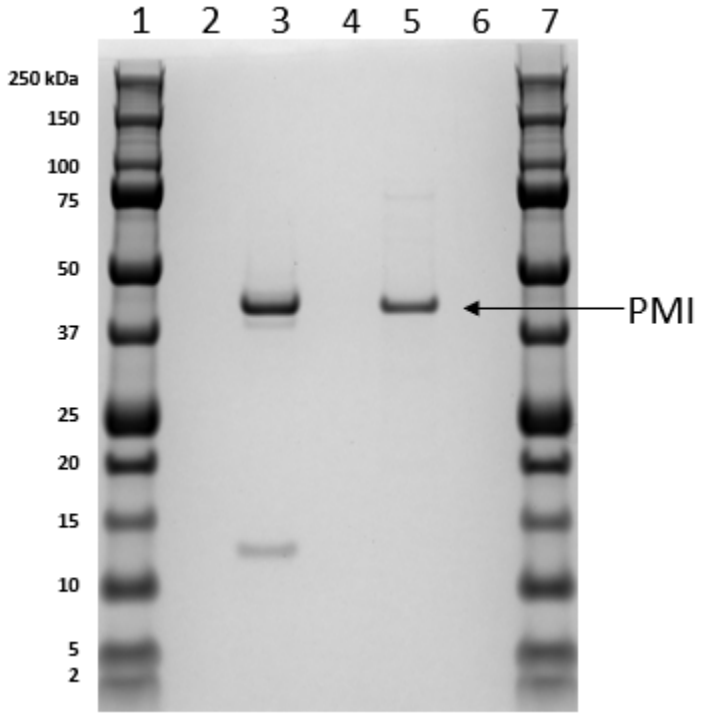

Lane	Sample Identification
1	Pre-stained Protein Molecular Weight Marker[a]
2	1X LDS/DTT Sample Buffer Blank
3	Microbially Derived PMI Protein (Lot # PCF-0055)[b]
4	1X LDS/DTT Sample Buffer Blank
5	DP910521 Maize-Derived PMI Protein
6	1X LDS/DTT Sample Buffer Blank
7	Pre-stained Protein Molecular Weight Marker[a]

Note: kilodalton (kDa) and lithium dodecyl sulfate containing dithiothreitol (LDS/DTT).

[a] Molecular weight markers were included to provide a visual verification that migration was within the expected range of the predicted molecular weight.

[b] Target concentration of 1 µg.

Figure 43. SDS-PAGE Analysis of DP910521 Maize-Derived PMI Protein

Western Blot Analysis

Samples of the PMI protein purified from DP910521 maize leaf tissue were analyzed by Western blot. As expected, the DP910521 maize-derived PMI was immunoreactive to a PMI monoclonal antibody and visible as a predominant band consistent with the expected molecular weight of approximately 43 kDa and a PMI protein reference substance (Figure 44).

Additional details regarding western blot analytical methods are provided in Appendix G.

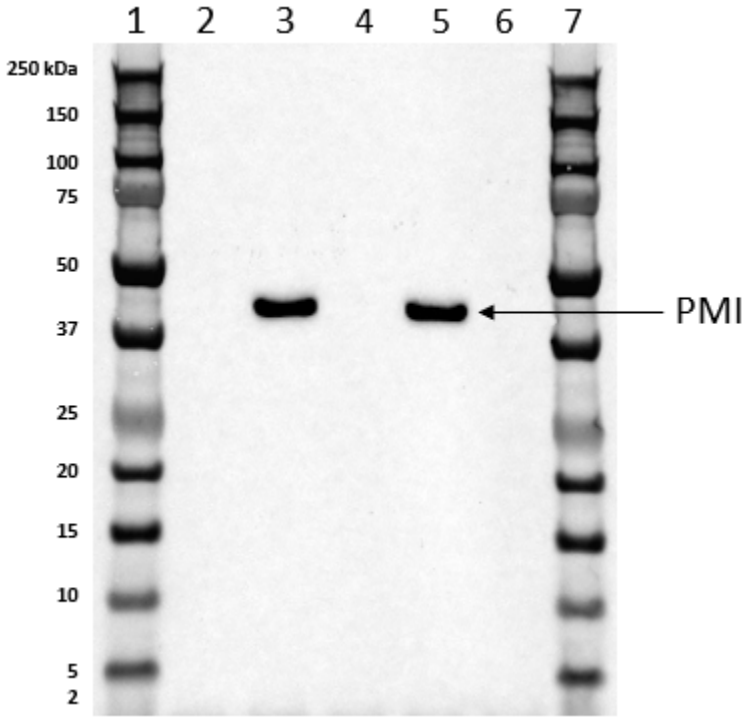

Lane	Sample Identification
1	Pre-stained Protein Molecular Weight Marker[a]
2	1X LDS/DTT Sample Buffer Blank
3	Microbially Derived PMI Protein (Lot # PCF-0055)[b]
4	1X LDS/DTT Sample Buffer Blank
5	DP910521 Maize-Derived PMI Protein
6	1X LDS/DTT Sample Buffer Blank
7	Pre-stained Protein Molecular Weight Marker[a]

Note: kilodalton (kDa) and lithium dodecyl sulfate containing dithiothreitol (LDS/DTT).

[a] Molecular weight markers were included to provide a visual verification that migration was within the expected range of the predicted molecular weight.

[b] Sample was diluted to ~ 10 ng.

Figure 44. Western Blot Analysis of DP910521 Maize-Derived PMI Protein

Glycosylation Analysis

The PMI protein purified from DP910521 maize leaf tissue was analyzed by SDS-PAGE. The gel also included a positive control (horseradish peroxidase) and a negative control (soybean trypsin inhibitor). The gel was stained using a Pierce Glycoprotein Staining Kit to visualize any glycoproteins. The gel was imaged and then stained with Coomassie based GelCode Blue Stain Reagent to visualize all protein bands.

Glycosylation was not detected for the the DP910521 maize-derived PMI protein (Figure 45). The horseradish peroxidase positive control was stained and clearly visible as a magenta-colored band. The soybean trypsin inhibitor negative control was not stained by the glycoprotein stain.

Additional details regarding glycosylation analytical methods are provided in Appendix G.

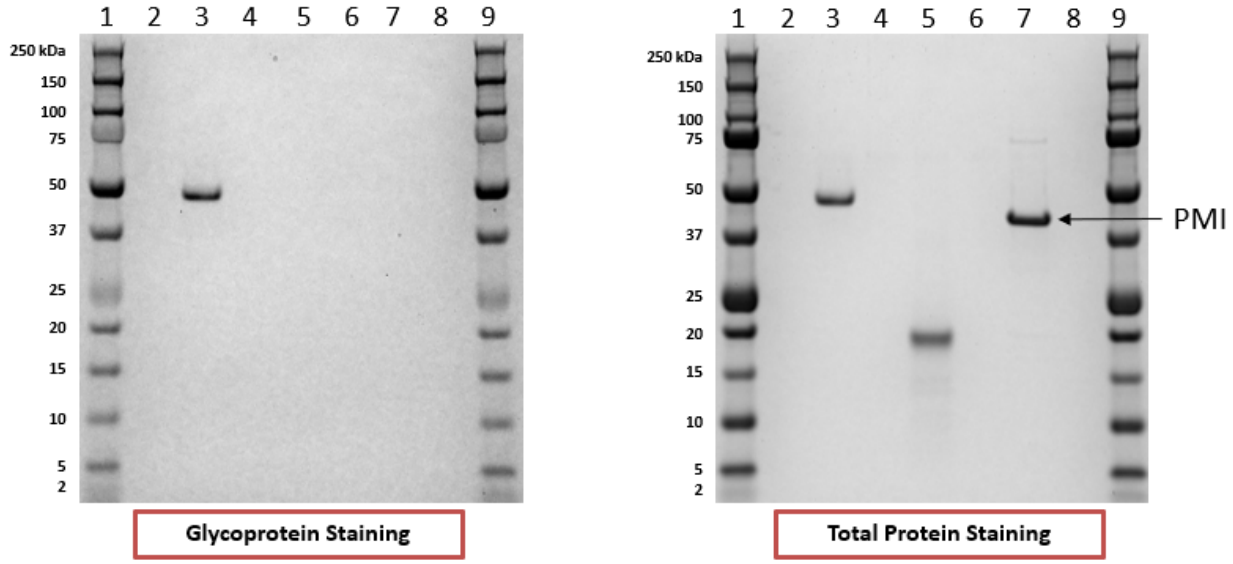

Lane	Sample Identification
1	Pre-stained Protein Molecular Weight Marker[a]
2	1X LDS/DTT Sample Buffer Blank
3	Horseradish Peroxidase (1.0 µg)
4	1X LDS/DTT Sample Buffer Blank
5	Soybean Trypsin Inhibitor (1.0 µg)
6	1X LDS/DTT Sample Buffer Blank
7	DP910521 Maize-Derived PMI Protein
8	1X LDS/DTT Sample Buffer Blank
9	Pre-stained Protein Molecular Weight Marker[a]

Note: The glycoprotein gel was stained with glycoprotein staining reagent. The total protein stain gel was stained with glycoprotein staining reagent followed by staining with Coomassie blue reagent for total proteins. Kilodalton (kDa) and lithium dodecyl sulfate containing dithiothreitol (LDS/DTT).

[a] Molecular weight markers were included to provide a visual verification that migration was within the expected range of the predicted molecular weight.

Figure 45. Glycosylation Analysis of DP910521 Maize-Derived PMI Protein

LC-MS Peptide Mapping and N-Terminal Amino Acid Sequencing Analyses

Samples of PMI protein purified from DP910521 maize leaf tissue were analyzed by SDS-PAGE. Protein bands were stained with Coomassie stain reagent, and the band containing PMI protein was excised for each sample. The excised PMI protein bands were digested with trypsin or chymotrypsin. Digested samples were analyzed using LC-MS, and an MS/MS ion search was used to match the detected peaks to peptides from the expected PMI protein sequence.

The identified tryptic and chymotrypic peptides for DP910521 maize-derived PMI protein are shown in Table 25 and Table 26. The combined sequence coverage was 95.9% (375/391) of the expected PMI amino acid sequence (Table 27 and Figure 46).

The N-terminal peptide was identified with the LC-MS as MQKLINSVQNY from the chymotryptic digestion. The results indicated the N-terminal methionine residue of the protein was acetylated.

Additional details regarding peptide mapping and N-terminal amino acid sequencing analytical methods are provided in Appendix G.

Table 25. Identified Tryptic Peptides of DP910521 Maize-Derived PMI Protein Using LC-MS Analysis

Matched Residue Position	Experimental Mass[a]	Theoretical Mass[b]	Identified Peptide Sequence
4–16	1478.7619	1478.7518	LINSVQNYAWGSK
17–43	2988.4231	2988.3819	TALTELYGMENPSSQPMAELWMGAHPK
48–59	1241.6813	1241.6728	VQNAAGDIVSLR
48–66	2028.0701	2028.0487	VQNAAGDIVSLRDVIESDK
60–76	1773 9515	1773.9360	DVIESDKSTLLGEAVAK
67–76	987 5659	987.5600	STLLGEAVAK
67–77	1143.6684	1143.6611	STLLGEAVAKR
77–86	1252.7074	1252.6968	RFGELPFLFK
78–86	1096.6054	1096.5957	FGELPFLFK
87–102	1773 9683	1773.9560	VLCAAQPLSIQVHPNK
87–111	2757.4658	2757.4384	VLCAAQPLSIQVHPNKHNSEIGFAK
103–111	1001.4977	1001.4930	HNSEIGFAK
112–124	1343.6213	1343.6139	ENAAGIPMDAAER
180–195	1807 9229	1807.9026	LSELFASLLNMQGEEK
198–203	627.4355	627.4319	ALAILK
204–218	1714.8281	1714.8275	SALDSQQGEPWQTIR
219–240	2479 3575	2479.3250	LISEFYPEDSGLFSPLLLNVVK
281–292	1372.7695	1372.7602	YIDIPELVANVK
293–307	1682 9472	1682.9355	FEAKPANQLLTQPVK
308–331	2675 3106	2675.2755	QGAELDFPIPVDDFAFSLHDLSDK
355–379	2598 3892	2598.3653	GSQQLQLKPGESAFIAANESPVTVK

[a] The experimental mass is the uncharged mass calculated from the mass to charge ratio of the observed ion.
[b] The theoretical mass is the *in silico* generated mass that matches closest to the experimental mass.

Table 26. Identified Chymotryptic Peptides of DP910521 Maize-Derived PMI Protein Using LC-MS Analysis

Matched Residue Position	Experimental Mass[a]	Theoretical Mass[b]	Identified Peptide Sequence
1–11	1394.7043	1394.6864	MQKLINSVQNY[cd]
5–11	836.4069	836.4028	INSVQNY
12–19	832.4486	832.4443	AWGSKTAL
12–22	1175.6307	1175.6186	AWGSKTALTEL
14–22	918 5099	918.5022	GSKTALTEL
14–23	1081 5763	1081.5655	GSKTALTELY
24–36	1389.6078	1389.5904	GMENPSSQPMAEL
24–37	1575.6924	1575.6697	GMENPSSQPMAELW[d]
59–69	1261.6618	1261.6514	RDVIESDKSTL
59–70	1374.7512	1374.7354	RDVIESDKSTLL
59–78	2233 2362	2233.2066	RDVIESDKSTLLGEAVAKRF
70–78	989 5733	989.5658	LGEAVAKRF
71–78	876.4848	876.4817	GEAVAKRF

Table 26. Identified Chymotryptic Peptides of DP910521 Maize-Derived PMI Protein Using LC-MS Analysis (continued)

Matched Residue Position	Experimental Mass[a]	Theoretical Mass[b]	Identified Peptide Sequence
71–83	1419.7701	1419.7510	GEAVAKRFGELPF
86–94	998 5650	998.5583	KVLCAAQPL
95–109	1705.8584	1705.8536	SIQVHPNKHNSEIGF
110–126	1819.8730	1819.8522	AKENAAGIPMDAAERNY
127–135	1076 5691	1076.5614	KDPNHKPEL
127–137	1322.7100	1322.6983	KDPNHKPELVF
143–151	1097 5400	1097.5328	LAMNAFREF
144–151	984.4553	984.4487	AMNAFREF
149–157	1078 5766	1078.5659	REFSEIVSL
149–158	1191.6639	1191.6499	REFSEIVSLL
158–171	1427.7818	1427.7674	LQPVAGAHPAIAHF
159–171	1314.6977	1314.6833	QPVAGAHPAIAHF
172–180	1068 5645	1068.5564	LQQPDAERL
172–183	1397.7327	1397.7150	LQQPDAERLSEL
173–184	1431.7185	1431.6994	QQPDAERLSELF
185–199	1661.8583	1661.8406	ASLLNMQGEEKSRAL[d]
188–199	1374.7010	1374.6925	LNMQGEEKSRAL
189–199	1261.6146	1261.6084	NMQGEEKSRAL
200–214	1641.8280	1641.8362	AILKSALDSQQGEPW
203–214	1344.6465	1344.6310	KSALDSQQGEPW
215–219	629 3878	629.3860	QTIRL
215–223	1105.6240	1105.6131	QTIRLISEF
215–230	1866 9675	1866.9363	QTIRLISEFYPEDSGL
236–248	1430.7778	1430.7592	LNVVKLNPGEAMF
237–248	1317.6911	1317.6751	NVVKLNPGEAMF
237–249	1430.7782	1430.7592	NVVKLNPGEAMFL
249–257	1047.5116	1047.5025	LFAETPHAY
250–257	934.4240	934.4185	FAETPHAY
251–257	787 3528	787.3501	AETPHAY
251–258	900.4456	900.4341	AETPHAYL
258–273	1671.8730	1671.8502	LQGVALEVMANSDNVL
259–273	1558.7921	1558.7661	QGVALEVMANSDNVL
264–273	1090 5063	1090.4965	EVMANSDNVL
274–281	904 5169	904.5130	RAGLTPKY
294–301	869.4647	869.4606	EAKPANQL
294–302	982 5515	982.5447	EAKPANQLL
294–312	2034 1419	2034.1109	EAKPANQLLTQPVKQGAEL
302–321	2228 1834	2228.1365	LTQPVKQGAELDFPIPVDDF
303–312	1069 5825	1069.5768	TQPVKQGAEL
303–321	2115.0962	2115.0525	TQPVKQGAELDFPIPVDDF
303–323	2333 1989	2333.1580	TQPVKQGAELDFPIPVDDFAF
313–323	1281.6081	1281.5918	DFPIPVDDFAF
324–343	2156 1273	2156.0961	SLHDLSDKETTISQQSAAIL
329–344	1737 9051	1737.8785	SDKETTISQQSAAILF
344–353	1196.5329	1196.5172	FCVEGDATLW
354–361	900 5087	900.5029	KGSQQLQL
354–368	1616.8700	1616.8522	KGSQQLQLKPGESAF
360–368	975 5098	975.5025	QLKPGESAF
369–384	1647 9144	1647.9056	IAANESPVTVKGHGRL

[a] The experimental mass is the uncharged mass calculated from the mass to charge ratio of the observed ion.
[b] The theoretical mass is the *in silico* generated mass that matches closest to the experimental mass.
[c] The N-terminal peptide was acetylated.
[d] This peptide was modified by methionine oxidation.

Table 27. Combined Sequence Coverage of Identified Tryptic and Chymotryptic Peptides of DP910521 Maize-Derived PMI Protein Using LC-MS Analysis

Protease	% Coverage	Combined % Sequence Coverage
Trypsin	64	95.9
Chymotrypsin	86	

```
  1 MQKLINSVQN YAWGSKTALT ELYGMENPSS QPMAELWMGA HPKSSSRVQN
 51 AAGDIVSLRD VIESDKSTLL GEAVAKRFGE LPFLFKVLCA AQPLSIQVHP
101 NKHNSEIGFA KENAAGIPMD AAERNYKDPN HKPELVFALT PFLAMNAFRE
151 FSEIVSLLQP VAGAHPAIAH FLQQPDAERL SELFASLLNM QGEEKSRALA
201 ILKSALDSQQ GEPWQTIRLI SEFYPEDSGL FSPLLLNVVK LNPGEAMFLF
251 AETPHAYLQG VALEVMANSD NVLRAGLTPK YIDIPELVAN VKFEAKPANQ
301 LLTQPVKQGA ELDFPIPVDD FAFSLHDLSD KETTISQQSA AILFCVEGDA
351 TLWKGSQQLQ LKPGESAFIA ANESPVTVKG HGRLARVYNK L
```

Red type	Bold red type indicates maize-derived PMI peptides identified using LC-MS analysis. The identified sequence is identical to the PMI sequence deduced by the translation of the *pmi* gene and the expected sequence used in LC-MS analysis.
Amino acid residue abbreviations	alanine (A), aspartic acid (D), glutamic acid (E), phenylalanine (F), glycine (G), histidine (H), isoleucine (I), lysine (K), leucine (L), methionine (M), asparagine (N), proline (P), glutamine (Q), arginine (R), serine (S), threonine (T), tryptophan (W), tyrosine (Y), and valine (V).

Figure 46. Identified Tryptic and Chymotryptic Peptide Amino Acid Sequence of DP910521 Maize-Derived PMI Protein Using LC-MS Analysis

Allergenicity and Toxicity Analyses of the PMI Protein

The PMI protein present in DP910521 maize is found in several approved events that are currently in commercial use. In accordance with the FSANZ Application Handbook, only the updated bioinformatics analysis is required for safety assessment in such a case. However, Corteva has very recently submitted bioinformatics data for the PMI protein to FSANZ within the A1270 and A1272 applications. Referrencing these two ongoing applications is considered sufficient for the assessment of DAS1131 maize. The data in question indicate that no new allergenicity or toxicity concern for humans arose from the updated bioinformatics assessment of the PMI protein.

Conclusions on the Safety of PMI Protein in DP910521 Maize

The amino acid sequence of the PMI protein present in DP910521 maize was demonstrated to be identical to the PMI protein found in a number of authorized GM events that are currently commercialized and have a history of safe use (ISAAA, 2019).

Protein characterization results via SDS-PAGE, western blot, peptide mapping, N-terminal amino acid sequence, and glycoprotein analysis have demonstrated that the PMI protein derived from DP910521 maize is of the expected molecular weight, immunoreactivity, amino acid sequence and showed a lack of glycosylation.

Currect bioinformatics analysis for the PMI protein, recently provided by Corteva within the A1270 and A1272 applications, indicate that no new allergenicity or toxicity concern for humans arose from the updated bioinformatics assessment of the PMI protein.

Based on this information there are no grounds to review the conclusions previously reached by FSANZ for the PMI protein that its consumption is unlikely to cause an adverse effect on humans.

B.3 Other (non-protein substances)

There are no other new substances associated with DP910521 maize.

B.4 Novel herbicide metabolites in GM herbicide-tolerant plants

There are no novel herbicide metabolites associated with DP910521 maize.

B.5 Compositional analyses of the food produced using gene technology

Trait Expression Assessment (PHI-2020-024 study)

The expression levels of the Cry1B.34, PAT, and PMI proteins were evaluated in DP910521 maize.

Tissue samples were collected during the 2020 growing season at six sites in commercial maize-growing regions of the United States and Canada. A randomized complete block design with four blocks was utilized at each site. The following tissue samples were collected: leaf (V6, V9, R1, and R4 growth stages), root (V9, R1, and R4 growth stages), pollen (R1 growth stage), stalk (R1 growth stage), forage (R4 growth stage), and grain (R6 growth stage). The concentrations of the Cry1B.34, PAT, and PMI proteins were determined using quantitative enzyme-linked immunosorbent assays (ELISAs).

Concentration results (means, ranges, and standard deviations) are summarized across sites in Table 28 to Table 30 for Cry1B.34 protein, PAT protein, and PMI protein, respectively. Individual sample results below the LLOQ were assigned a value equal to half of the LLOQ for calculation purposes.

Additional details regarding methods for trait expression analysis are provided in Appendix H.

Table 28. Across-Site Summary of Cry1B.34 Protein Concentrations in DP910521 Maize

Tissue (Growth Stage)	ng Cry1B.34/mg Tissue Dry Weight				Number of Samples <LLOQ/ Number of Samples Reported
	Mean	Range	Standard Deviation	Sample LLOQ[a]	
Herbicide-Treated DP910521 Maize					
Leaf (V6)	560	350 - 780	140	0.14	0/24
Leaf (V9)	440	230 - 720	150	0.14	0/24
Leaf (R1)	410	190 - 720	150	0.14	0/24
Leaf (R4)	810	350 - 1400	280	0.14	0/24
Root (V9)	330	140 - 570	100	0.28	0/24
Root (R1)	200	63 - 330	69	0.28	0/24
Root (R4)	140	54 - 200	35	0.28	0/24
Pollen (R1)	0.20[b]	<0.28 - 0.47	0.095[b]	0.28	17/24
Stalk (R1)	360	220 - 500	65	0.18	0/24
Forage (R4)	220	140 - 300	51	0.046	0/24
Grain (R6)	6.1	1.8 - 13	3.0	0.14	0/24

Note: Growth stages (Abendroth *et al.*, 2011). Herbicide-treated refers to treatment with glufosinate.

[a] Lower limit of quantification (LLOQ) in ng/mg tissue dry weight.

[b] Some, but not all, sample results were below the LLOQ. A value equal to half the LLOQ value was assigned to those samples to calculate the mean and standard deviation.

Table 29. Across-Site Summary of PAT Protein Concentrations in DP910521 Maize

Tissue (Growth Stage)	ng PAT/mg Tissue Dry Weight				Number of Samples <LLOQ/ Number of Samples Reported
	Mean	Range	Standard Deviation	Sample LLOQ[a]	
Herbicide-Treated DP910521 Maize					
Leaf (V6)	94	60 - 130	25	0.11	0/24
Leaf (V9)	99	55 - 120	15	0.11	0/24
Leaf (R1)	100	84 - 130	14	0.11	0/24
Leaf (R4)	100	37 - 140	24	0.11	0/24
Root (V9)	64	33 - 90	16	0.054	0/24
Root (R1)	50	15 - 75	17	0.054	0/24
Root (R4)	57	23 - 90	17	0.054	0/24
Pollen (R1)	65	49 - 95	9.7	0.22	0/24
Stalk (R1)	87	58 - 120	16	0.036	0/24
Forage (R4)	71	38 - 160	31	0.036	0/24
Grain (R6)	11	5.7 - 18	3.2	0.054	0/24

Note: Growth stages (Abendroth *et al.*, 2011). Herbicide-treated refers to treatment with glufosinate.

[a] Lower limit of quantification (LLOQ) in ng/mg tissue dry weight.

Table 30. Across-Site Summary of PMI Protein Concentrations in DP910521 Maize

Tissue (Growth Stage)	ng PMI/mg Tissue Dry Weight				Number of Samples <LLOQ/ Number of Samples Reported
	Mean	Range	Standard Deviation	Sample LLOQ[a]	
Herbicide-Treated DP910521 Maize					
Leaf (V6)	17	12 - 24	3.3	0.54	0/24
Leaf (V9)	14	7.2 - 35	6.6	0.54	0/24
Leaf (R1)	19	8.4 - 37	8.4	0.54	0/24
Leaf (R4)	34	17 - 78	11	0.54	0/24
Root (V9)	7.2	3.3 - 10	1.8	0.27	0/24
Root (R1)	4.9	1.7 - 6.9	1.3	0.27	0/24
Root (R4)	4.5	2.1 - 7.8	1.4	0.27	0/24
Pollen (R1)	23	16 - 34	4.3	1.1	0/24
Stalk (R1)	5.8	3.8 - 8.2	1.2	0.18	0/24
Forage (R4)	14	10 - 34	5.4	1.8	0/24
Grain (R6)	5.3	3.3 - 8.7	1.4	0.27	0/24

Note: Growth stages (Abendroth *et al.*, 2011). Herbicide-treated refers to treatment with glufosinate.
[a] Lower limit of quantification (LLOQ) in ng/mg tissue dry weight.

Nutrient Composition Assessment (PHI-2020-025/021 study)

An assessment of the compositional equivalence of a GM product compared to that of a conventional non-GM comparator with a history of safe use in food and feed is an important part of the weight-of-evidence approach used to evaluate the safety of genetically modified plant products (Codex Alimentarius Commission, 2008; OECD, 1993). Compositional assessments of DP910521 maize were evaluated in comparison to concurrently grown non-GM, near-isoline maize (referred to as control maize) to identify statistical differences, and subsequently were evaluated in the context of biological variation established from multiple sources of non-GM, commercial maize data (reference maize).

Forage (R4 growth stage) and grain (R6 growth stage) samples were collected during the 2020 growing season at eight sites in commercial maize-growing regions of the United States and Canada. A randomized complete block design with four blocks was utilized at each site. Each block included DP910521 maize, non-GM near-isoline control maize, and four non-GM commercial maize reference lines. A herbicide treatment of glufosinate was applied to DP910521 maize.

The samples were assessed for key nutritional components. Proximate, fiber, and mineral analytes were assessed in the forage samples (9 analytes total), and grain sample were assessed for proximate, fiber, fatty acid, amino acid, mineral, vitamin, secondary metabolite, and anti-nutrient analytes (70 analytes total). The analytes included in the compositional assessment were selected based on the OECD consensus document on compositional considerations for new varieties of maize (OECD, 2002). Procedures and methods for nutrient composition analyses of maize forage and grain were conducted in accordance with the requirements for the U.S. EPA Good Laboratory Practice (GLP) Standards, 40 CFR Part 160. The analytical procedures used were validated methods, with the majority based on methods published by AOAC International, AACC (American Association of Cereal Chemists), and AOCS (American Oil Chemists' Society).

Statistical analyses were conducted to evaluate and compare the nutrient composition of DP910521 maize and the control maize. Across-site comparisons were conducted for a total of 79 analytes, where 71 analytes were analyzed using mixed model analysis and 4 analytes did not meet criteria for sufficient quantities of observations above the LLOQ and were therefore subjected to Fisher's exact test. No statistical analysis was conducted on the remaining 4 analytes as all data values were below the LLOQ. For a given analyte in the mixed model analysis, if a statistical difference (P-value < 0.05) was observed between DP910521 maize and the control maize, the False Discovery Rate (FDR)-adjusted P-value was examined. In cases where the raw P-value indicated a significant difference but the FDR-adjusted P-value was non-significant, it was concluded that the difference was likely a false positive. Additionally, three reference ranges representing the non-GM maize population with a history of safe use (i.e., tolerance interval, literature range, and in-study reference range) were utilized to evaluate statistical differences in the context of biological variation. If the measured values of DP910521 maize for that analyte fell within at least one of the reference ranges, then this analyte would be considered comparable to conventional maize.

The outcome of the nutrient composition assessment is provided in Table 31. Nutrient composition analysis results are provided in Table 32 to Table 38. No statistically significant differences were observed between DP910521 maize and the control maize for 70 of the 75 analytes that went through across-site analysis via either mixed model analysis or Fisher's exact test. A statistically significant difference, before FDR adjustment, was observed in the across-site analysis between DP910521 maize and the control maize for five analytes (crude fiber [forage], ash [grain], zinc, vitamin B1 [thiamine], and *p*-coumaric acid). Although raw P-values were significant, the FDR-adjusted P-values for these analytes were not significant, indicating that the observed differences were likely false positives. All individual values for these analytes were within the tolerance interval, literature range, and/or in-study reference range, indicating DP910521 maize is within the range of biological variation for these analytes and the statistical differences are not biologically meaningful.

The results of the nutrient composition assessment demonstrated that nutrient composition of forage and grain derived from DP910521 maize was comparable to that of conventional maize represented by non-GM near-isoline control maize and non-GM commercial maize.

Additional details regarding methods for nutrient composition and statistical analyses are provided in Appendix I.

Table 31. Outcome of Nutrient Composition Assessment Across Sites

Subgroup	No Statistical Difference Identified	Statistical Difference Identified					Not Included in Statistical Analysis (All Data Values Below the Lower Limit of Quantification)
		All Data Values Within Tolerance Interval	One or More Data Values Outside Tolerance Interval, or Tolerance Interval Not Available			Adjusted P-Value < 0.05	
			All Data Values Within Literature Range	One or More Data Values Outside Literature Range			
				All Data Values Within Reference Data Range	One or More Data Values Outside Reference Data Range		
Forage (R4 Growth Stage)							
Proximates, Fiber, and Mineral Composition	Crude Protein Crude Fat ADF NDF Ash Carbohydrates Calcium Phosphorus	Crude Fiber	--	--	--	--	--
Grain (R6 Growth Stage)							
Proximates and Fiber Composition	Moisture (%) Crude Protein Crude Fat Crude Fiber ADF NDF Total Dietary Fiber Carbohydrates	Ash	--	--	--	--	--
Fatty Acid Composition	Myristic Acid (C14:0) Palmitic Acid (C16:0) Palmitoleic Acid (C16:1) Heptadecanoic Acid (C17:0) Heptadecenoic Acid (C17:1) Stearic Acid (C18:0) Oleic Acid (C18:1) Linoleic Acid (C18:2) α-Linolenic Acid (C18:3) Arachidic Acid (C20:0) Eicosenoic Acid (C20:1) Eicosadienoic Acid (C20:2) Behenic Acid (C22:0) Lignoceric Acid (C24:0)	--	--	--	--	--	Lauric Acid (C12:0)

Table 31. Outcome of Nutrient Composition Assessment Across Sites (continued)

Subgroup	No Statistical Difference Identified	Statistical Difference Identified					Not Included in Statistical Analysis (All Data Values Below the Lower Limit of Quantification)
		All Data Values Within Tolerance Interval	One or More Data Values Outside Tolerance Interval, or Tolerance Interval Not Available			Adjusted P-Value < 0.05	
			All Data Values Within Literature Range	One or More Data Values Outside Literature Range			
				All Data Values Within Reference Data Range	One or More Data Values Outside Reference Data Range		
Grain (R6 Growth Stage)							
Amino Acid Composition	Alanine Arginine Aspartic Acid Cystine Glutamic Acid Glycine Histidine Isoleucine Leucine Lysine Methionine Phenylalanine Proline Serine Threonine Tryptophan Tyrosine Valine	--	--	--	--	--	--
Mineral Composition	Calcium Copper Iron Magnesium Manganese Phosphorus Potassium Sodium	Zinc	--	--	--	--	--

Table 31. Outcome of Nutrient Composition Assessment Across Sites (continued)

Subgroup	No Statistical Difference Identified	Statistical Difference Identified					Not Included in Statistical Analysis (All Data Values Below the Lower Limit of Quantification)
		All Data Values Within Tolerance Interval	One or More Data Values Outside Tolerance Interval, or Tolerance Interval Not Available			Adjusted P-Value < 0.05	
			All Data Values Within Literature Range	One or More Data Values Outside Literature Range			
				All Data Values Within Reference Data Range	One or More Data Values Outside Reference Data Range		
Grain (R6 Growth Stage)							
Vitamin Composition	β-Carotene Vitamin B3 (Niacin) Vitamin B5 (Pantothenic Acid) Vitamin B6 (Pyridoxine) Vitamin B9 (Folic Acid) α-Tocopherol γ-Tocopherol δ-Tocopherol Total Tocopherols	Vitamin B1 (Thiamine)	--	--	--	--	Vitamin B2 (Riboflavin) β-Tocopherol
Secondary Metabolite and Anti-Nutrient Composition	Ferulic Acid Inositol Phytic Acid Raffinose Trypsin Inhibitor	*p*-Coumaric Acid	--	--	--	--	Furfural

Note: Growth stages (Abendroth *et al.*, 2011).

Proximate, Fiber, and Mineral Assessment of DP910521 Maize Forage

Proximates, fiber, and minerals were analyzed in forage derived from DP910521 maize and control maize. Results are shown in Table 32. No statistically significant differences (P-value < 0.05) were observed between DP910521 maize and control maize, with an exception for one analyte. A statistically significant difference (P-value < 0.05) was observed between DP910521 maize and control maize for crude fiber. All individual values for this analyte were within the tolerance interval, indicating DP910521 maize is within the range of biological variation for this analyte and the statistical difference is not biologically meaningful. The non-significant FDR-adjusted P-value indicates that this difference was likely a false positive.

These results demonstrate that the proximate, fiber, and mineral composition of forage derived from DP910521 maize is comparable to conventional maize represented by non-GM near-isoline control maize and non-GM commercial maize.

Table 32. Proximate, Fiber, and Mineral Results for DP910521 Maize Forage

Analyte	Reported Statistics	Control Maize	Herbicide-Treated DP910521 Maize	Tolerance Interval	Literature Range	Reference Data Range
Crude Protein	Mean	7 31	7 33	3 70 - 12 3	2 37 - 16 32	4 02 - 11 6
	Range	4 15 - 9 64	5 34 - 10 8			
	Confidence Interval	6 29 - 8 33	6 32 - 8 35			
	Adjusted P-Value	--	0 973			
	P-Value	--	0 891			
Crude Fat	Mean	3 78	3 96	0 867 - 6 50	NQ - 6 755	1 94 - 5 77
	Range	2 28 - 5 46	2 90 - 5 05			
	Confidence Interval	3 47 - 4 10	3 64 - 4 27			
	Adjusted P-Value	--	0 618			
	P-Value	--	0 248			
Crude Fiber	Mean	22 9	21 7	13 8 - 31 2	12 5 - 42	16 1 - 30 3
	Range	15 2 - 27 7	16 8 - 25 8			
	Confidence Interval	22 1 - 23 8	20 8 - 22 6			
	Adjusted P-Value	--	0 504			
	P-Value	--	0 0407*			
ADF	Mean	28 2	26 9	15 7 - 40 1	5 13 - 47 39	19 9 - 35 9
	Range	19 0 - 33 7	18 4 - 32 1			
	Confidence Interval	26 8 - 29 6	25 3 - 28 3			
	Adjusted P-Value	--	0 504			
	P-Value	--	0 0644			
NDF	Mean	48 0	45 7	28 8 - 63 2	18 30 - 67 80	36 4 - 56 9
	Range	39 7 - 55 7	35 1 - 53 4			
	Confidence Interval	45 8 - 50 1	43 6 - 47 9			
	Adjusted P-Value	--	0 504			
	P-Value	--	0 121			
Ash	Mean	4 84	4 90	2 42 - 9 35	0 66 - 13 20	2 94 - 8 02
	Range	3 12 - 7 72	2 81 - 8 56			
	Confidence Interval	3 81 - 5 87	3 88 - 5 93			
	Adjusted P-Value	--	0 900			
	P-Value	--	0 672			
Carbohydrates	Mean	84 1	83 7	76 7 - 91 2	73 3 - 92 9	77 8 - 89 0
	Range	78 9 - 88 0	77 5 - 87 5			
	Confidence Interval	82 5 - 85 7	82 1 - 85 3			
	Adjusted P-Value	--	0 633			
	P-Value	--	0 316			
Calcium	Mean	0 259	0 255	0 0768 - 0 528	0 04 - 0 58	0 110 - 0 530
	Range	0 130 - 0 400	0 140 - 0 490			
	Confidence Interval	0 216 - 0 303	0 211 - 0 298			
	Adjusted P-Value	--	0 915			
	P-Value	--	0 728			
Phosphorus	Mean	0 263	0 252	0 0919 - 0 433	0 07 - 0 55	0 160 - 0 380
	Range	0 160 - 0 410	0 190 - 0 370			
	Confidence Interval	0 232 - 0 293	0 221 - 0 283			
	Adjusted P-Value	--	0 648			
	P-Value	--	0 374			

Note: Not quantified (NQ); one or more assay values in the published literature references were below the lower limit of quantification (LLOQ) and were not quantified. Proximate, Fiber, and Mineral Composition are reported as % Dry Weight

* A statistically significant difference (P-Value < 0.05) was observed.

Proximate and Fiber Assessment of DP910521 Maize Grain

Proximates and fiber were analyzed in grain derived from DP910521 maize and control maize. Results are shown in Table 33. No statistically significant differences (P-value < 0.05) were observed between DP910521 maize and control maize, with an exception for one analyte. A statistically significant difference (P-value < 0.05) was observed between DP910521 maize and control maize for ash. All individual values for this analyte were within the tolerance interval, indicating DP910521 maize is within the range of biological variation for this analyte and the statistical difference is not biologically meaningful. The non-significant FDR-adjusted P-value indicates that this difference was likely a false positive.

These results demonstrate that the proximate and fiber composition of grain derived from DP910521 maize is comparable to conventional maize represented by non-GM near-isoline control maize and non-GM commercial maize.

Table 33. Proximate and Fiber Results for DP910521 Maize Grain

Analyte	Reported Statistics	Control Maize	Herbicide-Treated DP910521 Maize	Tolerance Interval	Literature Range	Reference Data Range
Moisture (%)	Mean	20 4	20 9			
	Range	13 0 - 29 2	12 7 - 30 7			
	Confidence Interval	15 6 - 25 2	16 1 - 25 7	3 74 - 38 1	5 1 - 40 7	12 1 - 32 3
	Adjusted P-Value	--	0 504			
	P-Value	--	0 107			
Crude Protein	Mean	9 27	9 37			
	Range	6 37 - 10 9	6 87 - 10 9			
	Confidence Interval	8 31 - 10 2	8 41 - 10 3	6 60 - 13 1	5 72 - 17 26	5 74 - 13 5
	Adjusted P-Value	--	0 643			
	P-Value	--	0 362			
Crude Fat	Mean	3 97	3 88			
	Range	3 22 - 4 79	2 93 - 4 82			
	Confidence Interval	3 71 - 4 22	3 63 - 4 13	2 58 - 6 41	1 363 - 7 830	3 11 - 5 47
	Adjusted P-Value	--	0 618			
	P-Value	--	0 229			
Crude Fiber	Mean	2 47	2 46			
	Range	2 01 - 2 97	1 81 - 2 86			
	Confidence Interval	2 32 - 2 63	2 30 - 2 62	1 61 - 3 52	0 49 - 5 5	1 73 - 3 18
	Adjusted P-Value	--	0 925			
	P-Value	--	0 812			
ADF	Mean	4 10	4 19			
	Range	3 24 - 5 16	3 09 - 5 45			
	Confidence Interval	3 86 - 4 34	3 95 - 4 43	2 69 - 6 14	1 41 - 11 34	2 69 - 6 71
	Adjusted P-Value	--	0 643			
	P-Value	--	0 358			
NDF	Mean	9 70	9 71			
	Range	8 44 - 11 9	8 00 - 11 7			
	Confidence Interval	9 10 - 10 3	9 11 - 10 3	7 60 - 18 1	4 28 - 24 30	7 62 - 17 5
	Adjusted P-Value	--	0 986			
	P-Value	--	0 956			
Total Dietary Fiber	Mean	8 99	9 24			
	Range	7 62 - 11 5	7 78 - 11 5			
	Confidence Interval	8 66 - 9 33	8 90 - 9 58	2 97 - 20 0	5 78 - 35 31	5 83 - 14 0
	Adjusted P-Value	--	0 560			
	P-Value	--	0 180			
Ash	Mean	1 32	1 28			
	Range	1 13 - 1 43	1 06 - 1 45			
	Confidence Interval	1 27 - 1 36	1 24 - 1 33	1 01 - 1 83	0 616 - 6 282	0 957 - 1 44
	Adjusted P-Value	--	0 504			
	P-Value	--	0 0367*			
Carbohydrates	Mean	85 5	85 5			
	Range	84 1 - 88 0	83 7 - 88 1			
	Confidence Interval	84 6 - 86 3	84 7 - 86 3	80 6 - 88 7	77 4 - 89 7	81 1 - 89 2
	Adjusted P-Value	--	0 984			
	P-Value	--	0 929			

Note: This table provides results from the mixed model analysis only. Proximate and Fiber Composition are reported as % Dry Weight or as Indicated

* A statistically significant difference (P-Value < 0.05) was observed.

Fatty Acid Assessment of DP910521 Maize Grain

Fatty acids were analyzed in grain derived from DP910521 maize and control maize. Results are shown in Table 34. No statistically significant differences (P-value < 0.05) were observed between DP910521 maize and control maize.

These results demonstrate that the fatty acid composition of grain derived from DP910521 maize is comparable to conventional maize represented by non-GM near-isoline control maize and non-GM commercial maize.

Table 34. Fatty Acid Results for DP910521 Maize Grain

Analyte	Reported Statistics	Control Maize	Herbicide-Treated DP910521 Maize	Tolerance Interval	Literature Range	Reference Data Range
Lauric Acid (C12:0)	Mean	<LLOQ[a]	<LLOQ[a]	0 - 0 423[r]	NQ - 0 698	<LLOQ[a]
	Range	<LLOQ[a]	<LLOQ[a]			
	Confidence Interval	NA	NA			
	Adjusted P-Value	--	NA			
	P-Value	--	NA			
Myristic Acid (C14:0)	Mean	0 0430	0 0466	0 - 0 267[r]	NQ - 0 288	0 0324 - 0 0788
	Range	0 0339 - 0 0863	0 0350 - 0 0877			
	Confidence Interval	NA	NA			
	Adjusted P-Value	--	NA			
	P-Value	--	NA			
Palmitic Acid (C16:0)	Mean	13 4	13 4	9 51 - 24 5	6 81 - 39 0	10 8 - 14 2
	Range	12 9 - 13 9	12 8 - 13 9			
	Confidence Interval	13 2 - 13 6	13 2 - 13 6			
	Adjusted P-Value	--	0 692			
	P-Value	--	0 409			
Palmitoleic Acid (C16:1)	Mean	0 118	0 116	0 - 0 421	NQ - 0 67	0 0421 - 0 205
	Range	0 104 - 0 133	0 104 - 0 133			
	Confidence Interval	0 113 - 0 123	0 111 - 0 121			
	Adjusted P-Value	--	0 504			
	P-Value	--	0 0918			
Heptadecanoic Acid (C17:0)	Mean	0 0958	0 0977	0 - 0 222	NQ - 0 203	0 0412 - 0 123
	Range	0 0429 - 0 126	0 0417 - 0 138			
	Confidence Interval	0 0785 - 0 113	0 0804 - 0 115			
	Adjusted P-Value	--	0 633			
	P-Value	--	0 328			
Heptadecenoic Acid (C17:1)	Mean	0 0419	<LLOQ[a]	0 - 0 135[r]	NQ - 0 131	0 0328 - 0 0872
	Range	0 0342 - 0 0728	<LLOQ[a]			
	Confidence Interval	NA	NA			
	Adjusted P-Value	--	NA			
	P-Value	--	NA			
Stearic Acid (C18:0)	Mean	1 54	1 55	1 32 - 3 66	NQ - 4 9	1 45 - 2 65
	Range	1 29 - 1 75	1 32 - 1 75			
	Confidence Interval	1 45 - 1 64	1 45 - 1 64			
	Adjusted P-Value	--	0 915			
	P-Value	--	0 761			
Oleic Acid (C18:1)	Mean	25 5	25 5	17 2 - 38 0	16 38 - 42 81	21 6 - 36 0
	Range	23 7 - 28 1	23 1 - 27 6			
	Confidence Interval	24 7 - 26 2	24 8 - 26 2			
	Adjusted P-Value	--	0 925			
	P-Value	--	0 821			
Linoleic Acid (C18:2)	Mean	55 9	55 8	32 0 - 65 2	13 1 - 67 68	45 7 - 60 3
	Range	53 0 - 58 0	53 2 - 58 7			
	Confidence Interval	54 8 - 56 9	54 8 - 56 8			
	Adjusted P-Value	--	0 915			
	P-Value	--	0 729			
α-Linolenic Acid (C18:3)	Mean	1 90	1 91	0 - 2 09	NQ - 2 33	1 34 - 2 15
	Range	1 66 - 2 13	1 72 - 2 21			
	Confidence Interval	1 80 - 1 99	1 82 - 2 01			
	Adjusted P-Value	--	0 633			
	P-Value	--	0 276			

Table 34. Fatty Acid Results for DP910521 Maize Grain (continued)

Analyte	Reported Statistics	Control Maize	Herbicide-Treated DP910521 Maize	Tolerance Interval	Literature Range	Reference Data Range
Fatty Acid Composition (% Total Fatty Acids)						
Arachidic Acid (C20:0)	Mean	0 502	0 502			
	Range	0 433 - 0 557	0 437 - 0 576			
	Confidence Interval	0 473 - 0 530	0 474 - 0 530	0 297 - 0 811	0 267 - 1 2	0 296 - 0 647
	Adjusted P-Value	--	0 973			
	P-Value	--	0 905			
Eicosenoic Acid (C20:1)	Mean	0 357	0 359			
	Range	0 315 - 0 397	0 317 - 0 395			
	Confidence Interval	0 340 - 0 373	0 342 - 0 376	0 140 - 0 441	NQ - 1 952	0 228 - 0 362
	Adjusted P-Value	--	0 560			
	P-Value	--	0 187			
Eicosadienoic Acid (C20:2)	Mean	0 0581	0 0530			
	Range	0 0375 - 0 0974	0 0357 - 0 0935			
	Confidence Interval	NA	NA	0 - 0 825[r]	NQ - 2 551	0 0330 - 0 0865
	Adjusted P-Value	--	NA			
	P-Value	--	NA			
Behenic Acid (C22:0)	Mean	0 310	0 312			
	Range	0 252 - 0 367	0 250 - 0 371			
	Confidence Interval	0 285 - 0 334	0 287 - 0 336	0 - 0 424	NQ - 0 5	0 0794 - 0 303
	Adjusted P-Value	--	0 838			
	P-Value	--	0 535			
Lignoceric Acid (C24:0)	Mean	0 290	0 297			
	Range	0 239 - 0 326	0 254 - 0 343			
	Confidence Interval	0 275 - 0 306	0 282 - 0 312	0 - 0 612	NQ - 0 91	0 209 - 0 396
	Adjusted P-Value	--	0 504			
	P-Value	--	0 0893			

Note: This table provides results from the mixed model analysis only. Not applicable (NA); mixed model analysis was not performed, or confidence interval was not determined. Not quantified (NQ); one or more assay values in the published literature references were below the lower limit of quantification (LLOQ) and were not quantified. Fatty acid composition is reported as % total fatty acids.

[a] < LLOQ, all fatty acid sample values were below the assay LLOQ.

[r] Historical reference data range was provided as tolerance interval was not calculated since the data did not meet the assumptions of any tolerance interval calculation method.

Amino Acid Assessment of DP910521 Maize Grain

Amino acids were analyzed in grain derived from DP910521 maize and control maize. Results are shown in Table 35. No statistically significant differences (P-value < 0.05) were observed between DP910521 maize and control maize.

These results demonstrate that the amino acid composition of grain derived from DP910521 maize is comparable to conventional maize represented by non-GM near-isoline control maize and non-GM commercial maize.

Table 35. Amino Acid Results for DP910521 Maize Grain

Analyte	Reported Statistics	Control Maize	Herbicide-Treated DP910521 Maize	Tolerance Interval	Literature Range	Reference Data Range
Alanine	Mean	0 705	0 716	0 448 - 1 06	0 40 - 1 48	0 408 - 1 13
	Range	0 461 - 0 871	0 489 - 0 864			
	Confidence Interval	0 617 - 0 793	0 627 - 0 804			
	Adjusted P-Value	--	0 643			
	P-Value	--	0 348			
Arginine	Mean	0 459	0 457	0 299 - 0 589	0 12 - 0 71	0 281 - 0 561
	Range	0 356 - 0 554	0 329 - 0 536			
	Confidence Interval	0 423 - 0 496	0 420 - 0 494			
	Adjusted P-Value	--	0 910			
	P-Value	--	0 692			
Aspartic Acid	Mean	0 615	0 615	0 412 - 0 890	0 30 - 1 21	0 380 - 0 886
	Range	0 437 - 0 716	0 443 - 0 744			
	Confidence Interval	0 561 - 0 670	0 561 - 0 669			
	Adjusted P-Value	--	0 986			
	P-Value	--	0 971			
Cystine	Mean	0 191	0 190	0 127 - 0 294	0 12 - 0 51	0 0966 - 0 251
	Range	0 121 - 0 237	0 115 - 0 242			
	Confidence Interval	0 167 - 0 215	0 166 - 0 214			
	Adjusted P-Value	--	0 922			
	P-Value	--	0 792			
Glutamic Acid	Mean	1 81	1 86	1 10 - 2 74	0 83 - 3 54	1 04 - 2 99
	Range	1 09 - 2 27	1 17 - 2 35			
	Confidence Interval	1 57 - 2 05	1 62 - 2 10			
	Adjusted P-Value	--	0 560			
	P-Value	--	0 188			
Glycine	Mean	0 390	0 393	0 285 - 0 481	0 184 - 0 685	0 263 - 0 472
	Range	0 317 - 0 439	0 304 - 0 445			
	Confidence Interval	0 364 - 0 417	0 367 - 0 419			
	Adjusted P-Value	--	0 875			
	P-Value	--	0 593			

Table 35. Amino Acid Results for DP910521 Maize Grain (continued)

Analyte	Reported Statistics	Control Maize	Herbicide-Treated DP910521 Maize	Tolerance Interval	Literature Range	Reference Data Range
Amino Acid Composition (% Dry Weight)						
Histidine	Mean	0 311	0 314	0 191 - 0 379	0 14 - 0 46	0 202 - 0 418
	Range	0 213 - 0 366	0 215 - 0 361			
	Confidence Interval	0 281 - 0 342	0 283 - 0 344			
	Adjusted P-Value	--	0 875			
	P-Value	--	0 612			
Isoleucine	Mean	0 337	0 344	0 207 - 0 491	0 18 - 0 69	0 194 - 0 541
	Range	0 221 - 0 417	0 234 - 0 410			
	Confidence Interval	0 297 - 0 376	0 305 - 0 383			
	Adjusted P-Value	--	0 566			
	P-Value	--	0 199			
Leucine	Mean	1 13	1 17	0 679 - 1 82	0 60 - 2 49	0 597 - 1 96
	Range	0 642 - 1 52	0 708 - 1 45			
	Confidence Interval	0 959 - 1 31	0 992 - 1 34			
	Adjusted P-Value	--	0 504			
	P-Value	--	0 0951			
Lysine	Mean	0 312	0 308	0 178 - 0 397	0 129 - 0 668	0 220 - 0 351
	Range	0 257 - 0 366	0 254 - 0 340			
	Confidence Interval	0 295 - 0 329	0 291 - 0 325			
	Adjusted P-Value	--	0 696			
	P-Value	--	0 422			
Methionine	Mean	0 216	0 214	0 105 - 0 312	0 10 - 0 47	0 110 - 0 331
	Range	0 149 - 0 281	0 146 - 0 279			
	Confidence Interval	0 189 - 0 244	0 187 - 0 241			
	Adjusted P-Value	--	0 875			
	P-Value	--	0 616			
Phenylalanine	Mean	0 491	0 494	0 299 - 0 729	0 24 - 0 93	0 262 - 0 803
	Range	0 297 - 0 675	0 312 - 0 615			
	Confidence Interval	0 425 - 0 558	0 427 - 0 560			
	Adjusted P-Value	--	0 915			
	P-Value	--	0 751			
Proline	Mean	0 800	0 815	0 551 - 1 24	0 46 - 1 75	0 491 - 1 32
	Range	0 511 - 1 01	0 541 - 0 968			
	Confidence Interval	0 698 - 0 902	0 713 - 0 917			
	Adjusted P-Value	--	0 618			
	P-Value	--	0 252			
Serine	Mean	0 467	0 475	0 309 - 0 678	0 15 - 0 91	0 273 - 0 690
	Range	0 326 - 0 561	0 326 - 0 560			
	Confidence Interval	0 415 - 0 518	0 424 - 0 527			
	Adjusted P-Value	--	0 504			
	P-Value	--	0 0952			
Threonine	Mean	0 359	0 367	0 248 - 0 485	0 17 - 0 67	0 228 - 0 496
	Range	0 271 - 0 434	0 264 - 0 420			
	Confidence Interval	0 328 - 0 391	0 336 - 0 399			
	Adjusted P-Value	--	0 504			
	P-Value	--	0 0746			
Tryptophan	Mean	0 0687	0 0684	0 0373 - 0 0982	0 027 - 0 215	0 0491 - 0 0825
	Range	0 0545 - 0 0789	0 0558 - 0 0801			
	Confidence Interval	0 0645 - 0 0728	0 0642 - 0 0725			
	Adjusted P-Value	--	0 917			
	P-Value	--	0 775			

Table 35. Amino Acid Results for DP910521 Maize Grain (continued)

Analyte	Reported Statistics	Control Maize	Herbicide-Treated DP910521 Maize	Tolerance Interval	Literature Range	Reference Data Range
Amino Acid Composition (% Dry Weight)						
Tyrosine	Mean	0 289	0 274	0 149 - 0 510	0 10 - 0 73	0 150 - 0 409
	Range	0 182 - 0 373	0 168 - 0 366			
	Confidence Interval	0 256 - 0 322	0 241 - 0 307			
	Adjusted P-Value	--	0 504			
	P-Value	--	0 0699			
Valine	Mean	0 464	0 470	0 300 - 0 627	0 21 - 0 86	0 287 - 0 663
	Range	0 331 - 0 544	0 341 - 0 552			
	Confidence Interval	0 417 - 0 511	0 424 - 0 517			
	Adjusted P-Value	--	0 633			
	P-Value	--	0.307			

Note: This table provides results from the mixed model analysis only. Amino acid composition is reported as % Dry W eight

Mineral Assessment of DP910521 Maize Grain

Minerals were analyzed in grain derived from DP910521 maize and control maize. Results are shown in Table 36. No statistically significant differences (P-value < 0.05) were observed between DP910521 maize and control maize, with an exception for one analyte. A statistically significant difference (P-value < 0.05) was observed between DP910521 maize and control maize for zinc. All individual values for this analyte were within the tolerance interval, indicating DP910521 maize is within the range of biological variation for this analyte and the statistical difference is not biologically meaningful. The non-significant FDR-adjusted P-value indicates that this difference was likely a false positive.

These results demonstrate that the mineral composition of grain derived from DP910521 maize is comparable to conventional maize represented by non-GM near-isoline control maize and non-GM commercial maize.

Table 36. Mineral Results for DP910521 Maize Grain

Analyte	Reported Statistics	Control Maize	Herbicide-Treated DP910521 Maize	Tolerance Interval	Literature Range	Reference Data Range
Calcium	Mean	0 00378	0 00389	0 00138 - 0 00735	NQ - 0 101	0 00203 - 0 00586
	Range	0 00265 - 0 00522	0 00271 - 0 00531			
	Confidence Interval	0 00327 - 0 00428	0 00338 - 0 00439			
	Adjusted P-Value	--	0 560			
	P-Value	--	0 189			
Copper	Mean	0 0000978	0 0000929	<0 0000625[b] - 0 000342	NQ - 0 0021	<0 0000625[b] - 0 000218
	Range	<0 0000625[b] - 0 000150	<0 0000625[b] - 0 000135			
	Confidence Interval	0 0000695 - 0 000126	0 0000646 - 0 000121			
	Adjusted P-Value	--	0 504			
	P-Value	--	0 128			
Iron	Mean	0 00178	0 00185	0 00115 - 0 00333	0 0000712 - 0 0191	0 00111 - 0 00246
	Range	0 00129 - 0 00237	0 00136 - 0 00255			
	Confidence Interval	0 00160 - 0 00197	0 00167 - 0 00204			
	Adjusted P-Value	--	0 504			
	P-Value	--	0 114			
Magnesium	Mean	0 116	0 115	0 0792 - 0 157	0 0035 - 1 000	0 0833 - 0 156
	Range	0 0912 - 0 138	0 0889 - 0 140			
	Confidence Interval	0 109 - 0 123	0 108 - 0 122			
	Adjusted P-Value	--	0 900			
	P-Value	--	0 650			
Manganese	Mean	0 000603	0 000627	0 000325 - 0 00120	0 0000312 - 0 0054	0 000341 - 0 00122
	Range	0 000428 - 0 000948	0 000442 - 0 000859			
	Confidence Interval	0 000508 - 0 000697	0 000532 - 0 000721			
	Adjusted P-Value	--	0 560			
	P-Value	--	0 180			
Phosphorus	Mean	0 344	0 340	0 211 - 0 414	0 010 - 0 750	0 265 - 0 393
	Range	0 275 - 0 379	0 298 - 0 383			
	Confidence Interval	0 330 - 0 357	0 327 - 0 354			
	Adjusted P-Value	--	0 838			
	P-Value	--	0 543			
Potassium	Mean	0 386	0 380	0 238 - 0 504	0 020 - 0 720	0 228 - 0 502
	Range	0 285 - 0 517	0 298 - 0 470			
	Confidence Interval	0 358 - 0 415	0 352 - 0 408			
	Adjusted P-Value	--	0 633			
	P-Value	--	0 330			
Sodium	Mean	0 000272	0 000241	<LLOQ[b] - 0 0136	NQ - 0 15	<0 0000625[b] - 0 00291
	Range	<0 0000625[b] - 0 00599	<0 0000625[b] - 0 00516			
	Confidence Interval	0 000177 - 0 000418	0 000157 - 0 000370			
	Adjusted P-Value	--	0 900			
	P-Value	--	0 669			
Zinc	Mean	0 00222	0 00232	0 00133 - 0 00343	0 0000283 - 0 0043	0 00159 - 0 00292
	Range	0 00176 - 0 00265	0 00185 - 0 00313			
	Confidence Interval	0 00204 - 0 00240	0 00214 - 0 00250			
	Adjusted P-Value	--	0 504			
	P-Value	--	0 0360*			

Note: This table provides results from the mixed model analysis only. Not quantified (NQ); one or more assay values in the published literature references were below the lower limit of quantification (LLOQ) and were not quantified. Minera l composition is reported as % Dry Weight.

[b] < LLOQ, one or more sample values were below the assay LLOQ.

* A statistically significant difference (P-Value < 0.05) was observed.

Vitamin Assessment of DP910521 Maize Grain

Vitamins were analyzed in grain derived from DP910521 maize and control maize. Results are shown in Table 37. No statistically significant differences (P-value < 0.05) were observed between DP910521 maize and control maize, with an exception for one analyte. A statistically significant difference (P-value < 0.05) was observed between DP910521 maize and control maize for Vitamin B1 (Thiamine). All individual values for this analyte were within the tolerance interval, indicating DP910521 maize is within the range of biological variation for this analyte and the statistical difference is not biologically meaningful. The non-significant FDR-adjusted P-value indicates that this difference was likely a false positive.

These results demonstrate that the vitamin composition of grain derived from DP910521 maize is comparable to conventional maize represented by non-GM near-isoline control maize and non-GM commercial maize.

Table 37. Vitamin Results for DP910521 Maize Grain

Analyte	Reported Statistics	Control Maize	Herbicide-Treated DP910521 Maize	Tolerance Interval	Literature Range	Reference Data Range
β-Carotene	Mean	0 488	0 472	0 - 3 86	0 3 - 5 81	<0 0500[b] - 0 945
	Range	0 168 - 0 786	0 184 - 0 748			
	Confidence Interval	0 335 - 0 641	0 318 - 0 625			
	Adjusted P-Value	--	0 560			
	P-Value	--	0 180			
Vitamin B1 (Thiamine)	Mean	2 61	2 77	1 12 - 4 85	NQ - 40 00	<0 900[b] - 3 70
	Range	<0 900[b] - 3 68	2 11 - 3 28			
	Confidence Interval	2 31 - 2 92	2 47 - 3 08			
	Adjusted P-Value	--	0 504			
	P-Value	--	0 0300[a]			
Vitamin B2 (Riboflavin)	Mean	<0 900[b]	<0 900[b]	<0 900[b] - 2 27[r]	NQ - 7 35	<0 900[b]
	Range	<0 900[b]	<0 900[b]			
	Confidence Interval	NA	NA			
	Adjusted P-Value	--	NA			
	P-Value	--	NA			
Vitamin B3 (Niacin)	Mean	15 1	14 7	7 75 - 30 5	NQ - 70	9 34 - 24 0
	Range	11 6 - 22 4	11 3 - 22 4			
	Confidence Interval	13 8 - 16 4	13 4 - 15 9			
	Adjusted P-Value	--	0 618			
	P-Value	--	0 241			
Vitamin B5 (Pantothenic Acid)	Mean	5 28	5 28	2 54 - 7 64	3 01 - 14	3 27 - 6 40
	Range	3 65 - 7 90	3 56 - 6 10			
	Confidence Interval	4 72 - 5 84	4 72 - 5 84			
	Adjusted P-Value	--	0 986			
	P-Value	--	0 972			
Vitamin B6 (Pyridoxine)	Mean	5 25	5 07	0 909 - 9 00	NQ - 12 14	2 53 - 11 0
	Range	2 53 - 10 7	2 84 - 9 02			
	Confidence Interval	4 34 - 6 15	4 17 - 5 98			
	Adjusted P-Value	--	0 633			
	P-Value	--	0 308			
Vitamin B9 (Folic Acid)	Mean	3 34	3 38	0 246 - 4 29	NQ - 3 50	1 04 - 8 50
	Range	1 07 - 6 90	1 23 - 5 86			
	Confidence Interval	2 62 - 4 06	2 66 - 4 10			
	Adjusted P-Value	--	0 973			
	P-Value	--	0 904			
α-Tocopherol	Mean	6 53	6 91	0 - 22 7	NQ - 68 67	1 93 - 15 5
	Range	3 05 - 11 0	3 35 - 10 7			
	Confidence Interval	5 27 - 7 80	5 64 - 8 17			
	Adjusted P-Value	--	0 504			
	P-Value	--	0 102			
β-Tocopherol	Mean	<0 500[b]	<0 500[b]	<0 500[b] - 1 10[r]	NQ - 19 80	<0 500[b] - 0 692
	Range	<0 500[b]	<0 500[b]			
	Confidence Interval	NA	NA			
	Adjusted P-Value	--	NA			
	P-Value	--	NA			

Table 37. Vitamin Results for DP910521 Maize Grain (continued)

Analyte	Reported Statistics	Control Maize	Herbicide-Treated DP910521 Maize	Tolerance Interval	Literature Range	Reference Data Range
γ-Tocopherol	Mean	25 4	24 5	0 - 44 4	NQ - 58 61	7 34 - 33 4
	Range	16 7 - 37 3	16 9 - 35 5			
	Confidence Interval	22 0 - 28 7	21 1 - 27 9			
	Adjusted P-Value	--	0 620			
	P-Value	--	0 262			
δ-Tocopherol	Mean	0 374	0 318	<0 500[b] - 2 61[r]	NQ - 14 61	<0 500[b] - 1 73
	Range	<0 500[b] - 0 915	<0 500[b] - 0 823			
	Confidence Interval	NA	NA			
	Adjusted P-Value	--	NA			
	P-Value	--	NA			
Total Tocopherols	Mean	32 5	32 0	0 - 57 9	NQ - 89 91	12 6 - 41 7
	Range	21 2 - 46 8	22 6 - 43 6			
	Confidence Interval	28 3 - 36 7	27 8 - 36 2			
	Adjusted P-Value	--	0 848			
	P-Value	--	0 561			

Note: This table provides results from the mixed model analysis only. Not applicable (NA); mixed model analysis was n ot performed, or confidence interval was not determined. Not quantified (NQ); one or more assay values in the publishe d literature references were below the lower limit of quantification (LLOQ) and were not quantified. Vitamin composition is reported as mg/kg Dry Weight

[b] < LLOQ, one or more sample values were below the assay LLOQ.

[r] Historical reference data range was provided as tolerance interval was not calculated since the data did not meet the ass umptions of any tolerance interval calculation method.

[*] A statistically significant difference (P-Value < 0.05) was observed.

Secondary Metabolite and Anti-Nutrient Assessment of DP910521 Maize Grain

Secondary metabolite and anti-nutrients were analyzed in grain derived from DP910521 maize and control maize. Results are shown in Table 38. No statistically significant differences (P-value < 0.05) were observed between DP910521 maize and control maize, with an exception for one analyte. A statistically significant difference (P-value < 0.05) was observed between DP910521 maize and control maize for *p*-coumaric acid. All individual values for this analyte were within the tolerance interval, indicating DP910521 maize is within the range of biological variation for this analyte and the statistical difference is not biologically meaningful. The non-significant FDR-adjusted P-value indicates that this difference was likely a false positive.

These results demonstrate that the secondary metabolite and anti-nutrient composition of grain derived from DP910521 maize is comparable to conventional maize represented by non-GM near-isoline control maize and non-GM commercial maize.

Table 38. Secondary Metabolite and Anti-Nutrient Results for DP910521 Maize Grain

Analyte	Reported Statistics	Control Maize	Herbicide-Treated DP910521 Maize	Tolerance Interval	Literature Range	Reference Data Range
p-Coumaric Acid	Mean	0 0248	0 0263	0 00781 - 0 0483	NQ - 0 08	0 0129 - 0 0473
	Range	0 0191 - 0 0305	0 0192 - 0 0321			
	Confidence Interval	0 0228 - 0 0267	0 0244 - 0 0282			
	Adjusted P-Value	--	0 504			
	P-Value	--	0 0145*			
Ferulic Acid	Mean	0 257	0 261	0 131 - 0 343	0 02 - 0 44	0 183 - 0 331
	Range	0 215 - 0 320	0 225 - 0 297			
	Confidence Interval	0 248 - 0 267	0 252 - 0 271			
	Adjusted P-Value	--	0 633			
	P-Value	--	0 296			
Furfural	Mean	<0 000100[b]	<0 000100[b]	<0 0000500[b]	NQ	<0 000100[b]
	Range	<0 000100[b]	<0 000100[b]			
	Confidence Interval	NA	NA			
	Adjusted P-Value	--	NA			
	P-Value	--	NA			
Inositol	Mean	0 0273	0 0269	0 00949 - 0 0571	0 00613 - 0 257	0 0117 - 0 0452
	Range	0 0204 - 0 0367	0 0162 - 0 0512			
	Confidence Interval	0 0246 - 0 0306	0 0243 - 0 0301			
	Adjusted P-Value	--	0 915			
	P-Value	--	0 756			
Phytic Acid	Mean	0 972	0 935	0 505 - 1 32	NQ - 1 940	0 643 - 1 12
	Range	0 771 - 1 15	0 711 - 1 19			
	Confidence Interval	0 911 - 1 03	0 875 - 0 995			
	Adjusted P-Value	--	0 504			
	P-Value	--	0 0500			
Raffinose	Mean	0 265	0 274	0 - 0 387	NQ - 0 466	<0 0800[b] - 0 424
	Range	0 138 - 0 416	0 149 - 0 477			
	Confidence Interval	0 218 - 0 311	0 227 - 0 320			
	Adjusted P-Value	--	0 714			
	P-Value	--	0 442			
Trypsin Inhibitor (TIU/mg DW)	Mean	2 37	2 37	1 06 - 8 12	NQ - 8 42	1 12 - 3 87
	Range	1 19 - 3 64	1 18 - 3 68			
	Confidence Interval	1 97 - 2 77	1 98 - 2 77			
	Adjusted P-Value	--	0 986			
	P-Value	--	0 986			

Note: This table provides results from the mixed model analysis only. Not applicable (NA); mixed model analysis was no t performed, or confidence interval was not determined. Not quantified (NQ); one or more assay values in the published literature references were below the lower limit of quantification (LLOQ) and were not quantified. Secondary Metabolite and Anti-Nutrient Composition (% Dry Weight or as Indicated)

[b] < LLOQ, one or more sample values were below the assay LLOQ.

* A statistically significant difference (P-Value < 0.05) was observed.

C. INFORMATION RELATED TO THE NUTRITIONAL IMPACT OF THE FOOD

In section *B.5 Compositional analyses of the food produced using gene technology*, the compositional equivalence of DP910521 maize to a conventional non-GM comparator with a history of safe use in food and feed was assessed. The results demonstrated that nutrient composition of forage and grain derived from DP910521 maize is comparable to that of conventional maize represented by non-GM near-isoline maize and non-GM commercial maize. Based on these analyses, the grain and forage of DP910521 maize are comparable to conventional maize with respect to nutrient composition.

Therefore, no nutritional impact of DP910521 is expected.

D. OTHER INFORMATION

Overall Risk Assessment Conclusions for DAS1131 Maize

This application presents information supporting the safety and nutritional comparability of DP910521 maize. The molecular characterization analyses conducted on DP910521 maize demonstrated that the introduced genes are integrated at a single locus, stably inherited across multiple generations, and segregate according to Mendel's law of genetics. The allergenic and toxic potential of the Cry1B.34, PAT, and PMI proteins were evaluated and found unlikely to be allergenic or toxic to humans. Based on the weight of evidence, consumption of the Cry1B.34, PAT, and PMI proteins is unlikely to cause an adverse effect on humans. A compositional equivalence assessment demonstrated that the nutrient composition of DP910521 maize forage and grain is comparable to that of conventional maize, represented by non-genetically modified (non-GM) near-isoline maize and non-GM commercial maize.

Overall, data and information contained herein support the conclusion that DP910521 maize containing the Cry1B.34, PAT, and PMI proteins is as safe and nutritious as non-GM maize.

REFERENCES

Abbitt SE, inventor, Aug. 8, 2017. SB-UBI terminator sequence for gene expression in plants. United States Patent, Patent No. US 9,725,731 B2

Abendroth LJ, Elmore RW, Boyer MJ, Marlay SK (2011) Corn Growth and Development. Iowa State University Extension, PMR 1009

AFSI (2021) Crop Composition Database, Version 8.0. Agriculture & Food Systems Institute, https://www.cropcomposition.org/

An G, Mitra A, Choi HK, Costa MA, An K, Thornburg RW, Ryan CA (1989) Functional Analysis of the 3' Control Region of the Potato Wound-Inducible Proteinase Inhibitor II Gene. The Plant Cell 1: 115-122

Benjamini Y, Hochberg Y (1995) Controlling the False Discovery Rate: a Practical and Powerful Approach to Multiple Testing. Journal of the Royal Statistical Society B 57: 289-300

CERA - ILSI Research Foundation (2011) A Review of the Environmental Safety of the PAT Protein. International Life Sciences Institute, Center for Environmental Risk Assessment

CERA - ILSI Research Foundation (2016) A Review of the Food and Feed Safety of the PAT Protein. International Life Sciences Institute, Center for Environmental Risk Assessment

Cheo DL, Titus SA, Byrd DRN, Hartley JL, Temple GF, Brasch MA (2004) Concerted Assembly and Cloning of Multiple DNA Segments Using In Vitro Site-Specific Recombination: Functional Analysis of Multi-Segment Expression Clones. Genome Research 14: 2111-2120

Christensen HM, Cong B, Crane V, Hu X, Lu AL, Mabry T, Rinehart Krebs K, Denise, Sandahl GA, inventors. 31 October 2019. Maize Event DP-023211-2 and Methods for Detection Thereof. World Intellectual Property Organization, Patent No. WO 2019/209700 A1

Codex Alimentarius Commission (2003) Alinorm 03/34: Appendix III: Draft guideline for the conduct of food safety assessment of foods derived from recombinant-DNA plants, and Appendix IV: Proposed Draft Annex of the Assessment of Possible Allergenicity. Food and Agriculture Organization of the United Nations, World Health Organization, Rome, pp 47-60

Codex Alimentarius Commission (2008) Guideline for the Conduct of Food Safety Assessment of Foods Derived from Recombinant-DNA Plants. Codex Alimentarius, CAC/GL 45-2003

Codex Alimentarius Commission (2019) Codex Standard for Named Vegetable Oils. Codex Alimentarius, CXS 210-1999

Cong B, Maxwell C, Luck S, Vespestad D, Richard K, Mickelson J, Zhong C (2015) Genotypic and Environmental Impact on Natural Variation of Nutrient Composition in 50 Non Genetically Modified Commercial Maize Hybrids in North America. Journal of Agricultural and Food Chemistry 63: 5321-5334

Crickmore N, Berry C, Panneerselvam S, Mishra R, Connor TR, Bonning BC (2021) A structure-based nomenclature for *Bacillus thuringiensis* and other bacteria-derived pesticidal proteins. Journal of Invertebrate Pathology 186: 107438

Dale EC, Ow DW (1990) Intra- and intramolecular site-specific recombination in plant cells mediated by bacteriophage P1 recombinase. Gene 91: 79-85

de Freitas FA, Yunes JA, da Silva MJ, Arruda P, Leite A (1994) Structural characterization and promoter activity analysis of the γ-kafirin gene from sorghum. Molecular and General Genetics 245: 177-186

Dey N, Maiti IB (1999) Structure and promoter/leader deletion analysis of mirabilis mosaic virus (MMV) full-length transcript promoter in transgenic plants. Plant Molecular Biology 40: 771-782

Diehen S, Nott A, Selinger DA, Simmons C, Bhyri P, Tavva V, inventors. Jul. 9, 2019. Regulatory sequences for modulating transgene expression in plants. United States Patent, Patent No. US 10,344,290 B2

Dong J, Feng Y, Kumar D, Zhang W, Zhu T, Luo M-C, Messing J (2016) Analysis of tandem gene copies in maize chromosomal regions reconstructed from long sequence reads. Proceedings of the National Academy of Sciences 113: 7949-7956

Dummitt B, Micka WS, Chang Y-H (2003) N-Terminal Methionine Removal and Methionine Metabolism in *Saccharomyces cerevisiae*. Journal of Cellular Biochemistry 89: 964-974

EFSA (2010) Scientific Opinion on the assessment of allergenicity of GM plants and microorganisms and derived food and feed. The EFSA Journal 8: 1700

EFSA Panel on Genetically Modified Organisms (GMO) (2011) Guidance for risk assessment of food and feed from genetically modified plants. The EFSA Journal 9: 2150

EnCor Biotechnology (2020) Ammonium Sulfate Calculator. EnCor Biotechnology Inc., http://www.encorbio.com/protocols/AM-SO4.htm

Ewing B, Green P (1998) Base-Calling of Automated Sequencer Traces Using *Phred*. II. Error Probabilities. Genome Research 8: 186-194

Ewing B, Hillier L, Wendl MC, Green P (1998) Base-Calling of Automated Sequencer Traces Using *Phred*. I. Accuracy Assessment. Genome Research 8: 175-185

FAO/WHO (2001) Evaluation of Allergencity of Genetically Modified Foods: Report of a Joint FAO/WHO Expert Consultation on Allergenicity of Foods Derived from Biotechnology, 22 - 25 January 2001. Food and Agriculture Organization of the United Nations, Rome

Fawcett R, Towery D (2003) Conservation Tillage and Plant Biotechnology: How New Technologies Can Improve the Environment By Reducing the Need to Plow. Conservation Technology Information Center, http://www.ctic.org/media/pdf/Biotech2003.pdf

Fernandez-Cornejo J, Hallahan C, Nehring R, Wechsler S (2012) Conservation Tillage, Herbicide Use, and Genetically Engineered Crops in the United States: The Case of Soybeans. AgBioForum 15: 231-241

Flannagan RD, Abad A, inventors. Jun. 2, 2009. *Bacillus thuringiensis CRY9* nucleic acids. United States Patent, Patent No. US 7,541,517 B2

Franck A, Guilley H, Jonard G, Richards K, Hirth L (1980) Nucleotide sequence of cauliflower mosaic virus DNA. Cell 21: 285-294

Gao H, Mutti J, Young JK, Yang M, Schroder M, Lenderts B, Wang L, Peterson D, St. Clair G, Jones S, Feigenbutz L, Marsh W, Zeng M, Wagner S, Farrell J, Snopek K, Scelonge C, Sopko X, Sander JD, Betts S, Cigan AM, Chilcoat ND (2020) Complex Trait Loci in Maize Enabled by CRISPR-Cas9 Mediated Gene Insertion. Frontiers in Plant Science 11: 535

Greger IH, Demarchi F, Giacca M, Proudfoot NJ (1998) Transcriptional interference perturbs the binding of Sp1 to the HIV-1 promoter. Nucleic Acids Research 26: 1294-1300

Guilley H, Dudley RK, Jonard G, Balàzs E, Richards KE (1982) Transcription of cauliflower mosaic virus DNA: detection of promoter sequences, and characterization of transcripts. Cell 30: 763-773

Hartley JL, Temple GF, Brasch MA (2000) DNA Cloning Using In Vitro Site-Specific Recombination. Genome Research 10: 1788-1795

Herman RA, Song P, Zhuang M (2011) Safety risks of cryptic reading frames and gene disruption due to crop transgenesis. What are the odds? GM Crops 2: 4-6

Hérouet C, Esdaile DJ, Mallyon BA, Debruyne E, Schulz A, Currier T, Hendrickx K, van der Klis R-J, Rouan D (2005) Safety evaluation of the phosphinothricin acetyltransferase proteins encoded by the *pat* and *bar* sequences that confer tolerance to glufosinate-ammonium herbicide in transgenic plants. Regulatory Toxicology and Pharmacology 41: 134-149

Hong B, Fisher TL, Sult TS, Maxwell CA, Mickelson JA, Kishino H, Locke MEH (2014) Model-Based Tolerance Intervals Derived from Cumulative Historical Composition Data: Application for Substantial Equivalence Assessment of a Genetically Modified Crop. Journal of Agricultural and Food Chemistry 62: 9916-9926

ISAAA (2019) GM Approval Database. International Service for the Acquisition of Agri-Biotech Applications, https://www.isaaa.org/gmapprovaldatabase/default.asp

ISAAA (2020) Gene: pmi (events list). International Service for the Acquisition of Agribiotech Applications, https://www.isaaa.org/gmapprovaldatabase/gene/default.asp?GeneID=37&Gene=pmi

Izumi Wilcoxon M, Yamamoto T, inventors. 21 April 2016. Insecticidal polypeptides having improved activity spectrum and uses thereof. World Intellectual Property Organization, Patent No. WO 2016/061197 A9

Katzen F (2007) Gateway® recombinational cloning: a biological operating system. Expert Opinion on Drug Discovery 2: 571-589

Keil M, Sanchez-Serrano J, Schell J, Willmitzer L (1986) Primary structure of a proteinase inhibitor II gene from potato (*Solanum tuberosum*). Nucleic Acids Research 14: 5641-5650

Kenward MG, Roger JH (2009) An improved approximation to the precision of fixed effects from

restricted maximum likelihood. Computational Statistics & Data Analysis 53: 2583-2595

La Paz JL, Pla M, Papazova N, Puigdomenech P, Vicient CM (2010) Stability of the MON 810 transgene in maize. Plant Molecular Biology 74: 563-571

Langmead B, Salzberg SL (2012) Fast gapped-read alignment with Bowtie 2. Nature Methods 9: 357-359

Lundry DR, Burns JA, Nemeth MA, Riordan SG (2013) Composition of Grain and Forage from Insect-Protected and Herbicide-Tolerant Corn, MON 89034 x TC1507 x MON 88017 x DAS-59122-7 (SmartStax), Is Equivalent to That of Conventional Corn (*Zea mays* L.). Journal of Agricultural and Food Chemistry 61: 1991-1998

Marçais G, Kingsford C (2011) A fast, lock-free approach for efficient parallel counting of occurrences of *k*-mers. Bioinformatics 27: 764-770

Martin M (2011) Cutadapt removes adapter sequences from high-througput sequencing reads. EMBnet.journal 17: 10-12

Mirsky HP, Cressman Jr RF, Ladics GS (2013) Comparative assessment of multiple criteria for the in silico prediction of cross-reactivity of proteins to known allergens. Regulatory Toxicology and Pharmacology 67: 232-239

NCGA (2020) World of Corn 2020. National Corn Growers Association, http://www.worldofcorn.com/#/

Negrotto D, Jolley M, Beer S, Wenck AR, Hansen G (2000) The use of phosphomannose-isomerase as a selectable marker to recover transgenic maize plants (*Zea mays* L.) via *Agrobacterium* transformation. Plant Cell Reports 19: 798-803

OECD (1993) Safety Evaluation of Foods Derived by Modern Biotechnology: Concepts and Principles. Organisation for Economic Cooperation and Development

OECD (1999) Consensus document on general information concerning the genes and their enzymes that confer tolerance to phosphinothricin herbicide. Organisation for Economic Co-operation and Development, ENV/JM/MONO(99)13

OECD (2002) Consensus Document on Compositional Considerations for New Varieties of Maize

(*Zea Mays*): Key Food and Feed Nutrients, Anti-Nutrients and Secondary Plant Metabolites. Organisation for Economic Co-operation and Development, ENV/JM/MONO(2002)25

Pawitan Y, Michiels S, Koscielny S, Gusnanto A, Ploner A (2005) False discovery rate, sensitivity and sample size for microarray studies. Bioinformatics 21: 3017-3024

Pearson WR, Lipman DJ (1988) Improved tools for biological sequence comparison. Proceedings of the National Academy of Sciences 85: 2444-2448

Perkins DN, Pappin DJC, Creasy DM, Cottrell JS (1999) Probability-based protein identification by searching sequence databases using mass spectrometry data. Electrophoresis 20: 3551-3567

Privalle LS (2002) Phosphomannose Isomerase, a Novel Plant Selection System. Annals of the New York Academy of Sciences 964: 129-138

Proteau G, Sidenberg D, Sadowski P (1986) The minimal duplex DNA sequence required for site-specific recombination promoted by the FLP protein of yeast *in vitro*. Nucleic Acids Research 14: 4787-4802

Reed J, Privalle L, Powell ML, Meghji M, Dawson J, Dunder E, Sutthe J, Wenck A, Launis K, Kramer C, Chang Y-F, Hansen G, Wright M (2001) Phosphomannose isomerase: An efficient selectable marker for plant transformation. In Vitro Cellular & Developmental Biology - Plant 37: 127-132

Roth Z, Yehezkel G, Khalaila I (2012) Identification and Quantification of Protein Glycosylation. International Journal of Carbohydrate Chemistry 2012: 640923

Schnepf E, Crickmore N, Van Rie J, Lereclus D, Baum J, Feitelson J, Zeigler DR, Dean DH (1998) *Bacillus thuringiensis* and Its Pesticidal Crystal Proteins. Microbiology and Molecular Biology Reviews 62: 775-806

Shearwin KE, Callen BP, Egan JB (2005) Transcriptional interference – a crash course. Trends in Genetics 21: 339-345

Shelton A (2012) Bacteria. Biological Control: A Guide to Natural Enemies in North America, http://www.biocontrol.entomology.cornell.edu/pathogens/bacteria.html

Sherman F, Stewart JW, Tsunasawa S (1985) Methionine or Not Methionine at the Beginning of a Protein. Bioessays 3: 27-31

Slein MW (1950) Phosphomannose Isomerase. Journal of Biological Chemistry 186: 753-761

Spelman RJ, Bovenhuis H (1998) Moving from QTL experimental results to the utilization of QTL in breeding programmes. Animal Genetics 29: 77-84

Sutcliffe JG (1978) Nucleotide sequence of the ampicillin resistance gene of *Escherichia coli* plasmid pBR322. Proceedings of the National Academy of Sciences 75: 3737-3741

Tao Y, Bidney D, Gordon-Kamm W, Lyznik L, inventors. January 25, 2007. Modified FRT Recombination Sites and Methods of Use. World Intellectual Property Organization, Patent No. WO2007/011733

US-EPA (1997) Escherichia coli K-12 Derivatives Final Risk Assessment. United States Environmental Protection Agency, https://www.epa.gov/sites/default/files/2015-09/documents/fra004.pdf

US-EPA (1998) R.E.D. Facts: *Bacillus thuringiensis*. United States Environmental Protection Agency, EPA-738-F-98-001

US-EPA (2001) Overview. In Biopesticides Registration Action Document: *Bt* Plant-Incorporated Protectants. United States Environmental Protection Agency, pp I1-I27, https://www3.epa.gov/pesticides/chem_search/reg_actions/pip/bt_brad2/1-overview.pdf

US-EPA (2004) Phosphomannose Isomerase and the Genetic Material Necessary for Its Production in All Plants; Exemption from the Requirement of a Tolerance. Federal Register 69: 26770-26775

USDA-APHIS (2001) Approval of Mycogen Seeds c/o Dow AgroSciences LLC and Pioneer Hi-Bred International, Inc., Request (00-136-01p) Seeking a Determination of Non-regulated Status for Bt Cry1F Insect Resistant, Glufosinate Tolerant Corn Line 1507: Environmental Assessment and Finding of No Significant Impact. United States Department of Agriculture, Animal and Plant Health Inspection Service

USDA-APHIS (2005) Mycogen Seeds/Dow AgroSciences LLC and Pioneer Hi-Bred International Inc.; Availability of Determination of Nonregulated Status for Genetically Engineered

Corn: Environmental Assessment and Finding of No Significant Impact. United States Department of Agriculture, Animal and Plant Health Inspection Service

USDA-APHIS (2013) Determination of nonregulated status for Pioneer Event DP-ØØ4114-3 corn. United States Department of Agriculture, Animal and Plant Health Inspection Service, https://www.aphis.usda.gov/brs/aphisdocs/11_24401p_det.pdf

USDA-APHIS (2020) Determination of Nonregulated Status for Pioneer DP202216 Maize. United States Department of Agriculture, Animal and Plant Health Inspection Service, https://www.aphis.usda.gov/brs/aphisdocs/19-101-01p-determination-final.pdf

USDA-NASS (2020) National Statistics for Corn: Corn - Acres Planted. United States Department of Agriculture, National Agricultural Statistics Service, https://www.nass.usda.gov/Statistics_by_Subject/result.php?12C29E97-8879-372A-B4F1-1BDFF54F7196&sector=CROPS&group=FIELD%20CROPS&comm=CORN

Waigmann E, Gomes A, Lanzoni A, Perry JN (2013) Editorial: New Commission Implementing Regulation on Risk Assessment of GM plant applications: novel elements and challenges. The EFSA Journal 11: e11121

Wang J, Jiang J, Oard JH (2000) Structure, expression and promoter activity of two polyubiquitin genes from rice (*Oryza sativa* L.). Plant Science 156: 201-211

Watson SA (1982) Corn: Amazing Maize. General Properties. In IA Wolff, ed, CRC Handbook of Processing and Utilization in Agriculture, Vol 2. CRC Press, Boca Raton, pp 3-29

Weber N, Halpin C, Hannah LC, Jez JM, Kough J, Parrott W (2012) Editor's Choice: Crop Genome Plasticity and Its Relevance to Food and Feed Safety of Genetically Engineered Breeding Stacks. Plant Physiology 160: 1842-1853

Weisser P, Krämer R, Sprenger GA (1996) Expression of the *Escherichia coli pmi* gene, encoding phosphomannose-isomerase in *Zymomonas mobilis*, leads to utilization of mannose as a novel growth substrate, which can be used as a selective marker. Applied and Environmental Microbiology 62: 4155-4161

Westfall PH, Tobias RD, Rom D, Wolfinger RD, Hochberg Y (1999) Concepts and Basic Methods for Multiple Comparisons and Tests. In Multiple Comparisons and Multiple Tests: Using SAS. SAS Institute Inc., Cary, NC, pp 13-40

Wohlleben W, Arnold W, Broer I, Hillemann D, Strauch E, Punier A (1988) Nucleotide sequence of the phosphinothricin *N*-acetyltransferase gene from *Streptomyces viridochromogenes* Tü494 and its expression in *Nicotiana tabacum*. Gene 70: 25-37

Yanisch-Perron C, Vieira J, Messing J (1985) Improved M13 phage cloning vectors and host strains: nucleotide sequences of the M13mpl8 and pUC19 vectors. Gene 33: 103-119

Zastrow-Hayes GM, Lin H, Sigmund AL, Hoffman JL, Alarcon CM, Hayes KR, Richmond TA, Jeddeloh JA, May GD, Beatty MK (2015) Southern-by-Sequencing: A Robust Screening Approach for Molecular Characterization of Genetically Modified Crops. The Plant Genome 8: 1-15

Zhang L, Lockhart B, Dahal G, Olszewski N (2008) Studies on biology and genomic characterization of a caulimo-like virus associated with a leaf distortion disease of *Lamium maculatum*. Archives of Virology 153: 1181-1184

STUDY INDEX

[redacted] (2021) “Characterization of DP-91Ø521-2 Maize for Insertion Stability in Five Generations Using Southern Blot Analysis” Corteva Agriscience study ID: PHI-2021-052

[redacted] et al. (2021) “Segregation Analysis and Tissue Production of Multiple Maize Generations Containing Event DP-91Ø521-2” Corteva Agriscience study ID: PHI-2020-067

[redacted]. (2021) “Characterization of Cry1B.34 Following In Vitro Pepsin and Sequential Pancreatin Digestion Using SDS-PAGE Analysis” Corteva Agriscience study ID: PHI-2021-056

[redacted] (2021) “Characterization of the In Vitro Pancreatin Resistance of Cry1B.34 Using SDS-PAGE and Western Blot Analysis” Corteva Agriscience study ID: PHI-2021-078

[redacted] (2021) “Characterization of the In Vitro Pepsin Resistance of Cry1B.34 Using SDS-PAGE and Western Blot Analysis” Corteva Agriscience study ID: PHI-2021-055

[redacted] et al. (2021) “Characterization of Cry1B.34 (PCF-0042) Protein Derived from a Microbial Expression System” Corteva Agriscience study ID: PHI-2020-093

[redacted]. et al. (2021) “Characterization of Cry1B.34 (PCF-0059) Protein Derived from a Microbial Expression System” Corteva Agriscience study ID: PHI-2021-027

[redacted] et al. (2021) “Characterization of Cry1B.34 Protein Derived from DP-91Ø521-2 Maize” Corteva Agriscience study ID: PHI-2021-115

[redacted] (2021) “Southern-by-Sequencing Analysis of the T1 Generation of DP-91Ø521-2 Maize” Corteva Agriscience study ID: PHI-2021-045

[redacted] (2021) “Cry1B.34: Acute Oral Toxicity Study in Mice” Corteva Agriscience study ID: PHI-2020-188

[redacted] et al. (2021) “Characterization of PAT Protein Derived from DP-91Ø521-2 Maize” Corteva Agriscience study ID: PHI-2021-134

[redacted] et al. (2021) "Determination of the Biological Activity of Heat-Treated Cry1B.34 Protein Incorporated in an Artificial Diet and Fed to *Spodoptera frugiperda*" Corteva Agriscience study ID: PHI-2021-067

[redacted] (2021) "Characterization of the Genomic Border Regions of Maize Event DP-91Ø521-2" Corteva Agriscience study ID: PHI-2021-194/230

[redacted] (2021) "Comparison of the Cry1B.34 Protein Sequence to the Protein Sequences in the Internal Toxin Database" Corteva Agriscience study ID: PHI-2021-204/211

[redacted] (2021) "Reading Frame Analysis at the Insertion Site of Maize Event DP-91Ø521-2" Corteva Agriscience study ID: PHI-2021-195/225

[redacted] (2021) "Development and Validation of an Event-Specific Quantitative Real-Time PCR (qPCR) Detection Method for Maize Event DP-91Ø521-2" Corteva Agriscience study ID: PHI-2021-104

[redacted] et al. (2021) "Expressed Trait Protein Concentration of a Maize Line Containing Event DP-91Ø521-2" Corteva Agriscience study ID: PHI-2020-024

[redacted] et al. (2021) "Nutrient Composition of an Herbicide-Treated Maize Line Containing Event DP-91Ø521-2" Corteva Agriscience study ID: PHI-2020-025/021

[redacted] (2021) "Comparison of the Amino Acid Sequence of the Cry1B.34 Protein to the Amino Acid Sequences of Known and Putative Protein Allergens" Corteva Agriscience study ID: PHI-2021-106/201

[redacted] et al. (2021) "Characterization of PMI Protein Derived from DP-91Ø521-2 Maize" Corteva Agriscience study ID: PHI-2021-153

[redacted] et al. (2021) "Sequence Characterization of Insert and Flanking Regions of DP-91Ø521-2 Maize" Corteva Agriscience study ID: PHI-2021-064

APPENDIX A. METHODS FOR SOUTHERN-BY-SEQUENCING ANALYSIS

Test and Control and Substances

The test substance in this study was defined as the DP-91Ø521-2 event contained within seed from the segregating T1 generation of DP910521 maize. The control substance was defined as the absence of the DP-91Ø521-2 event in untransformed PH184C maize seed (referred to as control maize). The unmodified line has a genetic background representative of the test substance background; however, it does not contain the DP910521 insertion.

DNA Extraction and Quantitation

Genomic DNA was separately extracted from leaf tissue of ten individual DP910521 maize plants and one control maize plant. The tissue was pulverized in tubes containing grinding beads using a Geno/Grinder™ (SPEX CertiPrep), and the genomic DNA was isolated using a standard Urea Extraction Buffer procedure. Following extraction, the DNA was quantified on a spectrofluorometer using the Quant-iT™ PicoGreen® dsDNA Assay Kit (Invitrogen) and visualized on an agarose gel to determine the DNA quality.

Southern-by-Sequencing

SbS was performed by Pioneer Hi-Bred International, Inc. Genomics Technologies (hereafter referred to as Genomics Technologies). SbS analysis utilizes probe-based sequence capture, Next Generation Sequencing (NGS) techniques, and bioinformatics procedures to capture, sequence, and identify inserted DNA within the maize genome (Zastrow-Hayes *et al.*, 2015). By compiling a large number of unique sequencing reads and mapping them against the linearized transformation plasmid maps, and control maize genome, unique junctions due to inserted DNA are identified in the bioinformatics analysis. This information is used to determine the number and organization of insertions within the plant genome and confirm the absence of plasmid backbone and other unintended plasmid sequences.

Genomic DNA isolated from the T1 generation of DP910521 maize was analyzed by SbS to determine the insertion copy number and organization. SbS was also performed on control maize DNA and positive control samples (control maize DNA spiked with PHP79620, [redacted], [redacted], PHP21875, PHP73572, or PHP5096 plasmid DNA at a level corresponding to one copy of plasmid per copy of the maize genome) to confirm that the assay could reliably detect plasmid fragments within the genomic DNA.

The following processes were performed by Genomics Technologies using standard methods and were based on the procedures described in Zastrow-Hayes *et al.* (2015).

Capture Probe Design and Synthesis

Biotinylated capture probes used to select plasmid sequences were designed and synthesized by Roche NimbleGen, Inc. The probe set was designed to target all sequences within the PHP79620, [redacted], PHP21875, PHP73572, and PHP5096 plasmids.

Sequencing Library Construction

NGS libraries were constructed for DNA samples from individual maize plants, including DP910521 maize plants, a control maize plant, and the positive control sample. Genomic DNA purified as described above was sheared to an average fragment size of 400 base pairs (bp) using an ultrasonicator. Sheared DNA was end-repaired, A-tailed, and ligated to NEXTflex-HT™ Barcode adaptors (Bioo Scientific Corp.) following the kit protocol so that samples would be indexed to enable identification after sequencing. The DNA fragment libraries were amplified by PCR for eight cycles prior to the capture process. Amplified libraries were analyzed using a fragment analyzer and diluted to 5 ng/µl with nuclease-free water.

Probe Hybridization and Sequence Enrichment

A double capture procedure was used to capture and enrich DNA fragments that contained sequences homologous to the capture probes. The genomic DNA libraries described above were mixed with hybridization buffer and blocking oligonucleotides corresponding to the adapter sequences and denatured. Following denaturation, the biotinylated probes were added to the genomic DNA library and incubated at 47 °C for 16 hours. Streptavidin beads were added to the hybridization mix to bind DNA fragments that were associated with the probes. Bound fragments were washed and eluted, PCR-amplified for five cycles, and purified using spin columns. The enriched DNA libraries underwent a second capture reaction using the same conditions to further enrich the sequences targeted by the probes. This was followed by PCR amplification for 16 cycles and purification as described above. The final double-enriched libraries were quantified and diluted to 2 nM for sequencing.

Next Generation Sequencing on Illumina Platform

Following sequence capture, the libraries were submitted for NGS (Illumina NextSeq500) to a depth of at least 100x for the captured sequences. The sequence reads were trimmed [redacted] (Ewing and Green, 1998; Ewing *et al.*, 1998) and assigned to the corresponding individual plant based on the indexing adapters. A complete sequence set from each plant is referred to as "AllReads" for bioinformatics analysis of that plant.

Quality Assurance of Sequncing Reads

The adapter sequences were trimmed from the NGS sequence using Cutadapt, v2.10 (Martin, 2011). Further analysis to eliminate sequencing errors used JELLYFISH, version 2.2.10 (Marçais and Kingsford, 2011), to [redacted] within "AllReads" as described in Zastrow-Hayes et al. (2015). This set of sequences was used for further bioinformatics analysis and is referred to as "CleanReads." Identical sequence reads were combined into non-redundant read groups (referred to as "Non-redundantReads") while retaining abundance information for each group and were used for further analysis, as described in Zastrow-Hayes *et al.* (2015).

Aligning Reads

Each set of "Non-redundantReads" was aligned to the plasmid sequences, including the plasmid backbone sequences, using Bowtie2, version 2.3.4.2 (Langmead and Salzberg, 2012), [redacted]

[redacted]. Remaining "Non-redundantReads" were aligned to the maize reference genome using Bowtie2, version 2.3.4.2[redacted].

Junction Detection

Following removal of "Non-redundantReads" with alignments to the maize reference genome or plasmid sequence identified during the quality assurance phase, the remaining "Non-redundantReads" were aligned to the full plasmid sequences using Bowtie2, version 2.3.4.2, with the soft-trimming feature enabled. Chimeric reads contain sequence that is non-contiguous with the plasmid sequence from the alignment, such as genome-plasmid junctions or rearrangements of the plasmid. These chimeric reads are referred to as junction reads or junctions. [redacted] This identifier (referred to as a 30_20 mer) includes 20 bp of sequence from PHP79620, [redacted], PHP21875, PHP73572, or PHP5096, and 30 bp of sequence adjacent to the plasmid-derived 20 bp within a sequencing read. The adjacent 30 bp either did not align to the plasmid contiguously to the known 20 bp or aligned to the genome. When the 20 bp from the plasmid and the adjacent 30 bp were identified as a 30_20 mer, they indicated the junction shown by the chimeric read. [redacted]. The total number of sequence reads (referred to as "TotalSupportingReads") for each unique junction was retained for filtering. [redacted]

Junction Identification

Variations between the maize reference genome used in the SbS analysis and the control maize genome may result in identification of junctions that are due to these differences in the endogenous maize sequences. In order to detect these endogenous junctions, control maize genomic DNA libraries were captured and sequenced in the same manner. The 30_20 mers of the endogenous junctions detected in the control sample were used to filter the same endogenous junctions in the DP910521 maize samples, so that the only junctions remaining in the DP910521 samples are due to actual insertions derived from PHP79620, [redacted], PHP21875, PHP73572, and PHP5096.

Data QC

The transgenic and null samples were compared to the control sample and a quality check was performed. If a junction was identified between two noncontiguous plasmid regions and after further review was identified to be a PCR amplicon, then it was masked in the final data. PCR amplicons are usually found in regions that have a duplicated sequence (within the plasmid or adapter) similar enough that a sequencing read can align to either sequence and function as a primer to initiate spurious PCR amplicons.

If regions of the plasmid backbone or other unintended plasmid sequences contain low to medium sequencing coverage compared to the control sample and no junctions were identified, the data was reviewed a second time. If no junctions were identified for these reads, there is no insertion of the plasmid into the genome. Contamination is a possible source of such reads and the

sequencing reads will be reviewed to determine the type of contaminant. If the sample is contaminated by a different sample that contains a similar plasmid with overlapping elements, most if not all of the sequencing reads will align to the plasmid being analyzed. If the sample is contaminated from a bacterial source that lives on the plant, the sequencing reads will likely not align exactly to the plasmid. If a null sample has additional regions on the map of the insertion that have low sequencing coverage and no junctions are identified, this is contamination from a transgenic plant.

SbS Results

Results for the control maize, positive control, one DP910521 maize plant (Plant ID 404181698), null segregant (negative) plant (Plant ID 404181702) are presented in the main body (Section 4a) of this document. Remaining plant results from SbS analysis are presented in Figures A1 to A5 (positive plants) below.

A. Alignment to Intended Insertion

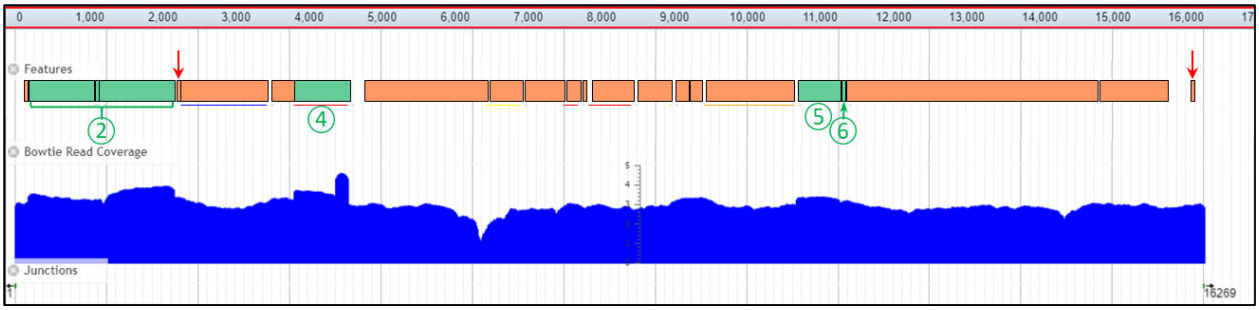

B. Alignment to PHP79620

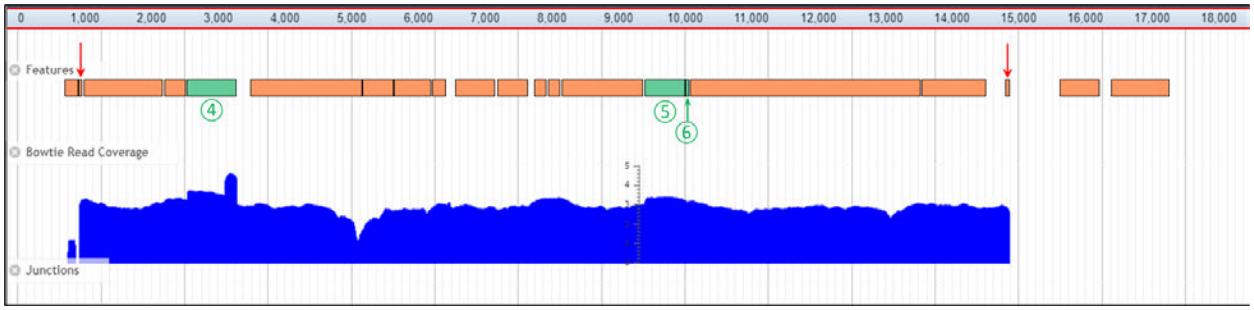

C. Alignment to [redacted]

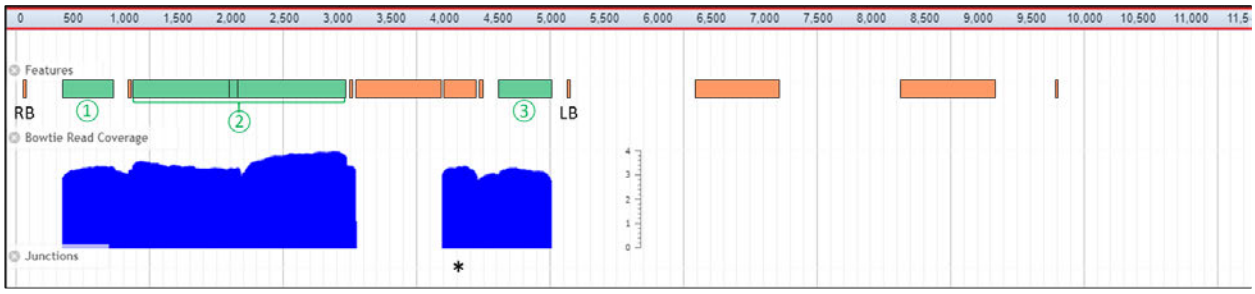

D. Alignment to [redacted]

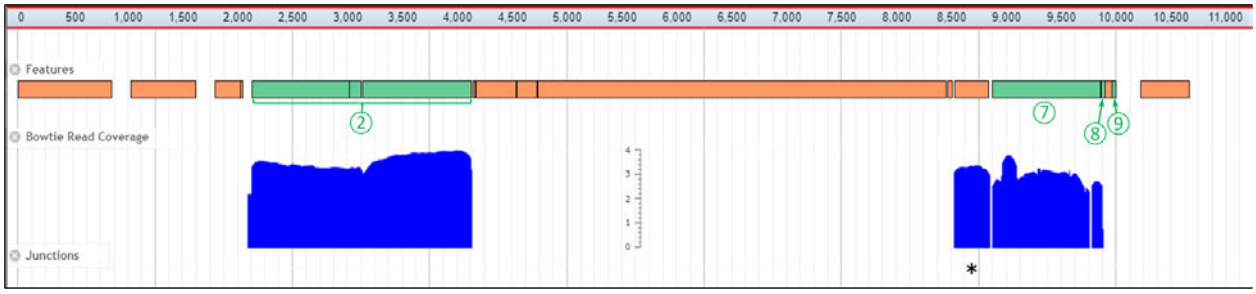

E. Alignment to [redacted]

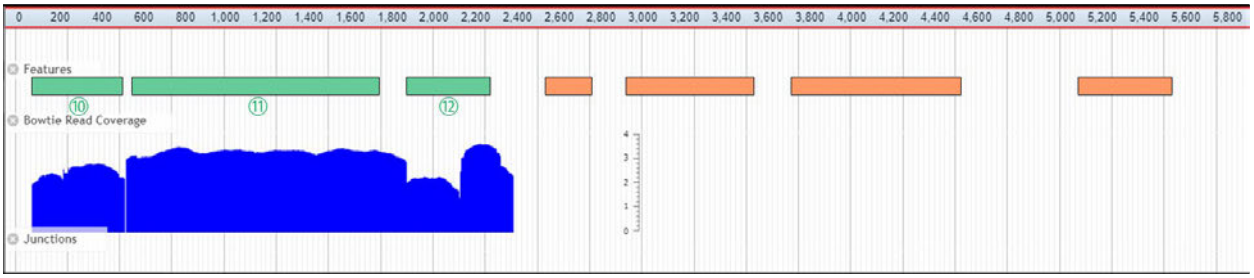

F. Alignment to PHP21875

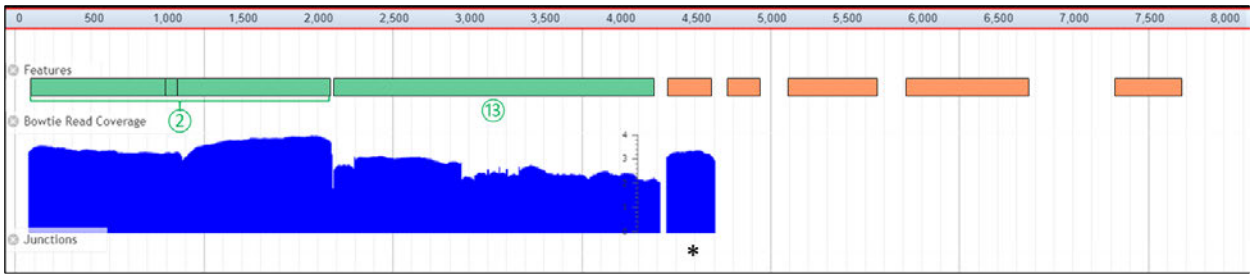

G. Alignment to PHP73572

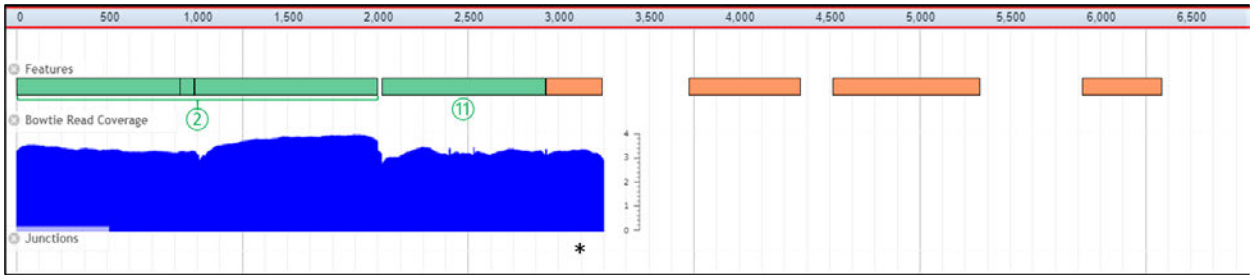

H. Alignment to PHP5096

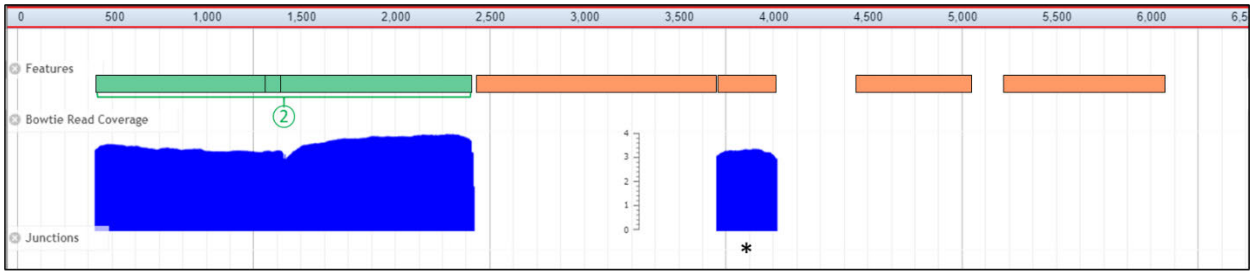

Figure A1. SbS Results for Plant ID 404181700 – DP910521 Maize (Transgenic)

The blue coverage graph shows the number of individual NGS reads aligned at each point on the intended insertion or plasmid using a logarithmic scale at the middle of the graph. Green bars above the coverage graph indicate endogenous genetic elements in each plasmid derived from the maize genome (identified by numbers; Table 5), while tan bars indicate genetic elements derived from other sources. FRT sites are

indicated by red arrows. **A)** SbS results aligned against the intended insertion (16,269 bp; Figure 10), indicating that this plant contains the intended insertion. Arrows below the graph indicate the two plasmid-to-genome sequence junctions identified by SbS; the numbers below the arrows refer to the bp location of the junction relative to the intended insertion (Figure 10). The presence of only two junctions demonstrates the presence of a single insertion in the DP910521 maize genome. **B)** SbS results aligned against the plasmid PHP79620 sequence (17,763 bp; Figure 6). Coverage was obtained for the elements between FRT1 and FRT87 transferred into DP910521 maize (region between the red arrows at top of graph). **C)** SbS results aligned against the plasmid [redacted] sequence [redacted] bp; Figure 1). Coverage was obtained for [redacted], and the elements found in the intended insertion (between [redacted] to FRT1 and between FRT87 to [redacted]), along with the *pin*II terminator element (*) in [redacted] due to alignment of reads derived from the *pin*II terminator in the *pmi* cassette of the intended insertion to the copy of this element in [redacted]. **D)** SbS results aligned against the plasmid [redacted] sequence ([redacted] bp; Figure 2). Coverage was obtained only for the endogenous elements along with the *pin*II terminator element (*). **E)** SbS results aligned against the plasmid [redacted] sequence ([redacted] bp; Figure 3). Coverage was obtained only for the endogenous elements. **F)** SbS results aligned against the plasmid PHP21875 sequence (7,842 bp; Figure 4). Coverage was obtained for the endogenous elements along with the *pin*II terminator element (*). **G)** SbS results aligned against the plasmid PHP73572 sequence (6,559 bp; Figure 8). Coverage was obtained for the endogenous elements along with the *pin*II terminator element (*). **H)** SbS results aligned against the plasmid PHP5096 sequence (6,269 bp; Figure 7). Coverage was obtained for the endogenous elements along with the *pin*II terminator element (*). The absence of any junctions other than to the intended insertion indicates that there are no additional insertions, plasmid backbone, or other unintended plasmid sequences present in DP910521 maize.

A. Alignment to Intended Insertion

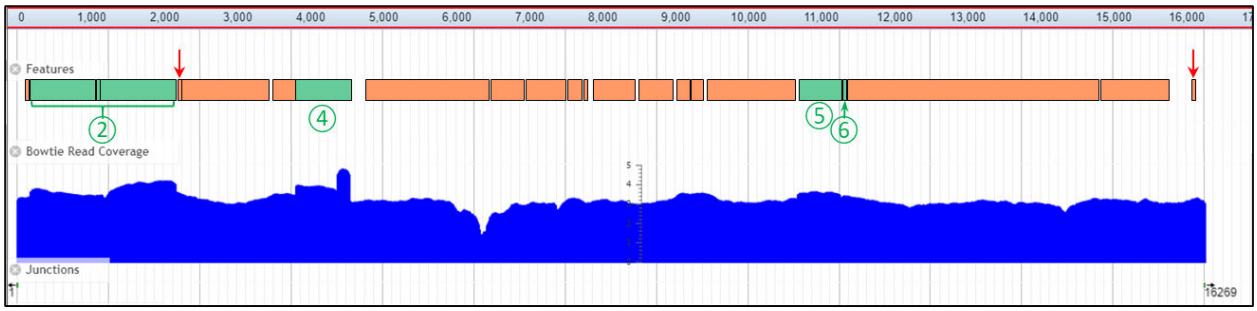

B. Alignment to PHP79620

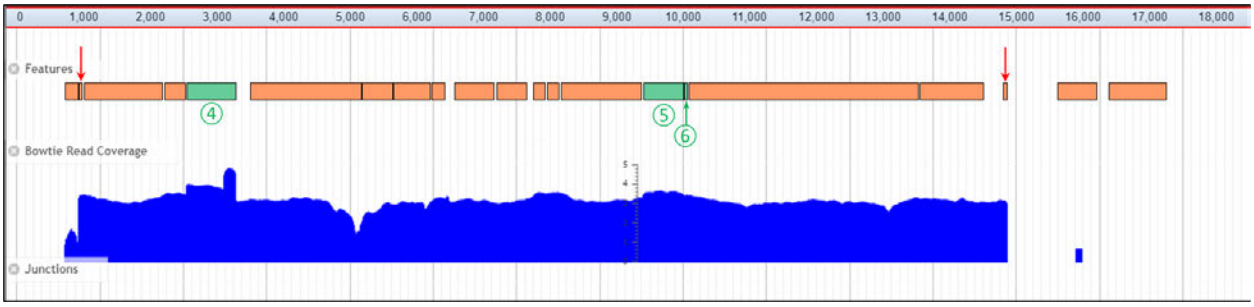

C. Alignment to [redacted]

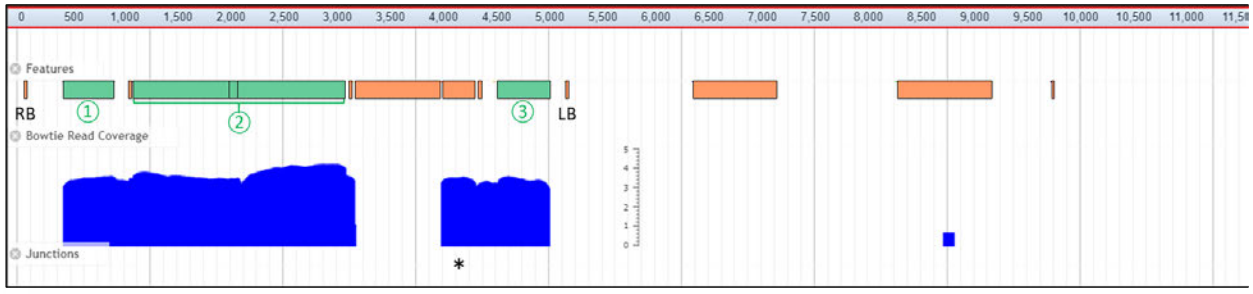

D. Alignment to [redacted]

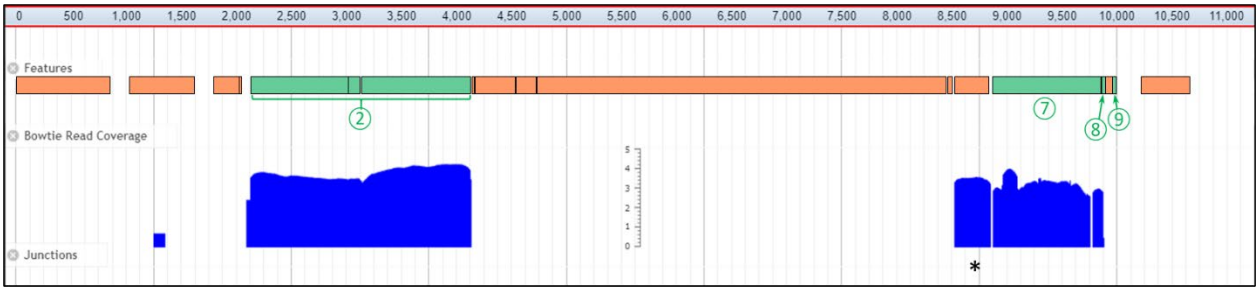

E. Alignment to [redacted]

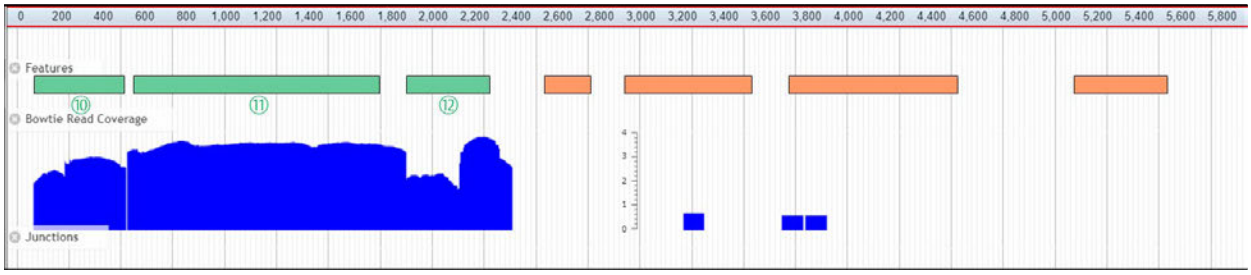

F. Alignment to PHP21875

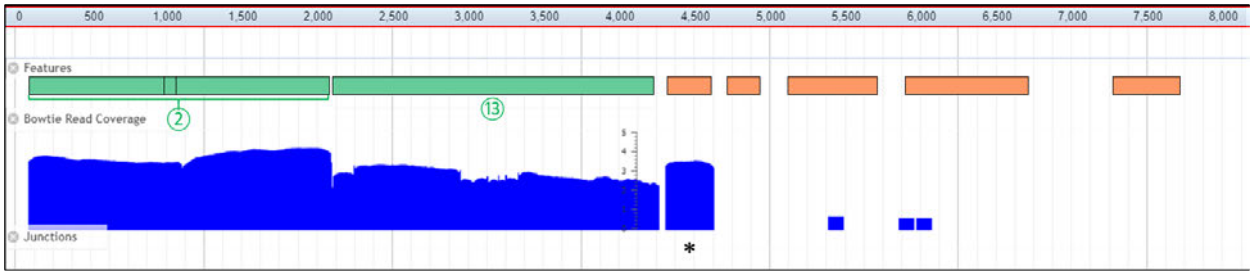

G. Alignment to PHP73572

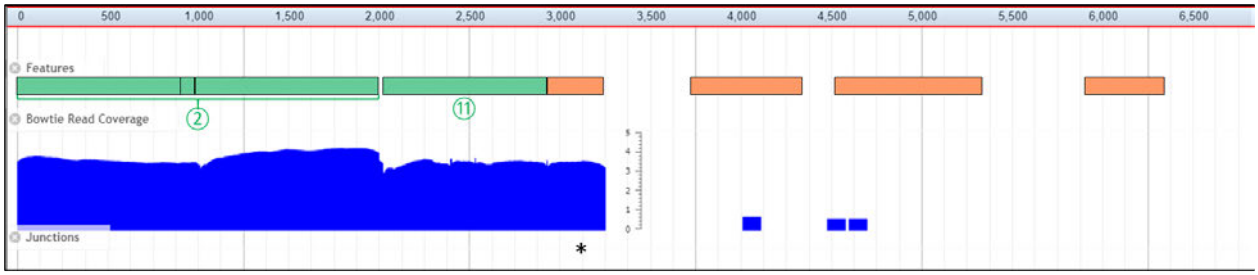

H. Alignment to PHP5096

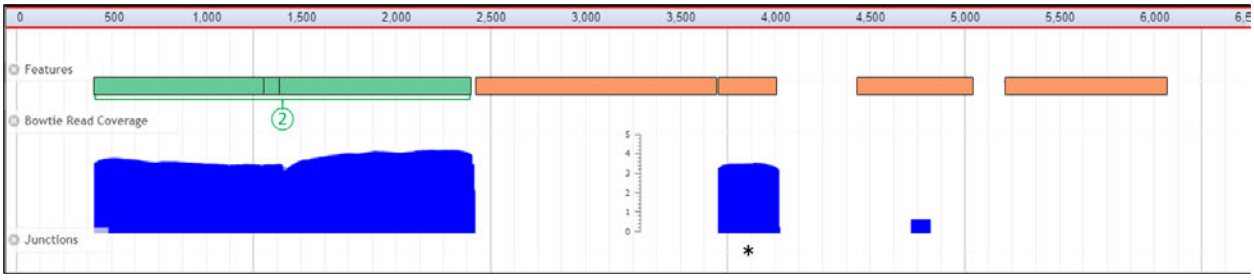

Figure A2. SbS Results for Plant ID 404181703 – DP910521 Maize (Transgenic)

The blue coverage graph shows the number of individual NGS reads aligned at each point on the intended insertion or plasmid using a logarithmic scale at the middle of the graph. Green bars above the coverage graph indicate endogenous genetic elements in each plasmid derived from the maize genome (identified by numbers; Table 5), while tan bars indicate genetic elements derived from other sources. FRT sites are indicated by red arrows. **A)** SbS results aligned against the intended insertion (16,269 bp; Figure 10),

indicating that this plant contains the intended insertion. Arrows below the graph indicate the two plasmid-to-genome sequence junctions identified by SbS; the numbers below the arrows refer to the bp location of the junction relative to the intended insertion (Figure 10). The presence of only two junctions demonstrates the presence of a single insertion in the DP910521 maize genome. **B)** SbS results aligned against the plasmid PHP79620 sequence (17,763 bp; Figure 6). Coverage was obtained for the elements between FRT1 and FRT87 transferred into DP910521 maize (region between the red arrows at top of graph). **C)** SbS results aligned against the plasmid [redacted] sequence ([redacted] bp; Figure 1). Coverage was obtained for [redacted], and the elements found in the intended insertion (between [redacted] to FRT1 and between FRT87 to [redacted]), along with the *pin*II terminator element (*) in [redacted] due to alignment of reads derived from the *pin*II terminator in the *pmi* cassette of the intended insertion to the copy of this element in [redacted]. **D)** SbS results aligned against the plasmid [redacted] sequence ([redacted] bp; Figure 2). Coverage was obtained only for the endogenous elements along with the *pin*II terminator element (*). **E)** SbS results aligned against the plasmid [redacted] sequence ([redacted] bp; Figure 3). Coverage was obtained only for the endogenous elements. **F)** SbS results aligned against the plasmid PHP21875 sequence (7,842 bp; Figure 4). Coverage was obtained for the endogenous elements along with the *pin*II terminator element (*). **G)** SbS results aligned against the plasmid PHP73572 sequence (6,559 bp; Figure 8). Coverage was obtained for the endogenous elements along with the *pin*II terminator element (*). **H)** SbS results aligned against the plasmid PHP5096 sequence (6,269 bp; Figure 7). Coverage was obtained for the endogenous elements along with the *pin*II terminator element (*). The absence of any junctions other than to the intended insertion indicates that there are no additional insertions, plasmid backbone, or other unintended plasmid sequences present in DP910521 maize.

A. Alignment to Intended Insertion

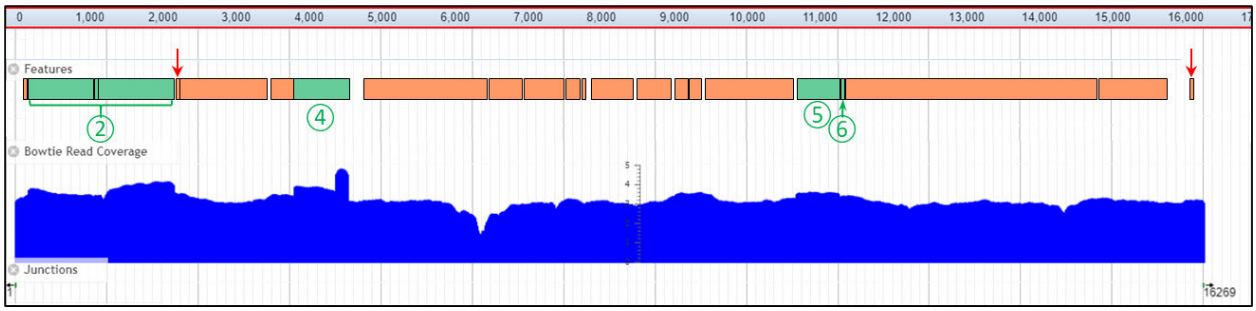

B. Alignment to PHP79620

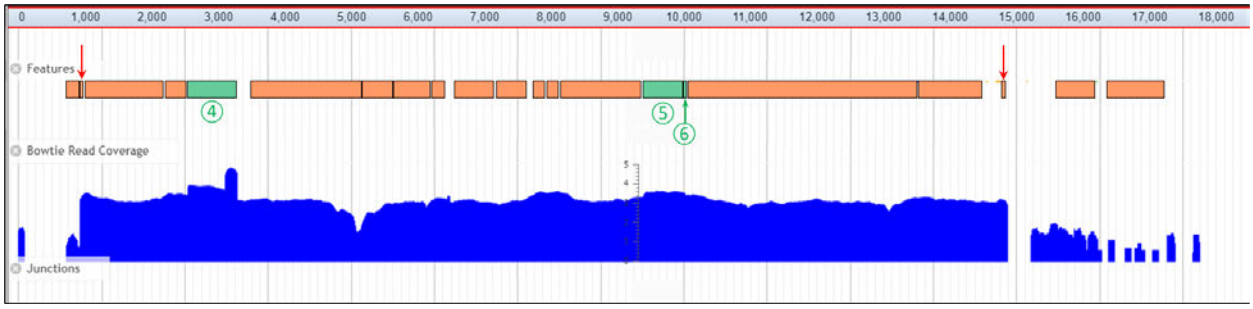

C. Alignment to [redacted]

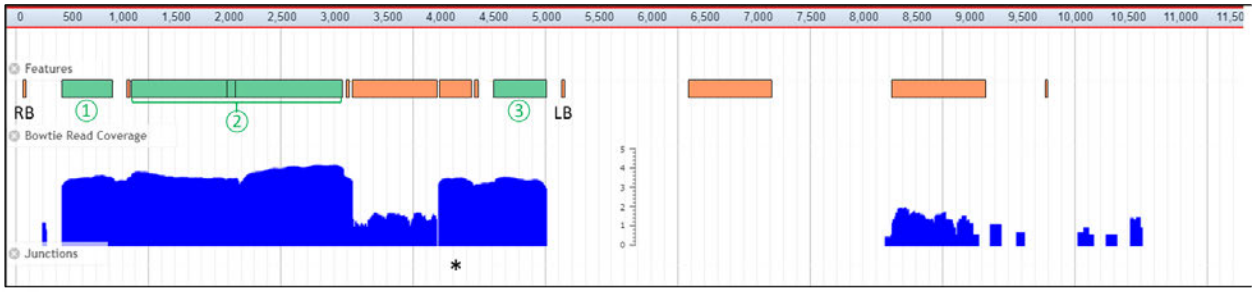

D. Alignment to [redacted]

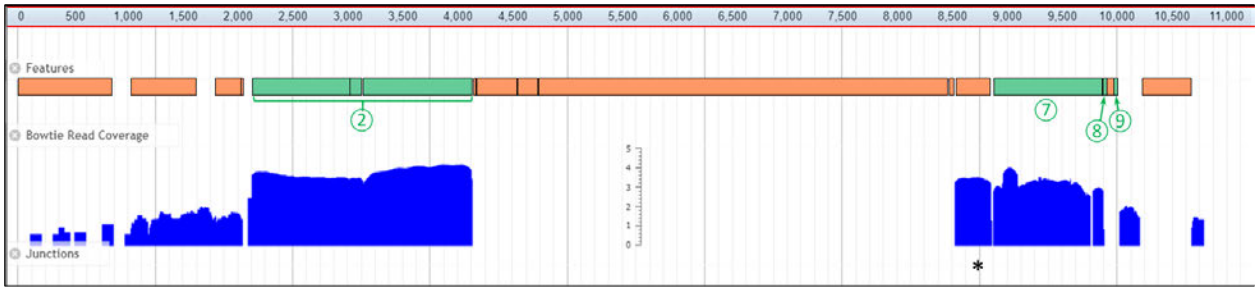

E. Alignment to [redacted]

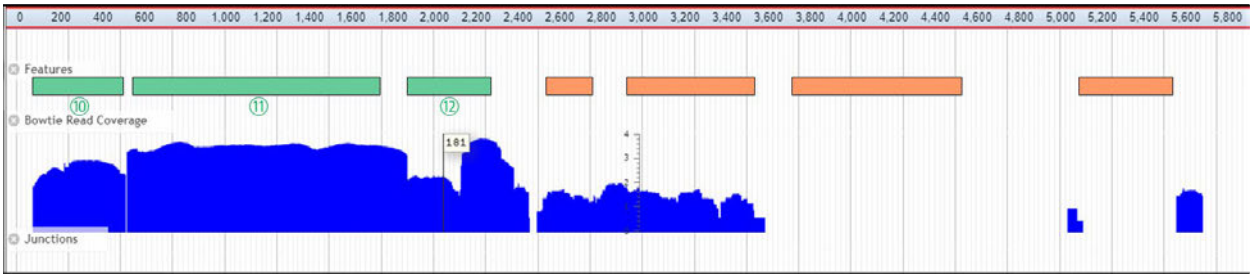

F. Alignment to PHP21875

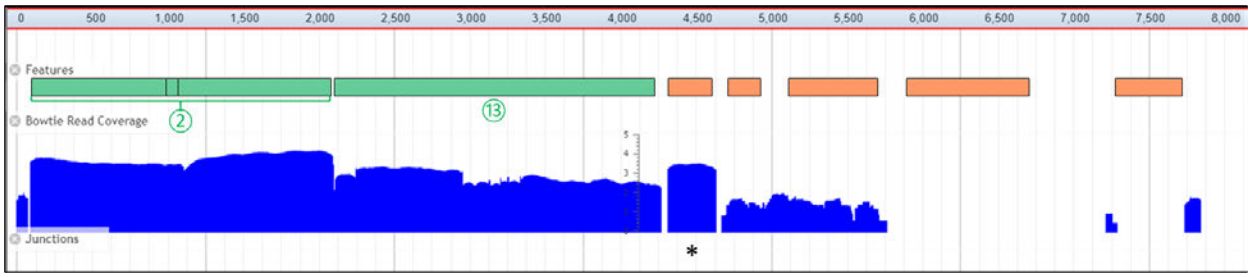

G. Alignment to PHP73572

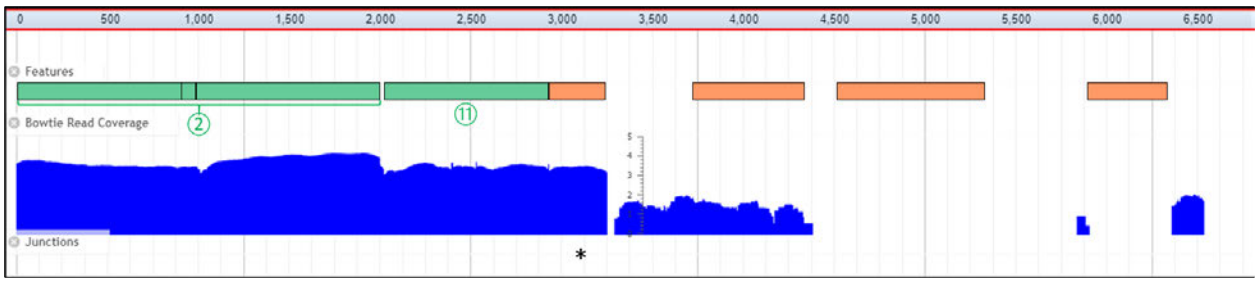

H. Alignment to PHP5096

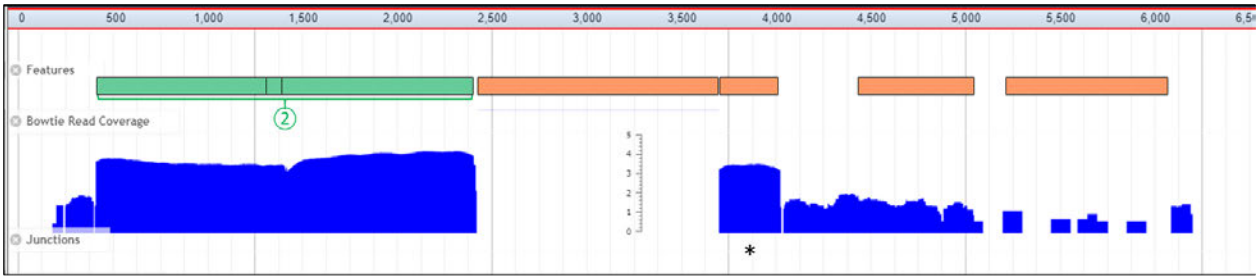

Figure A3. SbS Results for Plant ID 404181704 – DP910521 Maize (Transgenic)

The blue coverage graph shows the number of individual NGS reads aligned at each point on the intended insertion or plasmid using a logarithmic scale at the middle of the graph. Green bars above the coverage graph indicate endogenous genetic elements in each plasmid derived from the maize genome (identified by numbers; Table 5), while tan bars indicate genetic elements derived from other sources. FRT sites are

indicated by red arrows. **A)** SbS results aligned against the intended insertion (16,269 bp; Figure 10), indicating that this plant contains the intended insertion. Arrows below the graph indicate the two plasmid-to-genome sequence junctions identified by SbS; the numbers below the arrows refer to the bp location of the junction relative to the intended insertion (Figure 10). The presence of only two junctions demonstrates the presence of a single insertion in the DP910521 maize genome. **B)** SbS results aligned against the plasmid PHP79620 sequence (17,763 bp; Figure 6). Coverage was obtained for the elements between FRT1 and FRT87 transferred into DP910521 maize (region between the red arrows at top of graph). **C)** SbS results aligned against the plasmid [redacted] sequence ([redacted] bp; Figure 1). Coverage was obtained for [redacted], and the elements found in the intended insertion (between [redacted] to FRT1 and between FRT87 to [redacted]), along with the *pin*II terminator element (*) in [redacted] due to alignment of reads derived from the *pin*II terminator in the *pmi* cassette of the intended insertion to the copy of this element in [redacted]. **D)** SbS results aligned against the plasmid [redacted] sequence ([redacted] bp; Figure 2). Coverage was obtained only for the endogenous elements along with the *pin*II terminator element (*). **E)** SbS results aligned against the plasmid [redacted] sequence ([redacted] bp; Figure 3). Coverage was obtained only for the endogenous elements. **F)** SbS results aligned against the plasmid PHP21875 sequence (7,842 bp; Figure 4). Coverage was obtained for the endogenous elements along with the *pin*II terminator element (*). **G)** SbS results aligned against the plasmid PHP73572 sequence (6,559 bp; Figure 8). Coverage was obtained for the endogenous elements along with the *pin*II terminator element (*). **H)** SbS results aligned against the plasmid PHP5096 sequence (6,269 bp; Figure 7). Coverage was obtained for the endogenous elements along with the *pin*II terminator element (*). In this sample, all plasmids show low levels of sequencing reads to regions that are not incorporated in the final insertion and are not endogenous maize sequences. However, since no junctions were detected by these reads, they were reviewed more closely. It was determined that these reads are due to contamination of the sample by an outside source and do not indicate the presence of additional insertions. The absence of any junctions other than to the intended insertion indicates that there are no additional insertions, plasmid backbone, or other unintended plasmid sequences present in DP910521 maize.

A. Alignment to Intended Insertion

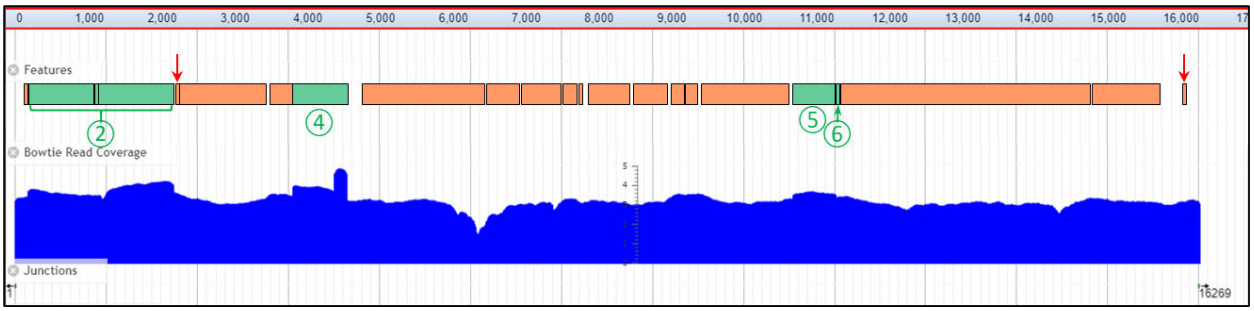

B. Alignment to PHP79620

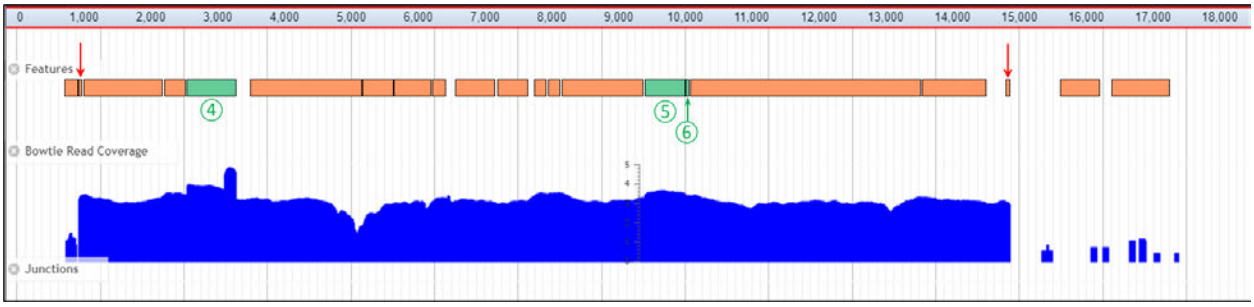

C. Alignment to [redacted]

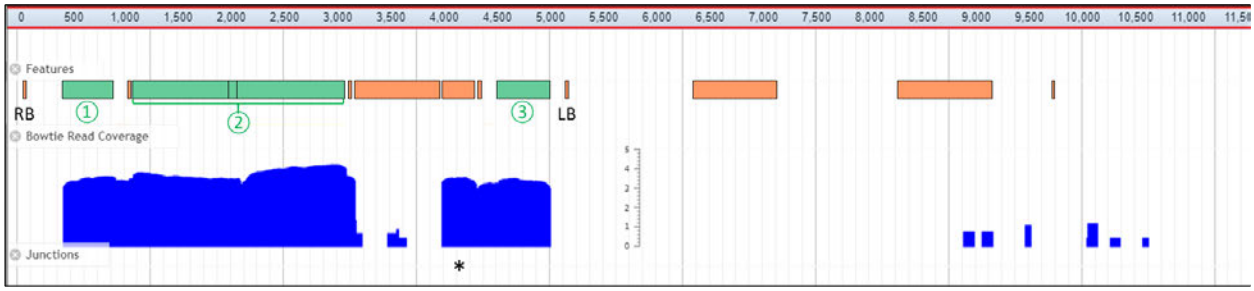

D. Alignment to [redacted]

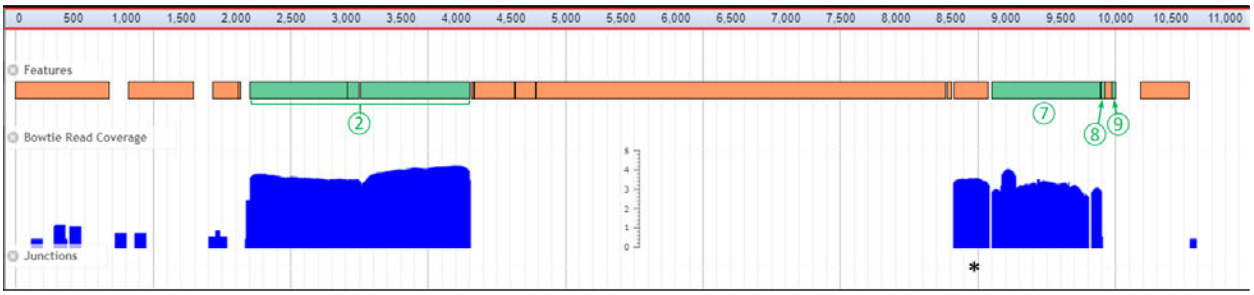

E. Alignment to [redacted]

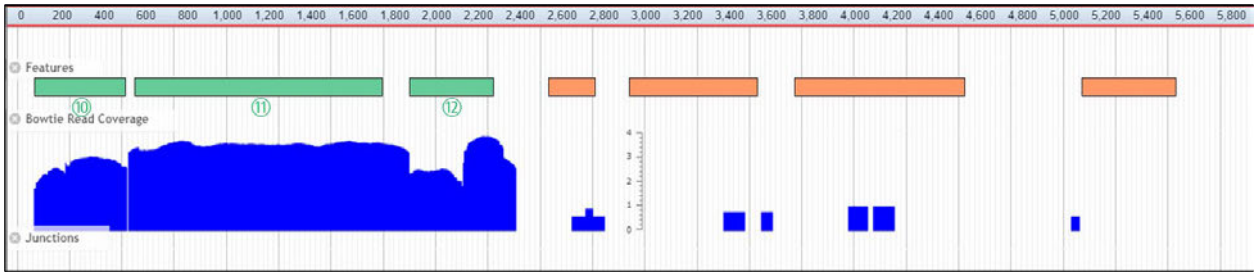

F. Alignment to PHP21875

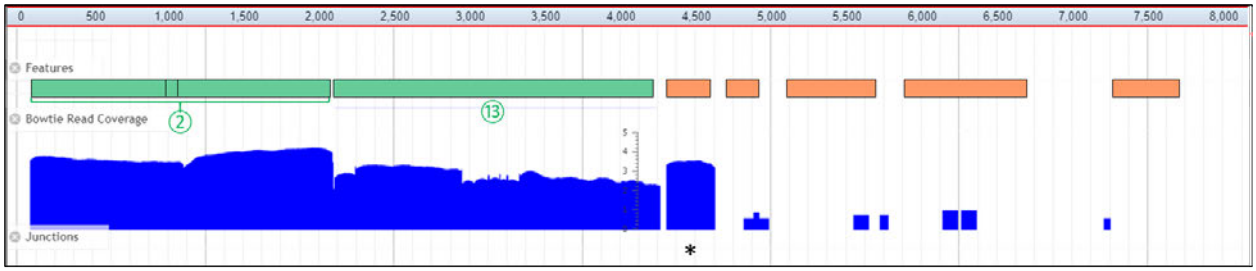

G. Alignment to PHP73572

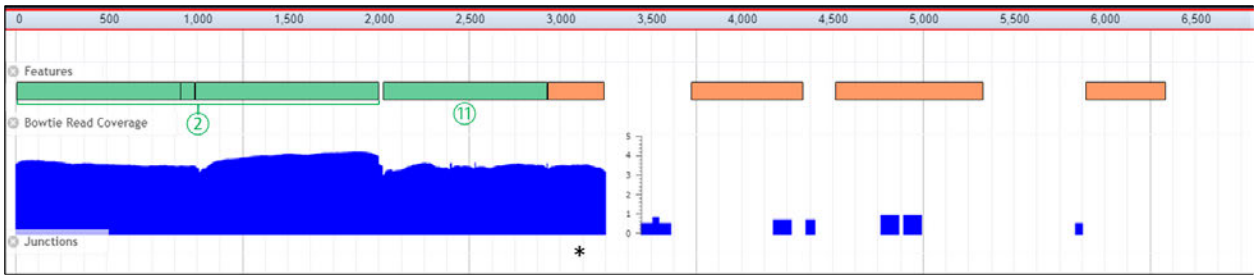

H. Alignment to PHP5096

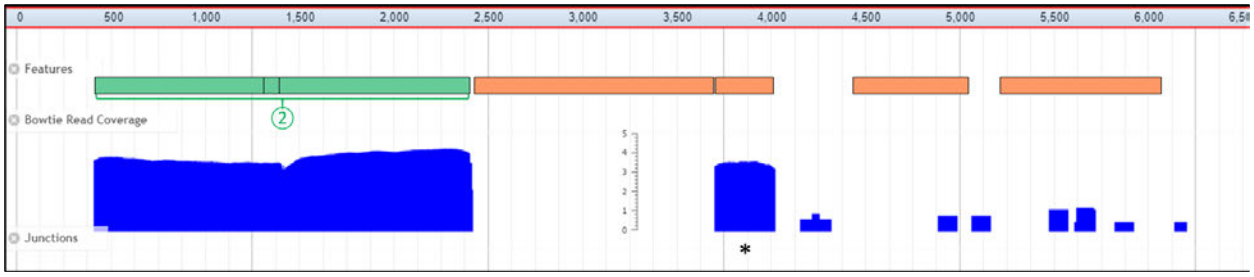

Figure A4. SbS Results for Plant ID 404181705 – DP910521 Maize (Transgenic)

The blue coverage graph shows the number of individual NGS reads aligned at each point on the intended insertion or plasmid using a logarithmic scale at the middle of the graph. Green bars above the coverage graph indicate endogenous genetic elements in each plasmid derived from the maize genome (identified by numbers; Table 5), while tan bars indicate genetic elements derived from other sources. FRT sites are

indicated by red arrows. **A)** SbS results aligned against the intended insertion (16,269 bp; Figure 10), indicating that this plant contains the intended insertion. Arrows below the graph indicate the two plasmid-to-genome sequence junctions identified by SbS; the numbers below the arrows refer to the bp location of the junction relative to the intended insertion (Figure 10). The presence of only two junctions demonstrates the presence of a single insertion in the DP910521 maize genome. **B)** SbS results aligned against the plasmid PHP79620 sequence (17,763 bp; Figure 6). Coverage was obtained for the elements between FRT1 and FRT87 transferred into DP910521 maize (region between the red arrows at top of graph). **C)** SbS results aligned against the plasmid [redacted] sequence ([redacted] bp; Figure 1). Coverage was obtained for [redacted], and the elements found in the intended insertion (between [redacted] to FRT1 and between FRT87 to [redacted]), along with the *pin*II terminator element (*) in [redacted] due to alignment of reads derived from the *pin*II terminator in the *pmi* cassette of the intended insertion to the copy of this element in [redacted]. **D)** SbS results aligned against the plasmid [redacted] sequence ([redacted] bp; Figure 2). Coverage was obtained only for the endogenous elements along with the *pin*II terminator element (*). **E)** SbS results aligned against the plasmid [redacted] sequence [redacted] bp; Figure 3). Coverage was obtained only for the endogenous elements. **F)** SbS results aligned against the plasmid PHP21875 sequence (7,842 bp; Figure 4). Coverage was obtained for the endogenous elements along with the *pin*II terminator element (*). **G)** SbS results aligned against the plasmid PHP73572 sequence (6,559 bp; Figure 8). Coverage was obtained for the endogenous elements along with the *pin*II terminator element (*). **H)** SbS results aligned against the plasmid PHP5096 sequence (6,269 bp; Figure 7). Coverage was obtained for the endogenous elements along with the *pin*II terminator element (*). The absence of any junctions other than to the intended insertion indicates that there are no additional insertions, plasmid backbone, or other unintended plasmid sequences present in DP910521 maize.

A. Alignment to Intended Insertion

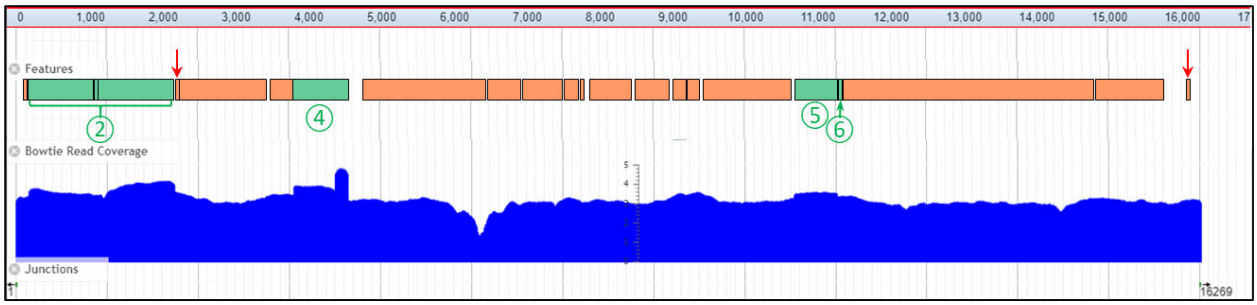

B. Alignment to PHP79620

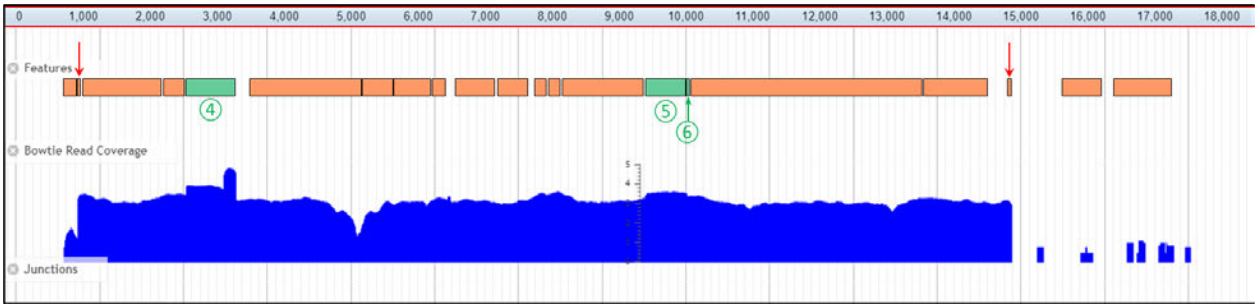

C. Alignment to [redacted]

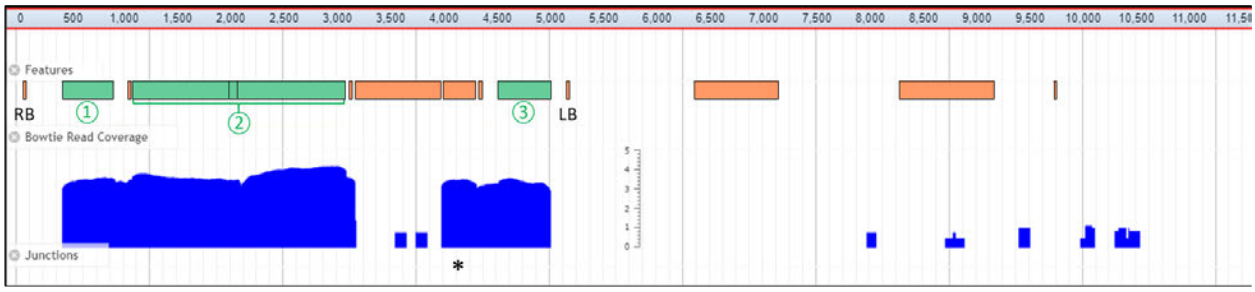

D. Alignment to [redacted]

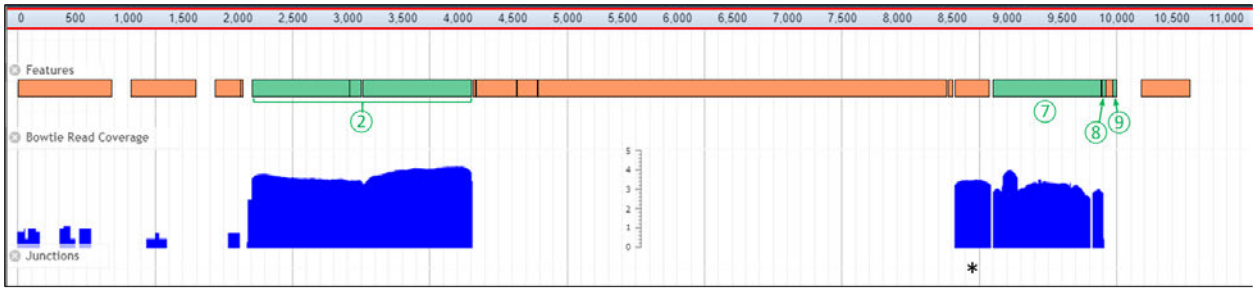

E. Alignment to [redacted]

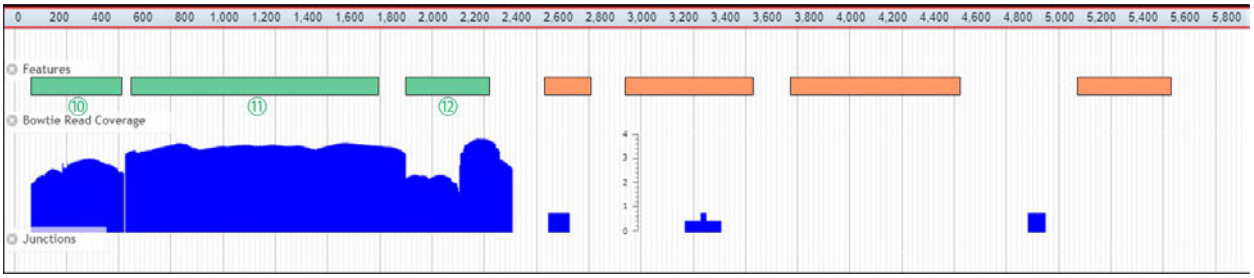

F. Alignment to PHP21875

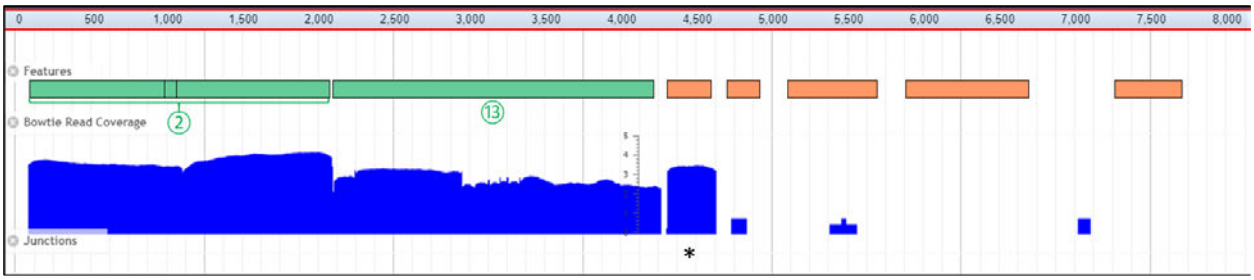

G. Alignment to PHP73572

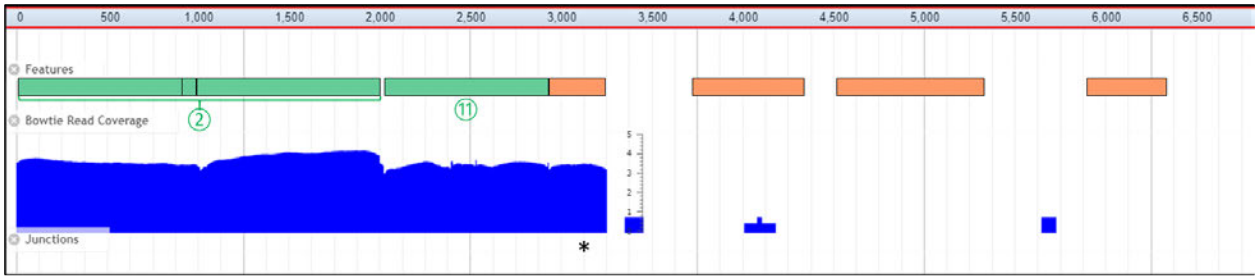

H. Alignment to PHP5096

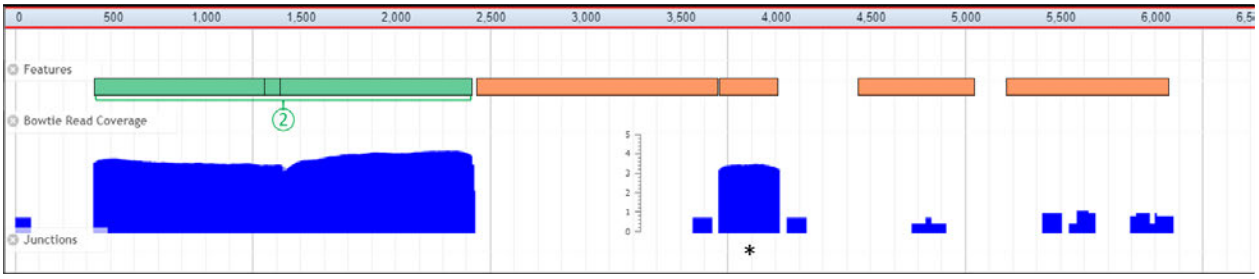

Figure A5. SbS Results for Plant ID 404181706 – DP910521 Maize (Transgenic)

The blue coverage graph shows the number of individual NGS reads aligned at each point on the intended insertion or plasmid using a logarithmic scale at the middle of the graph. Green bars above the coverage graph indicate endogenous genetic elements in each plasmid derived from the maize genome (identified by numbers; Table 5), while tan bars indicate genetic elements derived from other sources. FRT sites are indicated by red arrows. **A)** SbS results aligned against the intended insertion (16,269 bp; Figure 10),

indicating that this plant contains the intended insertion. Arrows below the graph indicate the two plasmid-to-genome sequence junctions identified by SbS; the numbers below the arrows refer to the bp location of the junction relative to the intended insertion (Figure 10). The presence of only two junctions demonstrates the presence of a single insertion in the DP910521 maize genome. **B)** SbS results aligned against the plasmid PHP79620 sequence (17,763 bp; Figure 6). Coverage was obtained for the elements between FRT1 and FRT87 transferred into DP910521 maize (region between the red arrows at top of graph). **C)** SbS results aligned against the plasmid [redacted] sequence ([redacted] bp; Figure 1). Coverage was obtained for [redacted], and the elements found in the intended insertion (between [redacted] to FRT1 and between FRT87 to [redacted]), along with the *pin*II terminator element (*) in [redacted] due to alignment of reads derived from the *pin*II terminator in the *pmi* cassette of the intended insertion to the copy of this element in [redacted]. **D)** SbS results aligned against the plasmid [redacted] sequence ([redacted] bp; Figure 2). Coverage was obtained only for the endogenous elements along with the *pin*II terminator element (*). **E)** SbS results aligned against the plasmid [redacted] sequence ([redacted] bp; Figure 3). Coverage was obtained only for the endogenous elements. **F)** SbS results aligned against the plasmid PHP21875 sequence (7,842 bp; Figure 4). Coverage was obtained for the endogenous elements along with the *pin*II terminator element (*). **G)** SbS results aligned against the plasmid PHP73572 sequence (6,559 bp; Figure 8). Coverage was obtained for the endogenous elements along with the *pin*II terminator element (*). **H)** SbS results aligned against the plasmid PHP5096 sequence (6,269 bp; Figure 7). Coverage was obtained for the endogenous elements along with the *pin*II terminator element (*). The absence of any junctions other than to the intended insertion indicates that there are no additional insertions, plasmid backbone, or other unintended plasmid sequences present in DP910521 maize.

APPENDIX B. METHODS FOR SOUTHERN BLOT ANALYSIS

Test, Control and Reference Substances

The test substances in the study were defined as seeds from DP910521 maize of the T1, BC1, BC1F1, BC1F2, and BC1F3 generations. The control substance was defined as seed from a maize line (PH184C) that was not transformed. PH184C maize has a similar genetic background to the test substance; however, it does not contain the DP910521 maize insertion.

Plasmid DNA of PHP79620 that was used for transformation to produce DP910521 maize was defined as a reference substance. This plasmid was used as a positive control for Southern analysis to verify probe hybridization. The *cry*1B.34*, mo-pat,* and *pmi* probes used in this analysis were derived from plasmid PHP79620.

DNA molecular weight markers for gel electrophoresis and Southern blot analysis were obtained from commercial vendors and were used as a reference to determine approximate molecular weights of DNA fragments. For Southern analysis, DNA Molecular Weight Marker III and VII, Digoxigenin (DIG)-labeled (Roche), were used as size standards for hybridizing fragments.

Sample Collection, Handling, Identification and Storage

Seed from each of the five generations of DP910521 maize and the control maize were planted in a controlled environment at Pioneer Hi-Bred International, Inc., Johnston, Iowa, USA. Fresh leaf tissue samples from test and control maize were harvested, stored frozen (< -50°C freezer unit), and then lyophilized. Lyophilized tissue samples were shipped to Regulatory Sciences, Multi Crop Research Center, Pioneer Hi-Bred Private Limited at Hyderabad, at ambient temperature. Upon arrival, samples were stored frozen (< -50°C freezer unit) until processing.

DNA Extraction and Quantification

Genomic DNA was isolated and analyzed from leaf tissue of one plant for each of the T1, BC1, BC1F1, BC1F2, and BC1F3 generations of DP910521 maize and one plant from the PH184C control maize.

The lyophilized leaf samples were pulverized with steel beads in tubes using a paint shaker (AGS Transact Technology Ltd). Care was taken to ensure leaf samples were ground sufficiently for DNA isolation. Genomic DNA was isolated using a high salt extraction buffer (2.0 M Sodium chloride, 100 mM Tris-Hydrochloride pH-8.0, 50 mM Sodium salt of EDTA, 3% β-mercaptoethanol (v/v) and 100 mM Sodium metabisulphite) and sequentially precipitated using potassium acetate and isopropyl alcohol. DNA was treated with Ribonuclease A, purified using

phenol/chloroform/isoamyl alcohol (25:24:1), and precipitated using sodium acetate and chilled ethanol. Following the extraction, DNA was quantified using Quant-iT™ PicoGreen® reagent (Molecular Probes, Invitrogen) and visualized on a 1% agarose gel to check the quality of the isolated DNA.

Digestion of DNA and Electrophoretic Separation

Genomic DNA (10 µg) isolated from both test and control maize leaves was digested with the restriction enzyme *Bcl* I (Thermo Fisher Scientific). PHP79620 plasmid DNA was added to the control maize DNA samples at a level equivalent to one plasmid copy per genomic copy and digested in the same manner. Following digestion with the restriction enzyme, the fragments produced were electrophoretically separated according to their sizes using an 0.9% agarose gel and documented by photographing the gel under UV illumination (BioRad Gel doc XR^+ System).

Southern Transfer

The DNA fragments separated on the agarose gel were denatured *in situ*, transferred to a nylon membrane (GE Healthcare, LC) and fixed to the membrane by UV crosslinking (UV Stratalinker, UVP).

Probe Labeling and Southern Blot Hybridization

The DNA fragments bound to the nylon membrane were detected as discrete bands when hybridized to a labeled probe. DNA probes specific to the *cry*1B.34*, mo-pat,* and *pmi* gene elements were labeled by incorporation of Digoxigenin (DIG) labeled nucleotide DIG-11-dUTP into the fragments by PCR labeling method.

Labeled probes were hybridized to the DNA on the nylon membrane for detection of the specific genomic DNA fragments. DNA Molecular Weight Marker III and VII, Digoxigenin (DIG) labeled (Roche) were used for visualization as the fragment size standards on the blot.

Detection of Hybridized Probes

After overnight hybridization, the membrane was washed and processed using a DIG Wash and Block Buffer Set (Roche). DIG-labeled DNA standards and single stranded DIG-labeled probes hybridized to DNA bound to the nylon membrane were visualized using CDP-Star Chemiluminescent Nucleic Acid Detection System. Blots were exposed for one or more time points to detect hybridizing fragments and to visualize molecular weight standards. Images were captured by detection with the Syngene G-Box Chemi XX6 (Syngene, Inc.). Detected bands were documented for each probe.

Stripping of Probes and Subsequent Hybridization

Following hybridization and detection, membranes were stripped of DIG-labeled probe to prepare blot for subsequent re-hybridization to a different probe. Membranes were rinsed briefly in distilled and de-ionized water and then stripped in a solution of 0.2 N NaOH and 0.1% SDS at 37°C with constant shaking. The membranes were then rinsed in 2x Saline sodium citrate and either used directly for subsequent hybridizations or stored for later use. The alkali-based stripping procedure effectively removed probes labeled with alkali-labile DIG used in these experiments.

APPENDIX C. METHODS FOR MULTI-GENERATION SEGREGATION ANALYSIS

Five generations of DP910521 maize (F1, F2, BC1, BC1S1, and BC1S3) were evaluated using real-time quantitative PCR (qPCR) and herbicide-tolerance testing to confirm Mendelian inheritance of genotype and phenotype.

Planting and Sample Collection

All seeds were grown in a controlled environment under suitable conditions for producing maize plants. For the F1, F2, BC1, BC1S1, and BC1S3 generations of DP910521 maize intended for genotypic and phenotypic analysis, approximately 160 seeds were planted per generation. Additional plantings were made for the BC1S1 and F2 generations, with 168 and 252 seeds planted for the BC1S1 and the F2 generations, respectively. Plants from the first planting of the BC1S1 and F2 generations were used for sample collection; PCR characterization results reported in this study are from the second planting of the BC1S1 generation and the second planting of the F2 generation. Prior to the second planting for the BC1S1 and F2 generations, seed chipping was conducted. Using a nail clipper, a small 'chip' of the seed containing seed coat and endosperm was removed from each seed and placed into individual wells of 96-well collection plates. Each seed (now with a chip removed) was placed into a corresponding well within 96-well bubble packs. Each plate and well and corresponding bubble pack were uniquely labeled to allow a given seed chip sample to be tracked back to the originating seed. The seed chip samples were used for genotypic PCR analysis. The seeds were planted and resulting plants were used for herbicide tolerance evaluation.

Prior to PCR sample collection, the F1, BC1, and BC1S3 generations were thinned by selecting healthy plants and one hundred plants were maintained from each generation of DP910521 maize for the intended purpose of genotypic and phenotypic analysis. For the F2 and BC1S1 generations intended for PCR characterization, all 252 seed chips and 168 seed chips, respectively, were used for genotypic analysis. All seeds of these two generations that successfully germinated and developed into plants were maintained and used for phenotypic analysis.

For leaf punch sampling for genotypic and phenotypic analysis (F1, BC1, and BC1S3), one sample per plant was collected at the V2-V4 growth stages (maize growth stage follows the descriptions in Growth stages (Abendroth et al., 2011) (Table H.1). Each sample consisted of three leaf punches collected into one bullet tube and placed on dry ice until transferred to a freezer for frozen storage. Individual plants and corresponding leaf punch samples were uniquely labeled to allow a given sample to be tracked back to the originating plant. Prior to conducting PCR, DNA was extracted from the leaf punches. For the BC1S1 and F2 generations, the seed chips collected prior to planting were ground and DNA was extracted and purified for genotypic PCR analysis.

Genotypic Analysis

Leaf punch samples from F1, BC1, and BC1S3 generations of DP910521 maize and seed chips from the BC1S1 and F2 generations of DP910521 maize were analyzed using either a qPCR assay

to confirm the copy number of event DP-91Ø521-2 (F1, BC1, BC1S1 and BC1S3 generations) or endpoint PCR to confirm presence or absence of event DP-91Ø521-2 (F2 generation).

Herbicide Application and Evaluation

A glyphosate herbicide treatment was applied when plants were at the V4 growth stage (occurs when the leaflets on the fourth leaf node have unrolled). The spray mixture consisted of Liberty 280 SL containing 2.34 pounds of glufosinate per gallon (0.28 kg ai/L) and ammonium sulfate at a rate of approximately 3.0 lb/A (3.4 kg/ha). No other adjuvants or additives were included in the spray mixture. Liberty 280 SL was applied at a target rate of 32 fl oz/A (2.34 L/ha) with a total spray volume of approximately 15-20 gal/A (140-187 L/ha) using a spray chamber to simulate a broadcast (over-the-top) application. Actual application rates were within ±10% of the target herbicide application rate.

Three to nine days after herbicide application, each plant was visually evaluated for herbicide tolerance in which presence of herbicide injury corresponded to an herbicide-susceptible phenotype and absence of herbicide injury corresponded to an herbicide-tolerant phenotype.

Statistical Analysis

A chi-square test was performed at the 0.05 significance level to compare the observed segregation ratios of the F1, F2, BC1 and BC1S1 generations of DP910521 maize to the expected segregation ratios (1:1 for the F1 and BC1 generations, 3:1 for the F2 and BC1S1 generations). A chi-square test was not performed for the BC1S3 generation of DP910521 maize as all plants were identified as positive as expected for a homozygous generation. Statistical analyses were conducted using SAS software, Version 9.4 (SAS Institute Inc.)

APPENDIX D. METHODS FOR SANGER SEQUENCING ANALYSIS

Test and Control Substances

The test substance in the study was defined as seeds from DP910521 maize of the BC1F2 generation. The control substance was defined as seed from a non-genetically modified (non-GM) maize line, PH184C, that has a similar genetic background as DP910521.

DNA Extraction and Quantification

Genomic DNA (gDNA) from DP910521 and control maize were extracted from separate pools of finely homogenized leaf tissue: ten DP910521 maize plants (~100 mg each) and two conventional maize plants (~250 mg each) of the same genetic background.

Pooled leaf samples were incubated for 30 min at 37°C in Urea Extraction Buffer [50 mM Tris-HCl (pH 8.0), 7 M Urea, 2% Sodium Chloride, 40 mM EDTA, 1% N-Lauroylsarcosine]. The slurry was partitioned by phenol/chloroform/isoamyl alcohol (25:24:1), followed by chloroform/isoamyl alcohol (24:1). The aqueous phase was collected and precipitated with 1/10th volume 3 M sodium acetate (pH 5.2) in equal volume isopropanol. After resuspension in 1× TE (10 mM Tris-HCl, 1 mM EDTA, pH 8.0), the gDNA was treated with RNaseA, and the treated gDNA was precipitated before being resuspended in 1× TE.

The quality of the purified gDNA was assessed by electrophoresis on a 1% agarose gel and visualized on a Molecular Imager Gel Doc XR+ (Bio-Rad). The gDNA concentration was determined by the NanoDrop 2000 Spectrophotometer (Thermo Fisher).

Polymerase Chain Reaction (PCR) Amplification of the DP910521 Insert and Flanking Genomic Regions

Six overlapping PCR fragments (**A**, **B**, **C**, **D**, **E and F**) spanning the insert and the 5' and 3' flanking border regions were amplified from the genomic DNA of DP910521 maize.

All PCR fragments were generated using Phusion High-Fidelity Master Mix with GC Buffer (Thermo Fisher) in a 20 µl reaction with 20 ng of gDNA template and each primer at a final concentration of 0.5 µM. PCR conditions were optimized for successful amplification of the targeted fragments (Table D.1).

Table D.1. PCR Amplification Conditions

Fragment (bp)	**A** (3995)	**B** (2933)	**C** (1931)	**D** (3133)	**E** (3819)	**F** (3532)
1x[b]	98ºC 00:30	98ºC 00:30	98ºC 00:30	98ºC 00:30	98ºC 00:30	98ºC 00:30
35x	98ºC 00:05 67ºC 00:05 72°C 00:45	98ºC 00:05 65ºC 00:05 72°C 00:30	98ºC 00:05 ----- ------ 72°C 00:30	98ºC 00:05 63ºC 00:05 72°C 00:45	98ºC 00:05 69ºC 00:05 72°C 00:45	98ºC 00:05 67ºC 00:05 72°C 00:45
1x	72ºC 03:00 4°C ∞	72ºC 10:00 4°C ∞	72ºC 10:00 4°C ∞	72ºC 03:00 4°C ∞	72ºC 03:00 4°C ∞	72ºC 03:00 4°C ∞

[a] Cycle time is indicated in minutes:seconds.

[b] x is cycle number.

Cloning of PCR Products

The pCR™4Blunt-TOPO® vector (Invitrogen) was used to clone all PCR products. The transformants were inoculated on LB-agar plates containing 50 ng/ml kanamycin. At least three colonies from each plate were selected and cultured in LB-kanamycin media. The plasmid DNA was isolated using a QIAprep Spin Miniprep Kit (Qiagen Inc.) and digested with a restriction enzyme to confirm the presence of the PCR product in the TOPO vector.

Sanger DNA Sequencing

Three positive plasmids (containing the insert of the expected size) from each independent PCR reaction (two independent PCR reactions for a total of six plasmids per fragment) were sent for Sanger sequencing ([redacted]). The complete sequence was covered by M13 forward and reverse primers on the TOPO vector and internal sequencing primers within each fragment.

Sequencher® 5.1 (Gene Codes Corporation) was used to analyze the received ABI trace files and assemble the sequences with default parameters. Low-quality data determined by the analysis software and vector sequences were trimmed from both 5' and 3' ends of each trace file when analyzing the sequencing results. All sequence reads were reviewed, and any ambiguous nucleotide was visually verified from the chromatograms and compared with sequence reads from the other clones to make a final base call. The final consensus sequence for the insert and flanking genomic regions in DP910521 maize was generated by creating the overlapping individual consensus sequences of the PCR fragments.

APPENDIX E. METHODS FOR CHARACTERIZATION OF CRY1B.34 PROTEIN

Test Materials

Plant-Derived Cry1B.34 Protein: Cry1B.34 protein was partially purified from DP910521 maize leaf tissue. The tissue samples were collected at the R1 growth stage (The stage when silks become visible; Abendroth *et al.*, 2011) from plants grown at a field location in Johnston, IA, USA. The tissue was lyophilized, homogenized and stored at ≤ -50 °C. The Cry1B.34 protein was extracted from lyophilized maize tissue by homogenization with a Waring blender using using phosphate-buffered saline containing polysorbate 20 (PBST) extraction buffer with protease inhibitor (20-30 ml buffer per g tissue). The sample extract was then clarified by centrifugation and filtration prior to purification by immunoaffinity chromatography. The immunoaffinity column was prepared by coupling a Cry1B.34 protein polyclonal antibody (R11957; Pioneer) to AminoLink Plus Coupling Resin. The partially purified Cry1B.34 protein samples were eluted off the column using IgG elution buffer. Elutions 2-5 from the immunoaffinity purification column were collected separately and immediately neutralized with 0.1 column volume of 1M Tris buffer, pH 8. These elutions were combined and concentrated using a centrifugal concentrator (30K Vivaspin Turbo 4; Sartorius) until the volume was reduced to approximately 280 µl.

Following extraction, purification, and concentration, the final volume in the concentrator was estimated and an equal volume of 2X LDS/DTT (50% 4X NuPAGE LDS Sample Buffer, 20% 10X NuPAGE Sample Reducing Agent containing DTT, and 30% ASTM [American Society for Testing and Materials] Type I water [referred to as water]) was added to the concentrated sample. The Cry1B.34 protein sample was heated at 70-100 °C for 5 (±1) minutes and transferred to a microcentrifuge tube. The sample was then heated at 90-100 °C for 5 (±1) minutes, and stored frozen (-20 °C freezer unit).

Microbially Derived Cry1B.34 *Protein*: Cry1B.34 protein was produced at Pioneer Hi-Bred International, Inc. using a microbial expression system. The protein was expressed in an E. coli protein expression system and purified using pellet washing and ion exchange chromatography. Tangential flow filtration was used to change the buffer to 50 mM ammonium bicarbonate. After lyophilization and mixing, a lot number was assigned.

SDS-PAGE Analysis

The partially purified maize-derived Cry1B.34 protein sample was removed from frozen storage, diluted as applicable with1X LDS/DTT (25% 4X NuPAGE LDS Sample Buffer, 10% 10X NuPAGE Sample Reducing Agent containing DTT, and 65% water), heated at 90-100 °C for 5 minutes, and then loaded into 4-12% Bis-Tris gels. Pre-stained protein molecular weight markers (Precision Plus Protein Dual Xtra Standards) were loaded into each gel to provide a visual verification that migration was within the expected range of the predicted molecular weight. For SDS-PAGE and western blot analysis, the Cry1B.34 protein reference substance was removed from frozen storage, diluted in 1X LDS/DTT to approximately the same concentration as the maize-derived protein, heated at 90-100 °C for 5 minutes, and loaded into the gel. Electrophoresis was conducted using a pre-cast gel electrophoresis system with MES running buffer and NuPAGE Antioxidant at a constant 200 volts (V) for 35 minutes.

Upon completion of electrophoresis, the gels were removed from the gel cassettes and used for Coomassie staining, western blot analysis, protein glycosylation analysis, or sample preparation for peptide mapping and N-terminal amino acid sequencing.

For Coomassie staining, the gel was washed with water three times for 5 minutes each wash and stained with GelCode Blue Stain Reagent for 60 minutes. Following staining, the gel was de-stained with water four times for at least 5 minutes each until the gel background was clear. Proteins were stained as blue-colored bands on the gel. The gel image was captured electronically using a ChemiDoc MP (Bio-Rad) imaging system.

Western Blot Analysis

Following SDS-PAGE, the resulting gel was assembled into a nitrocellulose (NC) iBlot Gel Transfer Stack. An iBlot Gel Transfer Device was used to transfer proteins from the gel to the NC membrane for 7 minutes with a pre-set program (P3).

Following protein transfer, the membrane was blocked in PBST containing 5% weight/volume (w/v) non-fat dry milk for 45 minutes at ambient laboratory temperature. Before and after the blocking step, the membrane was washed with PBST three times for 5 minutes each wash to reduce the background. The blocked membrane was incubated with a Cry1B.34 monoclonal antibody 10C2.D4.H10 (Pioneer) diluted 1:10,000 in PBST containing 1% w/v non-fat dry milk for 45 minutes at ambient laboratory temperature. Following primary antibody incubation, the membrane was washed in PBST three times for 5 minutes each wash. The membrane was incubated with a secondary antibody (anti-mouse IgG, horseradish peroxidase conjugate; Promega Corporation) diluted 1:10,000 in PBST containing 1% w/v non-fat dry milk for 45 minutes at ambient laboratory temperature. The membrane was washed with PBST four times for 5 minutes each wash. The membrane remained in PBST prior to incubating with a chemiluminescent substrate for 5 minutes. The chemiluminescent signal and the pre-stained markers were detected and captured using a ChemiDoc MP imaging system.

Peptide Mapping by Mass Spectrometry

Following SDS-PAGE, Coomassie staining, and gel imaging using the methods as described in Methods Section B, except no reference substance was loaded, the Cry1B.34 protein band was excised from a gel and stored frozen at ≤ -5 °C. The protein in the gel slices was reduced with DTT, alkylated with iodoacetamide, and then subsequently digested with trypsin or chymotrypsin. The digested samples were separated on a nanoACQUITY UPLC (Waters Corporation) fitted with a Peptide BEH C18 300 Å 1.7 µm column (75 µm x 100 mm; Waters Corporation) (for plant-derived Cry1B.34 Protein) or a Cortecs UPLC C18 1.6 µm column (2.1 x 100 mm; Waters Corporation) (for microbially derived Cry1B.34 Protein) by gradient elution. Eluent from the column was directed into an electrospray source, operating in positive ion mode, on a TripleTOF 5600+ hybrid quadrupole-TOF mass spectrometer (AB Sciex; currently Sciex). The resulting mass spectrometry (MS) data were processed using MS Data Converter (Beta 1.3) to produce a peak list. The peak list was used to perform an MS/MS ion search (Mascot Software version 2.7.0) and match peptides from the expected Cry1B.34 protein sequence (Perkins *et al.*, 1999). The following search parameters were used: peptide and fragment mass tolerance, ± 0.1 Da; fixed modifications, cysteine carbamidomethyl; variable modifications, methionine oxidation; and maximum missed

cleavages, 1 for trypsin and 2 for chymotrypsin. The Mascot-generated peptide ion score threshold was > 13 which indicates identity or extensive homology ($P < 0.05$). The combined sequence coverage was calculated with GPMAW (version 12.11.0 for study PHI-2021-115; version 12.1. for study PHI-2020-093).

N-Terminal Amino Acid Sequencing Analysis

Following SDS-PAGE, Coomassie staining, and gel imaging using the methods as described above, the resulting gel was incubated in cathode buffer (60 mM Tris, 40 mM CAPS, 0.075% SDS, pH 9.6) for 10-20 minutes. An Immobilon-P PVDF membrane was briefly wetted in 100% methanol, followed by immersion in anode buffer (60 mM Tris, 40 mM CAPS, 15% methanol, pH 9.6) for 10-20 minutes. A Trans-Blot SD Semi-Dry Electrophoretic Transfer Cell system was used to transfer proteins from the gel to the membrane at 10 V for 60 minutes.

Following transfer of the Cry1B.34 protein, the membrane was washed with water three times for at least 5 minutes each, stained with GelCode Blue stain reagent for 5 minutes, and then destained with water to visualize the Cry1B.34 protein. Two bands containing the Cry1B.34 protein was excised and stored frozen at ≤ -5 ° C.

Bands were analyzed using Edman degradation (Edman sequencing). Six or ten cycles of Edman sequencing were performed using a Shimadzu PPSQ-51A sequencer. During each cycle, the N-terminal amino acid was sequentially derivatized with phenylisothiocyanate (PITC), cleaved with trifluoracetic acid, and converted to PTH-amino acid which was identified through chromatography. LabSolutions Software was used to automatically identify the N-terminal sequence.

Glycoprotein Analysis

A Pierce Glycoprotein Staining Kit was used to determine whether the Cry1B.34 protein was glycosylated. The Cry1B.34 protein, a positive control protein (horseradish peroxidase), and a negative control protein (soybean trypsin inhibitor) were run by SDS-PAGE as described above.

Following electrophoresis, the gel was washed with water twice for 5 minutes each wash, fixed with 50% methanol for 30-35 minutes, and washed twice with 3% acetic acid for 10-15 minutes each wash. The gel was then incubated with oxidizing solution for 15-20 minutes and washed three times with 3% acetic acid for 5-7 minutes each wash. The gel was incubated with glycoprotein staining reagent for 15-20 minutes and then incubated in a reducing reagent for 5-7 minutes. The gel was then washed one to three times with 3% acetic acid for 5 minutes each wash and then rinsed one to twice in water for 5 minutes. Glycoproteins were detected as magenta-colored bands on the gel.

Following glycoprotein detection, the image of the gel was captured electronically. The same gel was then stained with GelCode Blue stain reagent for approximately 60 minutes followed by three washes with water (minimum 5 minutes each wash) to visualize all protein bands. The image of the GelCode stained gel was then captured electronically.

Bioactivity Bioassay

The biological activity of the Cry1B.34 protein was evaluated by conducting a 7-day bioassay using *Spodoptera frugiperda* (fall armyworm; Lepidoptera: Noctuidae), a species sensitive to the Cry1B.34 protein. Eggs were obtained from [redacted]) and their identity was recorded by study personnel.

The *S. frugiperda* bioassay utilized a generalized randomized block design containing 20 blocks. Each block consisted of a 12-well bioassay plate and contained one replicate from each of the following treatments for a target of 20 individuals per treatment:

- Treatment 1: Buffer Control Diet (containing a dosing solution of 10 mM CAPS buffer)
- Treatment 2: Test Diet (targeting 1.563 ng Cry1B.34 protein per mg diet wet weight)
- Treatment 3: Test Diet (targeting 3.125 ng Cry1B.34 protein per mg diet wet weight)
- Treatment 4: Test Diet (targeting 6.250 ng Cry1B.34 protein per mg diet wet weight)
- Treatment 5: Test Diet (targeting 12.50 ng Cry1B.34 protein per mg diet wet weight)
- Treatment 6: Test Diet (targeting 25.00 ng Cry1B.34 protein per mg diet wet weight)
- Treatment 7: Test Diet (targeting 50.00 ng Cry1B.34 protein per mg diet wet weight)

For each day of diet preparation, a Cry1B.34 protein stock solution was prepared by solubilizing test substance in buffer (10 mM CAPS, pH 10.5) to a target concentration of 1.0 mg/ml. The stock solution was diluted in ultrapure water to prepare the test dosing solutions at a concentration range of 2.1-67 ng/µl. The buffer control dosing solution consisted of 10 mM CAPS buffer. Dosing solutions were maintained chilled (refrigerated or on wet ice) until use. The carrier for the *S. frugiperda* bioassay consisted of Stonefly Heliothis diet. On each day of diet preparation, each dosing solution was combined with carrier at a 3:1 ratio (i.e., 3 ml of dosing solution to 1 g carrier) to generate Treatments 1-7.

S. frugiperda eggs were incubated in an environmental chamber until the eggs hatched. Neonates were used in the bioassay within 24 hours of hatching. On Day 0 of the bioassay, approximately 300 µl (i.e., 1 g of wet diet equated to 1 ml of wet diet) of freshly prepared diets were dispensed into individual wells of the bioassay plates. One *S. frugiperda* neonate was placed in each well containing diet, each bioassay plate was sealed with heat-sealing film and a small hole was poked over each well to allow for ventilation. The bioassay was conducted in an environmental chamber set at 25 °C, 65% relative humidity, and continuous dark. On Day 4, new bioassay plates were prepared with fresh diet as described for Day 0, with the exception that on Day 4, 600 µl was dispensed per well. The additional diet was needed to accommodate the increased nutritional needs of the growing organisms. After 7 days, the bioassay was complete, mortality was assessed, and surviving larvae were individually weighed. Only wells that contained one organism were included in the total number of observed individuals; organisms recorded as missing from a well were excluded from statistical analysis.

The bioassay acceptability criterion indicated the bioassay may be repeated if the combined number of dead and missing organisms exceeds 20% for the buffer control diet (Treatment 1) group. The bioassay met the acceptability criteria.

Thermolability Analysis

The test substance consisted of Cry1B.34 protein solubilized from a lyophilized powder (lot number PCF-0042). The carrier consisted of Stonefly Heliothis diet. The buffer control dosing solution used to prepare Treatment 1 consisted of 10 mM CAPS. The bulk dosing solution used to prepare Treatments 2-6 consisted of aliquots of the test substance diluted in 10 mM CAPS to achieve the targeted concentration in Treatments 2-6. The dosing solution aliquots used to prepare Treatments 3-6 were incubated for 30-35 minutes at several targeted temperatures.

The test system was *Spodoptera frugiperda* (fall armyworm; Lepidoptera: Noctuidae). The test system was chosen because *S. frugiperda* is an insect sensitive to the Cry1B.34 protein. *Spodoptera frugiperda* larvae were exposed via oral ingestion to one of the following six treatments:

- Treatment 1: Buffer Control Diet containing 10 mM CAPS
- Treatment 2: Control Diet containing the unheated Cry1B.34 protein dosing solution
- Treatment 3: Test Diet containing the Cry1B.34 protein dosing solution incubated at 25 °C
- Treatment 4: Test Diet containing the Cry1B.34 protein dosing solution incubated at 50 °C
- Treatment 5: Test Diet containing the Cry1B.34 protein dosing solution incubated at 75 °C
- Treatment 6: Test Diet containing the Cry1B.34 protein dosing solution incubated at 95 °C

The unheated control diet and each test diet contained a targeted concentration of 25 ng Cry1B.34 protein per mg diet wet weight. Treatments were arranged in a generalized randomized block design with a total of 10 blocks. Each block consisted of a 12-well bioassay plate and contained 2 replicates from each treatment. On Day 0, each treatment was provided to a target of 20 *S. frugiperda* individuals. The bioassay was conducted in an environmental chamber set at 25 °C, 65% relative humidity, and continuous dark. Larvae were refed on Day 4. After 7 days, the bioassay was complete, final mortality was assessed, and surviving organisms were individually weighed.

The bioassay acceptability criteria were as follows: The bioassay may be terminated and repeated if the combined number of dead and missing organisms is greater than 20% for the buffer control diet (Treatment 1) group. The bioassay may be terminated and repeated if the mortality of the unheated control diet (Treatment 2) group does not exceed 80%. The *S. frugiperda* bioassay met both acceptability criteria. An enzyme-linked immunosorbent assay (ELISA) was used to assess the homogeneity of the Cry1B.34 protein in Treatment 2 and concentration of the Cry1B.34 protein dosing solutions. The absence of Cry1B.34 protein in the buffer control dosing solutions was also assessed. Bias in the *S. frugiperda* bioassay was controlled through the randomization of treatments within blocks and the use of one or more control diets. Bias in the characterization portion of the study was controlled through the use of replicate testing and appropriate assay controls.

On each day of diet preparation, dosing solutions for Treatments 1-6 were prepared as described in Appendix A. Each dosing solution was mixed with carrier in a 3:1 ratio (i.e., 3 ml of dosing solution to 1 g of carrier), generating Treatments 1-6. Dosing solutions were maintained chilled (in a refrigerator set at 4 °C or on wet ice) until use. *S. frugiperda* eggs were incubated in an

environmental chamber until the eggs hatched. *S. frugiperda* neonates were used in the bioassay within 24 hours of hatching.

On Day 0, approximately 300 µl (i.e., 1 g of wet diet equated to 1 ml of wet diet) of freshly prepared diets were dispensed into wells of the bioassay plates. One *S. frugiperda* neonate was placed in each well containing diet. Each bioassay plate was sealed with heat-sealing film, a small hole was poked over each well to allow for ventilation, and the plates were placed in an environmental chamber. On Day 4, new bioassay plates were prepared with fresh diet as described for Day 0, with the exception that 600 µl was dispensed per well. Living *S. frugiperda* larvae were transferred to the new plates, missing or dead larvae were recorded, and the freshly prepared plates were placed in the environmental chamber. After 7 days, the bioassay was complete, mortality was assessed, and surviving larvae were individually weighed.

Statistical Analysis

Statistical analyses of data were conducted using SAS software, Version 9.4 (SAS Institute, Inc.). The response variable of interest was mortality. Statistical comparisons were made between mortality of *S. frugiperda* fed diet containing heat-treated Cry1B.34 protein (Treatments 3, 4, 5 and 6) and that of *S. frugiperda* fed the unheated Cry1B.34 protein control diet (Treatment 2).

Statistical analysis was conducted using Fisher's exact test to determine if the mortality rate of

S. frugiperda fed diets containing the heat-treated Cry1B.34 protein (m_T) was lower than the mortality rate of those fed the unheated Cry1B.34 protein control diet (m_C). The corresponding hypothesis test was

$$H_0: m_T - m_C = 0 \quad vs. \quad H_a: m_T - m_C < 0.$$

A significant difference was established if the P-value was < 0.05. SAS PROC MULTTEST was utilized to conduct the Fisher's exact test.

Digestibility in Simulated Gastric Fluid (SGF)

Test and control solutions were prepared as follows:

- The gastric control solution was prepared fresh on the day of use and was comprised of 0.2% weight per volume (w/v) NaCl in 0.7% volume per volume (v/v) HCl with a pH of ~1.2.
- The pepsin digestion solution, referred to as simulated gastric fluid (SGF), was prepared fresh on the day of use by dissolving pepsin (Sigma-Aldrich) into gastric control solution. The SGF was prepared so that the pepsin to protein ratio of the final digestion mixture was 10 units of pepsin per µg of test substance.
- The test substance consisted of Cry1B.34 protein solubilized from a lyophilized powder (lot number PCF-0042).

- To prepare the stock solutions for each of the control proteins (BSA and β-lactoglobulin), a sub-sample of 5.0 mg powder was weighed into an individual tube and solubilized by adding 1 ml of 10 mM CAPS pH 10.5 (for a final protein concentration of 5 mg/ml).
- The final concentration of the protein and pepsin in the SGF reaction mixture was 0.25 mg/ml Cry1B.34 protein and 2500 units/ml pepsin.

SGF solution (1,900 µl) was dispensed into a 7-ml glass vial and placed in a 37 °C water bath for 2-5 minutes prior to the addition of 100 µl of Cry1B.34 protein stock solution at Time 0. The digestion reaction mixture was mixed constantly using a stir bar and a submersible magnetic stirrer.

A 120-µl sub-sample of the Cry1B.34 protein digestion reaction mixture was removed from the vial at the following analytical time points (± 10 seconds): 0.5, 1, 2, 5, 10, 20, and 60 minutes. The sub-samples were inactivated by adding them to pre-labeled tubes containing 139 µl of a pre-mixed sample stop solution (consisting of 48 µl of 200 mM sodium carbonate, 65 µl NuPAGE 4X LDS sample buffer, and 26 µl NuPAGE 10X sample reducing agent) and heating to 90-100 °C for 5 minutes prior to frozen storage (-20 °C freezer unit).

To prepare control digestion samples at 1 and 60 minutes, a 114-µl sample of the appropriate digestion solution was pre-warmed in a 37 °C water bath for 2-5 minutes prior to adding 6 µl of the Cry1B.34 protein stock solution, control protein stock solution, or 10 mM CAPS buffer. The tubes were incubated in the water bath for the allotted time and then inactivated by mixing with 139 µl of the pre-mixed sample stop solution.

The Time 0 control reaction mixtures were prepared by first neutralizing 114 µl of the appropriate digestion solution with 139 µl of the pre-mixed sample stop solution, and then adding 6 µl of the Cry1B.34 protein stock solution, control protein stock solution, or 10 mM CAPS buffer to the appropriate tube and mixing.

Control digestion samples included in the SGF assay are provided in Table E.1. Following digestion and inactivation, all control reaction mixtures were heated at 90-100 °C for 5 minutes prior to frozen storage (-20 °C freezer unit).

Table E.1. Control Samples for Simulated Gastric Fluid (SGF) Digestibility Analysis

Protein	Digestion Solution	Digestion Time (min)		
		0	1	60
None (10 mM CAPS buffer), {SGF Control}	SGF	X	--	X
BSA	SGF	X	X	X
β-lactoglobulin	SGF	X	X	X
Cry1B.34	SGF	X	--	--
Cry1B.34	None (10 mM CAPS buffer)	X	--	X
Cry1B.34	Gastric Control Solution (No Pepsin)	--	--	X

SDS-PAGE Analysis

The Cry1B.34 protein digestion time-course samples and control digestion samples were removed from frozen storage, heated at 90-100 °C for 5 minutes, and loaded (20 µl/well) into 4-12% Bis-

Tris gels for SDS-PAGE analysis. To demonstrate the sensitivity of the SDS-PAGE gel and western blot analyses, an aliquot of the Cry1B.34 protein in SGF (Time 0) sample was loaded into the gel at a 1:20 dilution (116 ng Cry1B.34 protein) for protein staining, and at a 1:200 dilution (11.6 ng Cry1B.34 protein) for the western blot. Pre-stained protein molecular weight markers (Precision Plus Dual Xtra Standards) were also loaded into the gels to provide a visual estimate of molecular weight. Electrophoresis was conducted using a pre-cast gel electrophoresis system with 1X MES SDS running buffer at a constant 200 volts (V) for 35 minutes.

Upon completion of electrophoresis, the gels were removed from the gel cassettes for use in protein staining or western blot analyses. For protein staining, the gels were washed with water three times for 5 minutes each and stained with GelCode Blue Stain Reagent for 61 minutes. Following staining, the gels were destained with water four times for a minimum of 5 minutes each until the gel background was clear. Proteins were stained as blue-colored bands on the gels. The gel image was captured electronically using a ChemiDoc MP (Bio-Rad) imaging system.

Western Blot Analysis

The Cry1B.34 protein digestion time-course samples were also analyzed by western blot. Following SDS-PAGE, the gel intended for western blot analysis was assembled into a nitrocellulose (NC) iBlot Gel Transfer Stack. An iBlot Gel Transfer Device was used to transfer proteins from the gel to the NC membrane for 7 minutes with a pre-set program (P3).

Following protein transfer, the membrane was blocked in phosphate-buffered saline containing polysorbate 20 (PBST) containing 5% (w/v) non-fat dry milk for 46 minutes at ambient laboratory temperature. Before and after the blocking step, the membrane was washed with PBST three times for at least 5 minute each to reduce the background. The blocked membrane was incubated for 45 minutes at ambient laboratory temperature with a Cry1B.34 polyclonal antibody R11957 (Pioneer Hi-Bred International, Inc.) diluted 1:100,000 in PBST containing 1% (w/v) non-fat dry milk. Following primary antibody incubation, the membrane was washed in PBST three times for 5 minutes each. The membrane was incubated for 48 minutes at ambient laboratory temperature with a secondary antibody (anti-rabbit IgG, horseradish peroxidase conjugate; Promega Corporation) diluted 1:100,000 in PBST containing 1% (w/v) non-fat dry milk. The membrane was washed in PBST four times for 5 minutes each. The membrane remained in PBST prior to incubating with a chemiluminescent substrate for 5 minutes. The chemiluminescent signal and the pre-stained markers were detected and captured using a ChemiDoc MP imaging system.

<u>Digestibility in Simulated Intestinal Fluid (SIF)</u>

Test and control solutions were prepared as follows:

- The pancreatin digestion solution, referred to as simulated intestinal fluid (SIF), was prepared fresh on the day of use by dissolving 26.4 mg of pancreatin (Sigma-Aldrich) into 5 ml of intestinal control solution (I-Con 1X buffer) to a final concentration of 0.5% weight per volume (w/v) pancreatin and 50 mM KH_2PO_4, pH 7.5.
- The test substance consisted of Cry1B.34 protein solubilized from a lyophilized powder (lot number PCF-0042).

- To prepare the stock solutions for each of the control proteins (BSA and β-lactoglobulin), a 5.0-mg sub-sample of powder was weighed into an individual tube for each control and solubilized by adding 1.0 ml of 10 mM CAPS buffer (to a target protein concentration of 5.0 mg/ml).
- The final concentration of the protein and pancreatin in the SIF reaction mixture was 0.25 mg/ml Cry1Da2 protein and 0.5% (w/v) pancreatin.

SIF solution (1900 µl) was dispensed into a 7-ml glass vial and placed in a 37 °C water bath for 2-5 minutes prior to the addition of 100 µl of Cry1B.34 protein test substance at Time 0. The digestion reaction mixture was mixed constantly using a stir bar and a submersible magnetic stirrer.

A 120-µl sub-sample of the Cry1B.34 protein digestion reaction mixture was removed from the vial at the following analytical time points (± 10 seconds): 0.5, 1, 2, 5, 10, 20, 30, and 60 minutes. The sub-samples were inactivated by adding them to pre-labeled tubes containing 64 µl of pre-mixed sample solution (consisting of 46 µl NuPAGE 4X LDS Sample Buffer and 18 µl NuPAGE 10X Sample Reducing Agent) and heating to 90-100 °C for 5 minutes prior to frozen storage (-20 °C freezer unit).

To prepare control digestion samples at 1 and 60 minutes, a 114-µl sample of the appropriate digestion solution was pre-warmed in a 37 °C water bath for 2-5 minutes prior to adding 6 µl of the Cry1B.34 protein test substance, control protein stock solution, or 10 mM CAPS buffer. The tubes were incubated in the water bath for the allotted time and then inactivated by mixing with 64 µl of the pre-mixed sample solution.

The Time 0 control reaction mixtures were prepared by first neutralizing 114 µl of the appropriate digestion solution with 64 µl of the pre-mixed sample solution, and then adding 6 µl of the Cry1B.34 protein test substance, protein stock solution, or 10 mM CAPS buffer to the appropriate tube and mixing.

Following digestion and inactivation, all control reaction mixtures were heated at 90-100 °C for 5 minutes prior to frozen storage (-20 °C freezer unit).

Control digestion samples included in the SIF assay are provided in Table E.2.

Table E.2. Control Samples for Simulated Intestinal Fluid (SIF) Digestibility Analysis

Protein	Digestion Solution	Digestion Time (min)		
		0	1	60
None (10 mM CAPS buffer), {SIF Control}	SIF	X	--	X
BSA	SIF	X	X	X
β-lactoglobulin	SIF	X	X	X
Cry1B.34	SIF	X	--	--
Cry1B.34	10 mM CAPS	X	--	X
Cry1B.34	Intestinal Control Solution (No Pancreatin)	--	--	X

SDS-PAGE Analysis

The Cry1B.34 protein digestion time-course samples and control samples were removed from frozen storage, heated at 90-100 °C for 5 minutes, and loaded (10 µl/well) into 4-12% Bis-Tris gels for SDS-PAGE analysis. Pre-stained protein molecular weight markers (Precision Plus Dual Xtra Standards) were also loaded into each gel to provide a visual estimate of molecular weight. Electrophoresis was conducted using a pre-cast gel electrophoresis system with 1X MES SDS running buffer at a constant 200 volts (V) for 35 minutes.

Upon completion of electrophoresis, the gels were removed from the gel cassettes for use in protein staining or western blot analyses. For protein staining, the gels were washed three times for 5 minutes each with water and stained with GelCode Blue Stain Reagent for 60 minutes. Following staining, the gels were destained with water four times for a minimum of 5 minutes each until the gel background was clear. Proteins were stained as blue-colored bands on the gels. The gel image was captured electronically using a ChemiDoc MP (Bio-Rad) imaging system.

Western Blot Analysis

The Cry1B.34 protein digestion time-course samples were also analyzed by western blot. Following SDS-PAGE, one of the resulting gels was assembled into a nitrocellulose (NC) iBlot Gel Transfer Stack. An iBlot Gel Transfer Device was used to transfer proteins from the gel to the NC membrane for 7 minutes with a pre-set program (P3).

Following protein transfer, the membrane was blocked in phosphate-buffered saline containing polysorbate 20 (PBST) containing 5% (w/v) non-fat dry milk for 60 minutes at ambient laboratory temperature. Before and after the blocking step, the membrane was washed with PBST three times for 1 minute each to reduce the background. The blocked membrane was incubated for 60 minutes at ambient laboratory temperature with an Cry1B.34 polyclonal antibody R11956 (Pioneer Hi-Bred International, Inc.) diluted 1:100,000 in PBST containing 1% (w/v) non-fat dry milk. Following primary antibody incubation, the membrane was washed in PBST four times for 5 minutes each. The membrane was incubated for 60 minutes at ambient laboratory temperature with a secondary antibody (anti-rabbit IgG, horseradish peroxidase conjugate; Promega Corporation) diluted 1:100,000 in PBST containing 1% (w/v) non-fat dry milk. The membrane was washed in PBST four times for at least 5 minutes each. The membrane remained in PBST prior to incubating with a chemiluminescent substrate for 5 minutes. The chemiluminescent signal and the pre-stained markers were detected and captured using a ChemiDoc MP imaging system.

Sequential Digestibility Analysis with Simulated Gastric Fluid (SGF) and Simulated Intestinal Fluid (SIF)

Test solutions were prepared as follows:

- A concentrated (i.e., 2X) pepsin digestion solution, referred to as simulated gastric fluid (SGF), was prepared fresh on the day of use by solubilizing pepsin (Sigma-Aldrich) in a previously prepared 2X gastric control solution. The final concentration of gastric control solution in SGF was 0.2% weight per volume (w/v) NaCl and 0.7% volume per volume (v/v) HCl; pH ~1.2. The SGF was prepared so that the pepsin to protein ratio of the final digestion mixture was 10 units of pepsin per µg of test protein.

- A concentrated (i.e., 2.5X) pancreatin digestion solution, referred to as simulated intestinal fluid (SIF), was prepared fresh on the day of use by solubilizing pancreatin (Sigma-Aldrich) in 2.5X intestinal control solution (2.5X I-Con). The final concentration of intestinal control solution in SIF was 50 mM KH_2PO_4, with a pH of ~7.5. Pancreatin content in SIF was adjusted so that there was approximately 0.5% (w/v) pancreatin in the final digestion reaction mixture.
- The pre-mixed sample stop solutions used to inactivate samples were prepared fresh on the day of use. The solution for SGF reactions was prepared by mixing 1200 µl of 200 mM Na2CO3, 1625 µl NuPAGE 4X LDS Sample Buffer, and 650 µl NuPAGE 10X Sample Reducing Agent. The solution for SIF reactions was prepared by mixing 1150 µl NuPAGE 4X LDS Sample Buffer and 450 µl NuPAGE 10X Sample Reducing Agent.
- The test substance consisted of Cry1B.34 protein solubilized from a lyophilized powder (lot number PCF-0042).

In Vitro Pepsin Digestion

Cry1B.34 Protein in SGF 10 Minutes Sample for Sequential Digestion: An aliquot (1 ml) of the 2X SGF solution and 800 µl water were dispensed into a 7-ml glass vial and pre-warmed in the 37 °C water bath for 2-5 minutes prior to addition of 200 µl of the Cry1B.34 protein test substance. The SGF digestion reaction mixture was incubated and mixed constantly using a stir bar and submersible stir plate for 10 minutes (± 10 seconds) after adding the Cry1B.34 protein test substance. At the end of the time period, a 1.5-ml sample of the Cry1B.34 SGF digestion reaction mixture was transferred to a separate vial and inactivated by neutralization with 0.3 ml of 0.5 N NaOH. This sample was used for the sequential SIF digestion.

Cry1B.34 Protein in SGF 10 Minutes: A 120-µl control sample (Cry1B.34 in SGF 10 minutes) was taken out from the SGF digestion reaction mixture at the end of 10 minutes (± 10 seconds) and inactivated by neutralization with 139 µl of pre-mixed SGF sample stop solution. The neutralized sample was heated for 5 minutes at 90-100 °C prior to frozen storage (-20 °C freezer unit).

Cry1B.34 Protein in SGF Time 0: A control sample (Cry1B.34 in SGF Time 0) was prepared by first inactivating 60 µl of 2X SGF and 49 µl water in 139 µl of pre-mixed SGF sample stop solution and then adding 12 µl of Cry1B.34 protein test substance to the neutralized SGF. The neutralized sample was heated for 5 minutes at 90-100 °C prior to frozen storage (-20 °C freezer unit).

SGF-Only 10 Minutes Incubation: An SGF-only control sample without Cry1B.34 protein test substance (SGF Control 10 minute) was prepared by mixing 60 µl 2X SGF and 49 µl water in a tube and pre-warming at 37 °C for 2-5 minutes. Following the addition of 12 µl of 10 mM CAPS buffer, the tube was incubated in a 37 °C water bath for 10 minutes (± 10 seconds). After incubation, the sample was inactivated by neutralization with 139 µl of pre-mixed SGF sample stop solution. The neutralized sample was heated for 5 minutes at 90-100 °C prior to frozen storage (-20 °C freezer unit).

Sequential Pancreatin Digestion

Cry1B.34 Protein in SGF 10 Minutes, SIF 0.5-30 Minutes: For the sequential SIF digestion time course, a 1.2-ml sample of the neutralized Cry1B.34 SGF digestion reaction mixture was dispensed into a 7-ml glass vial and placed in a 37 °C water bath for 2-5 minutes prior to addition of 800 µl 2.5X SIF solution. The SIF digestion reaction mixture was mixed constantly using a stir bar and a submersible stir plate.

A 120-µl sub-sample of the SIF digestion reaction mixture was removed from the vial at each of the following analytical time points (± 10 seconds): 0.5, 1, 2, 5, 10, 20 and 30 minutes. Each sub-sample was neutralized by adding it to a pre-labeled tube containing 64 µl of pre-mixed SIF sample stop solution. The neutralized samples were inactivated by heating at 90-100 °C for 5 minutes.

Cry1B.34 Protein in SGF 10 Minutes, SIF Time 0: An SIF control sample (Cry1B.34 10 minutes SGF Time 0 SIF) was prepared by mixing 48 µl 2.5X SIF with 64 µl of pre-mixed SIF sample stop solution and then heating for 5 minutes at 90-100 °C. A sub-sample (72 µl) of the neutralized Cry1B.34 SGF digestion reaction mixture was added to the heat-inactivated SIF control sample and then heated again for 5 minutes at 90-100 °C.

After neutralization and heating, all SIF reaction samples were stored frozen (-20 °C freezer unit).

SDS-PAGE Analysis

The digestion samples were removed from frozen storage, heated at 90-100 °C for 5 minutes, and loaded (10 µl/well) into a 4-12% Bis-Tris gel for SDS-PAGE analysis. Pre-stained protein molecular weight markers (Precision Plus Dual Xtra Standards) were also loaded into the gel to provide a visual estimate of molecular weight. Electrophoresis was conducted using a pre-cast gel electrophoresis system with 1X MES running buffer at a constant 200 volts (V) for 35 minutes.

Upon completion of electrophoresis, the gel was removed from the gel cassette and washed three times for 5 minutes each with water and stained with GelCode Blue Stain Reagent for 60 minutes. Following staining, the gel was destained with water four times for a minimum of 3 minutes each until the gel background was clear. Proteins were stained as blue-colored bands on the gel. The gel image was captured electronically using a ChemiDoc MP (Bio-Rad) imaging system.

Appendix E.2 Characterization of Cry1B.34 (PCF-0059) Protein Derived from a Microbial Expression System

In order to have sufficient amounts of purified Cry1B.34 protein for the multiple studies required to assess its safety, the Cry1B.34 protein was expressed in an *Escherichia coli* protein expression system. The microbially derived protein was purified using pellet washing and ion exchange chromatography. Tangential flow filtration was used to change the buffer to 100 mM ammonium bicarbonate. After lyophilization and mixing, a lot number (PCF-0059) was assigned.

The microbially derived Cry1B.34 protein was characterized for concentration, purity, molecular weight, immunoreactivity, lack of glycosylation, amino acid sequence, and bioactivity. Methods used included amino acid composition analysis, sodium dodecyl sulfate polyacrylamide gel electrophoresis (SDS-PAGE) analysis, western blot analysis, protein glycosylation analysis, liquid chromatography-mass spectrometry (LC-MS), N-terminal amino acid sequencing, and a bioactivity assay.

SDS-PAGE Analysis

The microbially derived Cry1B.34 protein was analyzed by SDS-PAGE. As expected, the Cry1B.34 proteins migrated as a band consistent with the expected molecular weight of approximately 129 kDa, as shown in Figure E2.1. Densitometry analysis indicated that the purity of the Cry1B.34 protein was 89% on a total protein basis.

Additional details regarding SDS-PAGE analytical methods are provided in Appendix E.3.

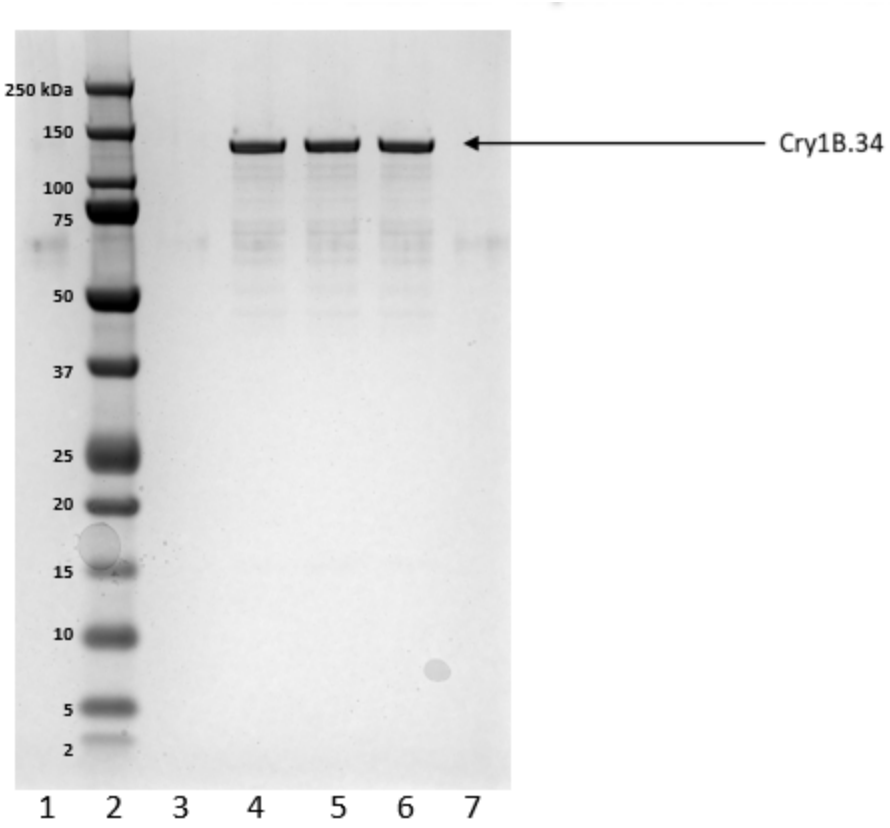

Lane	Sample Identification
1	1X LDS/DTT Sample Buffer Blank
2	Pre-stained Protein Molecular Weight Marker[a]
3	1X LDS/DTT Sample Buffer Blank
4	Microbially Derived Cry1B.34 Protein (1 µg)
5	Microbially Derived Cry1B.34 Protein (1 µg)
6	Microbially Derived Cry1B.34 Protein (1 µg)
7	1X LDS/DTT Sample Buffer Blank

Note: kilodalton (kDa) and microgram (µg).

[a] Molecular weight markers were included to provide a visual estimate that migration was within the expected range of the predicted molecular weight.

Figure E2.1. SDS-PAGE Analysis of the Microbially Derived Cry1B.34 Protein

Western Blot Analysis

The microbially derived Cry1B.34 protein was analyzed by Western blot. As expected, the microbially derived Cry1B.34 protein was immunoreactive to a Cry1B.34 monoclonal antibody and visible as a predominant band consistent with the expected molecular weight of approximately 129 kDa, as shown in Figure E2.2.

Additional details regarding Western blot analytical methods are provided in Appendix E.3.

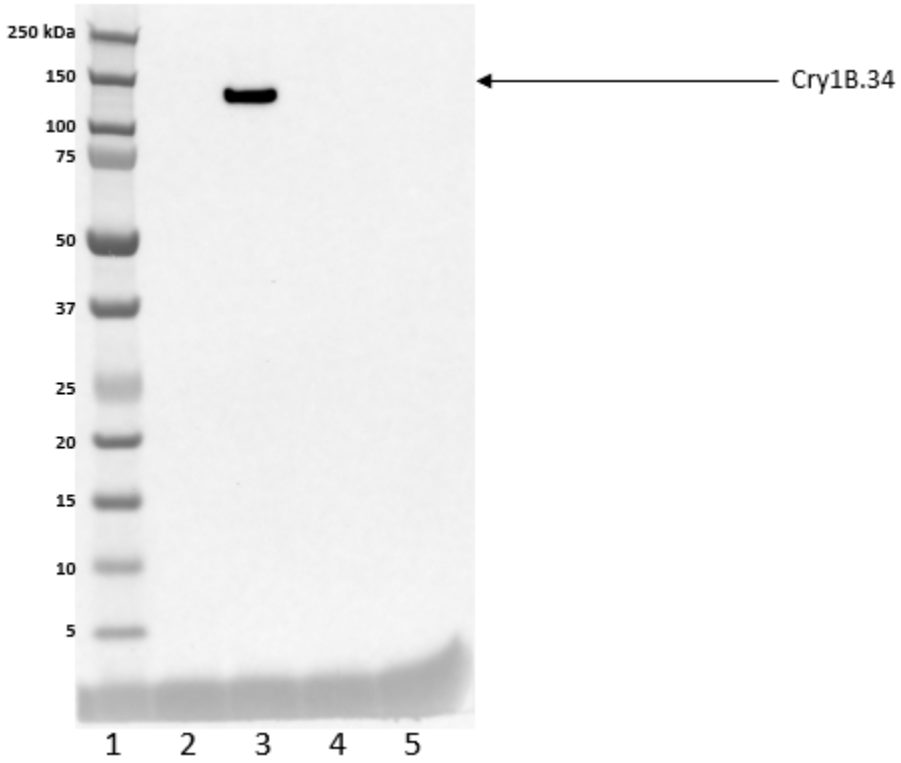

Lane	Sample Identification
1	Pre-stained Protein Molecular Weight Marker[a]
2	1X LDS/DTT Sample Buffer Blank
3	Microbially Derived Cry1B.34 Protein (5 ng)
4	1X LDS/DTT Sample Buffer Blank
5	1X LDS/DTT Sample Buffer Blank

Note: kilodalton (kDa) and nanogram (ng).

[a] Molecular weight markers were included to provide a visual estimate that migration was within the expected range of the predicted molecular weight.

Figure E2.2. Western Blot Analysis of the Microbially Derived Cry1B.34 Protein

Protein Glycosylation Analysis

The microbially derived Cry1B.34 protein was analyzed by SDS-PAGE. The gel also included a positive control (horseradish peroxidase) and negative control (soybean trypsin inhibitor). The gel was then stained using a Pierce Glycoprotein Staining Kit to visualize any glycoproteins. The gel was imaged and then stained with GelCode Blue stain reagent to visualize all protein bands.

Glycosylation was not detected for the microbially derived Cry1B.34 protein (Figures E2.3). The horseradish peroxidase positive control was clearly visible as a stained band. The soybean trypsin inhibitor negative control was not stained by the glycoprotein stain.

Additional details regarding glycosylation analytical methods are provided in Appendix E.3.

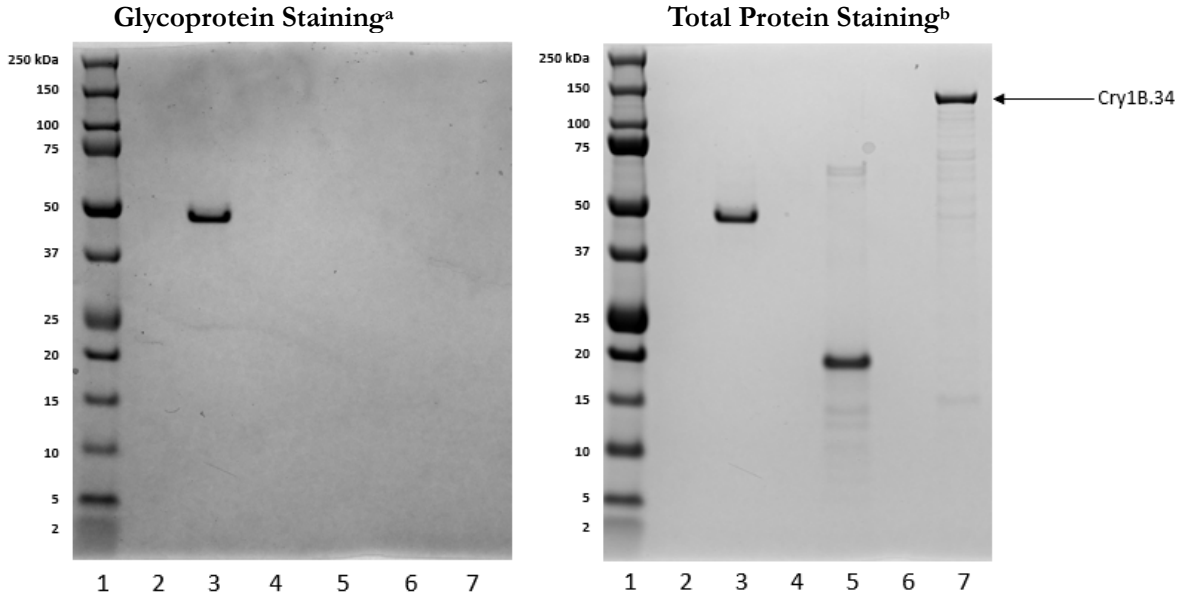

Lane	Sample Identification
1	Pre-stained Protein Molecular Weight Marker[c]
2	1X LDS/DTT Sample Buffer Blank
3	Horseradish Peroxidase Positive Control (1 µg)
4	1X LDS/DTT Sample Buffer Blank
5	Soybean Trypsin Inhibitor Negative Control (1 µg)
6	1X LDS/DTT Sample Buffer Blank
7	Microbially Derived Cry1B.34 Protein (1 µg)

Note: kilodalton (kDa) and microgram (µg).

[a] Gel was stained with glycoprotein staining reagent.

[b] Gel was stained with glycoprotein staining reagent followed by staining with Coomassie for total proteins.

[c] Molecular weight markers were included to provide a visual estimate that migration was within the expected range of the predicted molecular weight.

Figure E2.3. Glycosylation Analysis of Microbially Derived Cry1B.34 Protein

Mass Spectrometry Peptide Mapping Analysis

The microbially derived Cry1B.34 was analyzed by SDS-PAGE. Protein bands were stained with Coomassie stain reagent, and bands containing the Cry1B.34 protein were excised for each sample.

The excised Cry1B.34 protein bands were digested with trypsin or chymotrypsin. Digested samples were analyzed with ultra-performance liquid chromatography-mass spectrometry (LC-MS). The resulting MS data were used to search and match the peptides from the expected Cry1B.34 protein sequence, and the combined sequence coverage was calculated. The identified tryptic and chymotryptic peptides for microbially derived Cry1B.34 protein are shown in Tables E2.1 and E2.2, respectively. The combined sequence coverage account for 78.6% (901/1147) of the expected amino acid sequence of the microbially derived Cry1B.34 protein (Table E2.3.6 and Figure E2.4).

Additional details regarding peptide mapping analytical methods are provided in Appendix E.3.

Table E2.1. Tryptic Peptides of Microbially Derived Cry1B.34 Protein Identified Using LC-MS Analysis

Matched Residue Position	Experimental Mass[a]	Theoretical Mass[b]	Identified Peptide Sequence
5–28	2668.2851	2668.2874	KNENEIINAVSNHSAQMDLSLDAR
29–59	3261.6135	3261.6187	IEDSLCVAEVNNIDPFVSASTVQTGISIAGR
104–111	974.4740	974.4781	QQVTENTR
112–117	644.3582	644.3606	NTAIAR
118–123	643.3632	643.3653	LEGLGR
127–139	1622.7666	1622.7689	SYQQALETWLDNR
146–151	729.4361	729.4385	SIILER
192–216	2880.2585	2880.2661	DASLFGSEWGMSSADVNQYYQEQIR
217–237	2660.1738	2660.1714	YTEEYSNHCVQWYNTGLNNLR
238–246	1032.4950	1032.4988	GTNAESWLR
247–251	726.3425	726.3449	YNQFR
272–283	1363.7068	1363.7096	TYPINTSAQLTR
284–292	1062.5311	1062.5346	EIYTDPIGR
341–354	1803.7864	1803.7900	WSSTQHMNYWVGHR[c]
414–425	1553.7583	1553.7626	FNFINPQNIYER
426–464	4447.0589	4447.0517	GATTYSQPYQGVGIQLFDSETELPPETTERPNYESYSHR
465–477	1405.8390	1405.8405	LSHIGLIIGNTLR
478–486	1115.5463	1115.5512	APVYSWTHR
487–498	1316.6532	1316.6572	SATLTNTIDPER
499–506	923.5778	923.5804	INQIPLVK
510–529	1989.0287	1989.0320	VWGGTSVITGPGFTGGDILR
565–588	2341.2670	2341.2676	VIVLTGAASTGVGGQVSVNMPLQK[c]
589–599	1249.5937	1249.5972	TMEIGENLTSR
603–613	1379.6118	1379.6146	YTDFSNPFSFR
614–641	2890.4574	2890.4600	ANPDIIGISEQPLFGAGSISSGELYIDK
642–659	2034.0114	2034.0157	IEIILADATFEAESDLER
663–670	791.4257	791.4290	AGAGLFTR
671–686	1877.9232	1877.9232	TRDGLQVNVTDYQVDR
673–686	1620.7707	1620.7744	DGLQVNVTDYQVDR
687–703	1935.8580	1935.8632	AANLVSCLSDEQYSHDK
687–704	2063.9544	2063.9582	AANLVSCLSDEQYSHDKK
705–711	848.4217	848.4248	MLMEAVR
758–765	856.5096	856.5130	VLQLASAR
766–775	1317.6212	1317.6241	ENYPTYIYQK
776–786	1247.6857	1247.6874	VDASVLKPYTR
787–794	996.5363	996.5393	YRLDGFVK
789–794	677.3728	677.3748	LDGFVK
795–808	1648.8040	1648.8056	SSEDLEIDLVHQHK
814–830	1907.8283	1907.8320	NVPDNLVSDTYPDGSCR
888–913	2689.3395	2689.3446	TADGYATLGNLELVEVGPLSGESLER
921–927	844.4154	844.4191	WNAELGR
928–934	875.4079	875.4097	ERAETDR
935–940	663.3935	663.3955	VYLAAK
1000–1010	1328.6672	1328.6724	LQQASYLYTSR
1057–1062	730.3401	730.3432	VNPNCK
1071–1082	1220.6496	1220.6514	KVGGGDGYVTIR
1072–1082	1092.5523	1092.5564	VGGGDGYVTIR
1083–1088	691.3130	691.3150	DGAHHR
1114–1147	4011.8623	4011.8578	EVVFYPHTEHTWVEVSESEGAFYIDSIELIETQE

[a] The experimental mass is the uncharged mass calculated from the mass to charge ratio of the observed ion.

[b] The theoretical mass is the *in silico* generated mass that matches closest to the experimental mass.

[c] This peptide was modified by methionine oxidation (Oxidation-M).

Table E2.2. Chymotryptic Peptides of Microbially Derived Cry1B.34 Protein Identified Using LC-MS Analysis

Matched Residue Position	Experimental Mass[a]	Theoretical Mass[b]	Identified Peptide Sequence
1–23	2596.2281	2596.2299	PSNRKNENEIINAVSNHSAQMDL[c]
24–33	1117.5591	1117.5615	SLDARIEDSL
24–44	2376.1329	2376.1267	SLDARIEDSLCVAEVNNIDPF
92–101	1255.6449	1255.6448	EIFLEHVEQL
95–101	866.4471	866.4498	LEHVEQL
119–125	750.3627	750.3660	EGLGRGY
126–135	1280.6115	1280.6149	RSYQQALETW
129–135	874.4161	874.4185	QQALETW
129–136	987.5003	987.5025	QQALETWL
136–152	2090.0946	2090.0980	LDNRNDARSRSIILERY
137–152	1977.0109	1977.0140	DNRNDARSRSIILERY
156–165	1084.6012	1084.6016	ELDITTAIPL
166–175	1201.6419	1201.6455	FSIRNQEVPL
167–175	1054.5736	1054.5771	SIRNQEVPL
167–179	1560.8373	1560.8334	SIRNQEVPLLMVY
180–187	836.4479	836.4504	AQAANLHL
180–188	949.5314	949.5345	AQAANLHLL
190–196	820.4419	820.4443	LRDASLF
197–210	1529.6071	1529.6093	GSEWGMSSADVNQY
201–210	1070.4302	1070.4339	GMSSADVNQY
211–217	998.4803	998.4821	YQEQIRY
211–221	1520.6753	1520.6783	YQEQIRYTEEY
218–228	1451.5737	1451.5776	TEEYSNHCVQW
218–229	1614.6378	1614.6409	TEEYSNHCVQWY
222–228	929.3794	929.3814	SNHCVQW
230–244	1645.7756	1645.7808	NTGLNNLRGTNAESW
234–244	1260.5804	1260.5847	NNLRGTNAESW
237–244	919.4125	919.4148	RGTNAESW
237–245	1032.4950	1032.4988	RGTNAESWL
269–281	1478.7337	1478.7365	DTRTYPINTSAQL
287–299	1331.6440	1331.6470	TDPIGRTNAPSGF
305–320	1711.8217	1711.8206	FNNNAPSFSAIEAAIF
306–320	1564.7510	1564.7521	NNNAPSFSAIEAAIF
321–332	1460.7774	1460.7776	RPPHLLDFPEQL
336–341	692.3225	692.3242	SASSRW
342–349	966.3835	966.3865	SSTQHMNY
342–350	1152.4624	1152.4658	SSTQHMNYW
351–357	841.4525	841.4559	VGHRLNF
356–364	973.5311	973.5345	NFRPIGGTL
356–371	1674.8666	1674.8689	NFRPIGGTLNTSTQGL
358–364	712.4207	712.4232	RPIGGTL
358–371	1413.7548	1413.7576	RPIGGTLNTSTQGL
365–382	1873.9332	1873.9381	NTSTQGLTNNTSINPVTL
372–382	1172.5985	1172.6037	TNNTSINPVTL
372–384	1447.7308	1447.7307	TNNTSINPVTLQF
383–390	1014.4741	1014.4771	QFTSRDVY
385–390	739.3473	739.3501	TSRDVY
391–401	1174.5907	1174.5942	RTESNAGTNIL
391–402	1321.6576	1321.6626	RTESNAGTNILF
415–423	1121.5478	1121.5505	NFINPQNIY
415–430	1899.9163	1899.9115	NFINPQNIYERGATTY
417–423	860.4376	860.4392	INPQNIY
417–430	1638.7987	1638.8002	INPQNIYERGATTY
424–430	796.3695	796.3715	ERGATTY
435–442	860.4737	860.4756	QGVGIQLF
443–461	2255.9685	2255.9706	DSETELPPETTERPNYESY
462–470	1018.5650	1018.5672	SHRLSHIGL

Table E2.2. Identified Chymotryptic Peptides of the Microbially Derived Cry1B.34 Protein by LC-MS Analysis (continued)

Matched Residue Position	Experimental Mass[a]	Theoretical Mass[b]	Identified Peptide Sequence
466–476	1136.6550	1136.6554	SHIGLIIGNTL
477–483	877.4420	877.4446	RAPVYSW
484–490	784.4166	784.4191	THRSATL
491–504	1622.8635	1622.8628	TNTIDPERINQIPL
512–522	991.4956	991.4975	GGTSVITGPGF
512–528	1547.7869	1547.7832	GGTSVITGPGFTGGDIL
540–551	1431.7444	1431.7470	QVNINSPITQRY
558–568	1185.6804	1185.6830	ASSRDARVIVL
569–586	1644.8136	1644.8141	TGAASTGVGGQVSVNMPL
587–596	1161.5661	1161.5699	QKTMEIGENL
602–610	1145.5105	1145.5142	RYTDFSNPF
611–626	1755.9210	1755.9155	SFRANPDIIGISEQPL
613–626	1521.8150	1521.8151	RANPDIIGISEQPL
613–627	1668.8885	1668.8835	RANPDIIGISEQPLF
613–637	2527.3014	2527.2918	RANPDIIGISEQPLFGAGSISSGEL
627–638	1186.5477	1186.5506	FGAGSISSGELY
638–651	1623.8770	1623.8759	YIDKIEIILADATF
639–651	1460.8132	1460.8126	IDKIEIILADATF
652–668	1790.8748	1790.8799	EAESDLERAQKAGAGLF
669–682	1636.8126	1636.8169	TRTRDGLQVNVTDY
683–690	885.4647	885.4668	QVDRAANL
683–694	1344.6774	1344.6820	QVDRAANLVSCL
683–699	1966.9001	1966.9054	QVDRAANLVSCLSDEQY
691–699	1099.4455	1099.4492	VSCLSDEQY
754–759	718.4464	718.4490	FKGRVL
760–771	1411.6714	1411.6732	QLASARENYPTY
760–773	1687.8186	1687.8205	QLASARENYPTYIY
762–771	1170.5284	1170.5305	ASARENYPTY
762–773	1446.6767	1446.6779	ASARENYPTYIY
772–781	1134.6242	1134.6285	IYQKVDASVL
772–784	1522.8366	1522.8395	IYQKVDASVLKPY
774–781	858.4790	858.4811	QKVDASVL
774–784	1246.6893	1246.6921	QKVDASVLKPY
867–881	1617.7637	1617.7635	INTGDLNSSVDQGIW
885–892	908.4700	908.4716	KVRTADGY
885–895	1193.6372	1193.6404	KVRTADGYATL
896–906	1138.6237	1138.6234	GNLELVEVGPL
907–921	1803.8472	1803.8499	SGESLEREQRDNAKW
922–936	1777.8664	1777.8707	NAELGRERAETDRVY
922–937	1890.9531	1890.9547	NAELGRERAETDRVYL
926–936	1350.6625	1350.6640	GRERAETDRVY
937–947	1224.6958	1224.6979	LAAKQAINHLF
938–947	1111.6098	1111.6138	AAKQAINHLF
979–990	1291.6677	1291.6660	SDTVLQIPGISY
979–993	1696.8578	1696.8560	SDTVLQIPGISYEIY
984–993	1181.5940	1181.5968	QIPGISYEIY
994–1000	832.4259	832.4290	TELSDRL
994–1005	1409.6763	1409.6786	TELSDRLQQASY
997–1005	1066.5015	1066.5043	SDRLQQASY
1026–1041	1734.7261	1734.7268	NATTDASVQQDGNMHF
1026–1042	1847.8068	1847.8108	NATTDASVQQDGNMHFL
1026–1044	2059.9700	2059.9633	NATTDASVQQDGNMHFLVL
1042–1047	753.4146	753.4174	LVLSHW
1043–1047	640 3310	640.3333	VLSHW
1045–1055	1311.6168	1311.6208	SHWDAQVTQQL
1048–1055	901.4485	901.4505	DAQVTQQL
1056–1063	1049.5030	1049.5076	RVNPNCKY

Table E2.2. Identified Chymotryptic Peptides of the Microbially Derived Cry1B.34 Protein by LC-MS Analysis (continued)

Matched Residue Position	Experimental Mass[a]	Theoretical Mass[b]	Identified Peptide Sequence
1066–1078	1334.7039	1334.7055	RVTARKVGGGDGY
1079–1091	1503.7861	1503.7906	VTIRDGAHHRETL
1079–1093	1751.9033	1751.9067	VTIRDGAHHRETLTF
1111–1117	834.4830	834.4851	ITKEVVF
1111–1125	1885.9327	1885.9363	ITKEVVFYPHTEHTW
1111–1135	2920.3954	2920.3920	ITKEVVFYPHTEHTWVEVSESEGAF
1118–1135	2103.9140	2103.9174	YPHTEHTWVEVSESEGAF
1118–1136	2266.9820	2266.9807	YPHTEHTWVEVSESEGAFY
1126–1136	1215.5255	1215.5295	VEVSESEGAFY
1136–1147	1451.7052	1451.7031	YIDSIELIETQE
1137–1147	1288.6373	1288.6398	IDSIELIETQE

[a] The experimental mass is the uncharged mass calculated from the mass to charge ratio of the observed ion.
[b] The theoretical mass is the *in silico* generated mass that matches closest to the experimental mass.
[c] This peptide was modified by methionine oxidation (Oxidation-M).

Table E2.3. Combined Sequence Coverage of Identified Tryptic and Chymotryptic Peptides of Microbially Derived Cry1B.34 Protein Using LC-MS Analysis

Protease	% Coverage	Combined % Coverage
Trypsin	54	78.6
Chymotrypsin	68	

```
   1 PSNRKNENEI INAVSNHSAQ MDLSLDARIE DSLCVAEVNN IDPFVSASTV
  51 QTGISIAGRI LGVLGVPFAG QLASFYSFLV GELWPSGRDP WEIFLEHVEQ
 101 LIRQQVTENT RNTAIARLEG LGRGYRSYQQ ALETWLDNRN DARSRSIILE
 151 RYVALELDIT TAIPLFSIRN QEVPLLMVYA QAANLHLLLL RDASLFGSEW
 201 GMSSADVNQY YQEQIRYTEE YSNHCVQWYN TGLNNLRGTN AESWLRYNQF
 251 RRDLTLGVLD LVALFPSYDT RTYPINTSAQ LTREIYTDPI GRTNAPSGFA
 301 STNWFNNNAP SFSAIEAAIF RPPHLLDFPE QLTIYSASSR WSSTQHMNYW
 351 VGHRLNFRPI GGTLNTSTQG LTNNTSINPV TLQFTSRDVY RTESNAGTNI
 401 LFTTPVNGVP WARFNFINPQ NIYERGATTY SQPYQGVGIQ LFDSETELPP
 451 ETTERPNYES YSHRLSHIGL IIGNTLRAPV YSWTHRSATL TNTIDPERIN
 501 QIPLVKGFRV WGGTSVITGP GFTGGDILRR NTFGDFVSLQ VNINSPITQR
 551 YRLRFRYASS RDARVIVLTG AASTGVGGQV SVNMPLQKTM EIGENLTSRT
 601 FRYTDFSNPF SFRANPDIIG ISEQPLFGAG SISSGELYID KIEIILADAT
 651 FEAESDLERA QKAGAGLFTR TRDGLQVNVT DYQVDRAANL VSCLSDEQYS
 701 HDKKMLMEAV RAAKRLSRER NLLQDPDFNE INSTEENGWK ASNGIIISEG
 751 GPFFKGRVLQ LASARENYPT YIYQKVDASV LKPYTRYRLD GFVKSSEDLE
 801 IDLVHQHKVH LVKNVPDNLV SDTYPDGSCR GVNRCDEQHQ VDVQIDTEHH
 851 PMDCCEAAQT HEFSSYINTG DLNSSVDQGI WVVLKVRTAD GYATLGNLEL
 901 VEVGPLSGES LEREQRDNAK WNAELGRERA ETDRVYLAAK QAINHLFVDY
 951 QDQQLNPEIG LAEINEASNL VESITGVYSD TVLQIPGISY EIYTELSDRL
1001 QQASYLYTSR NAVQNGDFDS GLDSWNATTD ASVQQDGNMH FLVLSHWDAQ
1051 VTQQLRVNPN CKYVLRVTAR KVGGGDGYVT IRDGAHHRET LTFNACDYDV
1101 NGTYVNDNTY ITKEVVFYPH TEHTWVEVSE SEGAFYIDSI ELIETQE
```

Red bold type	Red bold type indicates microbially-derived Cry1B.34 peptides identified using LC-MS analysis.
Amino acid residue abbreviations	Alanine (A), cysteine (C), aspartic acid (D), glutamic acid (E), phenylalanine (F), glycine (G), histidine (H), isoleucine (I), lysine (K), leucine (L), methionine (M), asparagine (N), proline (P), glutamine (Q), arginine (R), serine (S), threonine (T), tryptophan (W), tyrosine (Y), and valine (V).

Figure E2.4. Amino Acid Sequence of Microbially Derived Cry1B.34 Protein Indicating Chymotryptic Peptides Identified Using LC-MS Analysis

N-Terminal Amino Acid Sequence Analysis

N-terminal amino acid sequence analysis identified a protein sequence of PSNRKNENEI.

Additional details regarding N-terminal amino acid sequence analytical methods are provided in Appendix E.3.

Bioactivity Assay

The bioactivity of the microbially derived Cry1B.34 protein was evaluated by conducting a 7-day bioassay using *Spodoptera frugiperda* (fall armyworm; Lepidoptera: Noctuidae), a species sensitive to the Cry1B.34 protein.

Bioactivity analysis demonstrated that Cry1B.34 protein had insecticidal activity toward a target insect, *Spodoptera frugiperda.* The biological activity of the test diet containing 50 ng Cry1B.34 protein/mg was demonstrated by 100% mortality in *S. frugiperda* fed Treatment 2 compared to 5.3 percent mortality in organisms fed the control diet.

Additional details are provided in Appendix E.3.

Table E2.4. Microbially Derived Cry1B.34 Protein Bioactivity Assay Using *Spodoptera frugiperda*

Treatment	Treatment Description	Concentration (ng Cry1B.34 Protein/mg)	Total Number of Observations	Number of Surviving Organisms	Mortality %
1	Buffer Control Diet	0	19[a]	18	5.3
2	Test Diet	50	20	0	100

[a] Organisms counted as missing during the bioassay were not included in the total number of observations for a given treatment.

Appendix E.3. Methods for Characterization of Microbially Derived Cry1B.34 Protein (PCF-0059)

Test Materials

Microbially Derived Cry1B.34 Protein: Cry1B.34 protein was produced by by Aldevron, using a microbial expression system. The protein was expressed in an *E. coli* protein expression system and purified using pellet washing and ion exchange chromatography. Tangential flow filtration was used to change the buffer to 100 mM ammonium bicarbonate. After lyophilization and mixing, a lot number (PCF-0059) was assigned.

SDS-PAGE Analysis

Cry1B.34 protein was solubilized to a target concentration of 1 mg/ml based on amino acid analysis in 1X LDS/DTT sample buffer (25% 4X NuPAGE LDS Sample Buffer, 10% 10X NuPAGE Sample Reducing Agent containing DTT, and 65% ASTM [American Society for Testing and Materials] Type I water [referred to as water]) and heated at 90-100 °C for 5 minutes. The sample was stored frozen (-20 °C freezer unit), as applicable, until SDS-PAGE analysis.

Prior to SDS-PAGE analysis, a sample was diluted in 1X LDS buffer. The diluted sample was heated for 5 minutes at 90-100 °C. The prepared protein samples were analyzed using 4-12% Bis-Tris gels. Pre-stained protein molecular weight markers (Precision Plus Protein Dual Xtra Standards) were also loaded into the gels to provide a visual verification that migration was within the expected range of the predicted molecular weight. Electrophoresis was conducted using a pre-cast gel electrophoresis system with MES SDS running buffer and NuPAGE Antioxidant at a constant 200 volts (V) for 35 minutes.

Upon completion of electrophoresis, the gels were removed from the gel cassettes and used for Coomassie staining, western blot analysis, protein glycosylation analysis, or sample preparation for N-terminal amino acid sequencing and peptide mapping.

For Coomassie staining, following electrophoresis, the gel was washed with water three times for 5 minutes each and stained with GelCode Blue Stain Reagent for 60 minutes. Following staining, the gel was de-stained with water four times for at least 5 minutes each or until the gel background was clear. Proteins were stained as blue-colored bands on the gels. The gel image was captured electronically using a ChemiDoc MP (Bio-Rad) imaging system.

For purity analysis, 1 µg of Cry1B.34 protein was loaded on to a gel in each of three lanes. With the image of the gel, densitometry analysis was conducted to evaluate the purity of the Cry1B.34 protein based on the relative intensity of the Cry1B.34 protein band compared to other protein bands in the same lane using an imaging software. The relative intensity of the bands was averaged across the three lanes to determine purity.

Western Blot Analysis

For western blot analysis, 5 ng of Cry1B.34 protein was loaded on to the gel. Following SDS-PAGE, the resulting gel was assembled into a nitrocellulose (NC) iBlot Gel Transfer Stack. An

iBlot Gel Transfer Device was used to transfer proteins from the gel to the NC membrane for 7 minutes with a pre-set program (P3).

Following protein transfer, the membrane was blocked in phosphate buffered saline containing polysorbate 20 (PBST) containing 5% weight/volume (w/v) non-fat dry milk for 45 minutes at ambient laboratory temperature. Before and after the blocking step, the membrane was washed with PBST three times for 5 minutes each to reduce the background. The blocked membrane was incubated for 45 minutes at ambient laboratory temperature with a Cry1B.34 monoclonal antibody 22A10.G4.F10 (Pioneer Hi-Bred International, Inc.) diluted 1:10,000 in PBST containing 1% w/v non-fat dry milk. Following primary antibody incubation, the membrane was washed 3 times in PBST for 5 minutes each. The membrane was incubated overnight in a 4 °C cold room with a secondary antibody (anti-mouse IgG, horseradish peroxidase conjugate; Promega Corporation) diluted 1:10,000 in PBST containing 1% non-fat dry milk. The membrane was washed 3 times with PBST for 5 minutes each. The blot remained in PBST prior to incubating with a chemiluminescent substrate for 5 minutes. The chemiluminescent signal and the pre-stained markers were detected and captured using a ChemiDoc MP imaging system.

Peptide Mapping by Mass Spectrometry

For mass spectrometry sequencing analyses, 4 µg of Cry1B.34 protein were loaded onto a gel in each of three lanes. Following SDS-PAGE, Coomassie staining, and gel imaging using the methods as described in Methods Section B, protein bands at the expected molecular weight of Cry1B.34 protein were excised from a gel and stored frozen (-20 °C freezer unit). The protein in two of the gel slices was reduced with DTT, alkylated with iodoacetamide, and then subsequently digested with trypsin or chymotrypsin. The digested samples were separated on an ACQUITY UPLC (Waters Corporation) fitted with a Cortecs UPLC C18 1.6 µm column (2.1 x 100 mm; Waters Corporation) by gradient elution. Eluent from the column was directed into an electrospray source, operating in positive ion mode, on a TripleTOF 5600+ hybrid quadrupole-TOF mass spectrometer (AB Sciex; currently Sciex). The resulting MS data were processed using MS Data Converter (Beta 1.3) to produce a peak list. The peak list was used to perform an MS/MS ion search (Mascot Software version 2.7.0) and match peptides from the expected Cry1B.34 protein sequence (Perkins *et al.*, 1999). The following search parameters were used: peptide and fragment mass tolerance, ± 0.1 Da; fixed modifications, cysteine carbamidomethyl; variable modifications, methionine oxidation; and maximum missed cleavages, 1 for trypsin and 2 for chymotrypsin. The Mascot-generated peptide ion score threshold was > 13, which indicates identity or extensive homology ($p < 0.05$). The combined sequence coverage was calculated with GPMAW version 12.11.0.

N-Terminal Amino Acid Sequencing Analysis

For N-terminal amino acid sequence analyses, 6 µg/lane of Cry1B.34 protein was loaded on to a gel in each of three lanes. Following SDS-PAGE, the resulting gel was incubated in cathode buffer (60 mM Tris, 40 mM CAPS, 0.075% SDS, pH 9.6) for 10-20 minutes. An Immobilon-P PVDF membrane was wetted in 100% methanol for 30 seconds, followed by immersion in anode buffer (60 mM Tris, 40 mM CAPS, 15% methanol, pH 9.6) for 10-20 minutes. A Trans-Blot SD Semi-Dry Electrophoretic Transfer Cell system was used to transfer proteins from the gel to the

membrane at 10 V for 60 minutes. Following protein transfer, the membrane was washed with water three times for 5 minutes each, stained with GelCode Blue stain reagent for 5 minutes, and then destained with water to visualize protein bands at the expected molecular weight of the Cry1B.34 protein. The bands containing the microbially derived Cry1B.34 protein were excised and stored frozen (-20 °C freezer unit). The bands were analyzed as a single sample using a Shimadzu PPSQ-51A sequencer. Ten cycles of Edman sequencing were performed. During each cycle, the N-terminal amino acid was sequentially derivatized with phenylisothiocyanate (PITC), cleaved with trifluoracetic acid, and converted to PTH-amino acid which was identified through chromatography. LabSolutions Software was used to automatically identify the N-terminal sequence.

Glycoprotein Analysis

A Pierce Glycoprotein Staining Kit was used to determine whether the Cry1B.34 protein was glycosylated. For glycosylation staining, 1 µg of Cry1B.34 protein was loaded on to the gel. The Cry1B.34 protein, a positive control protein (horseradish peroxidase), and a negative control protein (soybean trypsin inhibitor), were run by SDS-PAGE.

Following electrophoresis, the gel was washed with water twice for 5 minutes each wash, fixed with 50% methanol for 30-35 minutes, and washed twice with 3% acetic acid for 10-15 minutes each wash. The gel was then incubated with oxidizing solution for 15-20 minutes and washed three times with 3% acetic acid for 5-7 minutes each wash. The gel was incubated with glycoprotein staining reagent for 15-20 minutes and then incubated in a reducing reagent for 5-7 minutes. The gel was then washed three times with 3% acetic acid for 5 minutes each and then washed twice in water for 5 minutes. Glycoproteins were detected as bands stained a magenta color on the gel.

Following glycoprotein detection, the image of the gel was captured electronically using a ChemiDoc MP imaging system. The same gel was then stained with GelCode Blue stain reagent for 60 minutes followed by three washes with water for at least 5 minutes each to visualize all protein bands. The image of the GelCode stained gel was then captured electronically.

Bioactivity Bioassay

The biological activity of Cry1B.34 protein was evaluated by conducting a 7-day bioassay using *Spodoptera frugiperda* (fall armyworm; Lepidoptera: Noctuidae), a species sensitive to the Cry1B.34 protein. Eggs were obtained from [redacted] and their identity was recorded by study personnel.

The *S. frugiperda* bioassay utilized a generalized randomized block design containing four blocks. Each block consisted of a 12-well bioassay plate and contained five replicates from each of the following treatments for a target of 20 individuals per treatment:

- Treatment 1: Buffer Control Diet (containing a dosing solution of 10 mM CAPS buffer)
- Treatment 2: Test Diet (targeting 50 ng Cry1B.34 protein per mg diet wet weight)

For each day of diet preparation, a Cry1B.34 protein stock solution was prepared by solubilizing test substance in buffer (10 mM CAPS, pH 10.5) to a target concentration of 1.0 mg/ml. The stock solution was diluted in 10 mM CAPS to prepare the test dosing solution at a concentration range of 67 ng/µl. The buffer control dosing solution consisted of 10 mM CAPS buffer. Dosing solutions were maintained chilled (refrigerated or on wet ice) until use. The carrier for the *S. frugiperda* bioassay consisted of Stonefly Heliothis diet. On each day of diet preparation, each dosing solution was combined with carrier at a 3:1 ratio (i.e., 3 ml of dosing solution to 1 g carrier) to generate Treatments 1 and 2.

S. frugiperda eggs were incubated in an environmental chamber until the eggs hatched. Neonates were used in the bioassay within 24 hours of hatching. On Day 0 of the bioassay, approximately 300 µl (i.e., 1 g of wet diet equated to 1 ml of wet diet) of freshly prepared diets were dispensed into individual wells of the bioassay plates. One *S. frugiperda* neonate was placed in each well containing diet, each bioassay plate was sealed with heat-sealing film and a small hole was poked over each well to allow for ventilation. The bioassay was conducted in an environmental chamber set at 25 °C, 65% relative humidity, and continuous dark. On Day 4, new bioassay plates were prepared with fresh diet as described for Day 0, with the exception that on Day 4, 600 µl was dispensed per well. The additional diet was needed to accommodate the increased nutritional needs of the growing organisms. After 7 days, the bioassay was complete, mortality was assessed, and surviving larvae were individually weighed. Only wells that contained one organism were included in the total number of observed individuals; organisms recorded as missing from a well were excluded from statistical analysis.

The bioassay acceptability criterion indicated the bioassay may be repeated if the combined number of dead and missing organisms exceeds 20% for the buffer control diet (Treatment 1) group. The bioassay met the acceptability criteria.

APPENDIX F. METHODS FOR CHARACTERIZATION OF PAT PROTEIN

Test Materials

The reference substance consisted of lyophilized PAT protein derived from a microbial expression system (lot number PCF-0038). A 5.0-mg sample of the lyophilized protein was solubilized in 1.0 ml of 1X LDS/DTT sample buffer to a nominal concentration of 3.68 mg PAT protein/ml and heated at 90-100 °C for five minutes prior to SDS-PAGE analysis.

PAT protein was isolated from DP910521 maize leaf tissue. The tissue samples were collected at the R1 growth stage (the stage when silks become visible; Abendroth *et al.*, 2011) from plants grown at a field location in Johnston, IA, USA. The tissue was lyophilized, homogenized and stored at ≤ -50 °C.

The PAT protein was extracted from lyophilized maize tissue in two identical batches by homogenization in a pre-chilled Waring blender vessel using chilled phosphate-buffered saline containing polysorbate 20 (PBST) extraction buffer (500 ml buffer per ~25 g tissue per batch). The sample extract was then filtered through cheesecloth, clarified by centrifugation, and fractionated using ammonium sulfate (AS) precipitation. Beginning at 0% AS saturation and using an online calculator by EnCor Biotechnology Inc. (EnCor Biotechnology, 2020), AS was slowly added to the sample extract while stirring until 45% AS saturation was reached. The sample was centrifuged and the AS process was repeated with the supernatant, this time beginning at 45% AS saturation and progressing to 60%. The sample was centrifuged again, the supernatant was discarded, and the fractionated pellets were solubilized in phosphate-buffered saline and buffer-exchanged using Econo-Pac 10DG desalting columns from BioRad.

After desalting and buffer exchange, the sample was further purified by immunoaffinity chromatography. Two immunoaffinity columns were prepared by coupling a PAT monoclonal antibody (2C10.D5.G8) to AminoLink Plus Coupling Gel. Elutions 2-5 from each immunoaffinity purification column were collected separately and immediately neutralized with 1M Tris buffer, pH 8.

The PAT protein was further purified by ion exchange purification using a Q Sepharose column. Elutions 2-4 from each immunoaffinity purification column were pooled, diluted in 50 mM Tris, pH 8, and then added to the column containing the Q ion exchange resin. Collected fractions from elutions 2-5 were concentrated into one sample using a centrifugal concentrator (10K Vivaspin; Sartorius) and buffer-exchanged to a volume of approximately 200 µl.

Following extraction, purification, and concentration, the final volume in the concentrator was estimated and 25% 4X NuPAGE LDS sample buffer and 10% 10X NuPAGE DTT Sample Reducing Agent were added to the concentrated sample. The sample in the concentrator was heated for 2-5 minutes at 70-100 °C and then transferred to a microcentrifuge tube. The sample was then heat-treated at 90-100 °C for 5 (±1) minutes and stored frozen at ≤ -10 °C.

SDS-PAGE Analysis

The purified maize-derived PAT protein sample in LDS sample buffer from freezer storage was re-heated for 5 minutes at 90-100 °C, diluted as applicable, and then loaded into 4-12% Bis-Tris

gels. Pre-stained protein molecular weight markers (Precision Plus Protein Dual Xtra Standards) were loaded into each gel to provide a visual verification that migration was within the range of the predicted molecular weight. For SDS-PAGE and western blot analysis, the PAT protein reference substance was also re-heated for 5 minutes at 90-100 °C, diluted in 1X LDS/DTT to approximately the same concentration as the maize-derived protein, and loaded into the gel. Electrophoresis was conducted using a pre-cast gel electrophoresis system with MES running buffer and NuPAGE Antioxidant at a constant 200 volts (V) for 35 minutes.

Upon completion of electrophoresis, the gels were removed from the gel cassettes and used for Coomassie staining, western blot analysis, protein glycosylation analysis, or sample preparation for N-terminal amino acid sequencing and peptide mapping.

For Coomassie staining, the gel was washed with water three times for 5 minutes each and stained with GelCode Blue Stain Reagent for 60 minutes. Following staining, the gel was de-stained with water four times for at least 5 minutes each until the gel background was clear. Proteins were stained as blue-colored bands on the gel. The gel image was captured electronically using a ChemiDoc MP (Bio-Rad) imaging system.

Western Blot Analysis

Following SDS-PAGE, the resulting gel was assembled into a nitrocellulose (NC) iBlot Gel Transfer Stack. An iBlot Gel Transfer Device was used to transfer proteins from the gel to the NC membrane for 7 minutes with a pre-set program (P3).

Following protein transfer, the membrane was blocked in PBST containing 5% weight/volume (w/v) non-fat dry milk for 60 minutes at ambient laboratory temperature. Before and after the blocking step, the membrane was washed with PBST three times for 1 minute each to reduce the background. The blocked membrane was incubated for 60 minutes at ambient laboratory temperature with a PAT monoclonal antibody 22H2.G4 (Pioneer Hi-Bred International, Inc.) diluted 1:5000 in PBST containing 1% w/v non-fat dry milk. Following primary antibody incubation, the membrane was washed four times in PBST for 5 minutes each. The membrane was incubated for 60 minutes at ambient laboratory temperature with a secondary antibody (anti-mouse IgG, horseradish peroxidase conjugate; Promega Corporation) diluted 1:10,000 in PBST containing 1% w/v non-fat dry milk. The membrane was washed four times with PBST for at least 5 minutes each. The blot remained in PBST prior to incubating with a chemiluminescent substrate for 5 minutes. The chemiluminescent signal and the pre-stained markers were detected and captured using a ChemiDoc MP imaging system.

Peptide Mapping by Mass Spectrometry

Following SDS-PAGE, Coomassie staining, and gel imaging using the methods as described in Methods Section B, two PAT protein bands were excised from a gel and stored frozen at ≤ -5 °C. The protein in each gel slice was reduced with DTT, alkylated with iodoacetamide, and then subsequently digested with trypsin or chymotrypsin. The digested samples were separated on an ACQUITY UPLC (Waters Corporation) fitted with a Cortecs UPLC C18 1.6 µm column (2.1 x 100 mm; Waters Corporation) by gradient elution. Eluent from the column was directed into an electrospray source, operating in positive ion mode, on a TripleTOF 5600+ hybrid quadrupole-

TOF mass spectrometer (AB Sciex; currently Sciex). The resulting MS data were processed using MS Data Converter (Beta 1.3) to produce a peak list. The peak list was used to perform an MS/MS ion search (Mascot Software version 2.7.0) and match peptides from the expected PAT protein sequence (Perkins *et al.*, 1999). The following search parameters were used: peptide and fragment mass tolerance, ± 0.1 Da; fixed modifications, cysteine carbamidomethyl; variable modifications, methionine oxidation; and maximum missed cleavages, 1 for trypsin and 2 for chymotrypsin. The Mascot-generated peptide ion score threshold was > 13 which indicates identity or extensive homology ($p < 0.05$). The combined sequence coverage was calculated with GPMAW version 12.11.0.

N-Terminal Amino Acid Sequencing Analysis

Following SDS-PAGE as described in Methods Section B, the resulting gel was incubated in cathode buffer (60 mM Tris, 40 mM CAPS, 0.075% SDS, pH 9.6) for 10-20 minutes. An Immobilon-P^{SQ} PVDF membrane was wetted in 100% methanol for 1 minute, followed by immersion in anode buffer (60 mM Tris, 40 mM CAPS, 15% methanol, pH 9.6) for 10-20 minutes. A Trans-Blot SD Semi-Dry Electrophoretic Transfer Cell system was used to transfer proteins from the gel to the membrane at 12 V for 45 minutes. Following protein transfer, the membrane was stained with GelCode Blue stain reagent for 5 minutes, and then destained with water to visualize the PAT protein. A band containing the maize-derived PAT protein was excised and stored frozen at ≤ -5 °C. The band was analyzed using a Shimadzu PPSQ-51A sequencer. Ten cycles of Edman sequencing were performed. During each cycle, the N-terminal amino acid was sequentially derivatized with phenylisothiocyanate (PITC), cleaved with trifluoracetic acid, and converted to PTH-amino acid which was identified through chromatography. LabSolutions Software was used to automatically identify the N-terminal sequence.

Glycoprotein Analysis

The Pierce Glycoprotein Staining Kit was used to determine whether the maize-derived PAT protein was glycosylated. The purified maize-derived PAT protein, a positive control protein (horseradish peroxidase), and a negative control protein (soybean trypsin inhibitor) were run by SDS-PAGE as described above.

Following electrophoresis, the gel was washed with water twice for 5 minutes each wash, fixed with 50% methanol for 30-35 minutes, and washed twice with 3% acetic acid for 10-15 minutes each wash. The gel was then incubated with oxidizing solution for 15-20 minutes and washed three times with 3% acetic acid for 5-7 minutes each wash. The gel was incubated with glycoprotein staining reagent for 15-20 minutes and then incubated in a reducing reagent for 5-7 minutes. The gel was then washed twice with 3% acetic acid for 5 minutes each and then rinsed in water once for 5 minutes. Glycoproteins were detected as bands stained a magenta color on the gel.

Following glycoprotein detection, the image of the gel was captured electronically using a ChemiDoc MP imaging system. The same gel was then stained with GelCode Blue stain reagent for 60 minutes followed by two washes with water for 5 minutes each to visualize all protein bands. The image of the GelCode-stained gel was then captured electronically.

APPENDIX G. METHODS FOR CHARACTERIZATION OF PMI PROTEIN

Test Materials

The reference substance consisted of lyophilized PMI protein derived from a microbial expression system (lot number PCF-0055). A 5.0-mg sample of the lyophilized protein was solubilized in 3.4 ml of 1X LDS/DTT sample buffer to a nominal concentration of 1 mg PMI protein/ml and heated at 90-100 °C for five minutes prior to SDS-PAGE analysis.

PMI protein was isolated from DP910521 maize leaf tissue. The tissue samples were collected at the R1 growth stage (the stage when silks become visible; Abendroth *et al.*, 2011) from plants grown at a field location in Johnston, IA, USA. The tissue was lyophilized, homogenized and stored at ≤ -50 °C.

The PMI protein was extracted from lyophilized maize tissue by homogenization in a pre-chilled Waring blender vessel using phosphate-buffered saline containing polysorbate 20 (PBST) extraction buffer with protease inhibitor. The sample extract was then filtered through cheesecloth, clarified by centrifugation, and fractionated using ammonium sulfate (AS) precipitation. Beginning at 0% AS saturation and using an online calculator by EnCor Biotechnology Inc (EnCor Biotechnology, 2020), AS was slowly added to the sample extract while stirring until 45% AS saturation was reached. The sample was centrifuged and the AS process was repeated with the supernatant, this time beginning at 45% AS saturation and progressing to 60%. The sample was centrifuged again, the supernatant was discarded, and the fractionated pellets were solubilized and buffer-exchanged in phosphate-buffered saline using Econo-Pac 10DG desalting columns (BioRad).

Following buffer exchange, the sample was further purified by immunoaffinity chromatography. The immunoaffinity columns were prepared by coupling a PMI polyclonal antibody (R164; Pioneer) to AminoLink Plus Coupling Resin. The PMI protein sample was eluted off the column using IgG Elution buffer. Elutions 2-5 from the immunoaffinity purification column were collected separately. The elutions were then concentrated using a centrifugal concentrator (30K Vivaspin Turbo 4; Sartorius) to a volume of 2 ml.

The PMI protein was further purified by ion exchange purification using a GE Q HP ion exchange resin column. The concentrated sample from the immunoaffinity purification was removed from the concentrator, diluted in 6 ml of 50 mM Tris, pH 8, buffer and then added to the column containing the Q ion exchange resin. The protein was eluted off the resin with 50 mM Tris, pH 8, and 250 mM NaCl buffer, and concentrated using a centrifugal concentrator (30K Vivaspin Turbo 4) and buffer exchanged with 50 mM Tris buffer, pH 7.5, to a volume of approximately 100 µl.

Following extraction, purification, and concentration, the final volume in the concentrator was estimated and an equal volume of 2X LDS/DTT sample buffer (50% 4X NuPAGE LDS Sample Buffer, 20% 10X NuPAGE Sample Reducing Agent containing DTT, and 30% ASTM [American Society for Testing and Materials] Type I water [referred to as water]) was added to the concentrated sample. The sample was transferred to a microcentrifuge tube, heat-treated at 90-100 °C for 5 (±1) minutes, and stored frozen (-20 °C freezer unit).

SDS-PAGE Analysis

The partially purified maize-derived PMI protein sample in LDS/DTT sample buffer from freezer storage was re-heated for 5 minutes at 90-100 °C, diluted as applicable, and then loaded into 4-12% Bis-Tris gels. Pre-stained protein molecular weight markers (Precision Plus Protein Dual Xtra Standards) were loaded into each gel to provide a visual verification that migration was within the expected range of the predicted molecular weight. For SDS-PAGE and western blot analysis, the PMI protein reference substance was diluted in 1X LDS/DTT to approximately the same concentration as the maize-derived protein, re-heated for 5 minutes at 90-100 °C, and loaded into the gel. Electrophoresis was conducted using a pre-cast gel electrophoresis system with MES running buffer at a constant 200 volts (V) for 35 minutes.

Upon completion of electrophoresis, the gels were removed from the gel cassettes and used for Coomassie staining, western blot analysis, protein glycosylation analysis, or sample preparation for peptide mapping.

For Coomassie staining, the gel was washed with water three times for 5 minutes each wash and stained with GelCode Blue Stain Reagent for 60-62 minutes. Following staining, the gel was de-stained with water four times for at least 5 minutes each until the gel background was clear. Proteins were stained as blue-colored bands on the gel. The gel image was captured electronically using a ChemiDoc MP (Bio-Rad) imaging system.

Western Blot Analysis

Following SDS-PAGE, the resulting gel was assembled into a nitrocellulose (NC) iBlot Gel Transfer Stack. An iBlot Gel Transfer Device was used to transfer proteins from the gel to the NC membrane for 7 minutes with a pre-set program (P3).

Following protein transfer, the membrane was blocked in PBST containing 5% weight/volume (w/v) non-fat dry milk for 35 minutes at ambient laboratory temperature. Before and after the blocking step, the membrane was washed with PBST three times for at least 1 minute each wash to reduce the background. The blocked membrane was incubated with a PMI monoclonal antibody (13D11.F11.C12; Pioneer) conjugated to horseradish peroxidase diluted 1:10,000 in PBST containing 1% w/v non-fat dry milk for 67 minutes at ambient laboratory temperature. The membrane was washed with PBST four times for at least 5 minutes each wash. The membrane remained in PBST prior to incubating with a chemiluminescent substrate for 5 minutes. The chemiluminescent signal and the pre-stained markers were detected and captured using a ChemiDoc MP imaging system.

Peptide Mapping and N-Terminal Peptide Identification by Liquid Chromatography-Mass Spectrometry (LC-MS) Analysis

Following SDS-PAGE, Coomassie staining, and gel imaging using the methods as described in Methods Section B, the PMI protein band was excised from a gel and stored frozen at ≤ -5 °C. The protein in each gel slice was reduced with DTT, alkylated with iodoacetamide, and then subsequently digested with trypsin or chymotrypsin. The digested samples were separated on a nanoACQUITY UPLC (Waters Corporation) fitted with a Peptide BEH C18 300 Å 1.7 µm column (75 µm x 100 mm; Waters Corporation) by gradient elution. Eluent from the column was directed

into an electrospray source, operating in positive ion mode, on a TripleTOF 5600+ hybrid quadrupole-TOF mass spectrometer (AB Sciex; currently Sciex). The resulting mass spectrometry (MS) data were processed using MS Data Converter (Beta 1.3) to produce a peak list. The peak list was used to perform an MS/MS ion search (Mascot Software version 2.7.0) and match peptides from the expected PMI protein sequence (Perkins et al., 1999). The following search parameters were used: peptide and fragment mass tolerance, ± 0.1 Da; fixed modifications, cysteine carbamidomethyl; variable modifications, methionine oxidation; and maximum missed cleavages, 1 for trypsin and 2 for chymotrypsin. The Mascot-generated peptide ion score threshold was > 13 which indicates identity or extensive homology ($P < 0.05$). The combined sequence coverage was calculated with GPMAW version 12.11.0.

Protein Glycoprotein Analysis

The Pierce Glycoprotein Staining Kit was used to determine whether the maize-derived PMI protein was glycosylated. The partially purified maize-derived PMI protein, a positive control protein (horseradish peroxidase), and a negative control protein (soybean trypsin inhibitor), were run by SDS-PAGE as described as described above in the SDS-PAGE Analysis section.

Following electrophoresis, the gel was washed with water twice for at least 5 minutes each wash, fixed with 50% methanol for 30-35 minutes, and washed twice with 3% acetic acid for 10-15 minutes each wash. The gel was then incubated with oxidizing solution for 15-20 minutes and washed with 3% acetic acid three times for 5-7 minutes each wash. The gel was incubated with glycoprotein staining reagent for 15-20 minutes and then incubated in a reducing reagent for 5-7 minutes. The gel was then washed with 3% acetic acid for 5 minutes and then washed in water for 5 minutes. Glycoproteins were detected as bands stained a magenta color on the gel.

Following glycoprotein detection, the image of the gel was captured electronically using a ChemiDoc MP imaging system. The same gel was then stained with GelCode Blue stain reagent for 61 minutes followed by three washes with water for at least 5 minutes each wash to visualize all protein bands. The image of the GelCode-stained gel was then captured electronically.

APPENDIX H. METHODS FOR TRAIT EXPRESSION ANALYSES

Field Trial Experimental Design

A multi-site field trial was conducted during the 2020 growing season at six sites in commercial maize-growing regions of the United States (one site in Iowa, Illinois, Nebraska, Pennsylvania, and Texas) and Canada (one site in Ontario). A randomized complete block design with four blocks was utilized at each site. Procedures employed during the field trial to control the introduction of experimental bias included randomization of maize entries within each block and uniform maintenance treatments across each plot area. A herbicide treatment of glufosinate-ammonium was applied to DP910521.

Sample Collection

The following tissue samples were collected: Leaf (V6, V9, R1, and R4 growth stages), root (V9, R1, and R4 growth stages), pollen (R1 growth stage), stalk (R1 growth stage), forage (R4 growth stage), and grain (R6 growth stage). Growth stages are described in Table H.1. One sample per plot was collected for each tissue set. All samples were collected from impartially selected, healthy, representative plants to minimize potential bias.

Table H.1. Maize Growth Stage Descriptions

Growth Stage	Description
VE	The stage when the plant first emerges from the soil.
V1	The stage when the collar of the first leaf becomes visible.
V2	The stage when the collar of the second leaf becomes visible.
V3	The stage when the collar of the third leaf becomes visible.
V4	The stage when the collar of the fourth leaf becomes visible.
V5	The stage when the collar of the fifth leaf becomes visible.
V6	The stage when the collar of the sixth leaf becomes visible.
V7	The stage when the collar of the seventh leaf becomes visible.
V8	The stage when the collar of the eighth leaf becomes visible.
V9	The stage when the collar of the ninth leaf becomes visible.
V10	The stage when the collar of the tenth leaf becomes visible.
VT	The stage when the last branch of tassel is completely visible.
R1	The stage when silks become visible.
R2	The stage when kernels are white on the outside and resemble a blister in shape.
R3	The stage when kernels are yellow on the outside and the inner fluid is milky white.
R4	The stage when the material within the kernel produces a doughy consistency.
R5	The stage when all or nearly all the kernels are dented or denting.
R6	Typical grain harvest would occur. This stage is regarded as physiological maturity.

Note: Growth stages (Abendroth *et al.*, 2011).

Samples were collected as follows:

- Each root sample was obtained by cutting a circle 10-15 in. (25-38 cm) in diameter around the base of the plant to a depth of 7-9 in. (18-23 cm). The roots were thoroughly cleaned

with water and removed from the plant. No above ground brace roots were included in the sample. The root tissue was cut into sections of 3-4 in. (8-10 cm) or less in length and 1 cup (approximately 250 ml) of the root sections was collected into a pre-labeled, residue bag. At some sites, root tissue from more than one maize plant was pooled to achieve the sample volume.

- Each V6 growth stage leaf sample was obtained by pruning the youngest two leaves that have emerged at least 8 in. (20 cm) in length from the plant. Each V9, R1, and R4 growth stage sample was obtained by pruning the youngest leaf that has emerged at least 8 in. (20 cm) in length. The tissue was cut into sections of 1 in. (2.5 cm) or less in length and collected into a pre-labeled vial.
- Each pollen sample was obtained by bagging and shaking a selected tassel to dislodge the pollen. The tassel selected for sampling had one-half to three-quarters of the tassel's main spike shedding pollen. For some plots, pollen may have been pooled from multiple plants within the same plot in order to collect the appropriate amount. The pollen was screened for anthers and foreign material, and then collected to fill approximately 25-50% of the conical area of a pre-labeled vial.
- Each stalk sample was obtained by pruning a section of stalk, directly above the primary ear node. The leaf sheath tissue was removed, and the stalk section was cut in half length-wise. The half-sections were halved again, chopped into sections of 3-4 in. (8-10 cm) or less in length and collected into a pre-labeled, plastic-lined, cloth bag.
- Each forage sample was obtained by cutting the plants approximately 4-6 in. (10-15 cm) above the soil surface. Samples were composed of all above-ground plant parts, including the stalk, leaves, self-pollinated ear (husks, grain, and cob), and tassel. Leaves were cut into sections that were 12 in. (30 cm) or less in length and all other plant parts were cut into sections that were 3 in. (7.6 cm) or less in length. After tissues were cut to the appropriate lengths, samples were placed in pre-labelled, plastic-lined cloth bags. Samples were collected at the R4 growth stage and included all above-ground plant parts in order to produce samples that are representative of maize forage (whole aerial plant including grain harvested at high moisture content) that is fed to animals as silage.
- Each grain sample was obtained by husking and shelling the grain from one selected ear. Each ear selected for sampling was a primary ear that had previously been self-pollinated. For each sample, a representative sub-sample of 50 ml was collected into an individual pre-labeled vial. At some sites, ears from more than one maize plant were pooled to achieve the sample volume.

Sample Processing, Shipping, and Storage

Each sample was uniquely labeled with a sample identification number and barcode for sample tracking by site, entry, block, tissue, and growth stage. Samples were placed on dry ice within 10 minutes of collection in the field and transferred to frozen storage (-20 °C freezer unit) until shipment. Samples were then shipped frozen to Pioneer Hi-Bred International, Inc. for processing and analysis. Upon arrival, samples were stored frozen (-20 °C freezer unit).

Forage samples were coarsely homogenized on dry ice prior to lyophilization. All samples were lyophilized under vacuum until dry. Following lyophilization, root and stalk tissues were sub-sampled to fill approximately ½ - ¾ of a pre-labeled 50-ml vial. The tissue was cut into small pieces less than 1 in. (2.5 cm) in length and the vial was placed onto dry ice once filled. All remaining root and stalk tissues were retained in the original vials/residue bags and stored frozen. Following lyophilization of the grain samples, 15 kernels from each grain sample were removed and placed in a corresponding vial and placed on dry ice. All remaining kernels were retained in the original 50-ml vial and moved back into frozen storage for retention. Following lyophilization, pollen samples were stored frozen (-20 °C freezer unit) until analysis and leaf, root, stalk, forage, and grain samples were finely homogenized and stored frozen (-20 °C freezer unit) until analysis.

Protein Concentration Determination

The concentrations of Cry1B.34, PAT, and PMI proteins were determined using quantitative enzyme-linked immunosorbent assay (ELISA) methods that have been internally validated to demonstrate method suitability.

Processed tissue sub-samples were weighed at the following target weights: 5 mg for pollen; 10 mg for leaf; 20 mg for grain and root; and 30 mg for stalk and forage. Samples were extracted with 0.60 ml of chilled phosphate-buffered saline containing polysorbate 20 (PBST). All extracted samples were centrifuged, and then supernatants were removed and prepared for analysis. Experimental bias was controlled through the use of replicate testing, appropriate assay controls, and pre-determined data acceptability criteria.

ELISA Methods

ELISA methods were performed as follows:

- *Cry1B.34 Protein ELISA Method*: Prior to analysis, samples were diluted as applicable in PBST. Standards (typically analyzed in triplicate wells) and diluted samples (typically analyzed in duplicate wells) were incubated in a plate pre-coated with a Cry1B.34-specific antibody. Following incubation, unbound substances were washed from the plate. A different Cry1B.34-specific antibody, conjugated to the enzyme horseradish peroxidase (HRP), was added to the plate and incubated. Unbound substances were washed from the plate. Detection of the bound Cry1B.34-antibody complex was accomplished by the addition of substrate, which generated a colored product in the presence of HRP. The reaction was stopped with an acid solution and the optical density (OD) of each well was determined using a plate reader.
- *PAT Protein ELISA Method*: Prior to analysis, samples were diluted as applicable in PBST. Standards (typically analyzed in triplicate wells) and diluted samples (typically analyzed in duplicate wells) were co-incubated with a PAT-specific antibody conjugated to the enzyme HRP in a plate pre-coated with a different PAT-specific antibody. Following incubation, unbound substances were washed from the plate. Detection of the bound PAT-antibody complex was accomplished by the addition of substrate, which generated a colored product in the presence of HRP. The reaction was stopped with an acid solution and the OD of each well was determined using a plate reader.

- *PMI ELISA Method*: Prior to analysis, samples were diluted as applicable in PBST. Standards (typically analyzed in triplicate wells) and diluted samples (typically analyzed in duplicate wells) were incubated in a plate pre-coated with a PMI-specific antibody. Following incubation, unbound substances were washed from the plate and the bound PMI protein was incubated with a different PMI-specific antibody conjugated to the enzyme HRP. Unbound substances were washed from the plate. Detection of the bound PMI-antibody complex was accomplished by the addition of substrate, which generated a colored product in the presence of HRP. The reaction was stopped with an acid solution and the OD of each well was determined using a plate reader.

Calculations for Determining Cry1B.34, PAT, and PMI Protein Concentrations

SoftMax Pro GxP (Molecular Devices) microplate data software was used to perform the calculations required to convert the OD values obtained for each set of sample wells to a protein concentration value.

A standard curve was included on each ELISA plate. The equation for the standard curve was derived by the software, which used a quadratic fit to relate the OD values obtained for each set of standard wells to the respective standard concentration (ng/ml).

The sample concentration values were adjusted for a dilution factor expressed as 1:N by multiplying the interpolated concentration by N.

Adjusted Concentration = Interpolated Sample Concentration x Dilution Factor

Adjusted sample concentration values obtained from SoftMax Pro GxP software were converted from ng/ml to ng/mg sample weight as follows:

$$\text{Sample Concentration (ng protein/mg sample weight)} = \text{Sample Concentration (ng/ml)} \times \frac{\text{Extraction Buffer Volume (ml)}}{\text{Sample Target Weight (mg)}}$$

The reportable assay lower limit of quantification (LLOQ) in ng/ml was calculated as follows:

Reportable Assay LLOQ (ng/ml) = (lowest standard concentration - 10%) x minimum dilution

The LLOQ, in ng/mg sample weight, was calculated as follows:

$$\text{LLOQ} = \text{Reportable Assay LLOQ (ng/ml)} \times \frac{\text{Extraction Buffer Volume (ml)}}{\text{Sample Target Weight (mg)}}$$

Statistical Analysis

Statistical analysis of the Cry1B.34, PAT, and PMI protein concentration results consisted of the calculations of means, ranges, and standard deviations. Individual sample results below the LLOQ were assigned a value equal to half of the LLOQ for calculation purposes.

APPENDIX I. METHODS FOR NUTRIENT COMPOSITION ANALYSIS

Field Trial Experimental Design

A multi-site field trial was conducted during the 2020 growing season at eight sites in commercial maize-growing regions of the United States (one site in Iowa, Nebraska, Pennsylvania, Texas, and Wisconsin, and two sites in Illinois) and Canada (one site in Ontario). Each site included DP910521 maize, control maize, and four of the following non-GM commercial maize lines: P0506, XL5513, P0574, PB5646, P0760, G07F23, 207-27, BK5883, P0843, BKXL-5858, 209-50, P0928, P0993, 6046, P1093, DKC60-84, G10T63, and BK6076 maize (collectively referred to as reference maize). A randomized complete block design with four blocks was utilized at each site. A herbicide treatment of glufosinate-ammonium was applied to DP910521 maize. Procedures employed during the field trial to control the introduction of experimental bias included randomization of maize entries within each block and uniform maintenance treatments across each plot area.

Sample Collection

One forage sample (R4 growth stage) and one grain sample (R6 growth stage) were collected from each plot. Each forage sample (combination of three plants) was obtained by cutting the aerial portion of the plants from the root system approximately 4-6 in. (10-15 cm) above the soil surface line; the plants were chopped into sections of 3 in. (7.6 cm) or less in length, pooled, and approximately one-third of the chopped material was collected in a pre-labeled, plastic-lined, cloth bag. Each grain sample was obtained from five ears at typical harvest maturity from self-pollinated plants; the ears were husked and shelled, and the pooled grain was collected into a large, plastic, resealable bag and then placed into a pre-labeled, plastic-lined, cloth bag.

All samples were collected from impartially selected, healthy, representative plants to minimize potential bias. Reference maize and control maize samples were collected prior to the collection of DP910521 maize samples to minimize the potential for contamination. Each sample was uniquely labeled with a sample identification number and barcode for sample tracking, and is traceable by site, entry, block, tissue, and growth stage. Samples were placed into chilled storage (e.g., coolers with wet ice, artificial ice, or dry ice) after collection and, within three hours of collection, transferred to a freezer (≤ -10 °C) or placed on dry ice. Samples were shipped frozen from each site to [redacted] for nutrient composition analyses.

Nutrient Composition Analyses

The forage and grain samples were analyzed at [redacted] Experimental bias was controlled through the use of the same sample identification numbers assigned to the originally collected samples, the use of pre-set data acceptability criteria, sample randomization prior to homogenization, and through the arrangement of samples for analyses without consideration of sample identity. The following nutrient composition analytes were determined:

- *Forage proximate, fiber, and mineral composition*: moisture*, crude protein, crude fat, crude fiber, acid detergent fiber (ADF), neutral detergent fiber (NDF), ash, carbohydrates, calcium, and phosphorus
    - *moisture data were used to convert corresponding analyte values for a given sample to a dry weight basis, and were not included in subsequent statistical analysis and reporting of results.
- *Grain proximate and fiber composition*: moisture, crude protein, crude fat, total dietary fiber (TDF), crude fiber, acid detergent fiber (ADF), neutral detergent fiber (NDF), ash, and carbohydrates
- *Grain fatty acid composition*: lauric acid (C12:0), myristic acid (C14:0), palmitic acid (C16:0), palmitoleic acid (C16:1), heptadecanoic acid (C17:0), heptadecenoic acid (C17:1), stearic acid (C18:0), oleic acid (C18:1), linoleic acid (C18:2), α-linolenic acid (C18:3), arachidic acid (C20:0), eicosenoic acid (C20:1), eicosadienoic acid (C20:2), behenic acid (C22:0), and lignoceric acid (C24:0)
- *Grain amino acid composition*: alanine, arginine, aspartic acid, cysteine, glutamic acid, glycine, histidine, isoleucine, leucine, lysine, methionine, phenylalanine, proline, serine, threonine, tryptophan, tyrosine, and valine
- *Grain mineral composition*: calcium, copper, iron, magnesium, manganese, phosphorus, potassium, sodium, and zinc
- *Grain vitamin composition*: β-carotene, vitamin B1 (thiamine), vitamin B2 (riboflavin), vitamin B3 (niacin), vitamin B5 (pantothenic acid), vitamin B6 (pyridoxine), vitamin B9 (folic acid), α-tocopherol, β-tocopherol, γ-tocopherol, and δ-tocopherol
    - Note: an additional analyte (total tocopherols) was subsequently calculated as the sum of the α-, β-, γ-, and δ-tocopherol values for each sample for use in statistical analysis and reporting of results
- *Grain secondary metabolite and anti-nutrient composition*: *p*-coumaric acid, ferulic acid, furfural, inositol, phytic acid, raffinose, and trypsin inhibitor

Nutrient composition analytical methods and procedures are summarized in Table I.1.

Table I.1. Methods for Compositional Analysis

Nutritional Analyte	Method
Moisture	The analytical procedure for moisture determination was based on a method published by AOAC International. Samples were assayed to determine the percentage of moisture by gravimetric measurement of weight loss after drying in a forced air oven (forage) and a vacuum oven (grain).
Ash	The analytical procedure for ash determination was based on a method published by AOAC International. Samples were analyzed to determine the percentage of ash by gravimetric measurement of the weight loss after ignition in a muffle furnace.
Crude Protein	The analytical procedure for crude protein determination utilized an automated Kjeldahl technique based on a method provided by the manufacturer of the titrator unit (Foss-Tecator) and AOAC International. Ground samples were digested in the presence of a catalyst. The digestate was then distilled and titrated with a Foss-Tecator Kjeltec Analyzer unit.
Crude Fat	The analytical procedure for crude fat determination was based on methods provided by the American Oil Chemists' Society (AOCS) and the manufacturer of the hydrolysis and extraction apparatus (Ankom Technology). Samples were hydrolyzed with 3N hydrochloric acid at 90 °C for 80 minutes for forage and 60 minutes for grain. The hydrolysates were extracted with a petroleum ether/ethyl ether/ethyl alcohol solution at 90 °C for 60 minutes. The ether extracts were evaporated and the fat residue remaining determined gravimetrically.
Carbohydrates	The carbohydrate content in maize forage and grain on a dry weight basis was calculated using a formula obtained from the United States Department of Agriculture "*Energy Value of Foods,*" in which the percent dry weight of crude protein, crude fat, and ash was subtracted from 100%.
Crude Fiber	The analytical procedure for crude fiber determination was based on methods provided by the manufacturer of the extraction apparatus (Ankom Technology), AOAC International, and the AOCS. Samples were analyzed to determine the percentage of crude fiber by digestion and solubilization of other materials present.
Neutral Detergent Fiber	The analytical procedure for neutral detergent fiber (NDF) determination was based on a method provided by the manufacturer of the extraction apparatus (Ankom Technology), AOAC International, and the *Journal of AOAC International*. Samples were analyzed to determine the percentage of NDF by digesting with a neutral detergent solution, sodium sulfite, and alpha amylase. The remaining residue was dried and weighed to determine the NDF content.
Acid Detergent Fiber	The analytical procedure for acid detergent fiber (ADF) determination was based on a method provided by the manufacturer of the extraction apparatus (Ankom Technology) and AOAC International. Samples were analyzed to determine the percentage of ADF by digesting with an acid detergent solution and washing with reverse osmosis water. The remaining residue was dried and weighed to determine the ADF content.

Table I.1. Methods for Compositional Analysis (continued)

Nutritional Analyte	Method
Total Dietary Fiber	The analytical procedure for the determination of total dietary fiber in grain was based on methods provided by the manufacturer of the extraction apparatus (Ankom Technology), AOAC International, and the manufacturer of the protein titrator unit (Foss-Tecator). Duplicate samples were gelatinized with heat stable α-amylase, enzymatically digested with protease and amyloglucosidase to remove protein and starch, respectively, and then soluble dietary fiber precipitated with ethanol. The precipitate (residue) was quantified gravimetrically. Protein analysis was performed on one of the duplicate samples while the other duplicate sample was analyzed for ash. The weight of the protein and ash was subtracted from the weight of the residue divided by sample dry weight.
Minerals	The analytical procedure for the determination of minerals is based on methods published by AOAC International and CEM Corporation. The maize forage minerals determined were calcium and phosphorus. Additional grain minerals determined were copper, iron, magnesium, manganese, potassium, sodium, and zinc. The samples were digested in a microwave based digestion system and the digestate was diluted using deionized water. Samples were analyzed by inductively coupled plasma optical emission spectroscopy (ICP-OES).
Tryptophan	The analytical procedure for tryptophan determination was based on an established lithium hydroxide hydrolysis procedure with reverse phase ultra performance liquid chromatography (UPLC) with ultraviolet (UV) detection published by the *Journal of Micronutrient Analysis*.
Cystine and Methionine	The analytical procedure for cystine and methionine determination was based on methods obtained from Waters Corporation, AOAC International, and *Journal of Chromatography A*. The procedure converts cystine to cysteic acid and methionine to methionine sulfone, after acid oxidation and hydrolysis, to the 6-aminoquinolyl-N-hydroxysuccinimidyl carbamate derivatives which are then analyzed by reverse phase UPLC with UV detection.
Additional Amino Acids	Along with tryptophan, cystine, and methionine, 15 additional amino acids were determined. The analytical procedure for analysis of these amino acids was based on methods obtained from Waters Corporation and the *Journal of Chromatography A*. The procedure converts the free acids, after acid hydrolysis, to the 6-aminoquinolyl-N-hydroxysuccinimidyl carbamate derivatives, which are analyzed by reverse phase UPLC with UV detection.
Fatty Acids	The analytical procedure for determination of fatty acids was based on methods published by AOAC International and AOCS. The procedure converts the free acids, after ether extraction and base hydrolysis, to the fatty acid methyl ester (FAME) derivatives, which are analyzed by gas chromatography with flame ionization detection (GC/FID). Results are reported as percent total fatty acids but presented in the raw data as percent fresh weight.
Thiamine (Vitamin B1) and Riboflavin (Vitamin B2)	The analytical procedure for the determination of thiamine (vitamin B1) and riboflavin (vitamin B2) was based on a method published by the American Association of Cereal Chemists (AACC). The samples were extracted with 10% acetic acid/4.3% trichloroacetic acid solution. A 50-fold dilution was performed and then the samples were analyzed by reverse phase high pressure liquid chromatography (HPLC) tandem mass spectrometry (MS/MS).

Table I.1. Methods for Compositional Analysis (continued)

Nutritional Analyte	Method
Niacin (Vitamin B3)	The analytical procedure for the determination of niacin (vitamin B3) was based on a method published by the AACC. Niacin (vitamin B3) was extracted from the sample by adding deionized (DI) water and autoclaving. A tube array was prepared using three different dilutions of the samples. This tube array was inoculated with *Lactobacillus plantarum* and allowed to incubate for approximately 18 to 22 hours. After incubation, the bacterial growth was determined using a spectrophotometer at an absorbance of 660 nm. The absorbance readings were compared to a standard curve generated using known concentrations of nicotinic acid.
Pantothenic Acid (Vitamin B5)	The analytical procedure for the determination of pantothenic acid (vitamin B5) was based on a method from AOAC International. Pantothenic acid (vitamin B5) was determined using a microbiological assay. Pantothenic acid (vitamin B5) was extracted from the sample by adding an acetic acid buffer solution and autoclaving. The pH was adjusted and a tube array was prepared using three different dilutions of the samples. This tube array was inoculated with *Lactobacillus plantarum* and allowed to incubate for approximately 18-22 hours. After incubation, the microbial growth was determined using a spectrophotometer at an absorbance of 660 nm. The absorbance readings were compared to a standard curve generated using known concentrations of D-pantothenic acid hemicalcium salt.
Pyridoxine (Vitamin B6)	The analytical procedure for the determination of pyridoxine (vitamin B6) was based on a method from the AACC. Pyridoxine (vitamin B6) was determined using a microbiological assay. Pyridoxine (vitamin B6) was extracted from the sample by adding sulfuric acid and autoclaving. The pH was adjusted and a tube array was prepared using four different dilutions of the samples. This tube array was inoculated with *Saccharomyces cerevisiae* and allowed to incubate for approximately 18-22 hours. After incubation, the microbial growth was determined using a spectrophotometer at an absorbance of 600 nm. The absorbance readings were compared to a standard curve generated using known concentrations of pyridoxine hydrochloride.
Total Folate as Folic Acid (Vitamin B9)	The analytical procedure for determination of total folate as folic acid was based on a microbiological assay published by the AACC. Samples were hydrolyzed and digested by protease and amylase enzymes to release the folate from the grain. A conjugase enzyme was used to convert the naturally occurring folypolyglutamates. An aliquot of the extracted folates was mixed with a folate and folic acid free microbiological growth medium. The mixture was inoculated with *Lactobacillus casei*. The total folate content was determined by measuring the turbidity of the *Lactobacillus casei* growth response in the sample and comparing it to the turbidity of the growth response with folic acid standards using a spectrophotometer at 600 nm.
Total Tocopherols	The analytical procedure for determination of tocopherols was based on methods from the *Journal of the American Oil Chemists' Society* and *Analytical Sciences*. Alpha-, beta-, gamma-, and delta-tocopherols were extracted with hot hexane and the extracts were analyzed by normal phase UPLC with fluorescence detection.

Table I.1. Methods for Compositional Analysis (continued)

Nutritional Analyte	Method
β-Carotene	The analytical procedure for determination of beta-carotene was based on a method published by AOAC International. Samples were extracted using a 40:60 acetone:hexane with tert-butylhydroquinone (TBHQ) solution then analyzed by HPLC-UV.
Trypsin Inhibitor	The analytical procedure for the determination of trypsin inhibitor was based on a method published by the AOCS. Trypsin inhibitor was extracted with sodium hydroxide. Trypsin was added to the extracts to react with trypsin inhibitor. The residual trypsin activity was measured with a spectrophotometer using the chromogenic trypsin substrate Benzoyl-DL-arginine-p-nitroanilide hydrochloride (BAPNA). The amount of trypsin inhibitor was calculated based on the inhibition of trypsin activity.
Inositol and Raffinose	The analytical procedure for the determination of inositol and raffinose was based on a gas chromatography (GC) method published in the *Handbook of Analytical Derivatization Reactions*, an AACC method, and a method from the *Journal of Agricultural and Food Chemistry*. Extracted inositol and raffinose were analyzed by reverse phase HPLC with refractive index detection.
Furfural	The analytical procedure for the determination of furfural was based on methods published in the *Journal of Agricultural and Food Chemistry*. Ground maize grain was analyzed for furfural content by reverse phase HPLC with UV detection.
p-Coumaric and Ferulic Acid	The analytical procedure for the determination of *p*-coumaric and ferulic acids was developed based on methods published in *Journal of Agricultural and Food Chemistry* and *The Journal of Chemical Ecology*. Ground maize grain was analyzed to determine the amounts of *p*-coumaric acid and ferulic acid by separating the total content of phenolic acids using reverse phase HPLC and UV detection.
Phytic Acid	The analytical procedure for the determination of phytic acid was based on a method published by AOAC International. The samples were analyzed to determine the amount of phytic acid by extracting the phytic acid with dilute hydrochloric acid (HCl) and isolating it using an aminopropyl silica solid phase extraction column. Once isolated and eluted, the phytic acid was analyzed for elemental phosphorus by ICP-OES.

Statistical Analysis of Nutrient Composition Data

Prior to statistical analysis, the data were processed as follows:

- *LLOQ Sample Values*: For statistical analysis, nutrient composition values reported as below the assay lower limit of quantification (LLOQ) were each assigned a value equal to half the LLOQ

  Conversion of fatty acid assay values: The raw data for all fatty acid analytes were provided by [redacted] in units of percent fresh weight (%FW). Any fatty acid values below the %FW LLOQ were set to half the LLOQ value, and then all assay values were converted to units of % total fatty acids for statistical analyses.
  For a given sample, the conversion to units of % total fatty acids was performed by

dividing each fatty acid analyte value (%FW) by the total fresh weight of all fatty acids for that sample; for analyte values below the LLOQ, the half LLOQ value was used as the analyte value. Half LLOQ values were also included in the total fresh weight summations. After the conversion, a fixed LLOQ value was not available for a given individual fatty acid analyte on the % total fatty acids basis.

Calculation of additional analytes: One additional analyte (total tocopherol) was calculated for statistical analyses. The total amount of tocopherol for each sample was obtained by summing the assay values of α-tocopherol, β-tocopherol, γ-tocopherol, and δ-tocopherol in the sample.

If the assay value of an individual analyte was below the LLOQ for a given sample, half of the LLOQ value was used in computing the total. The total was considered below the LLOQ only when all the individual analytes contributing to its calculation were below the LLOQ.

Statistical analyses were conducted using SAS software, Version 9.4 (SAS Institute, Inc.). The following rules were implemented for each analyte:

- If both DP910521 maize and the control maize had < 50% of samples below the LLOQ, then an across-site mixed model analysis was conducted.
- If, either DP910521 maize or the control maize had ≥ 50% samples below the LLOQ, but not both entries had 100% of samples below the LLOQ across sites, then Fisher's exact test was conducted. The Fisher's exact test assessed whether there was a significant difference (P-value < 0.05) in the proportion of samples below the LLOQ between these two maize lines across sites.
- If, both DP910521 maize and the control maize had 100% of samples below the LLOQ, then statistical analyses was not performed (Table I.2).

Statistical Model for Across-Site Analysis

For a given analyte, data were analyzed using the following linear mixed model:

$$y_{ijk} = \mu_i + \ell_j + r_{k(j)} + (\mu\ell)_{ij} + \varepsilon_{ijk} \qquad \text{Model 1}$$

$\ell_j \sim iid\ N(0, \sigma^2_{Site})$, $r_{k(j)} \sim iid\ N(0, \sigma^2_{Rep})$, $(\mu\ell)_{ij} \sim iid\ N(0, \sigma^2_{Ent\times Site})$, and $\varepsilon_{ijk} \sim iid\ N(0, \sigma^2_{Error})$

where μ_i denotes the mean of the i^{th} entry (fixed effect), ℓ_j denotes the effect of the j^{th} site (random effect), $r_{k(j)}$ denotes the effect of the k^{th} block within the j^{th} site (random effect), $(\mu\ell)_{ij}$ denotes the interaction between the entries and sites (random effect), and ε_{ijk} denotes the effect of the plot assigned the i^{th} entry in the k^{th} block of the j^{th} site (random effect or residual). Notation $\sim iid\ N(0, \sigma^2_a)$ indicates random variables that are identically independently distributed (*iid*) as normal with zero mean and variance σ^2_a. Subscript a represents the corresponding source of variation.

The residual maximum likelihood estimation procedure was utilized to generate estimates of variance components and entry means across sites. The estimated means are known as empirical best linear unbiased estimators (hereafter referred to as LS-Means). The

statistical comparison was conducted by testing for a difference in LS-Means between DP910521 maize and the control maize. The approximated degrees of freedom for the statistical test were derived using the Kenward-Roger method (Kenward and Roger, 2009). A significant difference was identified if a P-value was < 0.05.

For each analyte, goodness-of-fit of the model was assessed in terms of meeting distributional assumptions of normally, independently distributed errors with homogeneous variance. Deviations from assumptions were addressed using an appropriate transformation or allowing for heterogeneous error variance among sites.

False Discovery Rate Adjustment

The false discovery rate (FDR) method (Benjamini and Hochberg, 1995; Westfall *et al.*, 1999) was used to control for false positive outcomes across all analytes analyzed using linear mixed models. A false positive outcome occurs if the difference in means between two entries is declared significant, when in fact the two means are not different. Since its introduction in the mid-1990s, the FDR approach has been widely employed across a number of scientific disciplines, including genomics, ecology, medicine, plant breeding, epidemiology, dairy science, and signal/image processing (e.g., Pawitan *et al.*, 2005; Spelman and Bovenhuis, 1998). In the FDR method, the false discovery rate is held at 5% across comparisons of multiple analytes via an adjustment to the P-value and is not inflated by the number of analytes in the comparison.

Interpretation of Statistical Results

For a given analyte, when a statistically significant difference (P-value from mixed model analysis < 0.05, or Fisher's exact test P-value < 0.05) was identified in the across-site analysis, the respective range of individual values from DP910521 maize was compared to a tolerance interval. Tolerance intervals are expected to contain at least 99% of the values for corresponding analytes of the conventional maize population with a 95% confidence level (Hong *et al.*, 2014). The tolerance intervals were derived from Pioneer and Dow AgroSciences proprietary accumulated data from non-GM maize lines, which were grown in commercial maize-growing regions between 2003 and 2019 in the United States, Canada, Chile, Brazil, and Argentina. The combined data represent 184 commercial maize lines and 185 unique environments. The selected commercial maize lines represent the non-GM maize population with a history of safe use, and the selected environments (site and year combinations) represent maize growth under a wide range of environmental conditions (i.e., soil texture, temperature, precipitation, and irrigation) and maize maturity group zones.

If the range of DP910521 maize contained individual values outside the tolerance interval, it was then compared to the respective literature range obtained from published literature (AFSI, 2021; Codex Alimentarius Commission, 2019; Cong *et al.*, 2015; Lundry *et al.*, 2013; OECD, 2002; Watson, 1982). Literature ranges complement tolerance intervals in that they are composed of non-proprietary data from additional non-GM commercial maize lines and growing environments, which are not included in Pioneer's proprietary database. If the range of DP910521 maize contained individual values outside the literature range, it was then compared to the respective in-study reference range comprised of all individual

values across-site from all non-GM reference maize lines grown in this study. In-study reference data ranges complement tolerance intervals and literature ranges in that they provide additional context of natural variation specific to the current study.

In cases when a raw P-value indicated a significant difference but the FDR-adjusted P-value was > 0.05, it was concluded that the difference was likely a false positive.

Table I.2. Number of Sample Values Below the Lower Limit of Quantification (sprayed)

Analyte	Number of Samples Below the LLOQ		Fisher's Exact Test P-Value
	Control Maize (n=32)	Herbicide-Treated DP910521 Maize (n=32)	
Fatty Acid Composition (% Total Fatty Acids)			
Lauric Acid (C12:0)	32	32	--
Myristic Acid (C14:0)	30	28	0.672
Heptadecanoic Acid (C17:0)[a]	5	7	--
Heptadecenoic Acid (C17:1)	31	32	1.00
Eicosadienoic Acid (C20:2)	19	24	0.287
Mineral Composition (% Dry Weight)			
Copper[a]	5	8	--
Sodium[a]	1	1	--
Vitamin Composition (mg/kg Dry Weight)			
Vitamin B1 (Thiamine)[a]	1	0	--
Vitamin B2 (Riboflavin)	32	32	--
β-Tocopherol	32	32	--
δ-Tocopherol	24	27	0.536
Secondary Metabolite and Anti-Nutrient Composition (% Dry Weight)			
Furfural	32	32	--

[a] This analyte had < 50% of sample values below the lower limit of quantification (LLOQ) in each maize line and was subjected to the mixed model analysis.